



New Natural Products from Endophytic Fungi-Structure Elucidation and Biological Activity

Neue Naturstoffe aus endophytischen Pilzen-Strukturaufklärung und biologisches Screening

Inaugural-Dissertation

**Zur Erlangung des Doktorgrades der
Mathematisch-Naturwissenschaftlichen Fakultät
der Heinrich-Heine-Universität Düsseldorf**

**vorgelegt von
Weaam N. E. Ebrahim
aus Mansoura, Ägypten**

Düsseldorf, 2012

Aus dem Institut für Pharmazeutische Biologie und Biotechnologie
der Heinrich-Heine Universität Düsseldorf

Gedruckt mit der Genehmigung der
Mathematisch-Naturwissenschaftlichen Fakultät der
Heinrich-Heine-Universität Düsseldorf .

Gedruckt mit der Unterstützung der
Kulturabteilung und Studienmission der Botschaft der Arabischen Republik Ägypten

Referent: Prof. Dr. Peter Proksch
Koreferent: Prof. Dr. Matthias U. Kassack

Tag der mündlichen Prüfung: 01.06.2012

“Das Leben ist wie ein Fahrrad...

**Man muss sich vorwärts bewegen,
um das Gleichgewicht nicht zu verlieren... ”**

(Albert Einstein)

**“Life is like riding a bicycle. To keep your balance
you must keep moving”**

(Albert Einstein)

**الحياه مثل الدراجة لكي تظل متوازنا يجب ان تتحرك باستمرار.
ألبرت أينشتاين.**

Erklärung

Hiermit erkläre ich ehrenwörtlich, dass ich die vorliegende Dissertation mit dem Titel „Neue Naturstoffe aus endophytischen Pilzen-Strukturaufklärung und biologisches Screening“ selbst angefertigt habe. Außer den angegebenen Quellen und Hilfsmitteln wurden keine weiteren verwendet. Diese Dissertation wurde weder in gleicher noch in abgewandelter Form in einem anderen Prüfungsverfahren vorgelegt. Weiterhin erkläre ich, dass ich früher weder akademische Grade erworben habe, noch dies versucht habe.

Düsseldorf, den 19.03.2012

Weaam N. E. Ebrahim

Acknowledgment

First and foremost thanks to the Almighty God “ALLAH” who has granted me all these graces to fulfill this work and blessed me by His power, mercy and patience during my life. To Him I extend my heartfelt thanks.

It is a great pleasure to get this opportunity to express my deepest appreciation and sincere gratitude to Prof. Dr. rer. nat. **Peter Proksch** for setting an example to what a sincere professor, scientist, and advisor should be. I am deeply grateful to him for giving me this valuable chance to pursue my predoctoral research and for the excellent work facilities at the Institute of Pharmaceutical Biology and Biotechnology, Heinrich-Heine University, Düsseldorf. I would like to express my sincere thanks and gratitude to him for supervising this study, suggesting the research project, his unforgettable support, his direct guidance, his generous considerations, his admirable supervision, his fruitful discussions, and his valuable suggestions in both work and life issues. I thank his scientific personality and the second personality which is the merciful big heart he has.

My special thanks to Prof. Dr. rer. nat. **Werner E. G. Müller** and Mrs. **Renate Steffen**, Institute of Physiological Chemistry and Pathobiochemistry, University of Mainz, for carrying out the cytotoxicity assays, Prof. Dr. rer. nat. **M. U. Kassack** and Dr. **Alexandra Hamacher**, Institut für Pharmazeutische und Medizinische Chemie, Düsseldorf for carrying out the cytotoxicity assays, and Dr. **Michael Kubbutat**, ProQinase GmbH, Freiburg, Germany for conducting the protein kinase inhibition assays.

My deep thanks and gratitude to Prof. Dr. rer. nat. Prof. Dr. rer. nat. **M. U. Kassack**, Institut für Pharmazeutische und Medizinische Chemie,

Heinrich-Heine University, Düsseldorf, for his guidance, conducting cytotoxicity assays and for accepting the co-supervision.

My appreciation to the sincere collaboration of Dr. **W. Peters** and Mr. **P. Behm**, Institute of Inorganic and Structure Chemistry, Heinrich-Heine University, Düsseldorf, for conducting 500 MHz NMR measurements, Dr. **H. Keck** and Dr. **P. Tommes**, Institute of Inorganic and Structure Chemistry, Heinrich-Heine University, Düsseldorf, for carrying out EI- and FAB-MS experiments, and my cordial thanks to Dr. **Victor Wray**, Helmholtz Centre for Infection Research, Braunschweig and Mrs. **C. Kakoschke** for 600 MHz NMR measurements, HR-MS experiments, and his generous help and his fruitful discussions by interpreting NMR data.

I would like to express my profound gratitude to my professors and colleagues from the Department of Pharmacognosy, Mansoura University, Mansoura, Egypt, especially Prof. Dr. **M-F Lahloub** for his guidance, supervision, his continuous encouragement, and his kind advices.

I would like to extend my thanks to my past and present colleagues and labmates Dr. **A. Hassan**, Dr. **A. Debbab**, Dr. **Daowan Lai**, Dr. **Festus Okoye**, Dr. **Zhiyong Guo**, Dr. **A. Putz**, Dr. **M. Bayer**, Dr. **S. Younes**, Dr. **Y. Wang**, Dr. **F. Riebe**, Dr. **J. Kjer**, Dr. **S. Ruhl**, Dr. **J. Xu**, **G** and Dr. **S. Ebada**, **G. Daletos**, **W. Döring**, **Y. Zhou**, **M. ElAmrani**, **B. Lipowicz**, **D. Rösberg**, **R. Bara**, **A. Ola**, **A. Marmann**, **L. Hammes Schmidt**, **C-D. Pham**, **H. Niemann**, **N. Aktas** and all the others for the nice multicultural time I spent with them, for their help and assistance whenever I needed it.

I would like to express my thanks to the practical students who I supervised during my stay here in Germany **K. Heinrich**, **G. Daletos**, **K.**

Goldner, M. Bendouma, N. Benayad and special thanking to **C. Pérez Hemphill** and **M. Moussa** for the very nice and productive period that i spend with them in the laboratory.

Special thanks to Mrs. **M. Thiel** and Mrs. **C. Eckelskemper** for their administrative help whenever needed, as well as Mrs. **W. Schlag**, Mrs. **S. Miljanovic**, Mrs. **H. Goldbach-Gecke**, and Mrs. **K. Friedrich** for their kind help in any technical problem encountered during the work.

My profound appreciation to the Egyptian Ministry of Higher Education, Missions Office for the predoctoral fellowship and for the financial support during my stay in Germany.

Last but not least, my gratitude, thankfulness, and my grand indebtedness to my **family**, my wife **Mona Elnekity**, my **mother**, and my **brothers** for their unfailing love, spiritual support and everlasting prayers.

At the end, my heartily thanks and prayers to my **father**, who passed away, and I will never forget that he was the first mentor in my life who inspired me how to set my own goals in life and to carry on to reach them. May Almighty ALLAH bless him.

To All of You, Thank You Very Much!

Zusammenfassung

Endophytische Pilze aus Pflanzen produzieren Naturstoffe mit einer großen Vielfalt an chemischen Verbindungen, welche medizinische oder agrarchemische Verwendung finden könnten. Die meisten dieser Sekundärstoffe zeigen biologische Aktivität in pharmazeutisch-relevanten Bioassay-Systemen und repräsentieren daher Leitstrukturen, die optimiert werden können, um effektive therapeutische und weitere bioaktive Verbindungen zu erhalten.

Ziel dieser Arbeit ist die Isolierung von Sekundärstoffen aus endophytischen Pilzen, gefolgt von Strukturaufklärung und der Analyse des pharmakologischen Potentials. Vier endophytische Pilzarten (*Corynespora cassicola*, *Stemphylium botryosum*, *Stemphylium solani* und *Embellisia eureka*) wurden als biologische Ressourcen ausgewählt. Die Pilze wurden sowohl auf flüssigem Wickerham-Medium, als auch auf Reis-Medium für eine Dauer von vier Wochen kultiviert. Die erhaltenen Extrakte wurden dann verschiedenen chromatographischen Trenn-Methoden unterzogen, um die Sekundärstoffe isolieren zu können.

Die Strukturaufklärung der Sekundärstoffe wurde auf der Grundlage von modernen Analysemethoden ausgeführt, einschließlich der Verwendung der Massenspektrometrie (MS) und der Kernspinresonanzspektroskopie (NMR). Zusätzlich wurden bei ausgewählten Naturstoffen mit optischer Aktivität chirale Derivatisierungs-Methoden angewendet, um die absolute Konfiguration feststellen zu können. Schließlich wurden alle isolierten Substanzen verschiedenen Bioassays unterzogen, um deren zytotoxische Aktivität zu überprüfen.

1. *Corynespora cassicola*

Corynespora cassicola wurde aus der Mangrove *Laguncularia racemosa*

(Combretaceae) isoliert. Achtzehn Substanzen wurden aus verschiedenen Kulturen von *Corynespora cassiicola* isoliert. Diese Substanzen sind den Substanzklassen der Naphthochinone, Octalactone, Decalactone und Depsidone zugehörig. Vierzehn dieser isolierten Substanzen sind neue Naturstoffe.

2. *Stemphylium botryosum*

Acht Substanzen wurden aus Reiskulturen von *Stemphylium botryosum* isoliert. Hauptsächlich handelt es sich bei diesen Substanzen um die Substanzklasse der Pyrone. Zwei der isolierten Substanzen sind neue Naturstoffe.

3. *Stemphylium solani*

Zwei Substanzen wurden aus Reiskulturen von *Stemphylium solani* isoliert. Eine dieser Substanzen ist ein neuer Naturstoff.

4. *Embellisia eureka*

Dreizehn Substanzen wurden aus Reiskulturen von *Embellisia eureka* isoliert. Diese Substanzen gehören zu den chemischen Substanzklassen der Phthalide, Isocoumarine und Pyrrocidine. Zehn der isolierten Substanzen sind neue Naturstoffe. Die beiden Pyrrocidin-Derivate zeigen starke zytotoxische Aktivitäten gegenüber L5178Y, A2780sens. und A2780CisR. Zelllinien.

Insgesamt wurden einundvierzig Substanzen während dieser Arbeit isoliert, wovon siebenundzwanzig als neue Naturstoffe identifiziert wurden. Sowohl die bekannten, als auch die neuen Naturstoffe wurden auf ihre biologische Aktivität hin in verschiedenen Bioassay-Systemen getestet.

Table of Contents

1. Introduction	1
1.1. Natural products	1
1.1.1. Natural products as drugs	1
1.1.2. Natural products as drugs in the past	2
1.2. Fungi as a fascinating source of natural products	3
1.3. Endophytes	5
1.3.1 Endophytes and phytochemistry	6
1.3.2. The relationship between the Endophyte and the host plant	7
1.4. Mangroves	8
1.4.1. Mangrove plants as source of endophytes	9
1.5. Aim and scope of the study	9
 2. Materials and Methods	 11
 2.1. Materials	 11
2.1.1. Biological materials	11
2.1.1.1. Plant material	11
2.1.1.2. Pure fungal strains isolated from the collected plants	11
2.1.2. Media	12
2.1.2.1. Composition of malt agar (MA) medium	12
2.1.2.2. Composition of Wickerham medium for liquid cultures	12
2.1.2.3. Composition of rice medium for solid cultures	12
2.1.2.4. Composition of Luria Bertani (LB) medium	12
2.1.2.5. Composition of yeast medium	13
2.1.2.6. Composition of fungal medium for bioassay	13
2.1.2.7. Composition of potato dextrose agar (PDA) medium for bioassay	14
2.1.2.8. Composition of trypticase soy broth (TSB)	14
2.1.3. Chemicals	14
2.1.3.1. General laboratory chemicals	14
2.1.3.2. Chemicals for culture media	15
2.1.3.3. Chemicals for agarose gel electrophoresis	16
2.1.4. Chromatography	16
2.1.4.1. Stationary phases	16
2.1.4.2. Spray reagents	16
2.1.5. Solvents	17
2.1.5.1. General solvents	17
2.1.5.2. Solvents for HPLC	17
2.1.5.3. Solvents for optical activity	17
2.1.5.4. Solvents for NMR	18

2.2. Methods	18
2.2.1. Fungal strains purification	18
2.2.2. Pure fungal strains cultivation	18
2.2.2.1. Short term storage cultivation	18
2.2.2.2. Small and large scale cultivation for screening	19
2.2.3. Secondary metabolites extraction	19
2.2.3.1. Liquid Wickerham cultures extraction	19
2.2.3.1.1. Total extraction method	19
2.2.3.1.2. Separate extraction method	20
2.2.3.2. Solid rice cultures extraction	22
2.2.3.3. Solvent-solvent extraction	22
2.2.4. Fungal strains identification	23
2.2.4.1. Fungal identification	23
2.2.4.2. Taxonomy	25
2.2.5. Isolation and purification of secondary metabolites	30
2.2.5.1. Isolation of secondary metabolites from <i>Corynespora cassiicola</i>	30
2.2.5.1.1. Secondary metabolites from liquid cultures of <i>Corynespora cassiicola</i>	30
2.2.5.1.2. Secondary metabolites from solid rice cultures of <i>Corynespora cassiicola</i>	31
2.2.5.2. Secondary metabolites from solid rice cultures of <i>Stemphylium botryosum</i>	33
2.2.5.3. Secondary metabolites from solid rice cultures of <i>Stemphylium solani</i>	34
2.2.5.4. Secondary metabolites from solid rice cultures of <i>Embellisia eureka</i>	35
2.2.5.5. Chromatographic methods for isolation	37
2.2.5.5.1. Thin layer chromatography (TLC)	37
2.2.5.5.2 Vacuum liquid chromatography (VLC)	37
2.2.5.5.3 Column chromatography	38
2.2.5.5.4. Preparative high pressure liquid chromatography (HPLC)	39
2.2.5.5.5. Semi-preparative high pressure liquid chromatography (HPLC)	39
2.2.5.5.6. Analytical high pressure liquid chromatography (HPLC)	40
2.2.6. Structure elucidation of isolated secondary metabolites	41
2.2.6.1. Mass spectroscopy (MS)	41
2.2.6.1.1. Electrospray ionization mass spectroscopy (ESI-MS)	41
2.2.6.1.2. Electron impact mass spectroscopy (EI-MS)	42
2.2.6.1.3. Fast atom bombardment mass spectroscopy (FAB-MS)	43
2.2.6.1.4. High resolution mass spectroscopy (HR-MS)	43
2.2.6.2. Nuclear magnetic resonance spectroscopy (NMR)	44
2.2.6.3. Optical activity	45

2.2.6.4. Determination of the absolute stereochemistry by Mosher reaction	45
2.2.6.5. Computational section for CD analysis	46
2.2.7. Testing the biological activity	47
2.2.7.1. Antimicrobial activity	47
2.2.7.1.1. Agar diffusion assay	47
2.2.7.2. Cytotoxicity test	47
2.2.7.2.1. Microculture tetrazolium (MTT) assay	47
2.2.7.2.2. MTT cell viability assays	49
2.2.7.2.3. Protein kinase assay	50
2.2.7.2.4. Soft agar assay	54
2.2.7.2.5. PBMC cytotoxicity assay	54
2.2.7.2.6. ORIS migration assay	55
2.2.7.2.7. Angiogenesis assay	55
2.2.8. General laboratory equipments	56
3. Results	58
3.1. Compounds isolated from the endophytic fungus <i>Corynespora cassicola</i>	58
3.1.1. Corynecassiidiol (1 , new compound)	59
3.1.2. 6-(3'-hydroxy- <i>n</i> -butyl)-7- <i>O</i> -methyl spinochrome B (2 , known compound)	61
3.1.3. 7- <i>O</i> -methyl spinochrome B (3 , known compound)	63
3.1.4. Coryneoctalactone A (4 , new compound)	69
3.1.5. Coryneoctalactone B (5 , new compound)	71
3.1.6. Coryneoctalactone C (6 , new compound)	73
3.1.7. Coryneoctalactone D/A (7/4 , new compounds)	75
3.1.8. Coryneoctalactone E (8 , new compound)	84
3.1.9. Coryneoctalactone F (9 , new compound)	86
3.1.10. Corynesidone A (10 , known compound)	90
3.1.11. Corynesidone B (11 , known compound)	92
3.1.12. Corynesidone D (12 , new compound)	94
3.1.13. Xestodecalactone D (13 , new compound)	100
3.1.14. Xestodecalactone D/E (13/14 , new compounds)	103
3.1.15. Xestodecalactone F (15 , new compound)	109
3.1.16. Xestodecalactone G (16 , new compound)	115
3.1.17. Corynecassiicol A/B (17/18 , new compounds)	127
3.2. Compounds isolated from the endophytic fungus <i>Stemphylium botryosum</i>	134
3.2.1. Phomapyrone D/H (19/20 , D (known) and H (new))	135
3.2.2. Stemphpyrone (21 , known compound)	140
3.2.3. Infectopyrone (22 , known compound)	143

3.2.4. Stemphbotrydione (23 , new compound)	146
3.2.5. Stemphperyleneol (24 , known compound)	151
3.2.6. Macrosporin (25 , known compound)	154
3.2.7. Indole-3-carbaldehyde (26 , known compound)	157
3.3. Compounds isolated from the endophytic fungus <i>Stemphylium solani</i>	160
3.3.1. Altersolanol A (27 , known compound)	161
3.3.2. Stemsolantrione (28 , new compound)	164
3.4. Compounds isolated from the endophytic fungus <i>Embellisia eureka</i>	169
3.4.1. Embepthalide A (29 , new compound)	170
3.4.2. Embepthalide B (30 , new compound)	173
3.4.3. Embepthalide C (31 , new compound)	176
3.4.4. Embepthalide D (32 , new compound)	179
3.4.5. Embepthalide E (33 , new compound)	182
3.4.6. Embeurekol A (34 , new compound)	195
3.4.7. Embeurekol B (35 , new compound)	197
3.4.8. Embeurekol C (36 , new compound)	200
3.4.9. p-hydroxy benzaldehyde (37 , known compound)	208
3.4.10. 2-Anhydromevalonic acid (38 , known compound)	211
3.4.11. Endocrocin (39 , known compound)	214
3.4.12. Pyrrocidine D (40 , new compound)	217
3.4.13. Pyrrocidine E (41 , new compound)	221
4. Discussion	235
4.1. Culturing media	235
4.2. Methodologies for profiling of the metabolites	235
4.2.1. HPLC/UV	236
4.2.2. HPLC/ESI-MS	236
4.3. Isolation of natural products	237
4.4. Compounds isolated from purified fungal strains	237
4.4.1. Compounds isolated from the endophytic fungus <i>Corynespora cassiicola</i>	237
4.4.1.1. Biosynthesis of octalactones and decalactones	238
4.4.1.2. Bioactivity of isolated compounds from <i>Corynespora cassiicola</i> .	239
4.4.2. Compounds isolated from the endophytic fungus <i>Stemphylium botryosum</i>	239
4.4.2.1. Biosynthesis of stemphperyleneol	240
4.4.2.2. Biosynthesis of pyrones	241
4.4.3. Compounds isolated from the endophytic fungus <i>Stemphylium</i>	241

<i>solani</i>	
4.4.3.1. Biosynthesis of altersolanol A	242
4.4.4. Compounds isolated from the endophytic fungus <i>Embellisia eureka</i>	242
4.4.4.1. Biosynthesis of pyrrocidines	242
4.4.4.2. Biosynthesis pathway of phthalides and isocoumarines	246
4.4.4.3. Bioactivity of isolated compounds from <i>Embellisia eureka</i> .	246
4.4.4.4. What is NF- κ B?	247
4.4.4.6. NF- κ B in cancer	250
4.4.4.6. NF- κ B inhibition	253
5. Conclusion	255
6. References	264
7. List of abbreviation	288
8. Attachment	291
Curriculum	311

1. Introduction

1.1. Natural Products

1.1.1. Natural products as drugs

Natural Drugs have been classified as original natural products, products from semi synthetic origin, or synthetic products based on natural product models. Analysis of the number and sources of biologically active agents (Debbab *et al.*, 2011), indicates that over 60% of the approved drugs and pre-NDA candidates (for the period 1989-1995), excluding biologics, developed in these disease areas are of natural origin (Aly *et al.*, 2011a; Cragg *et al.*, 1997).

Natural products are an important source of drugs, and a lot of successful drugs were synthesized to mimic the action of molecules found in nature (Kingston, 1996). Natural products are highly diverse and provide highly specific biological activities. This follows from the proposition that essentially all natural products have some receptor binding capacity (Verdine, 1996). Natural molecules, however, differ substantially from synthetic ones. These differences appear to be amplified when the products of combinatorial synthesis are considered. Although an important aim in combinatorial chemistry is to generate highly diverse libraries, the need for speed and automation introduces new structural idiosyncrasies into the method (Fehler and Schmidt, 2003).

Natural products are chemical substances that are derived from living organisms throughout the six kingdoms Eubacteria, Archaeobacteria, Protista, Fungi, Plantae and Animalia (Woese *et al.*, 1977). These chemical compounds have diverse nature and also biological activities. Since the origin of mankind until now natural products have been used to cure many diseases (Fehler and Schmidt, 2003).

1.1.2. Natural products as drugs in the past

For thousands of years, and through the use of traditional medicines and natural poisons, medicine and natural products (NPs) have been closely linked (Newman et al, 2000). Clinical, pharmacological, and chemical studies of these traditional medicines, which were derived predominantly from plants, were the basis of most early medicines such as aspirin, digitoxin, morphine, quinine, and pilocarpine (Buss *et al.*, 2003). The drug discovery research was strongly enhanced by the discovery of “penicillin” by Fleming in 1928, re-isolation and clinical studies by Chain, Florey, and co-workers in the early 1940s and commercialization of synthetic penicillins (Mann, 1999). Following the success of penicillin, drug companies and research groups soon assembled large microorganism culture collections in order to discover new antibiotics. The output from the early years of this antibiotic research was prolific and included examples such as streptomycin, chloramphenicol, chlortetracycline, cephalosporin C, erythromycin, and vancomycin (Wainwright, 1990).

With Christianity in Europe, a sophisticated system of recording and spreading knowledge was established. Monasteries have been the first institutions operating libraries and exchanging documents. Following the Christian values, nuns and monks provided help for the sick, but this was mostly limited to nursing. Active treatment by drugs was considered as an intrusion in Gods will, and a doctor’s work rejected as sinful or at least useless (Keil, 1989).

This was drastically changed by the Lorsch Pharmacopeia, written in a monastery near Worms, Germany in the late 8th century. The book contained numerous medical compositions as well as an index allowing the reader to quickly find the right remedy. In the introduction, the big gap between religion and science was closed and the medicine was legally put in the service for mankind not as a right, but as a duty (Keil, 1989). Since this time, monasteries cultured medicinal plants in their gardens.

Even though the industrial drugs displaced them already a long time ago, the spirit is still found today in the name of the pharmaceutical company “Klosterfrau”, which is specialized on natural remedies.

In Asia, traditional medicine was and is still widely used. Ayurveda, the traditional medicine in India has been used for more than three thousand years. In China, the traditional system of medicine has been used also for several thousand years. The Chinese herbal medicine was first recorded in the Emperor Shennung’s classic herbals, about 2700 BC (Patwardhan *et al.*, 2004).

1.2. Fungi as a fascinating source of natural products

Fungi are biosynthetically active organisms capable of producing a wide range of chemically diverse and biologically intriguing small molecules. The majority of scientific interests in fungal natural products have centered on their pharmaceutical applications, roles as mycotoxins, and various ecological functions (Bergmann *et al.*, 2007). Fungi comprise a wide range of subtypes. Saprotrophic fungi are important in the cycling of nutrients, especially the carbon that is sequestered in wood and other plant tissues. Pathogenic and parasitic fungi attack effectively all groups of organisms, including bacteria, plants, other fungi, and animals, including humans (Debbab *et al.*, 2011). Other fungi function as mutualistic symbionts, including mycorrhizal associates of insects, mycorrhizae, lichens, and endophytes. Through these symbioses, fungi have enabled a diversity of other organisms to exploit novel habitats and resources. Indeed, the establishment of mycorrhizal associations may be a key factor that enabled plants to make the transition from aquatic to terrestrial habitats (Lutzoni *et al.*, 2004).

The exploration of fungal bioactive secondary metabolites was initiated by the discovery of penicillin in 1928 by Alexander Fleming, further re-isolation and clinical studies by Chain, Florey and coworkers in early 1940s, and its

subsequent commercialization in a synthetic form (Butler, 2004). About twenty years after the discovery of penicillin, potent anticancer agent, taxol (Strobel *et al.*, 1996) and antimicrobial agent such griseofulvin (Grove *et al.*, 1952) had been discovered from fungi. Furthermore, cyclosporine A which was isolated from the fungus *Tolypocladium inflatum* (Traber *et al.*, 1982 and 1987), and lovastatin (Endo, 1979) are fungal metabolites used as immunosuppressant during organ transplantation and antihyperlipidemic agents, respectively.

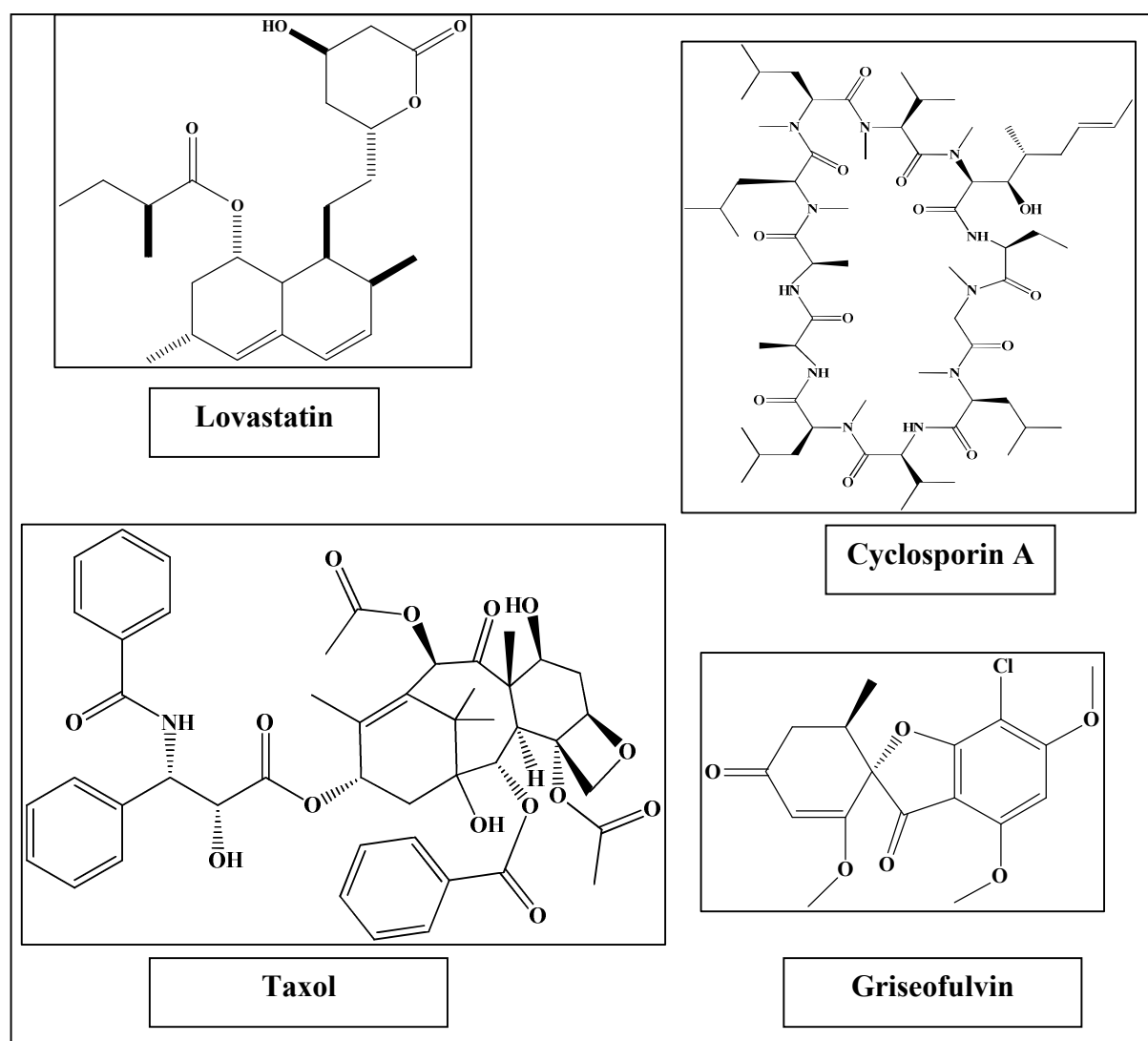


Fig. 1.1: Some fungal products as drugs.

Some secondary metabolites can stimulate spore formation and inhibit or stimulate germination. Since formation of secondary metabolites and spores are

regulated by similar factors, this phenomenon can ensure secondary metabolites production during sporulation. Thus, the secondary metabolites can slow down germination until a less competitive environment and more favorable conditions for growth exist, protect the dormant or initiated spore from consumption by amoebae or cleanse the immediate environment of competing microorganisms during germination (Demain, 2000).

1.3. Endophytes

Endophytes are microorganisms that reside in the internal tissues of living plants without causing any immediate overt side effects (Bacon and white, 2000), but may turn pathogenic during host senescence (Rodriguez *et al.*, 2008). The majority of endophytes are transmitted horizontally to their host plants through airborne spores. In contrast, some endophytes are transmitted vertically to the next plant generation via seeds (Hartley and Gange, 2009). They are relatively unstudied and potential sources of novel natural products for exploitation in medicine, agriculture, and industry. It is noteworthy that, of the nearly 300,000 plant species that exist on the earth, each individual plant is host to one or more endophytes. Only a few of these plants have ever been completely studied relative to their endophytic biology (Aly *et al.*, 2011a). Consequently, the opportunity to find new and interesting endophytic microorganisms among myriads of plants in different settings and ecosystems is great (Strobel and Daisy, 2003; Aly *et al.*, 2011b).

It is clear that the new and useful compounds provide assistance and relief to the human. The appearance of resistant bacteria, life threatening viruses, the recurring problems with disease in persons with organ transplants, and the wide spread of fungal infections in the world's population only underscore our inadequacy to cope with these medical problems (Aly *et al.*, 2011a). Added to this there are enormous difficulties in raising enough food on certain areas of the Earth to support local human populations. Environmental degradation, loss of

biodiversity, and spoilage of land and water also add to problems facing mankind (Strobel and Daisy, 2003)

It is hypothesized that there are no neutral interactions, but rather that endophyte-host interactions involve a balance of antagonisms. There is always at least a certain degree of virulence on the part of the fungus enabling infection, whereas defense of the plant host limits development of fungal invaders and disease (Schulz and Boyle, 2005). Many endophytes are closely related to pathogenic fungi, and presumably evolved from them via an extension of latency periods and a reduction of virulence (White *et al.*, 1993). It is also hypothesized that endophytes, in contrast to known pathogens, generally have far greater phenotypic plasticity and thus more options than pathogens including infection, local but also extensive colonization, latency, virulence, pathogenicity, or saprophytism (Schulz and Boyle, 2005).

1.3.1. Endophytes and phytochemistry

It is believed that the reason why some endophytes produce certain drugs might be related to a genetic recombination of the endophyte with the host that occurs in evolutionary time (Tan and Zou, 2001). Furthermore, it is recognized that a microbial source of a valued product may be easier and more economical to produce, effectively reducing its market price. Frequently, many endophytes (biotypes) of the same species are isolated from the same plant and only one of the endophytes will produce a highly biologically active compound in culture (Li *et al.*, 1996; Aly *et al.*, 2011b).

It is also uncertain of what an endophyte produces in culture and what it may produce in nature. It does seem apparent that the production of certain bioactive compounds by the endophyte *in situ* may facilitate the domination of its biological niche within the plant or even provide protection to the plant from harmful invading pathogens. This may be especially true if the bioactive product

of the endophyte is unique to it and is not produced by the host. Seemingly, this would more easily facilitate the study of the role of the endophyte and its role in the plant (Strobel and Daisy, 2003).

1.3.2. The relationship between the Endophyte and the host plant

Endophytic fungi, which live within host plant tissues without causing any visible symptoms of disease (Wilson, 1995) are known to occur in almost all higher plants (Azevedo *et al.*, 2000) and are important mediators of plant-herbivore interactions (Rajagopal and Suryanarayanan, 2000). However, there are isolates and/or species of fungal endophytes that span the symbiotic continuum by expressing different lifestyles, ranging from mutualism through commensalism to parasitism (Rodriguez *et al.*, 2008). Although the genetic basis of symbiotic communication is not yet known, studies examining the relation between host genotype and symbiotic lifestyle expression revealed that individual isolates of some fungal species can express either parasitic or mutualistic lifestyles depending on the host genotype colonized (Redman *et al.*, 2001; Unterseher and Schnittler 2010). Some endophytes are generally viewed at as mutualists; by receiving nutrition and protection from their host plants, the endophytes enhance resistance of the host plant against insect herbivores or pathogens (Clay, 1990).

The mechanisms underlying anti-herbivore properties of endophytic fungi are attributed mainly to the production of various alkaloid-based defensive compounds in the plant tissue (Faeth, 2002) or through alteration of plant nutritional quality (e.g., phytosterols) (Bernays, 1993). However, other cues, such as plant volatiles or secondary plant metabolites may influence the growth of the fungus within the plant tissue and may contribute to behavioral changes of herbivorous insects feeding on endophyte associated host plants (Bernays, 1993).

It is possible to imagine that some of these endophytic microbes may have devised genetic systems allowing for the transfer of information between themselves and the higher plant and *vice versa* (Stierle *et al.*, 1993; Strobel, 2002). Obviously, this would permit a more rapid and reliable mechanism of the endophyte to deal with environmental conditions and perhaps allow for more compatibility with the plant host leading to symbiosis (Strobel, 2002).

In return, plants provide spatial structure, protection from desiccation, nutrients, photosynthates and, in the case of vertical-transmission, dissemination to the next generation of hosts (Clay, 1988; Wolock-Madej and Clay, 1991; Knoch *et al.*, 1993; Saikkonen *et al.*, 1998; Faeth and Fagan, 2002; Rudgers *et al.*, 2004). It is also possible that the plant may provide compounds critical for the completion of the life cycle of the endophyte or essential for its growth or self-defense (Metz *et al.*, 2000; Strobel, 2002). However, in cases in which herbivores facilitate spore or hyphal dispersal, non-systemic endophyte interactions with their host plants should fall near the antagonistic end of the interaction spectrum (Saikkonen *et al.*, 1998).

Recent studies suggested that plant and endophyte genotypic combinations together with environmental conditions are an important source of variation in endophyte-plant interactions (Faeth and Fagan, 2002). It would seem that many factors changing in the host as related to the season, age, environment and location may influence the biology of the endophyte (Strobel and Daisy, 2003).

1.4. Mangroves

Mangroves are tropical and subtropical forests comprising trees of many unrelated genera that share the common ability to grow in estuarine and coastal environments. They are open systems with respect to both energy and matter

and thus couple upland terrestrial and coastal estuarine ecosystems (Lugo and Snedaker, 1974).

1.4.1. Mangrove Plants as host for Endophytes

Mangrove vegetation contributes to the primary production in the aquatic environment in the form of leaf and litter fall. Decomposition of this organic material by bacteria and fungi results in protein enriched fragments of detritus. Fungi rather than bacteria have been considered to be principal sources of this increase in nitrogen (Odum and Heald, 1972). Despite a better understanding of the importance of mangroves, they continue to be destroyed at an alarming rate (Ong, 1995). Therefore it is imperative to record and quantify the abundance of marine fungi in the mangrove ecosystem and to culture them to ensure their conservation for future biochemical, genetic and molecular studies (Jones and Mitchell, 1996). Although mangroves are the second important habitats for marine fungi after driftwood, reports on fungi from mangroves were not published until Cribb and Cribb (1955) (Cribb and Cribb, 1955) reported their collections of fungi on mangrove roots in Australia. Investigations on mangrove fungi have however, received considerable attention. The mycota of several of the tropical and subtropical mangrove substrata have been documented. Apart from isolating several interesting fungi, information was also gathered on the biogeography and ecology of these fungi (Hyde and Lee, 1995).

1.5. Aim and scopes of the study

Being poorly investigated, endophytes are obviously a rich and reliable source of bioactive and chemically novel compounds with huge medicinal and agricultural potential. The aim of this study was the purification of endophytic fungal strains from mangrove and terrestrial plants, the isolation, characterization and structure elucidation of biologically active secondary metabolites from the extracts of these endophytic fungal strains, and the preliminary evaluation of their pharmaceutical potential. Four endophytic fungi,

Corynespora cassiicola, *Stemphylium botryosum*, *Stemphylium solani* and *Embellisia eureka* were investigated as biological sources of the study.

In order to isolate the secondary metabolites, the fungi were grown in static liquid Wickerham medium as well as on solid rice medium at room temperature. The cultures were allowed to grow for 3-4 weeks, followed by harvesting and subsequent extraction with organic solvents. The obtained crude extracts were then fractionated and separated using various chromatographic techniques and their fractions were analyzed by HPLC-DAD for their purity and ESI-LC/MS for their molecular weight and fragmentation patterns. The pure compounds were submitted to state-of-the-art one- and two-dimensional NMR techniques for structure elucidation. In addition, selected compounds were derivatized in order to determine their absolute stereochemistry.

Furthermore, fractions and pure compounds were subjected to selected bioassays to determine their pharmaceutical potential. Thus, antimicrobial activity was studied using the agar diffusion assay, whereas cytotoxicity was studied *in vitro* using mouse lymphoma (L5178Y), A2780 and A2780 Cis.R. cell lines. Moreover, some pure compounds were also tested for their protein kinase inhibitory activity. The latter three assays were conducted in cooperation with Prof. W. E. G. Müller, Mainz, Prof. M. U. Kassack, Düsseldorf, and ProQinase, Freiburg, respectively.

2. Materials and Methods

2.1. Materials

2.1.1. Biological materials

2.1.1.1. Plant material

Plant samples were collected from Hainan Island and Morocco. Small stems and leaves were cut from the plants and placed in plastic bags after any excess moisture was removed. Every attempt was made to store the materials at 4° C until isolation procedures could be performed.

2.1.1.2. Pure fungal strains isolated from the collected plants

Table 2.1: shows a list of the endophytic fungal strains isolated from different Plants and their corresponding botanical sources.

Fungal code	Plant Part	Source
JCM 23.3	Leaves	<i>Laguncularia racemosa</i> (Combretaceae)
<i>Stemphylium botryosum</i>		<i>Lupinus</i> Sp. (Fabaceae)
Slts2	Stems	<i>Mentha pulegium</i> (Lamiaceae)
Cats2	Stems	<i>Cladanthus arabicus</i> (Asteraceae)

2.1.2. Media

2.1.2.1. Composition of malt agar (MA) medium

MA medium was used for short term storage of fungal cultures or fresh seeding for preparation of liquid cultures.

Agar-agar	15.0 g
Malt extract	15.0 g
Distilled water	to 1000 mL
pH	7.4 -7.8 (adjusted with NaOH/HCl)

For the isolation of endophytic fungi from plant tissues chloramphenicol or streptomycin (0.2 or 0.1 g, respectively) were added to the medium to suppress bacterial growth.

2.1.2.2. Composition of Wickerham medium for liquid cultures

Yeast extract	3.0 g
Malt extract	3.0 g
Peptone	5.0 g
Glucose	10.0 g
Distilled water	to 1000 mL
pH	7.2 -7.4 (adjusted with NaOH/HCl)

2.1.2.3. Composition of rice medium for solid cultures

Rice	3.0 g
Distilled water	3.0 g

Water was added to the rice and kept overnight before autoclaving.

2.1.2.4. Composition of Luria Bertani (LB) medium

This medium was used to conduct antibacterial assays.

Peptone	10.0 g
Malt extract	5.0 g
NaCl	10.0 g
Distilled water	to 1000 mL
pH	7.0 (adjusted with NaOH/HCl)

To prepare the agar plates, 15.0 g agar were added to 1 L broth media.

2.1.2.5. Composition of yeast medium

This medium was used to perform bioassays using *Saccharomyces cerevisiae*.

Peptone	5.0 g
Yeast extract	5.0 g
Malt extract	3.0 g
Glucose	10.0 g
Distilled water	to 1000 mL

To prepare the agar plates, 15.0 g agar were added to 1 L broth media.

2.1.2.6. Composition of fungal medium for bioassay

Mannitose	50.0 g
Saccharose	50.0 g
Succinic acid	5.4 g
Yeast extract	3.0 g
K ₂ HPO ₄	0.1 g
MgSO ₄	0.3 g
FeSO ₄	10.0 mg
ZnSO ₄	10.0 mg

Distilled water to 1000 mL

pH 5.4 (adjusted with NaOH/HCl)

2.1.2.7. Composition of potato dextrose agar (PDA) medium for bioassay

Potato infusion (see below) to 1000 mL

Dextrose 20.0 g

Agar 15.0 g

Potato infusion: The potatoes (200 g) were first washed and cut into small pieces, then boiled in 1000 mL distilled water for 1 hour and filtered to get the potato infusion.

2.1.2.8. Composition of trypticase soy broth (TSB)

Peptone from casein 17.0 g

Peptone from soymeal 3.0 g

Glucose 2.5 g

NaCl 5.0 g

K₂HPO₄ 2.5 g

Distilled water to 1000 mL

pH 7.3 (adjusted with NaOH/HCl).

2.1.3. Chemicals

2.1.3.1. General laboratory chemicals

Anisaldehyde Merck

(4-methoxybenzaldehyde) Merck

(-)-2-Butanol Merck

Dimethylsulfoxide	Merck
Formaldehyde	Merck
L-(+)-Ascorbic acid	Merck
Hydrochloric acid	Merck
Potassium hydroxide	Merck
Pyridine	Merck
Concentrated sulphuric acid	Merck
Trifluoroacetic acid (TFA)	Merck
Concentrated ammonia solution	Fluka
Acetic anhydride	Merck
Ortho-phosphoric acid 85% (p.a.)	Merck
Sodium hydrogen carbonate	Sigma

2.1.3.2. Chemicals for culture media

Agar-agar	Galke
Chloramphenicol	Sigma
Glucose	Caelo
Malt extract	Merck
NaCl	Merck
Peptone	BD
Streptomycin	Sigma
Yeast extract	Sigma

2.1.3.3. Chemicals for agarose gel electrophoresis

Agarose	Serva
TBE-buffer	Sigma
Ethidium bromide	Serva
Standards	NEB

2.1.4. Chromatography

2.1.4.1. Stationary phases

Pre-coated TLC plates, Silica Gel 60 F ₂₅₄ , layer thickness 0.2 mm	Merck
Silica Gel 60, 0.04 - 0.063 mm mesh size	Merck
Pre-coated TLC plates, RP-18, F ₂₅₄ S, layer thickness 0.25 mm	Merck
RP-18, 0.04 - 0.063 mm mesh size	Merck
Sephadex LH 20, 0.25 - 0.1 mm mesh size	Merck
Diaion HP20	Supelco

2.1.4.2. Spray reagents

The reagents were stored in amber-colored bottles and kept refrigerated until use. TLC was used to monitor the identity of each of the fractions and the qualitative purity of the isolated compounds. It was also utilized to optimize the solvent system that would be applied for column chromatography.

Anisaldehyde/H₂SO₄ Spray Reagent

Methanol	85 mL
Glacial acetic acid	10 mL

Conc. H ₂ SO ₄	(added slowly) 0.5 mL
Anisaldehyde	5 mL

Vanillin/ H₂SO₄ Spray Reagent

Methanol	85 mL
Conc. H ₂ SO ₄	15 mL
Vanillin	1 g

2.1.5. Solvents

2.1.5.1. General solvents

Acetone, acetonitrile, dichloromethane, ethanol, ethyl acetate, n-hexane and methanol were used. The solvents were purchased from the Institute of Chemistry, University of Düsseldorf. They were distilled before using and special grades were used for spectroscopic measurements.

2.1.5.2. Solvents for HPLC

Acetonitrile	LiChroSolv HPLC grade (Merck)
Methanol	LiChroSolv HPLC grade (Merck)
Nanopure water	distilled and heavy metals free water obtained by passing distilled water through nano- and ion-exchange filter cells (Barnstead, France)

2.1.5.3. Solvents for optical activity

Acetone	Spectral grade (Sigma)
Chloroform	Spectral grade (Sigma)
Methanol	Spectral grade (Sigma)

Dimethylsulfoxide Spectral grade (Merck)

2.1.5.4. Solvents for NMR

Acetone- d_6 Uvasol, Merck

DMF- d_7 Uvasol, Merck

DMSO- d_6 Uvasol, Merck

Methanol- d_4 Uvasol, Merck

Pyridine- d_5 Uvasol, Merck

2.2. Methods

2.2.1. Fungal strains purification

Different plant parts were cut into very small pieces, washed with sterilized water, then only the surface of them is thoroughly treated with 70% ethanol for 1-2 minutes and then air dried under the flow hood. This is done in to avoid surface contaminating microbes. With a sterile scalpel, outer tissues were removed from the plant samples and the inner tissues were carefully dissected under sterile conditions and placed onto malt agar plates containing antibiotics. Then, hyphal tips of the fungi were removed and transferred to fresh malt agar medium. Plates are prepared in duplicates to eliminate the possibility of contamination. Pure strains were isolated by repeated inoculation.

2.2.2. Pure fungal strains cultivation

2.2.2.1. Short term storage cultivation

Fungi were grown on malt agar medium under room temperature for several days. When fungal hyphae almost cover the surface of the malt agar plate, cultures were stored at 4° C for a maximum period of 6 months, and then re-inoculated onto fresh malt agar media.

2.2.2.2. Small and large scale cultivation for screening

This is done by transferring fresh fungal cultures into Erlenmeyer flasks (1L each) containing 300 mL of Wickerham medium for liquid cultures or 100 g rice for solid cultures. The cultures were then incubated at room temperature (no shaking) for 21 and 30 days, respectively. Large scale cultivation was carried out using 20 1L Erlenmeyer flasks for liquid and solid rice cultures, respectively.

2.2.3. Secondary metabolites extraction

2.2.3.1. Liquid Wickerham cultures extraction

2.2.3.1.1. Total extraction method

To each 1L Erlenmeyer about 250 mL EtOAc were added and left overnight to stop cell growth. Culture media and mycelia were then extracted in the Ultraturrax for 10 min for cell destruction, followed by vacuum filtration using Buchner. The mycelium residue was discarded while culture filtrates were collected and extracted with EtOAc and *n*-BuOH till exhaustion. The combined EtOAc phases were washed with distilled water and then taken to dryness. The dry residue was then partitioned between *n*-hexane and 90% MeOH. The extraction scheme is described in Fig. 2.1.

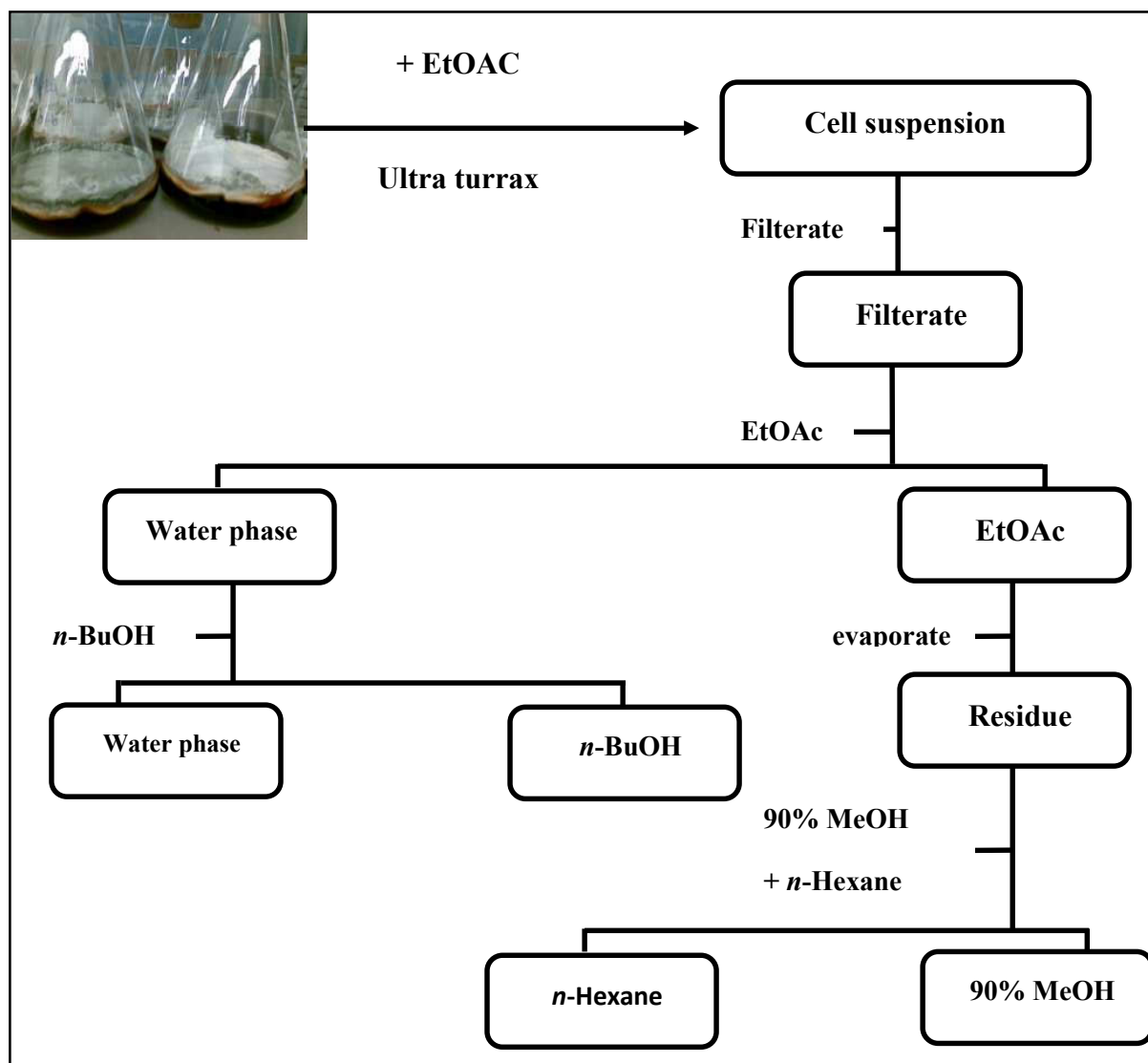


Fig. 2.1: Total extraction of culture media and mycelia.

2.2.3.1.2. Separate extraction method

This is done by separation of fungal mycelia from culture media and left in MeOH overnight. Using Ultraturrax cells were destructed and extracted for 10 min., followed by filtration and repeated extraction till exhaustion. The culture media were extracted in the same manner as described above in 2.2.3.1.1 to obtain the EtOAc extract. The extraction scheme is described in Fig. 2.2.

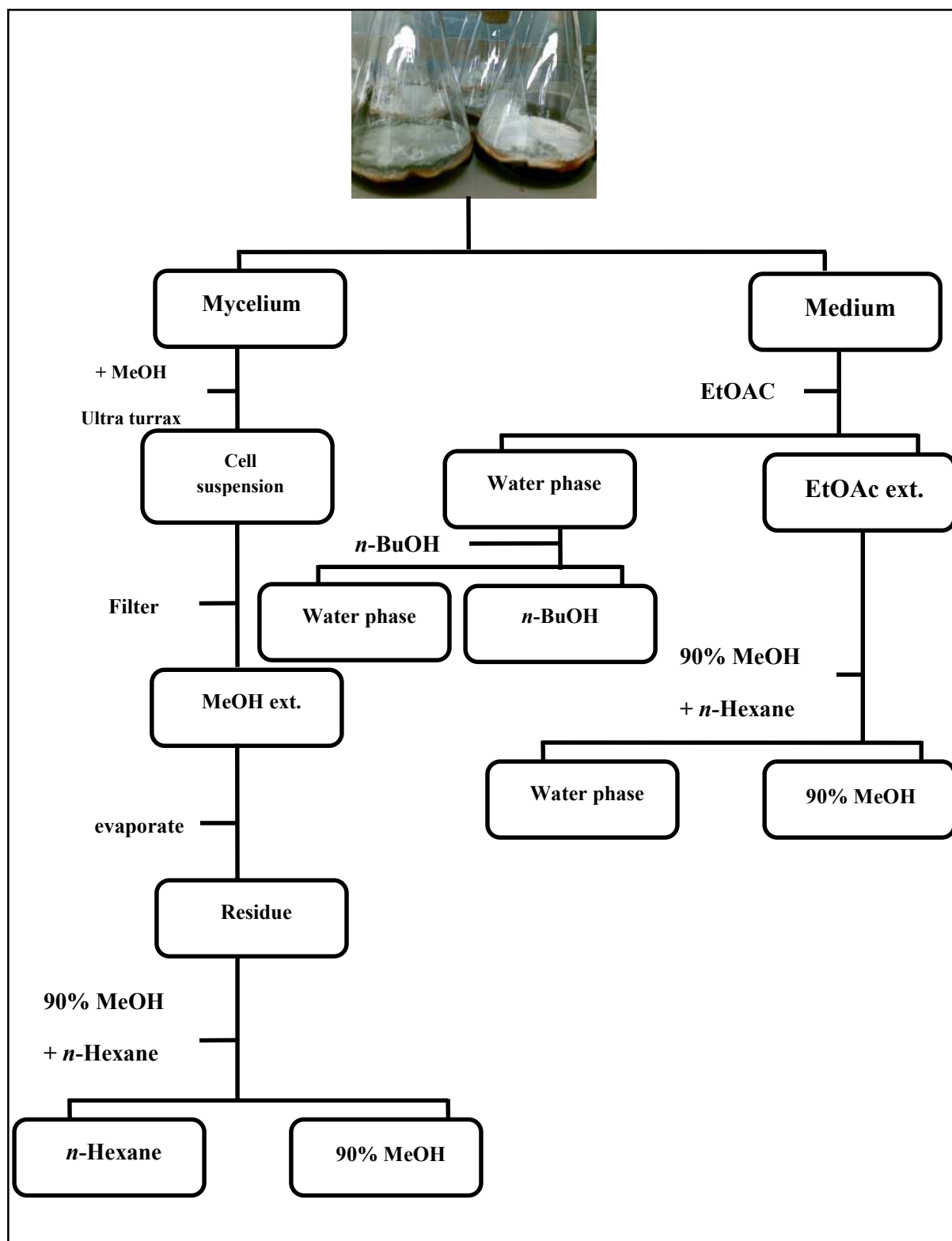


Fig. 2.2: Separate extraction of culture media and mycelia.

2.2.3.2. Solid rice cultures extraction

To each 1L Erlenmeyer about 250 mL EtOAc were added and left overnight. Then the culture media are cut into very small pieces and re-extracted with fresh EtOAc three times till nearly all the secondary metabolites are extracted.

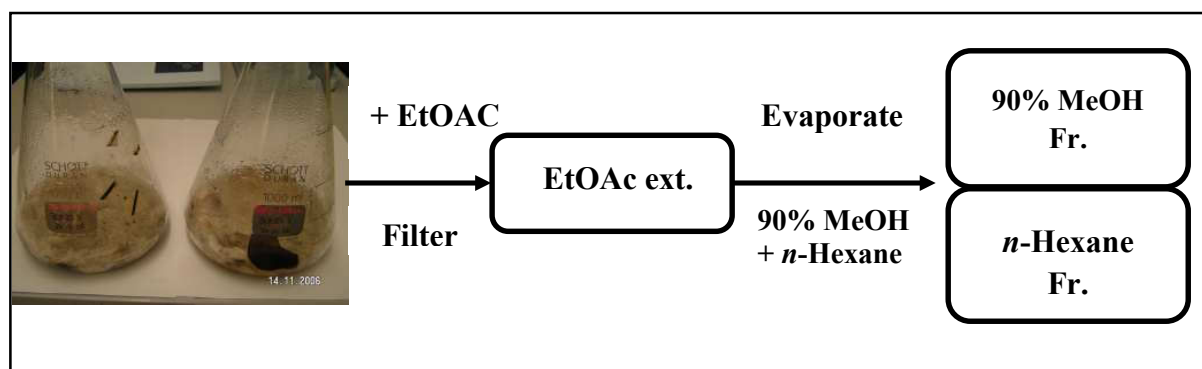


Fig. 2.3: Extraction of solid rice culture.

The combined EtOAc phases were washed with distilled water and then taken to dryness. The dry residues obtained from EtOAc and MeOH extracts were partitioned between *n*-hexane and 90% MeOH. The extraction scheme is described in Fig. 2.3.

2.2.3.3. Solvent-solvent extraction

It is a widely employed technique to separate organic compounds from a mixture. It involves the distribution of compounds into two immiscible solvents. Since the technique is based upon an unequal distribution of solutes between two solvents with different polarities, the solutes will be more soluble in one solvent compared to the other. The distribution of a component A between two phases can be expressed by the distribution coefficient (K):

$$\text{phase K} = \frac{[A]_{\text{top}}}{[A]_{\text{lower phase}}}$$

where, [A] is the concentration of solute A.

These should be considered in choosing the solvents:

- The solvents involved in the extraction must be immiscible
- The solvents must not react with the components that will be separated
- The solvents should be easily removed by evaporation after the process

In this study, solvent-solvent extraction was the first step in the separation process. It was meant to “clean” the ethyl acetate extract from salts and other undesirable polar constituents.

2.2.4. Fungal strains identification

2.2.4.1. Fungal identification

This is carried out using a molecular biology protocol. This was carried out by Mustapha El Amrani at the Institut für Pharmazeutische Biologie und Biotechnologie, Heinrich-Heine-Universität Düsseldorf.

Isolation of DNA

This is done using DNeasy® Plant Mini Kit (QIAGEN). The lyophilized mycelia were pulverized and disrupted with the help of glass beads. Then cell lysis was carried out by addition of lysis Buffer AP-1 and RNase-A solution followed by incubation of the mixture at 65° C. The remaining detergent, protein and polysaccharide were precipitated by addition of Buffer AP-2 to the lysate. The lysate was then applied to the Qias shredder™ Mini Spin Column and centrifuged to remove the cell debris and other remaining precipitates. The lysate was then transferred to a new tube.

An adequate volume of ethanolic Buffer AP3/E was added to the lysate and the mixture was then applied to DNeasy Mini Spin Column. After centrifugation, the filtrate was discarded. The column was washed by addition of ethanol Buffer AW followed by centrifugation. Another portion of Buffer AW was added to the

column and centrifuged at maximum speed to dry the membrane in the column from residual ethanol.

Fungal DNA, which is incorporated into the membrane, was eluted by addition of Buffer AE directly to the membrane in the DNeasy column. The column was then incubated at room temperature for 5 minutes and then centrifuged to collect the filtrate, which was the fungal DNA dissolved in Buffer AE.

The amplification of DNA

DNA was then amplified by Polymerase Chain Reaction (PCR). The PCR was carried out using HotStarTaq Master Mix Kit (QIAGEN). The Master Mix contains HotStarTaq[®] DNA Polymerase, PCR buffer (with MgCl₂) and dNTPs.

ITS 1 (with base sequences TCCGTAGGTGAACCTGCGG) and ITS 4 (with base sequences TCCTCCGCTTATTGATATGC) (Invitrogen), as primers, were mixed with HotstarTaq Master Mix Kit and DNA template. Thus, each PCR reaction mixture contained 5- 10 ng of genomic DNA, 1 µM each of the primers ITS 1 and ITS 4, and 1 U of Hot start TaqPolymerase (Invitrogen) in a total volume of 50 µL. The mixture was then applied to the thermal cycler (BioRad) using the programmed PCR cycle as outlined below:

- Initial activation step in 95° C for 15 minutes to activate HotStarTaq[®]DNA Polymerase

- Cycling steps which were repeated 35 times:

Denaturing: 1 minute at 95° C, annealing: 1 minute at 56° C, extension: 1 minute at 72° C

- Final extension for 10 minutes at 72° C

PCR products purification and DNA sequencing

PCR product was purified using 2% Agarose-Gel-Electrophoresis at 75 V for 60 minutes in TBE buffer. The agarose gel was then stained using 1% ethidium bromide. A 500 bp stained DNA fragment was then excised from the agarose gel. The next step of PCR product purification was performed using Perfectprep® Gel Cleanup Kit (Eppendorf). The binding buffer was mixed to the PCR product and incubated at 50° C for 10 minutes in an eppendorf thermomixer at 1000 rpm. The mixture was mixed with a volume of isopropanol and then centrifuged. The filtrate was discarded and the column was washed with wash buffer twice followed by centrifugation.

Amplified fungal DNA (PCR product), which was incorporated into the column, was eluted by addition of elution buffer or molecular biology grade water to the centre of the column. The column was then centrifuged to collect the filtrate, which was the fungal DNA dissolved in elution buffer. The amplified fungal DNA was then submitted for sequencing by a commercial service and the base sequence was compared with publicly available databases such as GenBank with the help of Blast-Algorithmus.

2.2.4.2. Taxonomy

Corynespora cassiicola

The fungus *Corynespora cassiicola* was isolated from fresh leaves of the medicinal plant *Laguncularia racemosa* (Combretaceae) (see Fig. 2.4). The plant was collected in 2006 from Hainan Island, China.

Taxonomy

Phylum	Ascomycota;
Subphylum	Pezizomycotina;
Class	Dothideomycetes;

Order Pleosporales;
Family Pleosporaceae;
Genus *Corynespora*;
Species *C. cassiicola*.

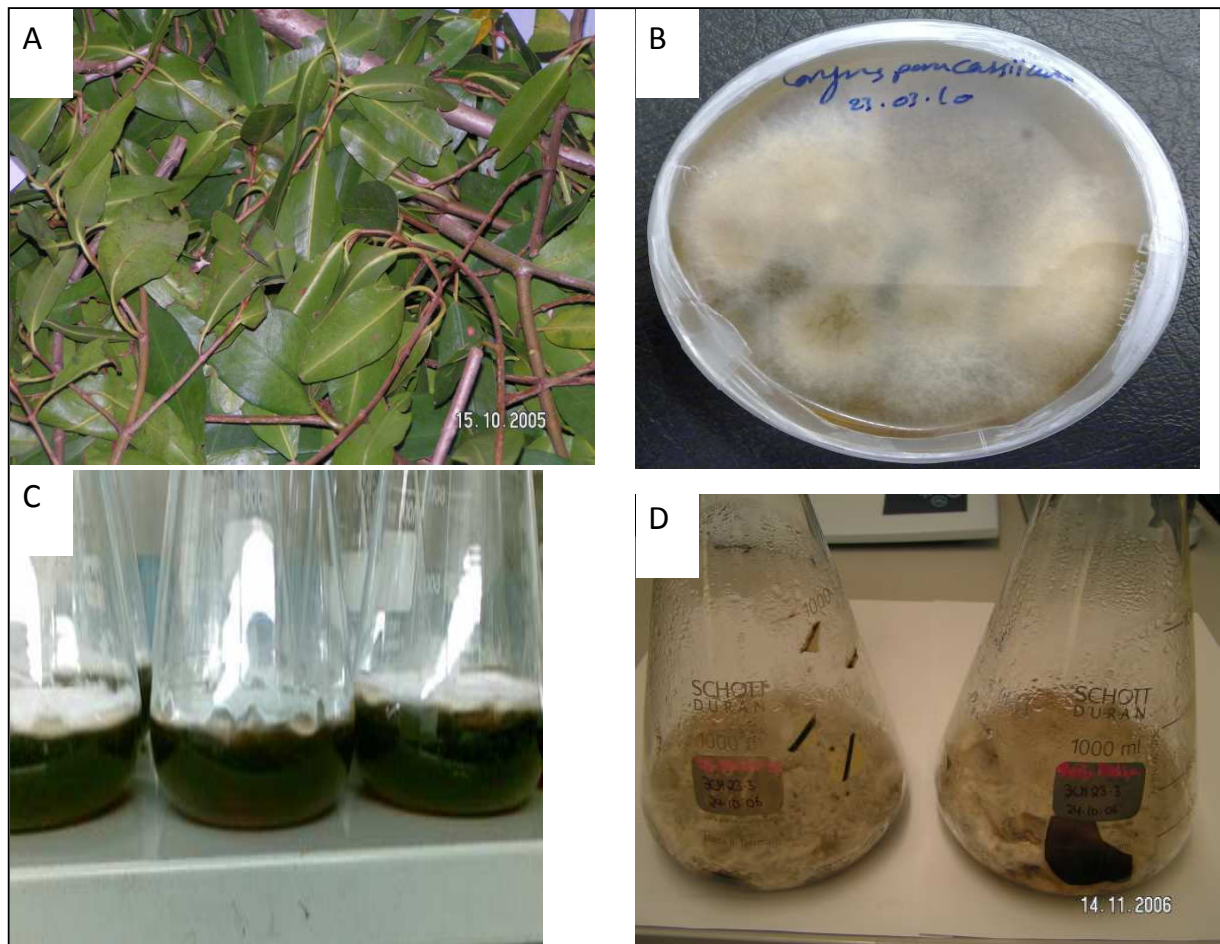


Fig. 2.4: (A: *Laguncularia racemosa* B: Pure strain of *Corynespora cassiicola* on malt agar plate C: Liquid Wickerham culture D: Rice culture).

Stemphylium botryosum

The fungus *Stemphylium botryosum* was isolated from the plant *Lupinus* sp. (Fabaceae) (see Fig. 2.5).

Taxonomy

Phylum	Ascomycota;
Subphylum	Pezizomycotina;
Class	Dothideomycetes;
Order	Pleosporales;
Family	Pleosporaceae;
Genus	<i>Stemphylium</i> ;
Species	<i>S. botryosum</i> .

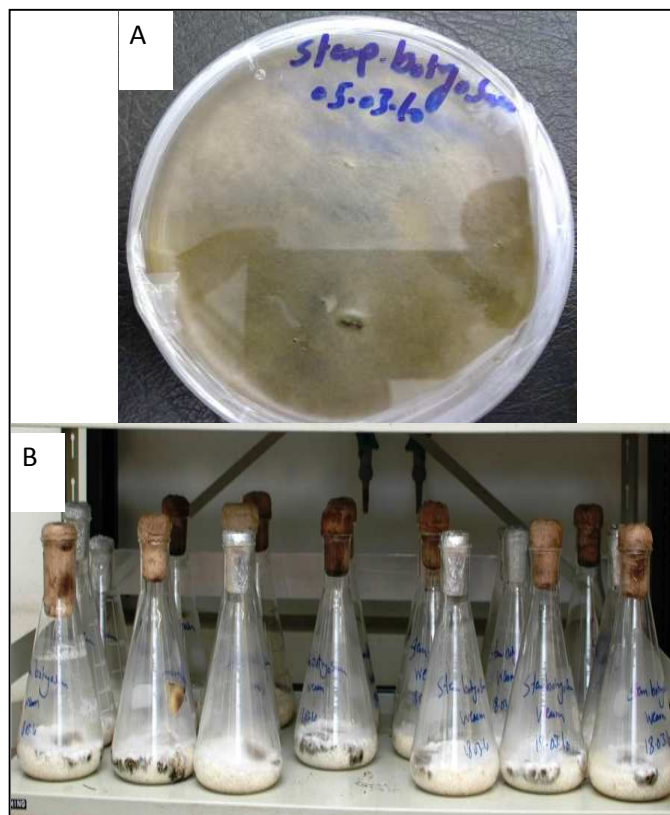


Fig. 2.5: (A: Pure strain of *Stemphylium botryosum* on malt agar plate B: Rice culture).

Stemphylium solani

The fungus *Stemphylium botryosum* was isolated from the stem of the medicinal plant *Mentha pulegium* (Lamiaceae) (see Fig. 2.6). The plant was collected in 2009 from Morocco.

Taxonomy

Phylum	Ascomycota;
Subphylum	Pezizomycotina;
Class	Dothideomycetes;
Order	Pleosporales;
Family	Pleosporaceae;
Genus	<i>Stemphylium</i> ;
Species	<i>S. solani</i> .

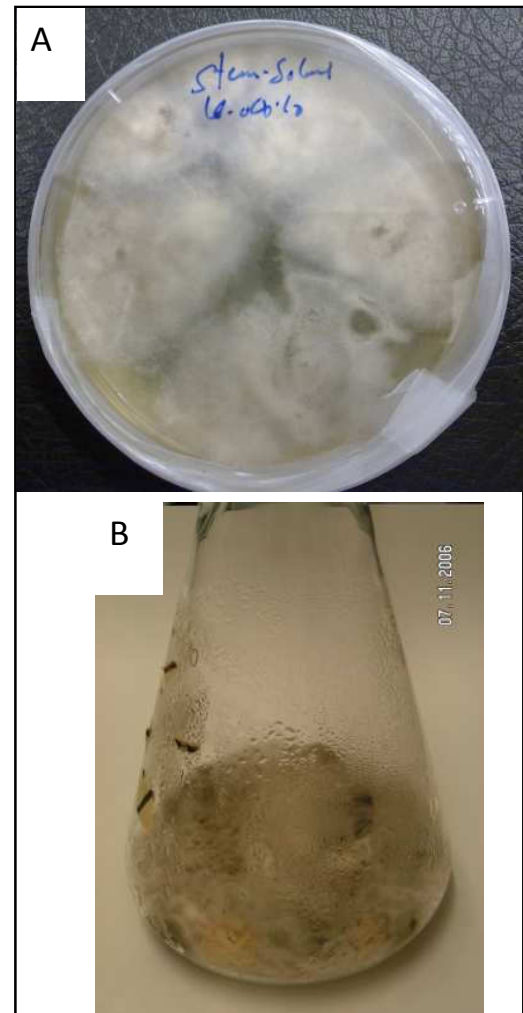


Fig. 2.6: (A: Pure strain of *Stemphylium solani* on malt agar plate B: Rice culture).

Embellisia eureka

The fungus *Embellisia eureka* was isolated from the plant *Cladanthus arabicus* (Asteraceae) (see Fig. 2.7). The plant was collected in 2010 from Morocco.

Taxonomy

Phylum	Ascomycota;
Subphylum	Pezizomycotina;
Class	Dothideomycetes;
Order	Pleosporales;
Family	Pleosporaceae;
Genus	<i>Embellisia</i> ;
Species	<i>E. eureka</i> .

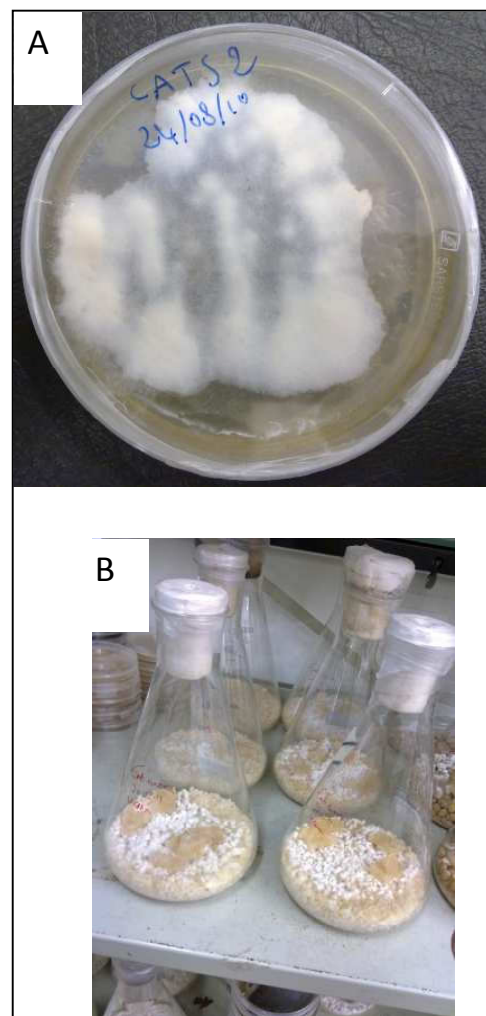
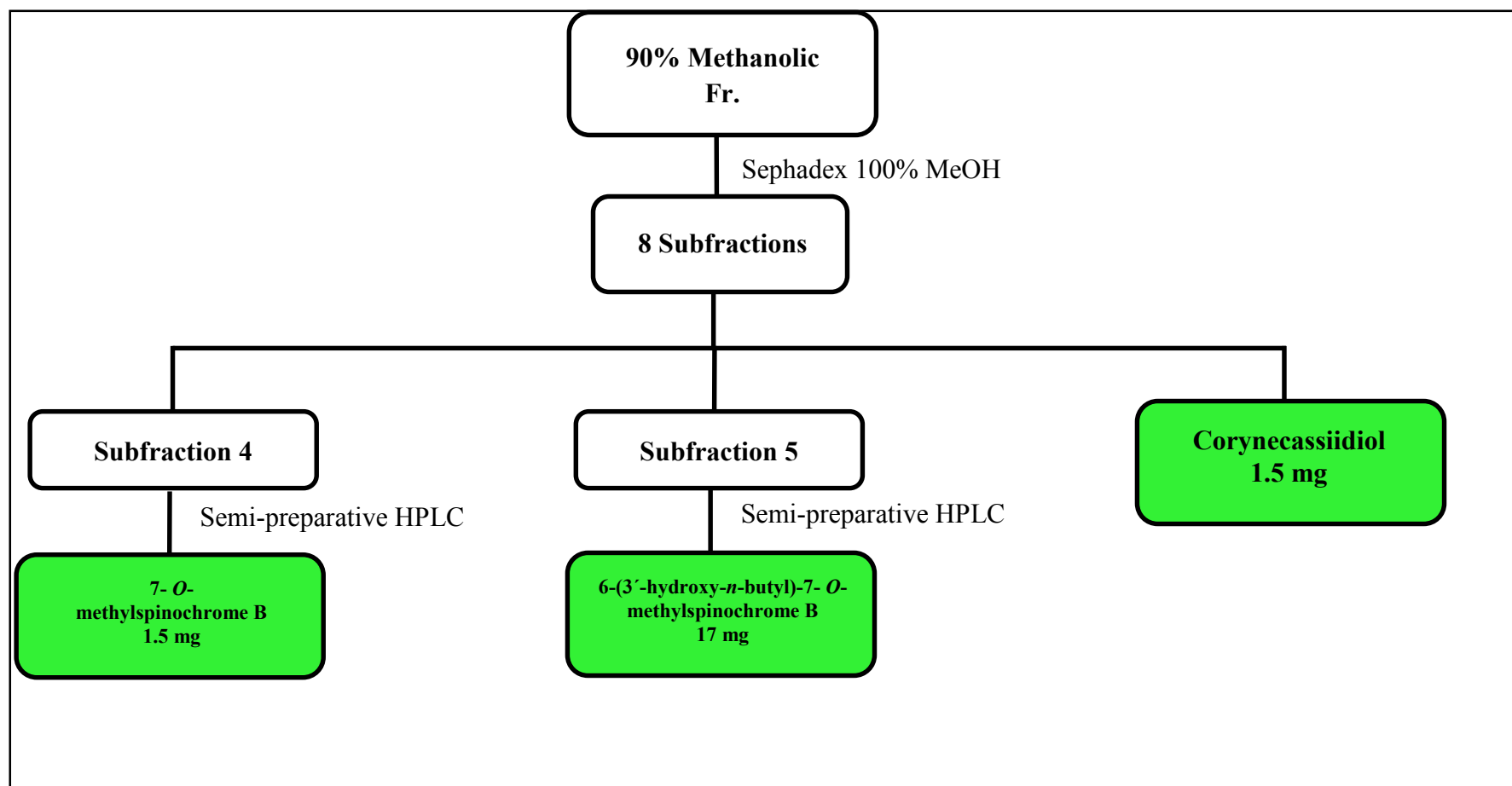


Fig. 2.7: (A: Pure strain of *Embellisia eureka* on malt agar plate B: Rice culture).

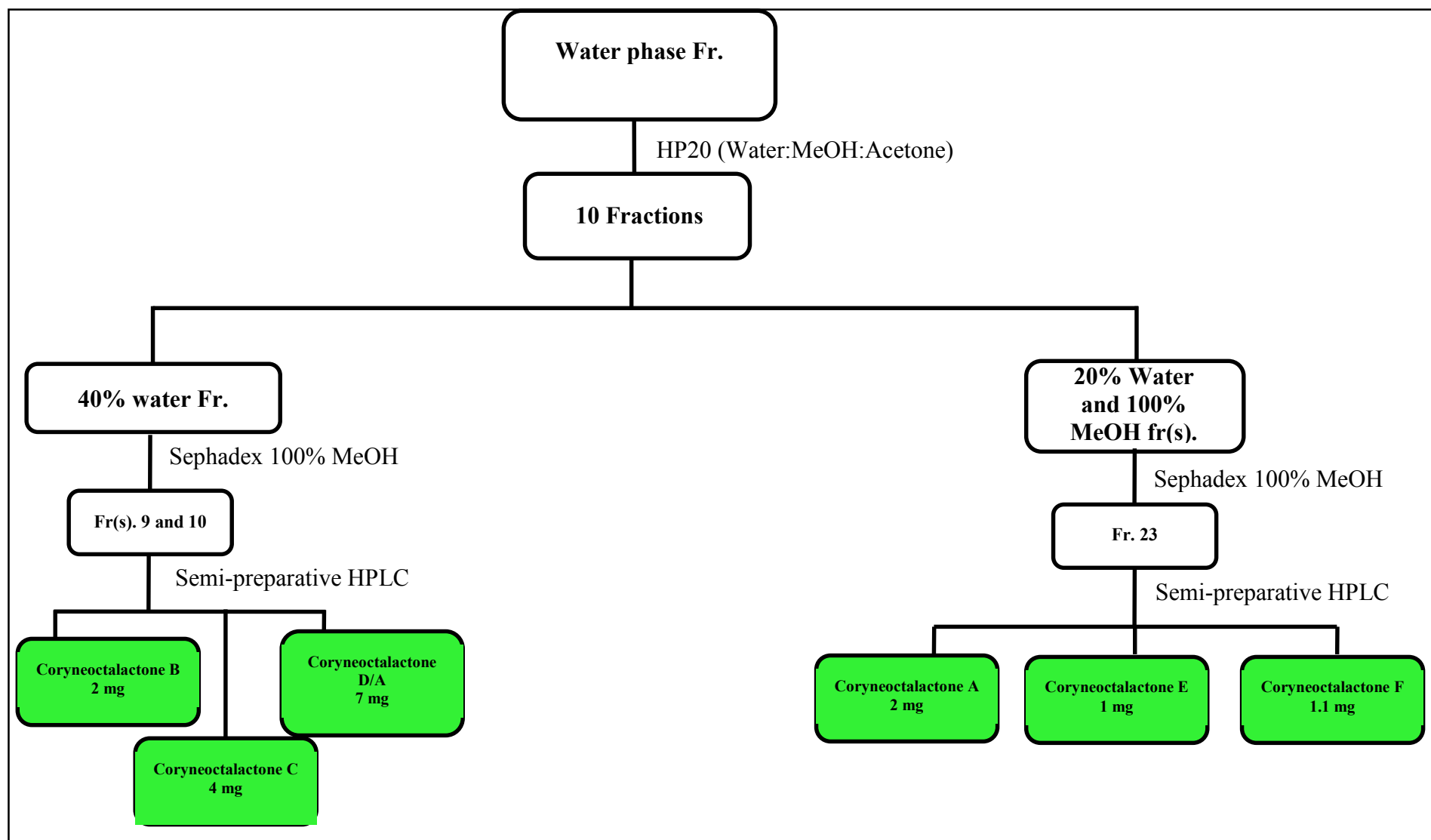
2.2.5. Isolation and purification of secondary metabolites

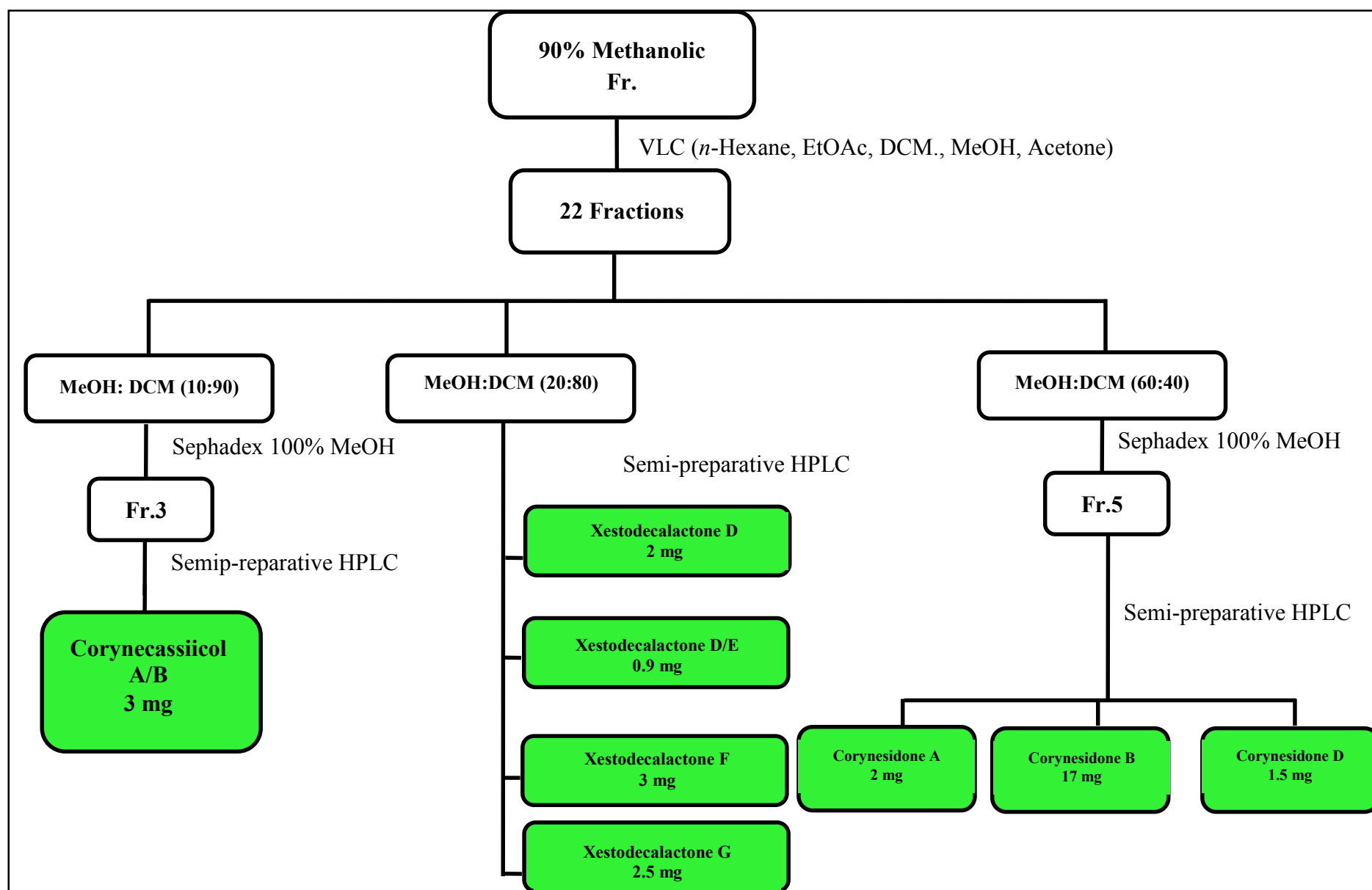
2.2.5.1. Isolation of the secondary metabolites from *Corynespora cassicola*.

2.2.5.1.1. Secondary metabolites isolated from liquid cultures of *Corynespora cassicola*

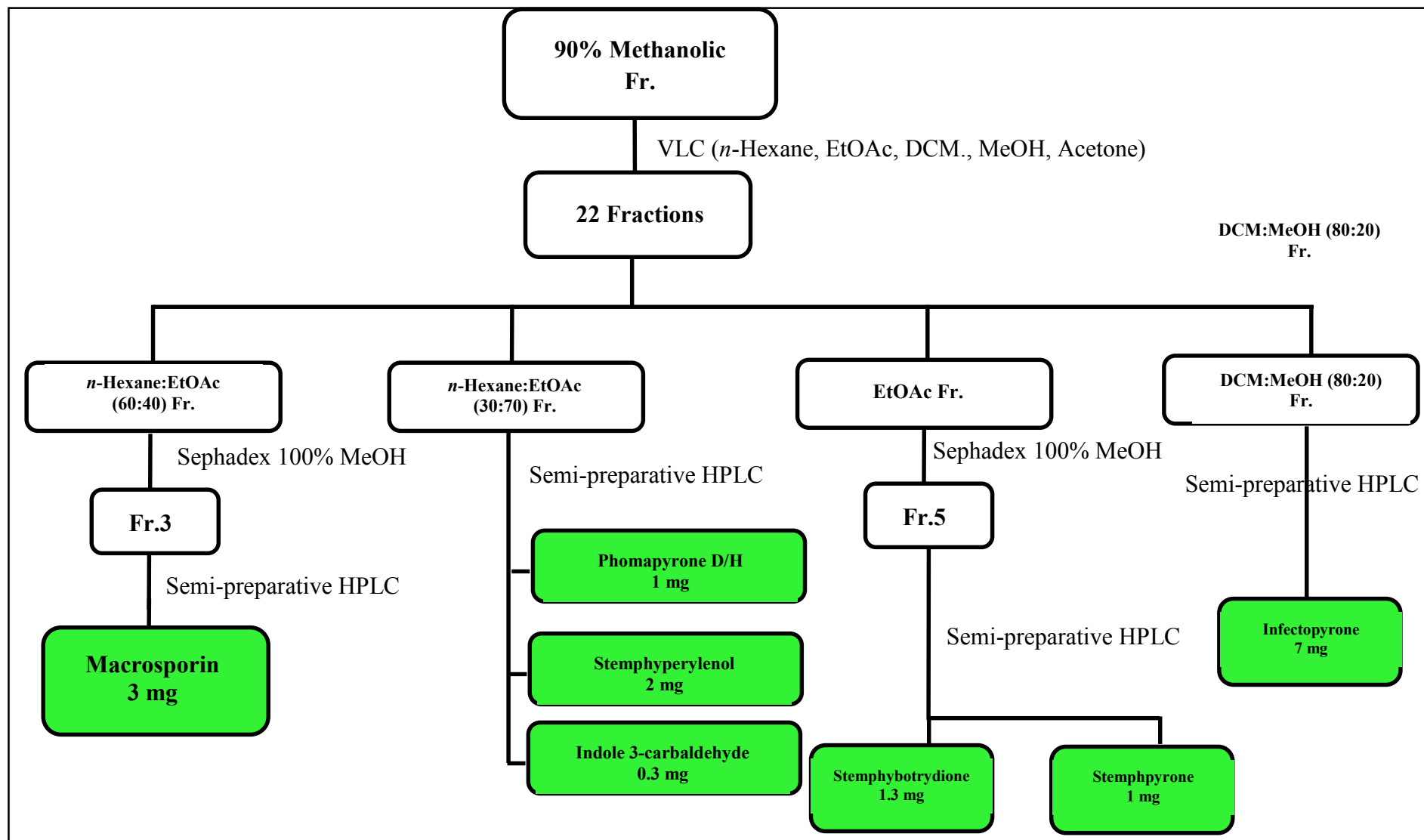


2.2.5.1.2. Secondary metabolites isolated from solid rice cultures of *Corynespora cassiicola*

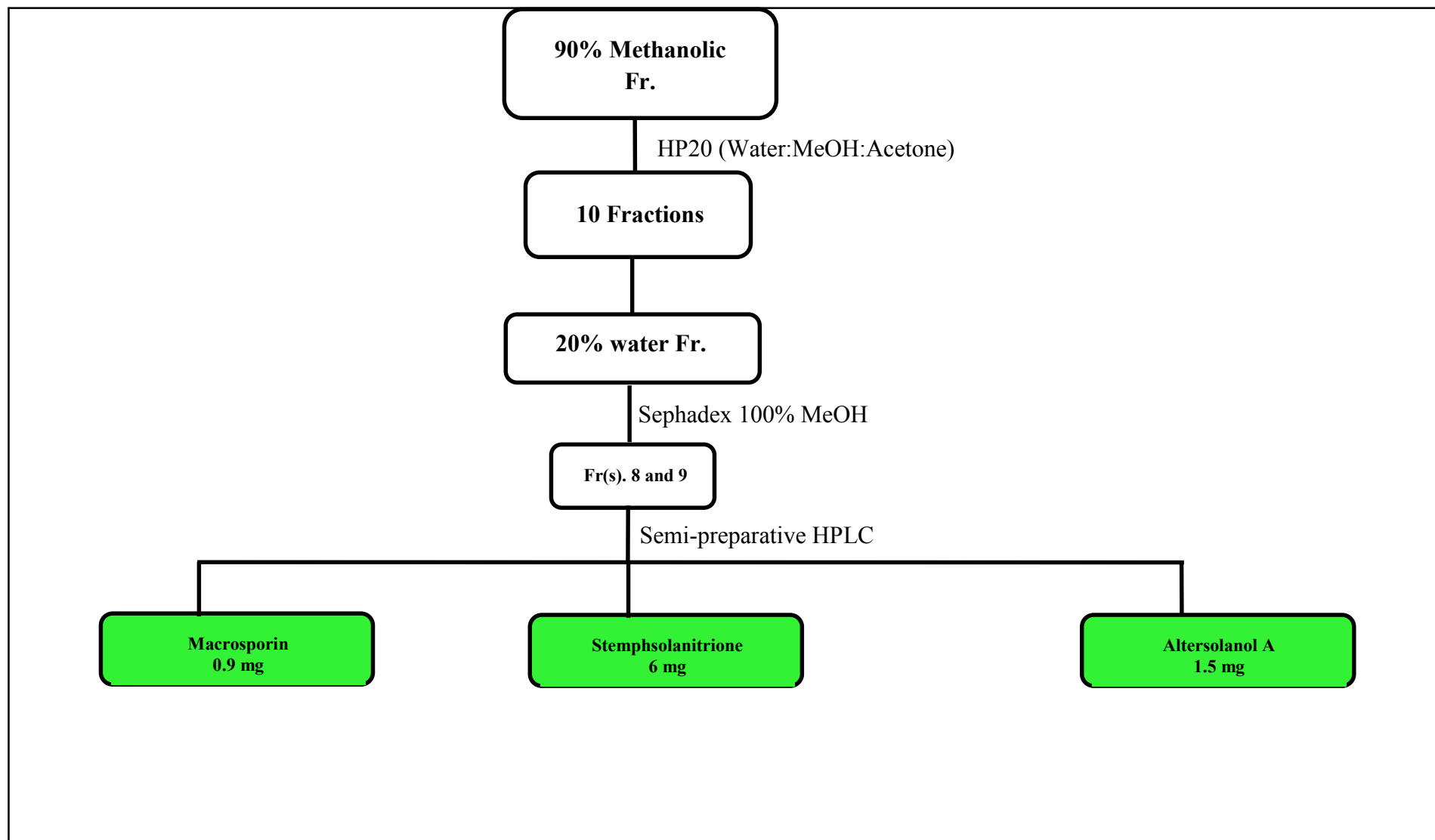




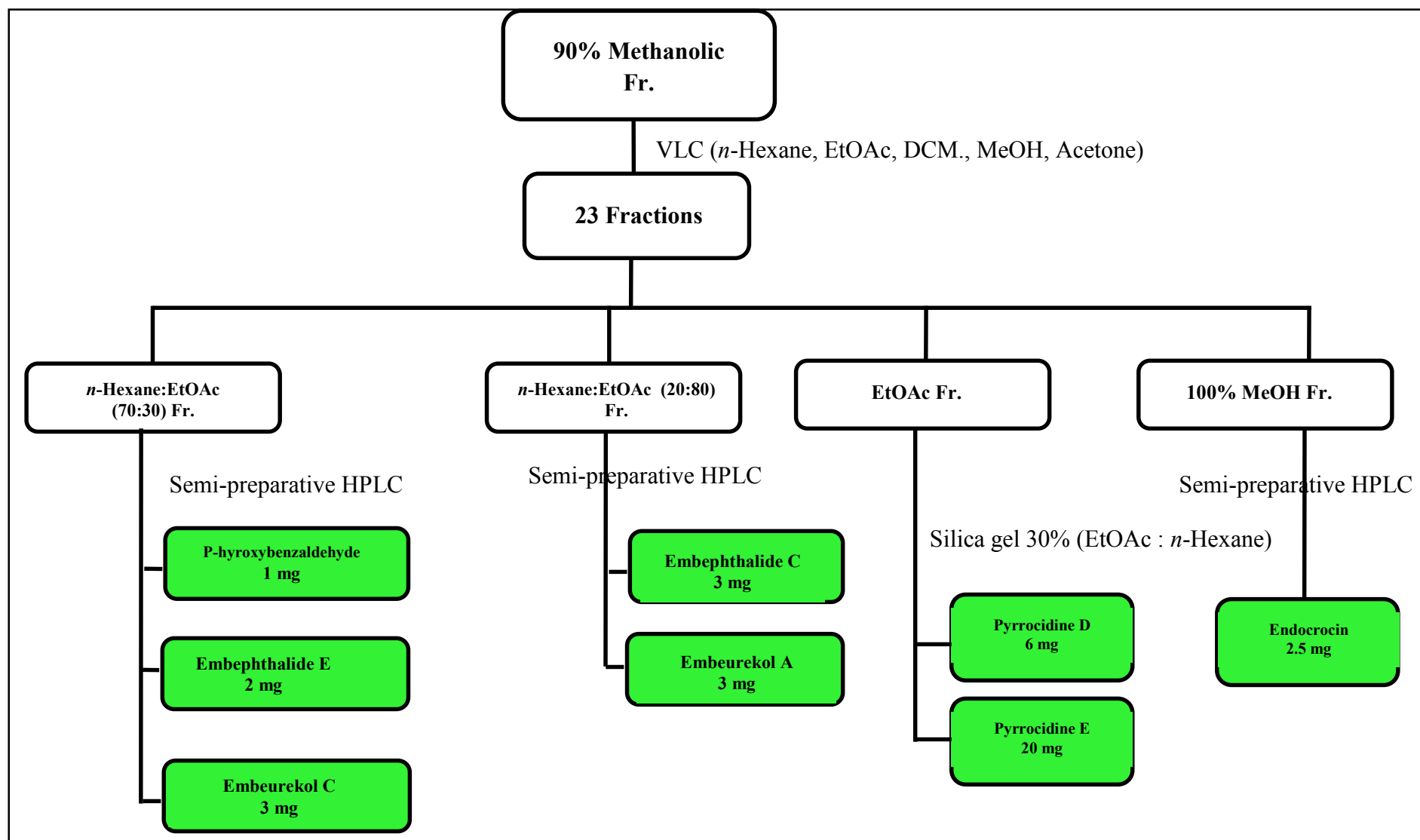
2.2.5.2. Secondary metabolites isolated from solid rice cultures of *Stemphylium botryosum*

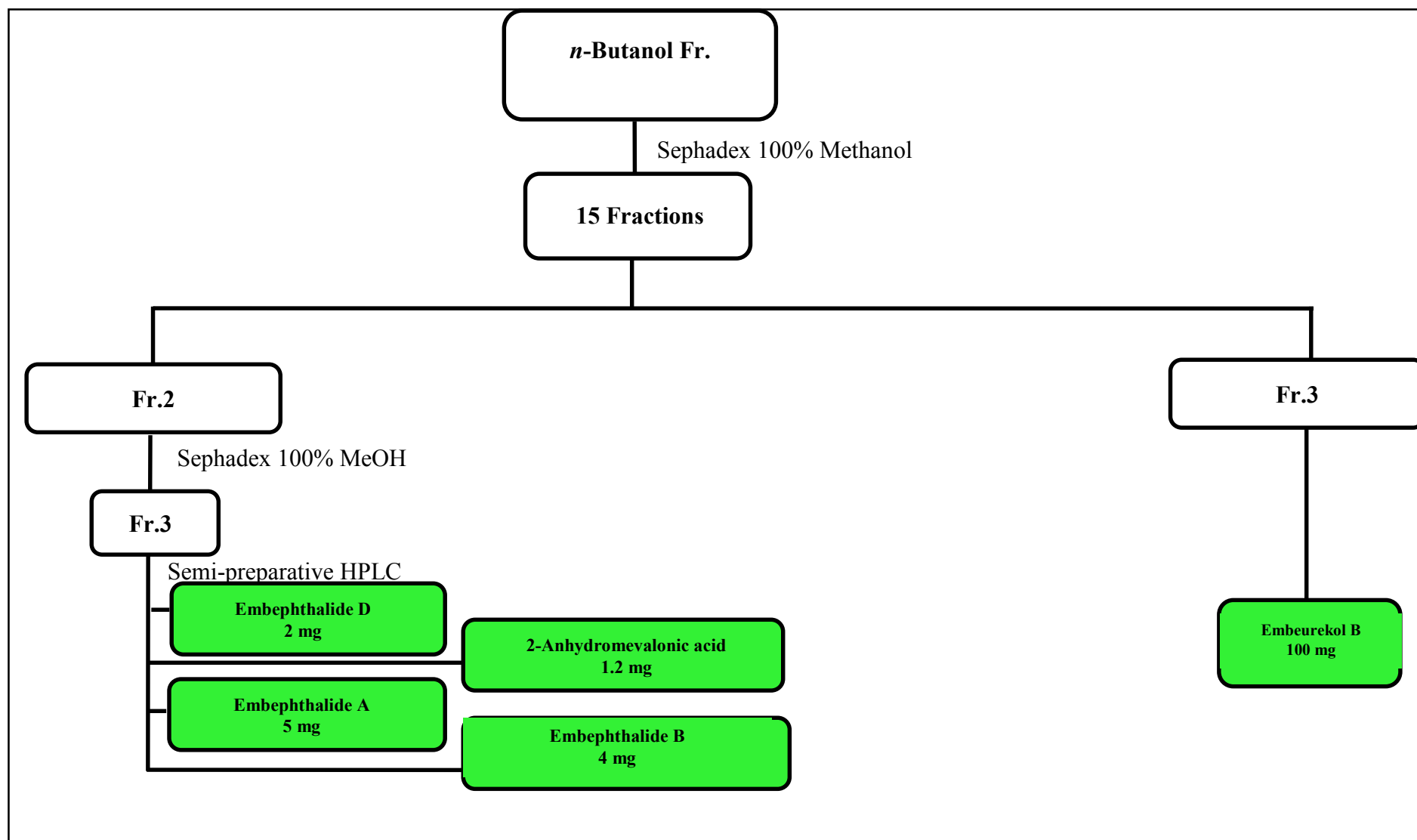


2.2.5.3. Secondary metabolites isolated from solid rice cultures of *Stemphylium Solani*



2.2.5.4. Secondary metabolites isolated from solid rice cultures of *Embellisia eureka*





2.2.5.5. Chromatographic methods for isolation

2.2.5.5.1. Thin layer chromatography (TLC)

TLC was performed on pre-coated TLC plates with silica gel 60 F₂₅₄ (layer thickness 0.2 mm, E. Merck, Darmstadt, Germany) with the following eluents:

For polar compounds	MeOH: H ₂ O (30:5:4, 30:6:5 and 30:7:6)
For semi-polar compounds	DCM:MeOH (95:5, 90:10, 85:15, 80:20 and 70:30) DCM:MeOH:EtOAc (90:10:5 and 80:20:10)
For non-polar compounds	<i>n</i> -Hexane:EtOAc (95:5, 90:10, 85:15, 80:20 and 70:30) <i>n</i> -Hexane:MeOH (95:5 and 90:10)

TLC on reversed phase RP18 F₂₅₄ (layer thickness 0.25 mm, Merck, Darmstadt, Germany) was used for polar substances and using the different solvent systems of MeOH: H₂O (90:10, 80:20, 70:30 and 60:40). The band separation on TLC was detected under UV lamp at 254 and 366 nm, followed by spraying the TLC plates with anisaldehyde/H₂SO₄ or vaniline/H₂SO₄ reagent and subsequent heating at 110 °C.

2.2.5.5.2. Vacuum liquid chromatography (VLC)

VLC apparatus consists of a 500 cm sintered glass filter funnel with an inner diameter of 12 cm. Silica gel 60 was packed to a hard cake at a height of 5-10 cm under applied vacuum. The sample used was adsorbed onto a small amount of silica gel using volatile solvents. The resulting sample mixture was then packed onto the top of the column. Using step gradient elution with non-polar solvent (e.g. *n*-Hexane or DCM) and increasing amounts of polar solvent (e.g. EtOAc or

MeOH) successive fractions were collected. The flow was produced by vacuum and the column was allowed to run dry after each fraction collected.

2.2.5.5.3. Column chromatography

Fractions derived from VLC were subjected to repeated separation through column chromatography using appropriate stationary and mobile phase solvent systems previously determined by TLC. The following separation systems were used:

- Normal phase chromatography using a polar stationary phase, typically silica gel, in conjunction with a non-polar mobile phase (e.g. *n*-Hexane, DCM) with gradually increasing amounts of a polar solvent (e.g. EtOAc or MeOH). Thus hydrophobic compounds elute more quickly than do hydrophilic compounds.
- Reversed phase (RP) chromatography using a non polar stationary phase and a polar mobile phase (e.g. H₂O, MeOH). Thus hydrophilic compounds elute more quickly than do hydrophobic compounds. Elution was performed using H₂O with gradually increasing amounts of MeOH.
- Size exclusion chromatography which is based on molecular size of compounds being analyzed. The stationary phase consists of porous beads (Sephadex LH-20). The larger compounds will be eluted first. The smaller compounds will be eluted according to their ability to exit from the small sized pores they were internalized through. Elution was performed using 100% MeOH or MeOH: DCM (1:1).
- Ion exclusion chromatography uses ion exchange resin beds (Diaion HP-20) that act as a charged solid separation medium. The components of the processed sample have different electrical affinities to this medium and are, as a result, differently retained by the resins due to these different affinities. Therefore, by elution, these components can be recovered separately at the

outlet of the resins bed. Elution was performed using H₂O with gradually increasing amounts of MeOH and acetone.

2.2.5.5.4. Preparative high pressure liquid chromatography (HPLC)

This was used for isolation and purification of compounds from fractions previously separated using column chromatographic separation. The most appropriate solvent systems were determined before running the HPLC separation. The mobile phase combination was MeOH or acetonitrile and nano-pure H₂O with or without 0.01 % TFA or 0.1% formic acid, pumped in gradient or isocratic manner depending on the compounds retention time. Each injection consisted of 20-80 mg of the fraction dissolved in 400 mL of the solvent system. The solvent system was pumped through the column at a rate of 20 mL/min. The eluted peaks were detected by the online UV detector and collected separately in Erlenmeyer flasks.

Preparative HPLC system specifications are described as follows:

Pump	Varian, PrepStar 218
Detector	Varian, ProStar 320 UV-Vis detector
HPLC Program	Varian Star (V. 6)
Column	Varian Dynamax (250 × 4.6 mm, ID and 250 × 21.4 mm, ID), pre-packed with Microsorb 60-8 C18, with integrated pre-column.

2.2.5.5.5. Semi-preparative high pressure liquid chromatography (HPLC)

This process was used for purification of compounds from fractions previously separated using column chromatographic separation. The most appropriate solvent system was determined before running the HPLC separation. The mobile phase combination was MeOH and nano-pure H₂O with or without

0.01 % TFA or 0.1 % formic acid, pumped in gradient or isocratic manner depending on the compounds retention time. Each injection consisted of 1-3 mg of the fraction dissolved in 1 mL of the solvent system. The solvent system was pumped through the column at a rate of 5 mL/min. The eluted peaks were detected by the online UV detector and collected separately in Erlenmeyer flasks. The separation column (125 × 4 mm, ID) was pre-filled with Eurospher C18 (Knauer, Berlin, Germany).

Semi-preparative HPLC system specifications are described as follows:

Pump	Merck Hitachi L-7100
Detector	Merck Hitachi UV detector L-7400
Column	Knauer (300 × 8 mm, ID), pre-packed with Eurosphere 100-10 C18, with integrated pre-column.

2.2.5.5.6. Analytical high pressure liquid chromatography (HPLC)

Analytical HPLC was used to identify the distribution of peaks either from extracts or fractions, as well as to evaluate the purity of isolated compounds. The solvent gradient used started with MeOH:nano-pure H₂O (10:90), adjusted to pH 2 with phosphoric acid, and reached to 100 % MeOH in 35 minutes. The auto-sampler injected 20 µL samples. All peaks were detected by UV-VIS photodiode array detector. In some cases, special programs were used. HPLC instrument consists of the pump, the detector, the injector, the separation column and the reservoir of mobile phase. The separation column (125 × 2 mm, ID) was pre-filled with Eurospher-100 C18 (5 µm), with integrated pre-column (Knauer, Berlin, Germany).

LC/UV system specifications are described as follows:

Pump	Dionex P580A LPG
------	------------------

Detector	Dionex Photodiode Array Detector UVD 340S
Column thermostat	STH 585
Auto-sampler	ASI-100T
HPLC program	Chromeleon (V. 6.3)
Column	Knauer (125 × 4 mm, ID), pre-packed with Eurosphere 100-5 C18, with integrated pre-column.

2.2.6. Structure elucidation of the isolated secondary metabolites

2.2.6.1. Mass spectrometry (MS)

Mass spectrometers use the difference in mass-to-charge ratio (m/z) of ionized molecules to separate them from each other. Mass spectrometry is therefore useful for quantification of atoms or molecules and also for determination of chemical and structural information of molecules. A mass spectrometer consists of an ion source, ion detector and mass-selective analyzer. The output of mass spectrometers shows a plot of relative intensity vs. the mass-to-charge ratio (m/z).

2.2.6.1.1. Electrospray ionization mass spectrometry (ESI-MS)

A mass spectrometer is an analytical instrument used to determine the molecular weight of a compound. Basically, mass spectrometers are divided into three parts; ionization source, analyzer and detector, which should be maintained under high vacuum conditions in order to maintain the ions travel through the instrument without any hindrance from air molecules. Once a sample was injected into the ionization source, the molecules are ionized. The ions were then passed and extracted into the analyzer. In the analyzer, the ions were separated according to their mass (m) to charge (z) ratio (m/z). Once the separated ions flow into the

detector, the signals are transmitted to the data system where the mass spectrum is recorded.

Liquid chromatography mass spectrometry (LC/MS)

High pressure liquid chromatography is a powerful method for the separation of complex mixtures, especially when many of the components may have similar polarities. If a mass spectrum of each component can be recorded as it elutes from the LC column, quick characterization of the components is greatly facilitated. Usually, ESI-MS is interfaced with LC to make an effective on-line LC/MS. HPLC/ESI-MS was carried out using a Finnigan LCQ-DECA mass spectrometer connected to a UV detector. The samples were dissolved in water/MeOH mixtures and injected to HPLC/ESI-MS set-up. For standard MS/MS measurements, a solvent gradient that started with acetonitrile:nano-pure H₂O (10:90), adjusted with 0.1 % HCOOH, and reached to 100 % acetonitrile in 35 minutes was used. LC/UV/MS system specifications are described as follows:

HPLC system	Agilent 1100 series (pump, detector and auto-sampler) Finnigan LC Q-DECA
MS spectrometer	Knauer, (250 × 2 mm, ID), pre-packed with Eurosphere 100-5
Column	C18, with integrated pre-column.

2.2.6.1.2. Electron impact mass spectrometry (EI-MS)

Analysis involves vaporizing a compound in an evacuated chamber and then bombarding it with electrons having 25.80 eV (2.4-7.6 MJ/mol) of energy. The high energy electron stream not only ionizes an organic molecule (requiring about 7-10 eV) but also causes extensive fragmentation (the strongest single

bonds in organic molecules have strengths of about 4 eV). The advantage is that fragmentation is extensive, giving rise to a pattern of fragment ions which can help to characterize the compound. The disadvantage is the frequent absence of a molecular ion.

Low resolution EI-MS was measured on a Finnigan MAT 8430 mass spectrometer. Measurements were done by Dr. Peter Tommes, Institut für Anorganische und Strukturchemie, Heinrich-Heine Universität, Düsseldorf.

2.2.6.1.3. Fast atom bombardment mass spectrometry (FAB-MS)

This was the first widely accepted method that employs energy sudden ionization. FAB is useful for compounds, especially polar molecules, unresponsive to either EI or CI mass spectrometry. It enables both non-volatile and high molecular weight compounds to be analyzed. In this technique, a sample is dissolved or dispersed in a polar and relatively nonvolatile liquid matrix, introduced into the source on a copper probe tip. Then, this matrix is bombarded with a beam of atoms of about 8 Kev. It uses a beam of neutral gas (Ar or Xe atoms) and both positive and negative ion FAB spectra can be obtained.

Low resolution FAB-MS was measured on a Finnigan MAT 8430 mass spectrometer. Measurements were done by Dr. Peter Tommes, Institut für Anorganische and Strukturchemie, Heinrich-Heine Universität, Düsseldorf.

2.2.6.1.4. High resolution mass spectrometry (HR-MS)

High resolution is achieved by passing the ion beam through an electrostatic analyzer before it enters the magnetic sector. In such a double focusing mass spectrometer, ion masses can be measured with an accuracy of about 1 ppm. With measurement of this accuracy, the atomic composition of the molecular ions can be determined.

HRESI-MS was measured on a Micromass Qtof 2 mass spectrometer at Helmholtz Centre for Infection Research, Braunschweig. The time-of-flight analyzer separates ions according to their mass-to-charge ratios (m/z) by measuring the time it takes for ions to travel through a field free region known as the flight.

2.2.6.2. Nuclear magnetic resonance spectroscopy (NMR)

Nuclear magnetic resonance is a phenomenon which occurs when the nuclei of certain atoms are immersed in a static magnetic field and exposed to a second oscillating magnetic field. Some nuclei experience this phenomenon, and others do not, dependent upon whether they possess a property called spin. It is used to study physical, chemical, and biological properties of matter. As a consequence, NMR spectroscopy finds applications in several areas of science. NMR spectroscopy is routinely used by chemists to study chemical structure using simple one dimensional technique. Two dimensional techniques are used to determine the structure of more complicated molecules.

NMR spectra were recorded at 300° K on a Bruker ARX-500 by Dr. Peter Tommes, Institut für Anorganische und Strukturchemie, Heinrich-Heine Universität, Düsseldorf. Some measurements were also performed at the Helmholtz Centre for Infection Research, Braunschweig, by Dr. Victor Wray using an AVANCE DMX-600 NMR spectrometer. All 1D and 2D spectra were obtained using the standard Bruker software. The samples were dissolved in different solvents, the choice of which was dependent on the solubility of the samples. Residual solvent signals were used as internal standards (reference signal). The observed chemical shift (δ) values were given in ppm and the coupling constants (J) in Hz.

2.2.6.3. Optical activity

Optically active compounds contain at least one chiral centre. Optical activity is a microscopic property of a collection of these molecules that arises from the way they interact with light. Optical rotation was determined on a Perkin-Elmer-241 MC polarimeter. The substance was stored in a 0.5 mL cuvette with 0.1 dm length. The angle of rotation was measured at the wavelength of 546 and 579 nm of a mercury vapour lamp at room temperature (25° C). The specific optical rotation was calculated using the expression:

$$[\alpha]_D^T = \frac{[\alpha]_{579} \times 3.199}{4.199 - \frac{[\alpha]_{579}}{[\alpha]_{546}}}$$

With $[\alpha]_D^T$ = the specific rotation at the wavelength of the sodium D-line, 589 nm, at certain temperature T.

$[\alpha]_{579}$ and $[\alpha]_{546}$ = the optical rotation at wavelengths 579 and 546 nm, respectively, calculated using the formula:

$$[\alpha]_\lambda = \frac{100a}{l \times c}$$

Where a = the measured angle of rotation in degrees,

l = the length in dm of the polarimeter tube,

c = the concentration of the substance expressed in g/100 mL.

2.2.6.4. Determination of absolute stereochemistry by Mosher reaction

The reaction was performed according to a modified Mosher ester procedure described by Su *et al.* (Ohtani *et al.*, 1991; Su *et al.*, 2002).

Reaction with (*R*)-(-)-a-(trifluoromethyl) phenylacetyl chloride

The compounds (1 mg of each) were transferred into NMR tubes and were dried under vacuum. Deuterated pyridine (0.5 mL) and (*R*)-MTPA chloride were added into the NMR tube immediately under a N₂ gas stream. The reagent was added in the ratio of 0.14 mM reagent to 0.10 mM of the compound (Dale and Mosher, 1973). The NMR tubes were shaken carefully to mix the samples and MTPA chloride evenly. The reaction NMR tubes were permitted to stand at room temperature and monitored by ¹H-NMR until the reaction was found to be complete. ¹H-¹H COSY was measured to confirm the assignment of the signals.

Reaction with (*S*)-MTPA chloride

Another portion of each compound (1 mg) was transferred into a NMR tube. The reaction was performed in the same manner as described before to yield the (*S*)-MTPA ester.

2.2.6.5. Computational section for CD analysis

Conformational searches were carried out by means of the Macromodel 9.7.21 software using Merck Molecular Force Field (MMFF) with implicit solvent model for chloroform. Geometry reoptimizations at B3LYP/6-31G(d) level of theory followed by TDDFT calculations using various functionals (B3LYP, BH&HLYP, PBE0) and TZVP basis set were performed by the Gaussian 03 package. Boltzmann distributions were estimated from the ZPVE corrected B3LYP/6-31G(d) energies. ECD spectra were generated as the sum of Gaussians with 3000 and 2100 cm⁻¹ half-height width (corresponding to ca. 19 and 13 nm at 250 nm, respectively), using dipole-velocity computed rotational strengths for conformers above 3%. The MOLEKEL software package was used for visualization of the results.

2.2.7. Testing the biological activity

Finding biologically important compounds from endophytic fungi is only achieved if, and when, assay systems have been devised that will allow for successful biologically guided fractionation of the culture extracts.

2.2.7.1. Antimicrobial assay

2.2.7.1.1. Agar diffusion assay

This method was used to detect the capability of a substance to inhibit the growth of microorganisms by measuring the diameter of inhibition zone around a tested compound on an agar plate. The agar diffusion assay was performed according to the Bauer-Kirby-Test (Bauer *et al.*, 1966).

Microorganisms

Crude extracts and isolated pure compounds were tested for activity against the following standard strains:

Gram-positive bacteria *Bacillus subtilis*

Gram-negative bacteria *Escherichia coli*

yeast *Saccharomyces cerevisiae*

and the fungi *Cladosporium cucumerinum*

and *C. herbarum*.

2.2.7.2. Cytotoxicity tests

2.2.7.2.1. Microculture tetrazolium (MTT) assay

Cytotoxicity tests were carried out by Prof. Dr. W. E. G. Müller, Institut für Physiologische Chemie und Pathobiochemie, University of Mainz, Mainz. The cytotoxicity was tested against L5178Y mouse lymphoma cells using the

microculture tetrazolium (MTT) assay, and compared to that of untreated controls (Carmichael, DeGraff, Gazdar, Minna, and Mitchell, 1987).

Cell cultures

L5178Y mouse lymphoma cells were grown in Eagle's minimal essential medium supplement with 10% horse serum in roller tube culture. The medium contained 100 units/mL penicillin and 100 µg/mL streptomycin. The cells were maintained in a humidified atmosphere at 37° C with 5% CO₂.

MTT colorimetric assay

Of the test samples, stock solutions in ethanol 96% (v/v) were prepared. Exponentially growing cells were harvested, counted and diluted appropriately. Of the cell suspension, 50 µL containing 3750 cells were pipetted into 96-well microtiter plates. Subsequently, 50 µL of a solution of the test samples containing the appropriate concentration was added to each well. The concentration range was 3 and 10 µg/mL. The small amount of ethanol present in the wells did not affect the experiments. The test plates were incubated at 37° C with 5% CO₂ for 72 h. A solution of 3-(4,5-dimethylthiazol-2-yl)-2,5-diphenyltetrazolium bromide (MTT) was prepared at 5 mg/mL in phosphate buffered saline (PBS; 1.5 mM KH₂PO₄, 6.5 mM Na₂HPO₄, 137 mM NaCl, 2.7 mM KCl; pH 7.4) and from this solution, 20 µL was pipetted into each well. The yellow MTT penetrates the healthy living cells and in the presence of mitochondrial dehydrogenases, MTT is transformed to its blue formazan complex. After an incubation period of 3h 45 min at 37° C in a humidified incubator with 5% CO₂, the medium was centrifuged (15 min, 20 °C, 210 x g) with 200 µL DMSO, the cells were lysed to liberate the formed formazan product. After thorough mixing, the absorbance was measured at 520 nm using a scanning microliter-well spectrophotometer. The color intensity is correlated with the number of healthy living cells. Cell survival was calculated using the

formula:

$$\text{Survival \%} = 100 \times \frac{\text{Absorbance of treated cells} - \text{absorbance of culture medium}}{\text{Absorbance of untreated cells} - \text{absorbance of culture medium}}$$

All experiments were carried out in triplicates and repeated three times. As controls, media with 0.1% EGMME/DMSO were included in the experiments.

2.2.7.2.2. MTT cell viability assays

Cytotoxicity tests were carried out by Prof. Dr. M. U. Kassack, Institut für Pharmazeutische und Medizinische Chemie, Heinrich-Heine University, Düsseldorf.

Materials, cell lines and cell culture

The human ovarian carcinoma cell line A2780 (A2780 sens) was obtained from European Collection of Cell Cultures (ECACC, Salisbury, UK). A2780 cells were exposed to weekly cycles of 2 µmol/L cisplatin over a period of 24 weeks. Cisplatin-resistant cells were denoted A2780 CisR. The human chronic myelogenous leukemia cell line K562 was obtained from the German Collection of Microorganisms and Cell Cultures (DSMZ, Germany). All other reagents were supplied by Sigma Chemicals unless otherwise stated.

All cell lines were grown at 37 °C under humidified air supplemented with 5% CO₂ in RPMI 1640 (PAN Biotech, Germany) containing 10% fetal calf serum (PAN Biotech, Germany), 100 IU/mL penicillin and 100 µg/mL streptomycin. The cells were grown to 80% confluency before using them for the MTT cell viability assay.

MTT cell viability assays

The rate of cell-survival under the action of test substances was evaluated by an improved MTT assay (Müller *et al.* 2004). The assay is based on the ability of viable cells to metabolize yellow 3-(4,5-dimethylthiazol-2-yl)-2,5-diphenyl

tetrazolium bromide (MTT, Applichem, Germany) to violet formazane crystals that can be detected spectrophotometrically. In brief, A2780 cells were seeded at a density of 8.000 cells/well and K562 at a density of 30,000 cells/well in 96well plates (Corning, Germany). After 24 h, cells were exposed to the test compounds at concentrations of 10^{-5} M and 10^{-4} M. Incubation was stopped after 72 h and cell survival was determined by addition of MTT solution (5 mg/mL in phosphate buffered saline). The formazan precipitate was dissolved in DMSO. Absorbance was measured at 544 nm and 620 nm in a FLUOstar microplate-reader (BMG LabTech, Offenburg, Germany). The absorbance of untreated control cells was taken as 100% viability. All tests were performed in triplicate.

2.2.7.2.3. Protein kinase assay

Protein kinase assays were carried out by Dr. Michael Kubbutat (ProKinase GmbH, Freiburg, Germany).

Protein kinase enzymes are integral components of numerous signal transduction pathways involved in the regulation of cell growth, differentiation, and response to changes in the extracellular environment. Consequently, kinases are major targets for potentially developing novel drugs to treat diseases such as cancer and various inflammatory disorders.

The inhibitory potency of the samples was determined using 24 protein kinases (see Table 2.2). The IC_{50} profile of compounds/fractions showing an inhibitory potency of $\geq 40\%$ with at least one of the 24 kinases at an assay concentration of 1×10^{-6} g/mL was determined. IC_{50} values were measured by testing 10 concentrations of each sample in singlicate ($n=1$).

Sample preparation

The compounds/fractions were provided as 1×10^{-3} g/mL stock solutions in 100% DMSO (1000 or 500 μ L) in micronic boxes. The boxes stored at -20° C. Prior to the assays, 100 μ L of the stock solutions were transferred into

separate microtiter plates. Subsequently, they were subjected to serial, semi-logarithmic dilution using 100% DMSO as a solvent resulting in 10 different concentrations. 100% DMSO was used as control. Subsequently, $7 \times 5 \mu\text{L}$ of each concentration were aliquoted and diluted with $45 \mu\text{L}$ H_2O only a few minutes before the transfer into the assay plate to minimize precipitation. The plates were shaken thoroughly and then used for the transfer of $5 \mu\text{L}$ compound solution into the assay plates.

Recombinant protein kinases

All protein kinases were expressed in Sf9 insect cells as human recombinant GST-fusion proteins or His-tagged proteins by means of the baculovirus expression system. Kinases were purified by affinity chromatography using either GSH-agarose (Sigma) or NiNTH-agarose (Qiagen). Purity was checked by SDS-PAGE/silver staining and the identity of each kinase was verified by western blot analysis with kinase specific antibodies or by mass spectrometry.

Protein kinase assay

A proprietary protein kinase assay (33PanKinase[®] Activity Assay) was used for measuring the kinase activity of the protein kinases. All kinase assays were performed in 96- well Flash Plates[™] from Perkin Elmer/NEN (Boston, MA, USA) in a $50 \mu\text{L}$ reaction volume. The reaction mixture was pipetted in the following order: $20 \mu\text{L}$ assay buffer, $5 \mu\text{L}$ ATP solution in H_2O , $5 \mu\text{L}$ test compound in 10% DMSO and $10 \mu\text{L}$ substrate/ $10 \mu\text{L}$ enzyme solution (premixed). The assay for all enzymes contained 60 mM HEPES-NaOH (pH 7.5), 3 mM MgCl_2 , 3mM MnCl_2 , 3 pM Na-orthovanadate, 1.2 mM DTT, 50 pg/mL PEG20000, 1 pM [γ - ^{33}P]-ATP. The reaction mixtures were incubated at 30°C for 80 minutes and stopped with $50 \mu\text{L}$ 2% (v/v) H_3PO_4 . The plates were aspirated and washed two times with $200 \mu\text{L}$ of 0.9% (w/v) NaCl or $200 \mu\text{L}$ H_2O . Incorporation of ^{33}Pi was determined with a microplate scintillation

counter (Microbeta Trilux, Wallac). All assays were performed with a Beckman Coulter/Sagian robotic system.

Table 2.2: List of Protein kinases and their substrates

Family	Kinase	Substrate	Oncologically relevant mechanism	Disease
Serine/threonine kinases	AKT1/PKB Alpha*	GSC3 (14-27)	Apoptosis	Gastric cancer (Staal, 1987)
	ARK5*	Autophos.	Apoptosis	Colorectal cancer (Kusakai <i>et al.</i> , 2004)
	Aurora A	Tetra(LRRWSLG)	Proliferation	Pancreatic cancer (Li <i>et al.</i> , 2003)
	Aurora B*	Tetra(LRRWSLG)	Proliferation	Breast cancer (Keen and Tylor 2004)
	CDK2/cyclin A	Histone H1	Proliferation	Pancreatic cancer (Iseki <i>et al.</i> , 1998)
	CDK4/cyclin D1	Rb-CTF	Proliferation	Breast cancer (Yu <i>et al.</i> , 2006)
	CK2-alpha1	P53-CTM	Proliferation	Rahbdomyosarcoma (Izeradjene <i>et al.</i> , 2004)
	COT	Autophos.	Proliferation	Breast cancer (Sourvinos , 1999)
	PLK-1*	Casein	Proliferation	Prostate cancer (Weichert <i>et al.</i> , 2004)
	B-RAF-VE	MEK1-KM	Proliferation	Thyroid cancer (Ouyang <i>et al.</i> , 2006)
	SAK	Autophos.	Proliferation	Colorectal cancer (Macmillan <i>et al.</i> , 2001)
	MEK1 wt*	ERK2-KR	Apoptosis	Multiple cancers (Ryan <i>et al.</i> , 2000)
	NEK2*	RB-CTF	Apoptosis	Ewing's tumors & B cell lymphoma (Schultz <i>et al.</i> , 1994)
	NEK6*	GSK3(14-27)	Apoptosis	Multiple cancers (Li <i>et al.</i> , 2003)
	PIM1*	GSK3(14-27)	Apoptosis	prostate cancer (Dhanasekaran <i>et al.</i> , 2001)
	PRK1*	RB-CHKtide	Proliferation	Prostate cancer (Manser <i>et al.</i> , 1994)

Family	Kinase	Substrate	Oncologically relevant mechanism	Disease
Receptor tyrosine kinase	EGFR	Poly(glu,Tyr) _{4:1}	Proliferation	Glioblastoma multiforme (National Cancer Institute, 2005)
	EPHB4	Poly(glu,Tyr) _{4:1}	Angiogenesis	Prostate cancer (Xia <i>et al.</i> , 2005)
	ERBB2	Poly(glu,Tyr) _{4:1}	Proliferation	Gastric carcinoma (Lee <i>et al.</i> , 2005)
	FLT3	Poly(Ala,glu,Lys,Tyr) _{6:2:4:1}	Proliferation	Leukemia (Menezes <i>et al.</i> , 2005)
	IGF1-R [*]	Poly(glu,Tyr) _{4:1}	Apoptosis	Breast cancer (Zhang and Yee 2000)
	INS-R	Poly(Ala,glu,Lys,Tyr) _{6:2:4:1}	``counter kinase``	Ovarian cancer (Kalli <i>et al.</i> , 2002)
	MET wt [*]	Poly(Ala,glu,Lys,Tyr) _{6:2:4:1}	Metastasis	Lung cancer (Qiao <i>et al.</i> , 2002)
	PDGFR-beta	Poly(Ala,glu,Lys,Tyr) _{6:2:4:1}	Proliferation	Prostate cancer (Hofer <i>et al.</i> , 2004)
	TIE-2	Poly(glu,Tyr) _{4:1}	Angiogenesis	Rheumatoid arthritis (DeBusk <i>et al.</i> , 2003)
	VEGF-R2 [*]	Poly(glu,Tyr) _{4:1}	Angiogenesis	Pancreatic cancer (Li <i>et al.</i> , 2003)
	VEGF-R3	Poly(glu,Tyr) _{4:1}	Angiogenesis	Breast cancer (Garces <i>et al.</i> , 2006)
	ALK [*]	poly(Glu,Tyr) _{4:1}	Apoptosis	anaplastic large-cell lymphoma (Morris <i>et al.</i> , 1994)
	AXL [*]	poly(Glu,Tyr) _{4:1}	Proliferation	Ovarian, gastric and breast cancer (Liu <i>et al.</i> , 1988)

Soluble tyrosine kinase	FAK*	Poly(glu,Tyr) _{4:1}	Metastasis	Breast cancer (Schmitz <i>et al.</i> , 2005)
	SRC*	Poly(glu,Tyr) _{4:1}	Metastasis	Colon cancer (Dehm <i>et al.</i> , 2001)

* Protein kinases involved in the present study.

2.2.7.2.4. Soft agar assay

To measure the impact of compounds on the transformed status of cells, 96 well suspension cell culture plates were prepared as follows: 100 µL of the soft agar bottom layer (0.6% final concentration in complete medium) was poured and left to solidify. 50 µL of the soft agar top layer (0.4% final concentration) containing 2.500 A549 or HCT116 cells were then added on top, solidified and such 96 well plates incubated at 37°C, 10% CO₂. Next day, compounds were added at indicated final concentrations. The assay was developed 7 days after seeding of cells. Staurosporine at 1E-5M was used as low control, 0.1% DMSO as high control.

2.2.7.2.5. PBMC cytotoxicity assay

To measure the impact of compounds on the viability of peripheral blood mononuclear cells, frozen PBMC kept in liquid nitrogen were thawed and 96-wellplates seeded with 120.000 PBMC/well in 150 µL complete medium (termed cellplate). Outer wells are not used and filled with medium alone. Viability of PBMC is determined by Trypan Blue in a Neubauer counting chamber and should exceed 90%. 10 µL of the predilution-plate are added to cell-plate and incubation takes place at 37°C at 10% CO₂. Subsequently 10 µL Alamar Blue reagent is added and measurement of fluorescence at 590 nm after 5h incubation at 37°C, 5% CO₂. Staurosporine at 1E-5M was used as low control, 0.1% DMSO as high control.

2.2.7.2.6. ORIS migration assay

To measure the impact of compounds on the migration of cells, confluent A375 or MDA MB231 were harvested with Accutase and seeded with a multichannel-pipette (40.000 in 100 μ L /well) on a Collagen I-precoated ORIS-96 well plate. 24h later, stopper inserts were removed except for controls (high control: 0.1% DMSO. Low control: remaining stopper insert). Medium was removed and exchanged for 100 μ L compound containing medium from the Compound-predilution plate. Again 1 $\frac{1}{2}$ days later control stopper inserts were removed, and 75 μ L DMEM w/o Phenolred containing Calcein-AM (5 μ g/mL) was added for 10 min at 37°C. Finally fluorescent cells in the insert-defined area were detected by Fluostar (BMG) with FITC-settings (Ex:485 nm/ Ex:520 nm). Subsequently fluorescence photos were taken.

2.2.7.2.7. Angiogenesis assay

The assay was pursued in modification of the originally published protocol (Korff and Augustin, 1999). In brief, spheroids were prepared as previously described (Korff and Augustin, 1998) by pipetting 500 HUVEC in a hanging drop on plastic dishes to allow overnight spheroid aggregation. Fifty HUVEC spheroids were then seeded in 0.9 mL of a collagen gel and pipetted into individual wells of a 24 well plate to allow polymerization. The test compounds in combination with VEGF-A [25 ng/mL final assay concentration] were added after 30 min by pipetting 100 μ L of a 10-fold concentrated working dilution on top of the polymerized gel. Plates were incubated at 37°C for 24 h and fixed by adding 4% paraformaldehyde. Sprouting intensity of HUVEC spheroids treated with the test compounds were scanned under the microscope by two independent observers for changes compared to VEGF-A control and documented. Sprouting intensity of HUVEC spheroids treated with the identified inhibitors and stimulators or sunitinib were quantified by an image analysis system determining the cumulative sprout length per spheroid using an inverted

microscope and the digital imaging software Analysis 3.2 (Soft imaging system, Münster, Germany). The mean of the cumulative sprout length of 10 randomly selected spheroids was analyzed as an individual data point. To determine IC₅₀ values, seven concentrations (10 µM to 10 nM) of each compound were tested in singlicate and the calculations were performed using GraphPad Prism version 5.02 software.

2.2.8. General laboratory equipments

Autoclave	Varioklav, H&P
Balances	Mettler 200, Mettler AT 250, Mettler PE 1600, Sartorius MC1 AC210S Biofuge pico, Heraeus
Centrifuge	Biofugr pico, Heraeus
Cleanbench	HERAsafe, Heraeus
Digital pH meter	420Aplus, Orion
Drying Ovens	Kelvitron t, Heraeus
Fraction collector	Cygnet, ISCO
Freeze dryer	Lyovac GT2, Steris
- 80 °C Freezer	Forma Scientific, 86-Freezer
Hot plate	Camag
Magnetic stirrer	Combi Mag, IKA
Rotary evaporator	Vacuubrand, IKA
Sonicator	Sonorex RK 102, Bandelin
Syringes	Hamilton
Ultra Turrax	T18 basic, IKA

| *Materials and Methods*

UV Lamp Camag (254 and 366)

Vacuum centrifuge SpeedVac SPD 111V, Savant

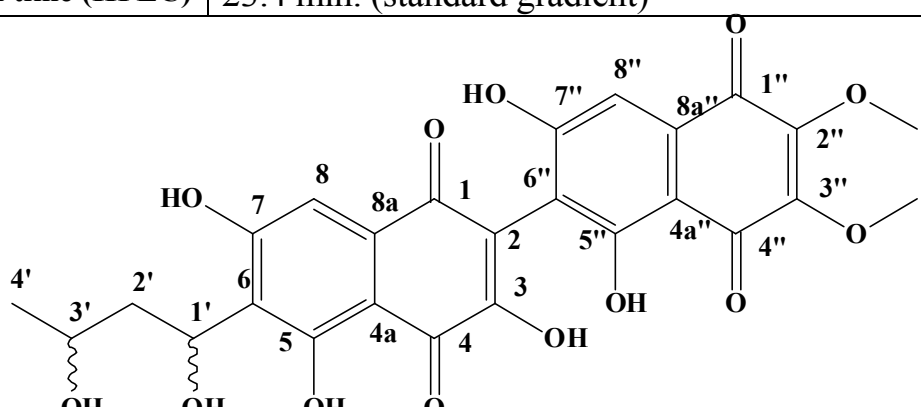
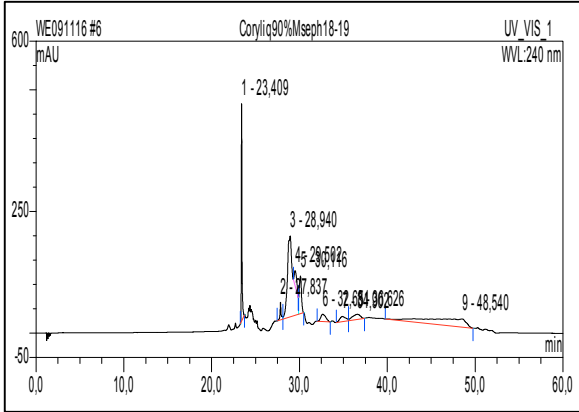
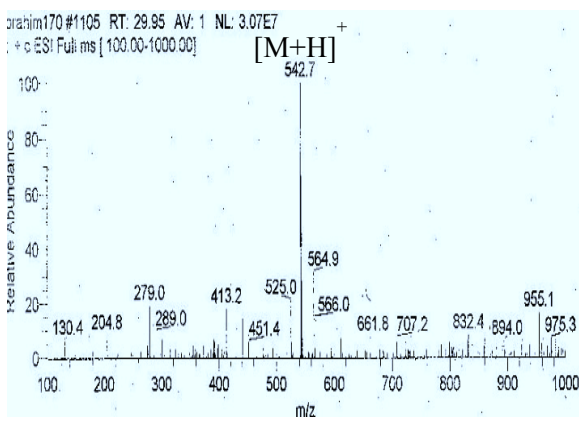
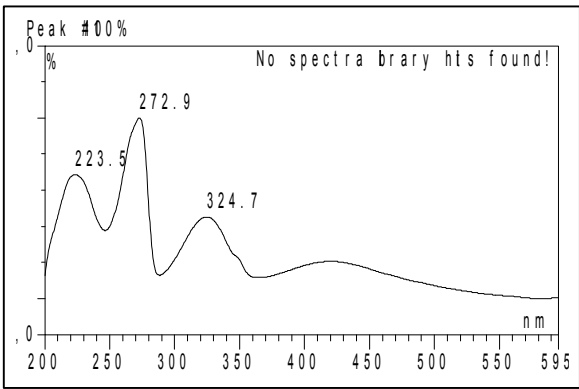
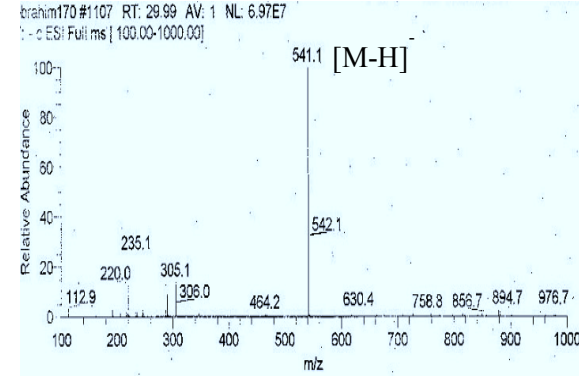
3. Results

3.1. Compounds isolated from the endophytic fungus *Corynespora cassiicola* isolated from the Mangrove plant *Laguncularia racemosa*

This endophytic fungal strain of the genus *Corynespora* was isolated from leaves of *Laguncularia racemosa* growing in China. The pure fungal strain was cultivated in liquid Wickerham medium and on rice solid medium. Interestingly, chemical screening studies indicated a clear difference between *Corynespora* extracts obtained from liquid Wickerham medium and rice cultures. Comparison of the HPLC chromatograms of the EtOAc extracts of both cultures showed a different chemical pattern. Three compounds were isolated from the liquid Wickerham medium; corynecassiidiol (**1**), 6-(3'-hydroxy-*n*-butyl)-7-*O*-methyl spinochrome B (**2**) and 7-*O*-methyl spinochrome B (**3**). Fifteen compounds were isolated from the solid rice cultures; coryneoctalactone A (**4**), coryneoctalactone B (**5**), coryneoctalactone C (**6**), coryneoctalactone D/A (**7/4**), coryneoctalactone E (**8**), coryneoctalactone F (**9**), corynesidone A (**10**), corynesidone B (**11**), corynesidone D (**12**), xestodecalactone D (**13**), xestodecalactone D/E (**14/3**), xestodecalactone F (**15**), xestodecalactone G (**16**) and corynecassiicol A/B (**17**, **18**). Moreover, extracts obtained from solid cultures were subjected to some preliminary biological screening assays, i.e. antibacterial, antifungal and cytotoxicity assays. Interestingly, extracts obtained from rice cultures showed cytotoxic activity.

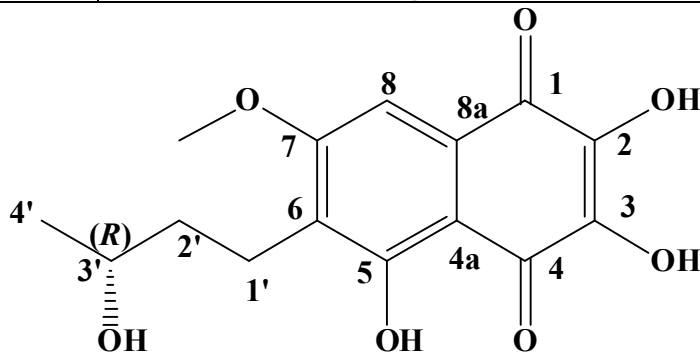
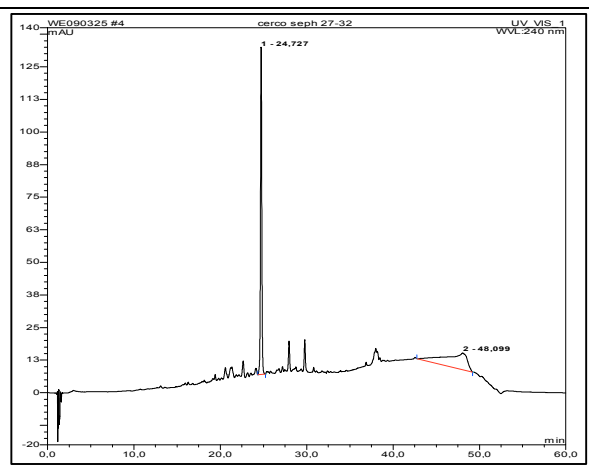
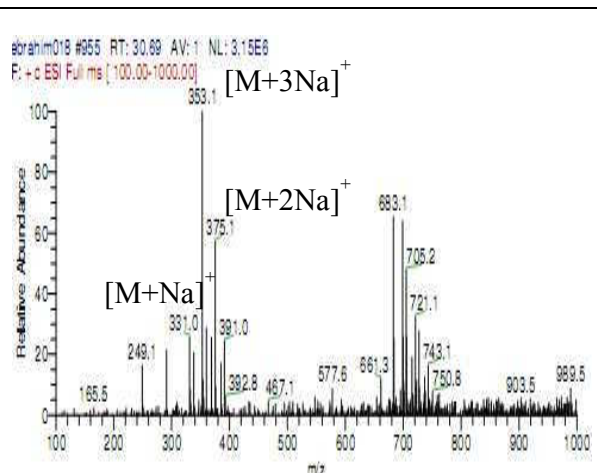
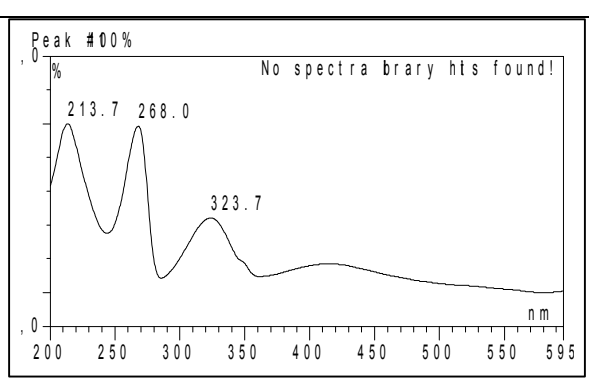
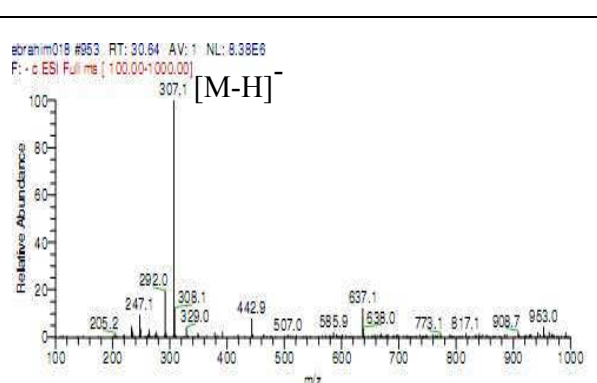
In this part of the investigation results on the natural products produced by *Corynespora cassiicola* when grown in liquid Wickerham medium and on solid rice medium are presented.

3.1.1. Corynecassiidiol (1, new compound)

Corynecassiidiol	
Synonym(s)	6-(1,3-dihydroxybutyl)-1',3,3',5,7-pentahydroxy-6',7'-dimethoxy-[2,2'-binaphthalene]-1,4,5',8'-tetraone
Sample code	Coryliqseph1819
Biological source	<i>Corynespora cassiicola</i>
Sample amount	1.5 mg
Physical properties	reddish amorphous solid
Molecular formula	C ₂₆ H ₂₂ O ₁₃
Molecular weight	542 g/mol
Optical rotation $[\alpha]_D^{20}$	+0.4 (c 0.00635, MeOH)
Retention time (HPLC)	23.4 min. (standard gradient)
	
	
	

Corynecassiidiol (**1**) was isolated from the EtOAc extract of liquid cultures of *Corynespora cassiicola* as reddish amorphous solid (1.5 mg). It showed UV absorbance maxima at λ_{max} (MeOH) 223.5, 272.9 and 324.7 nm. Positive and negative ESI-MS showed molecular ion peaks at m/z 542.7 $[\text{M}+\text{H}]^+$ (base peak) and m/z 541.1 $[\text{M}-\text{H}]^-$ (base peak), respectively, indicating a molecular weight of 542 g/mol. The molecular formula $\text{C}_{26}\text{H}_{22}\text{O}_{13}$ (calculated 543.1139, Δ 0.0013) was obtained from HRESI-MS, which exhibited a strong peak at m/z 543.1152 $[\text{M}+\text{H}]^+$. The UV and NMR data suggested that **1** is a dimer of two different naphthoquinone units. Structural elucidation of **1** was based on results of 1D and 2D NMR spectral analysis including ^1H NMR, ^1H - ^1H COSY and HMBC spectra (Table 3.1) as well as on comparison of the NMR data with known naphthoquinones units (Chimura *et al.*, 1973; Assante *et al.*, 1977). This indicated the presence of two aromatic singlets 8 and 8'' appearing at δ_{H} 7.01 ppm and 7.04 ppm, respectively, a doublet at δ_{H} 1.18 ppm ($J=6.3$ Hz) attributed to 4'-Me, two singlets at δ_{H} 3.92 ppm and 3.93 ppm for 2''-OMe and 3''-OMe respectively, two multiplets at δ_{H} 2.27 ppm and 2.55 ppm for H-2' A and B, respectively, a multiplet at δ_{H} 3.76 ppm for H-3' and a triplet at δ_{H} 5.27 ppm ($J=7.5$ Hz) for H-1'. Inspection of COSY spectrum revealed a continuous spin system starting from 4'-Me at δ_{H} 1.18 ppm to H-1' at δ_{H} 5.27 ppm. The attachment of the side chain at position 6 was confirmed by HMBC correlation of H-1' to C-7 (Table 3.1). The attachment of the two methoxy groups at δ_{H} 3.92 and 3.93 ppm to positions 2'' and 3'' is confirmed also through HMBC correlations as well as by a NOE experiment as the methoxy group showed no effect on the aromatic protons. Moreover, HMBC indicated correlations of H-8 at δ_{H} 7.01 ppm to C-1 and C-7 and of H-8'' at δ_{H} 7.04 ppm to C-4'' and C-6''. Thus compound **1** was then identified as a new natural product corynecassiidiol. Unfortunately, the absolute stereochemistry of the side chain at C-1' and C-3' was not detected due to the small amount of the compound and compound **1** could be a racemate and this is clear from $[\alpha]_{\text{D}}$.

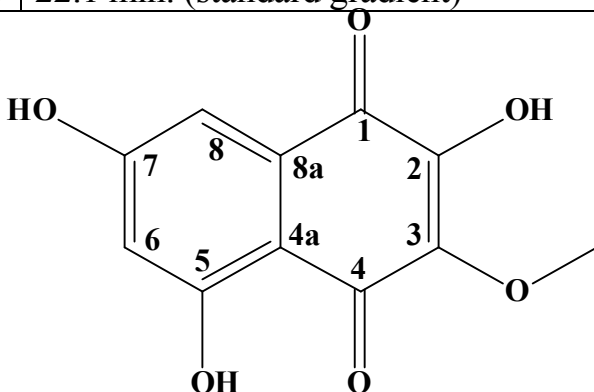
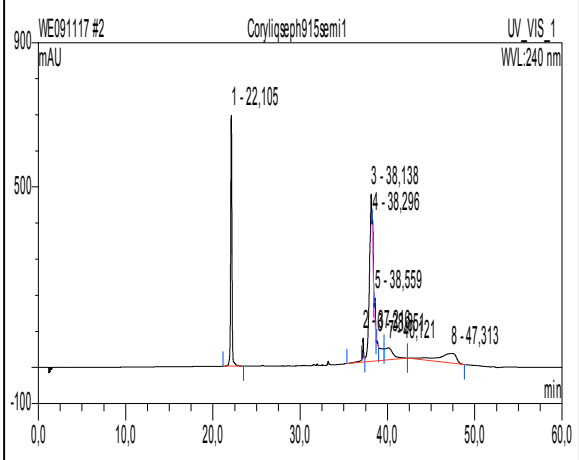
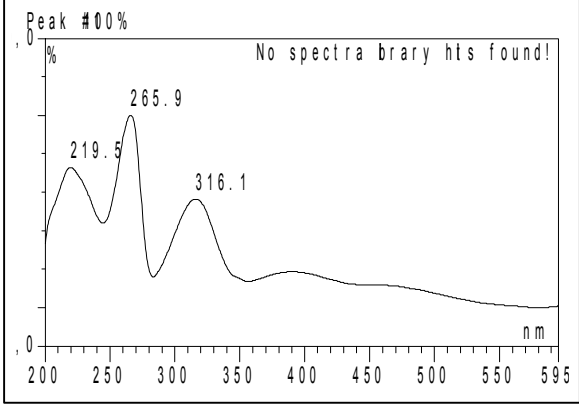
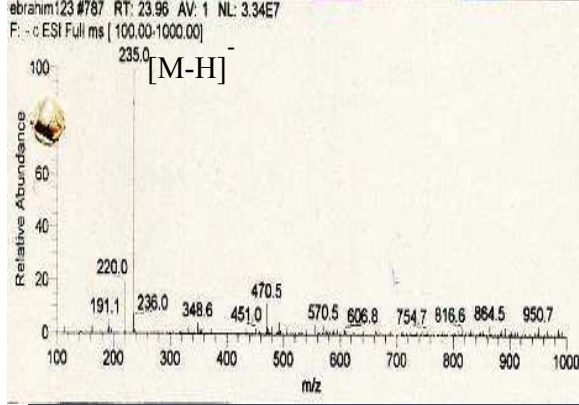
3.1.2. 6-(3'-hydroxy-*n*-butyl)-7-*O*-methyl spinochrome B (2, known compound)

6-(3'-hydroxy- <i>n</i> -butyl)-7- <i>O</i> -methypspinochrome B	
Synonym(s)	(<i>R</i>)-2,3,5-trihydroxy-6-(3-hydroxybutyl)-7-methoxynaphthalene-1,4-dione
Sample code	Coryseph2732
Biological source	<i>Corynespora cassicola</i>
Sample amount	17 mg
Physical properties	reddish amorphous solid
Molecular formula	C ₁₅ H ₁₆ O ₇
Molecular weight	308 g/mol
Optical rotation[α] _D ²⁰	-12 (c 0.025, Acetone)
Retention time (HPLC)	24.7 min. (standard gradient)
	
	
	

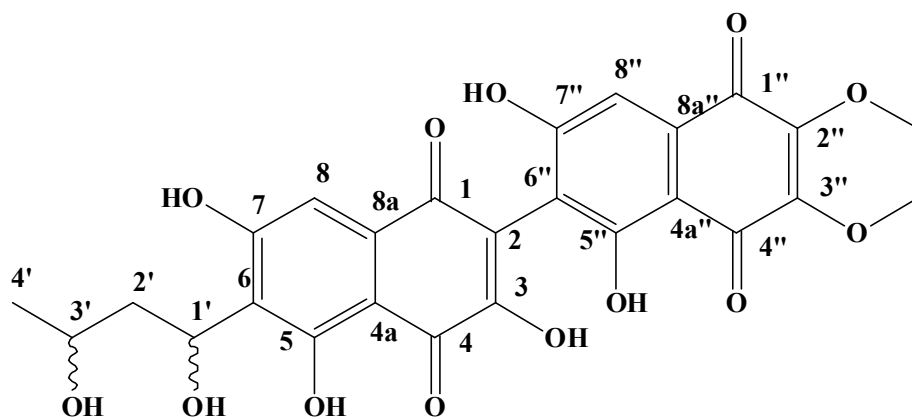
6-(3'-hydroxy-*n*-butyl)-7-*O*-methyl spinochrome B (**2**) was isolated from the EtOAc extract of liquid cultures of *Corynespora cassiicola* as reddish amorphous solid (17 mg). It showed UV absorbance maxima at λ_{max} (MeOH) 213.7, 268 and 323.7 nm. Positive and negative ESI-MS showed molecular ion peaks at m/z 331 $[\text{M}+\text{Na}]^+$ (base peak) and m/z 307.1 $[\text{M}-\text{H}]^-$ (base peak), respectively, indicating a molecular weight of 308 g/mol. Structural elucidation of **1** was based on results of 1D and 2D NMR spectral analysis including ^1H NMR, ^1H - ^1H COSY and HMBC spectra (Table 3.2). This indicated the presence of one aromatic singlet H-8 at δ_{H} 7.04 ppm, a doublet at δ_{H} 1.18 ($J=6.3$ Hz) indicated for 4'-Me, a singlet at δ_{H} 3.78 ppm for 7-OMe, a multiplet at δ_{H} 2.65 and 2.63 ppm for CH_2 -1', a multiplet at δ_{H} 1.51 and 1.49 ppm for CH_2 -2' and a multiplet at δ_{H} 3.60 ppm for H-3'. The COSY spectrum showed a spin system from 4'-Me to CH_2 -1'. The attachment of the side chain at position 6 was confirmed by the HMBC correlation of H-1' to C-5 (Table 3.2). The attachment of the methoxy groups at δ_{H} 3.78 ppm to position 7 is confirmed through HMBC by the correlation to C-7. Moreover, HMBC shows correlation of H-8 to C-6a, C-7, C-9 and C-10.

In order to determine the absolute configuration of this metabolite, we applied the modified Mosher procedure in NMR tube. The observed shift differences between the (*S*)-MTPA ester and its (*R*)-MTPA ester epimer led to the assignment of the chiral centre at C-3' of 6-(3'-hydroxy-*n*-butyl)-7-*O*-methyl spinochrome B (Table 3.2a). The compound **2** was then identified as a known natural product 6-(3'-hydroxy-*n*-butyl)-7-*O*-methypspinochrome B which was isolated from *Corynespora cassiicola* (Chimura *et al.*, 1973), for which we clarified the absolute configuration of the aliphatic side chain for the first time as (*R*)-conformer.

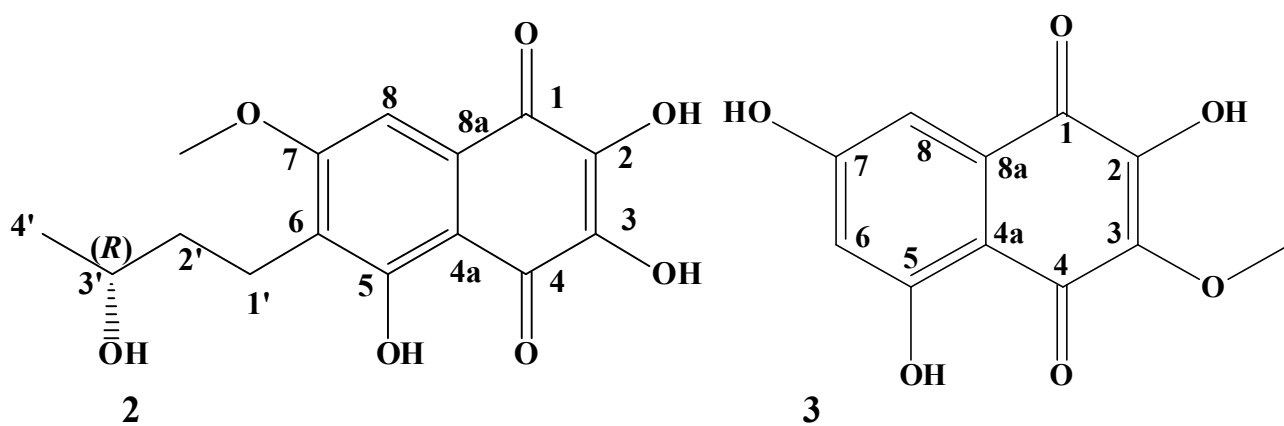
3.1.3. 7-*O*-methyl spinochrome B (3, known compound)

7- <i>O</i> -methypspinochrome B	
Synonym(s)	2,5,7-trihydroxy-3-methoxynaphthalene-1,4-dione
Sample code	Coryliqseph915 semi1
Biological source	<i>Corynespora cassicola</i>
Sample amount	1.5 mg
Physical properties	reddish amorphous solid
Molecular formula	C ₁₁ H ₈ O ₆
Molecular weight	236 g/mol
Retention time (HPLC)	22.1 min. (standard gradient)
	
	(+)-ESI-MS: no ionization
	

7-*O*-methyl spinochrome B (**3**) was isolated from the EtOAc extract of liquid cultures of *Corynespora cassiicola* as reddish amorphous solid (1.5 mg). It showed UV absorbance maxima at λ_{max} (MeOH) 219.5, 265.9 and 316.1 nm. Negative ESI-MS showed the molecular ion peak at m/z 235 $[\text{M-H}]^-$ (base peak) indicating a molecular weight of 236 g/mol. Structural elucidation of **1** was based on results of 1D and 2D NMR spectral analysis including ^1H NMR, NOE and HMBC spectra (Table 3.2). This indicated the presence of one pair of *meta*-coupled protons 6 and 8 at δ_{H} 6.45 ppm and 6.90 ppm, respectively (each doublet, $J=2.2$), a methoxy group at δ_{H} 3.82 ppm. The HMBC spectrum confirms the attachment of the methoxy groups to position 3 by correlation to C-3 by applying NOE experiment to **3** (confirms its position) by irradiating the methoxy group as no effect on any of the aromatic protons (H-6 and H-8). The structure was confirmed also by comparison with the literature (Assante *et al.*, 1977). The compound **3** was then identified as a known natural product 7-*O*-methypspinochrome B which was previously isolated from *Cercospora melonis* (the old name of *Corynespora cassiicola*) (Assante *et al.*, 1977).



1



Nr.	Compound
1	Corynecassiidiol
2	6-(3'-hydroxy- <i>n</i> -butyl)-7- <i>O</i> -methyl spinochrome B
3	7- <i>O</i> -methyl spinochrome B

Table 3.1: ^1H , COSY and HMBC spectra of compound **1**

Position	1 δ_{H} (MeOD)	COSY	HMBC
1			
2			
3			
4			
4a			
5			
6			
7			
8	7.01, s		1, 7
8a			
1'	5.27, t (7.5)	2'A, 2'B	7
2'	A 2.27, m B 2.55, m	1', 3'	
3'	3.76, m	2', 4'	
4'	1.18, d (6.3)	3'	
1''			
2''			
3''			
4''			
4a''			
5''	7.04, s		4'', 6''
6''			
7''			
8''			
8a''			
2''-OMe	3.92, s		2''
3''-OMe	3.93, s		3''

Table 3.2: ^1H , ^{13}C , COSY and HMBC spectra of compounds **2** and **3**

Position	2				2^a	3				3^b
	δ_{C} (DMSO)	δ_{H} (DMSO)	COSY	HMBC	δ_{H} (DMSO)	δ_{C} (DMSO)	δ_{H} (DMSO)	COSY	HMBC	δ_{H} (DMSO)
1	181.2					182.1				
2	161.1					163.3				
3	147.7					140.3				
4	185.7					184.5				
4a	105.8					106.7				
5	160.9					162.5				
6	122.3					107.7	6.45, d (2.2)	8	5, 8	6.50, d (2.5)
7	140.4					157.6				
8	107.3	7.04, s		6a, 7, 9, 10	7.06, s	107.8	6.90, d (2.2)	6	1, 6	6.94, d (2.5)
8a	128.6					131.9				
1'	19.2	A 2.65, m B 2.63*, m	2'	5, 6, 2', 3' 5, 6, 2', 3'	A 2.65, t (6) B 2.65, t (6)					
2'	38.9	A 1.51, m B 1.49, m	1', 3'	1', 3', 4' 1', 3', 4'	1.50, m 1.50, m					
3'	66.1	3.60, m	2', 4'	1'	3.50, m					
4'	23.4	1.09, d (6.3)	3'	2', 3'	1.10, d (6)					
3-OMe						60	3.82, s		3	3.88, s
7-OMe	60.3	3.78, s		7	3.85, s					
OH-5		12.61, s		5, 6, 4a	12.65, s		12.5, br. s			12.2, s
OH-5							10.9, br. s			

a) (Chimura *et al.*, 1973)

b) (Assante *et al.*, 1977)

Table 3.2a: Chemical shift difference between the (*S*)-MTPA and (*R*)-MTPA esters of **2**.

Proton no.	Chemical shift (δ_{H} , in $\text{C}_5\text{D}_5\text{N}$, at 500 MHz)			$\Delta \delta S - \delta R$
	2	(<i>S</i>)-MTPA ester	(<i>R</i>)-MTPA ester	
1'	3.31	2.27	2.33	-0.04
2'	2.16	1.61	1.90	-0.29
4'	1.40	1.30	1.28	+0.02

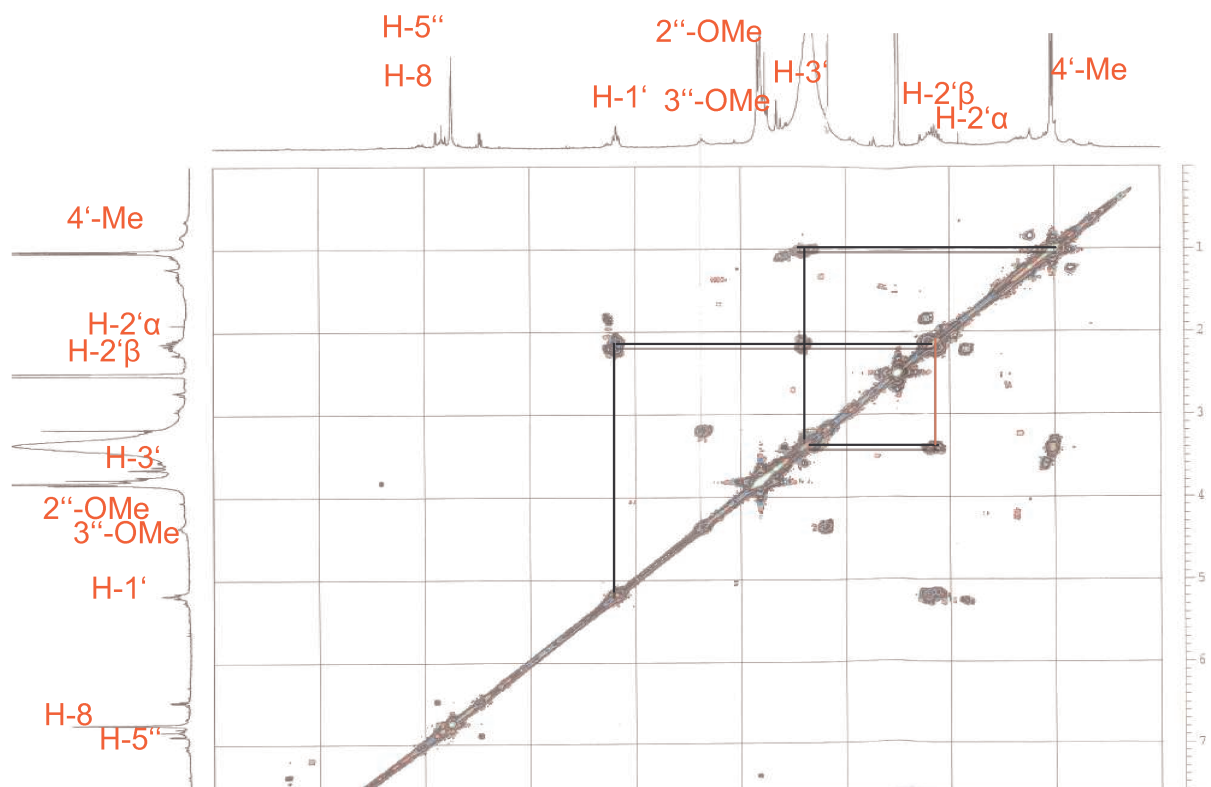


Fig. 3.1: COSY spectrum of compound 1.

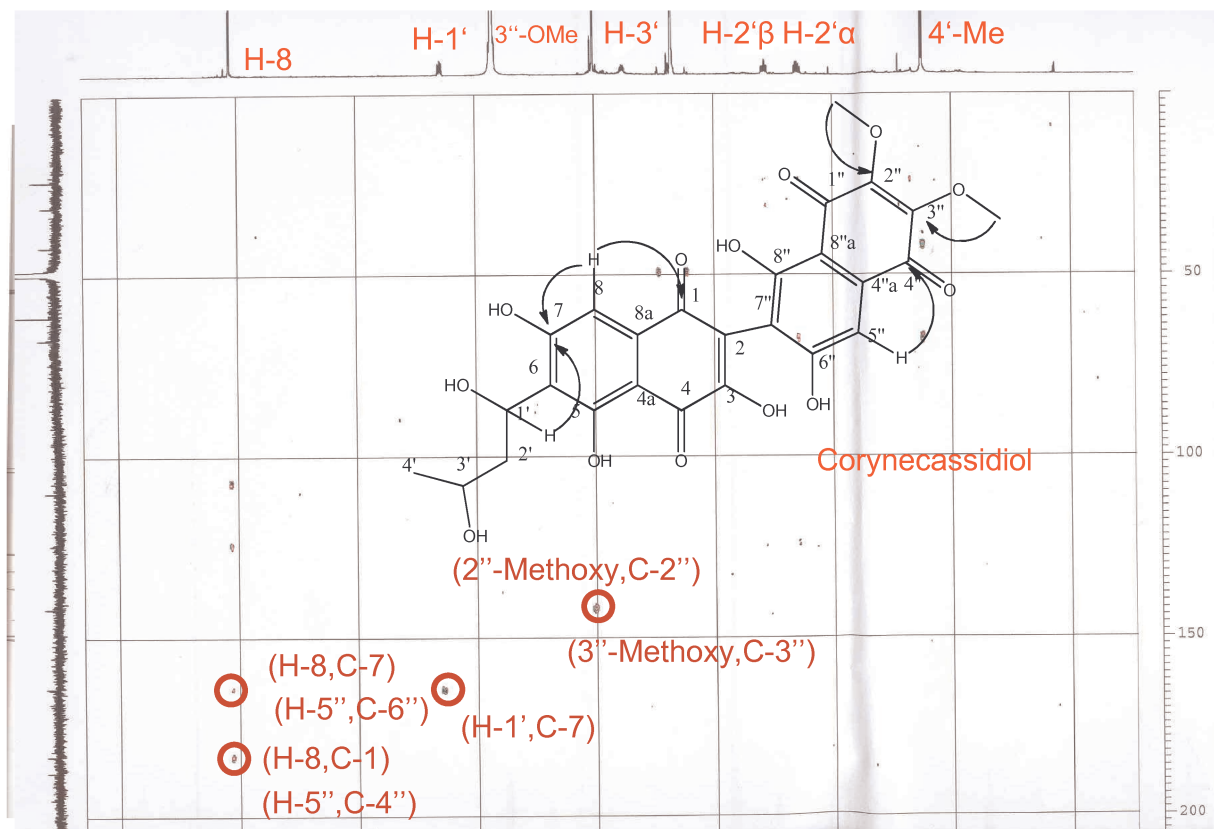
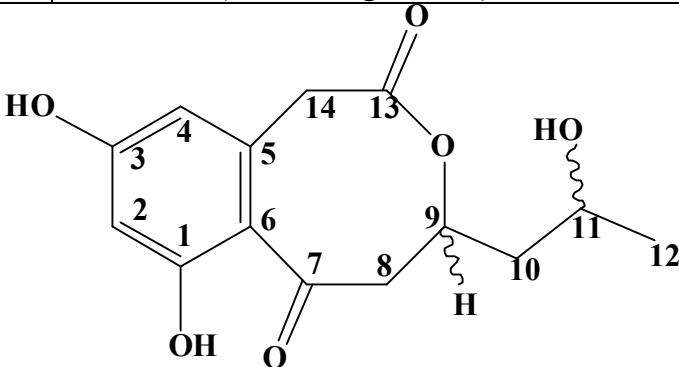
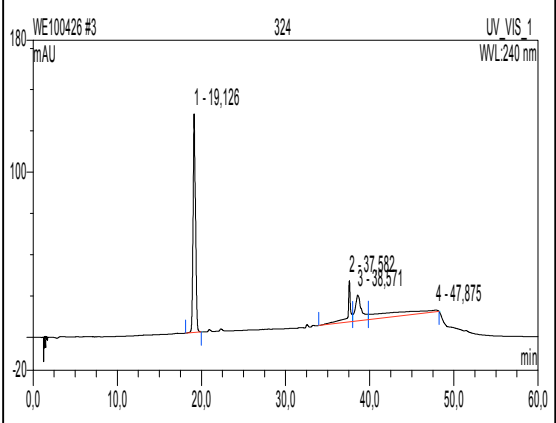
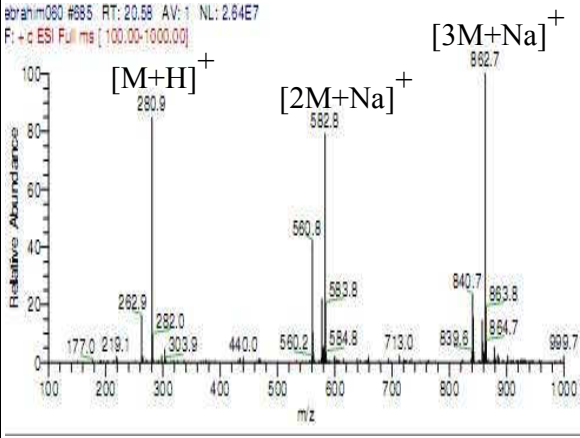
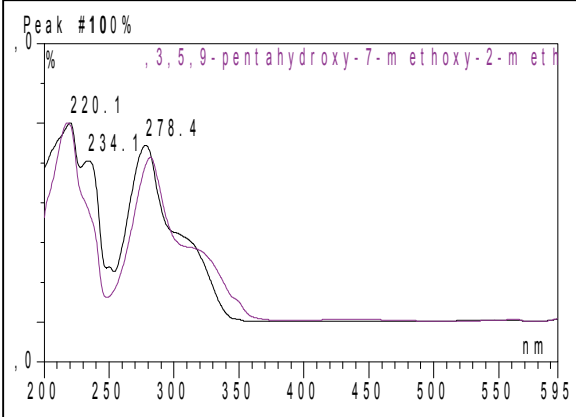
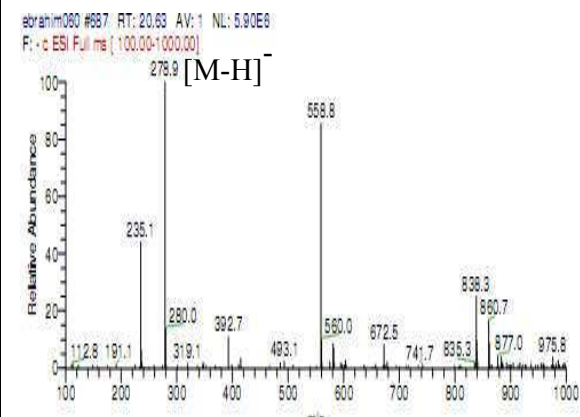


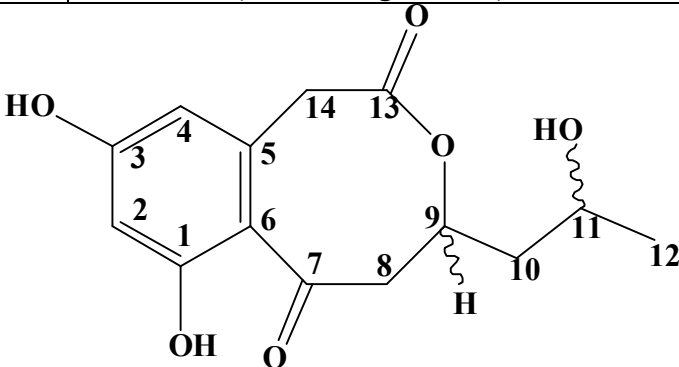
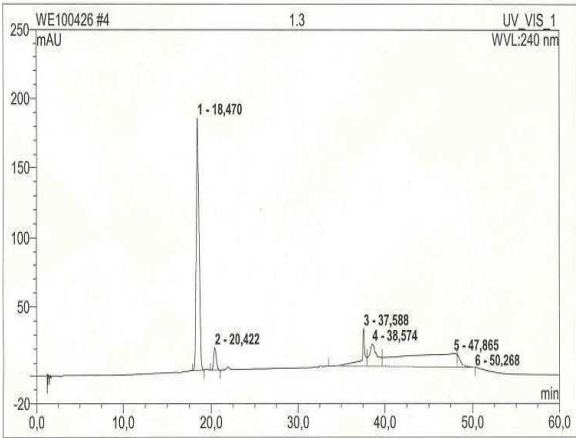
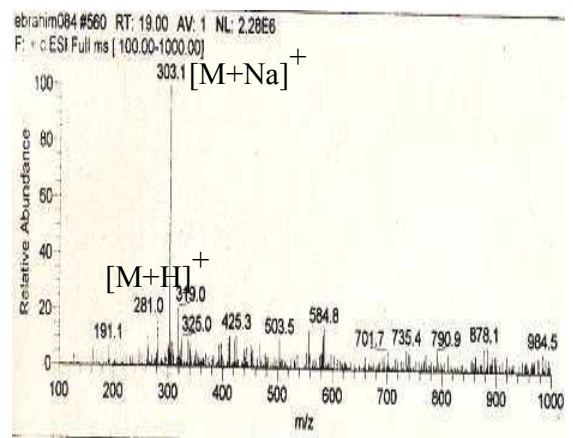
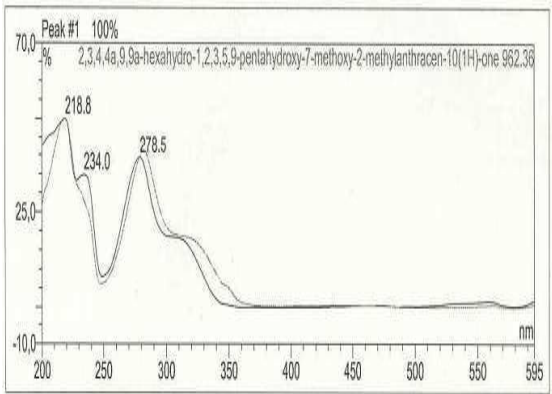
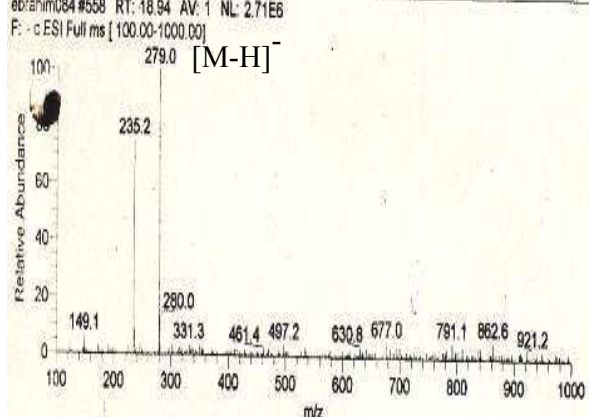
Fig. 3.2: HMBC spectrum of compound 2.

3.1.4. Coryneoctalactone A (4, new compound)

Coryneoctalactone A	
Synonym(s)	7,9-dihydroxy-4-(2-hydroxypropyl)-4,5-dihydro-1H-benzo[d]oxocine-2,6-dione
Sample code	Corysep2832semi 6
Biological source	<i>Corynespora cassiicola</i>
Sample amount	2 mg
Physical properties	yellowish white residue
Molecular formula	C ₁₄ H ₁₆ O ₆
Molecular weight	280 g/mol
Optical rotation $[\alpha]_D^{20}$	-32 (<i>c</i> 0.025, MeOH)
Retention time (HPLC)	19.1 min. (standard gradient)
	
	
	

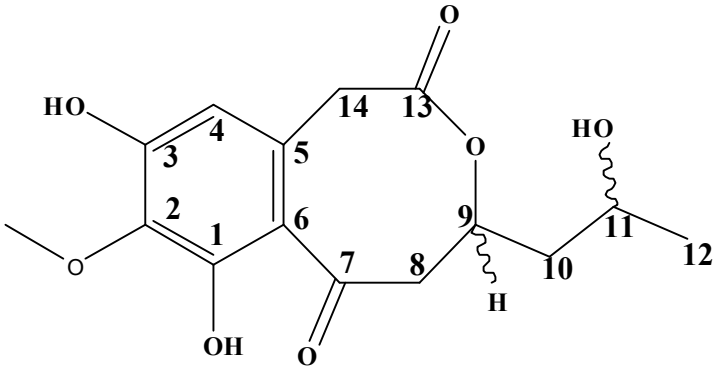
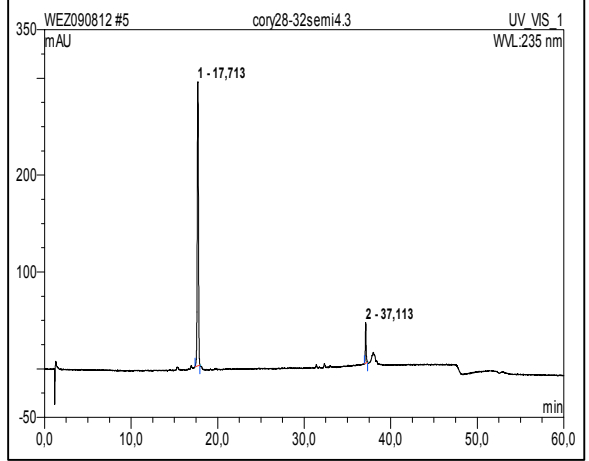
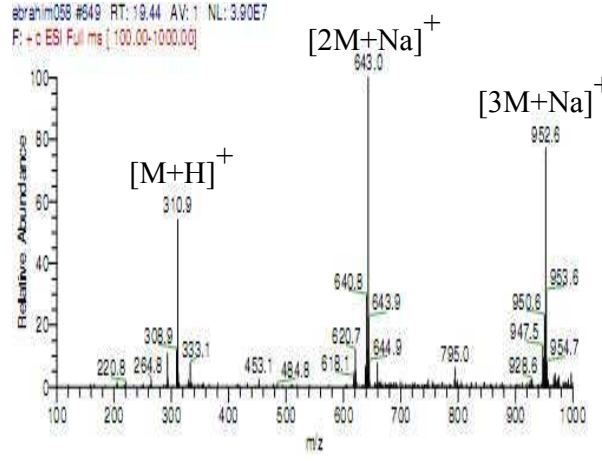
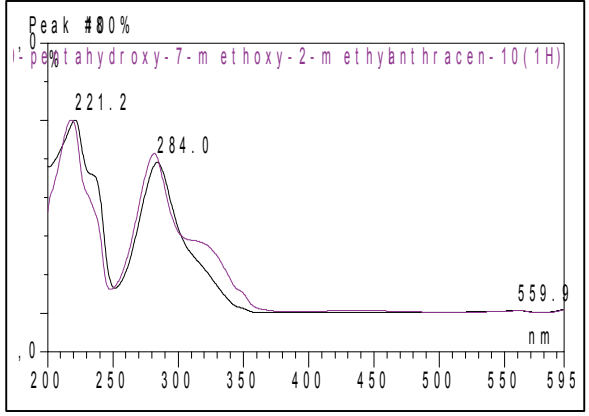
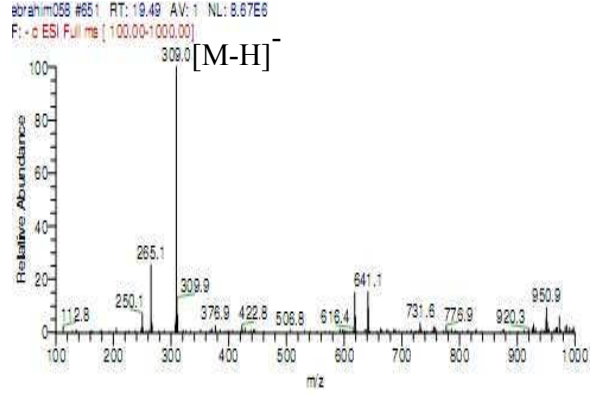
Coryneoctalactone A **4** was isolated from the EtOAc extract of rice cultures of *Corynespora cassiicola* as a yellowish white residue (2 mg). It showed UV absorbances at λ_{max} (MeOH) 220.0, 234.1, 278.4 nm. Positive and negative ESI-MS showed molecular ion peaks at m/z 280.9 $[M+H]^+$ (base peak) and m/z 278.9 $[M-H]^-$ (base peak), respectively, indicating a molecular weight of 280 g/mol. The HRESI-MS exhibited a strong peak at m/z 281.1023 $[M+H]^+$ indicating a molecular formula $C_{14}H_{16}O_6$ (calculated 281.1025, Δ 0.0002). 1D ^1H -NMR and 2D COSY and HMBC spectra indicated the presence of spin systems belonging to two substructures. The phenylacetic acid substructure was composed of the aromatic protons H-2 at δ_{H} 6.24 ppm and H-4 at δ_{H} 6.29 ppm, in which the latter showed a correlation with C-14 at δ_{C} 40.5 ppm in the HMBC spectrum. Further diagnostic correlations in the HMBC spectrum of CH_2 -14 at δ_{H} 3.79 ppm, H-4 at δ_{H} 6.29 ppm and H-2 at δ_{H} 6.24 ppm (Table 3.3), confirmed the substructure. The second spin system, from CH_2 -8 at (δ_{H} A 2.53 ppm and B 2.58 ppm) to 12-Me at δ_{H} 1.09 ppm, detected in the COSY spectrum was attached to the aromatic system via carbonyl C-7 at δ_{C} 191.4 ppm from its correlations with CH_2 -8 at (δ_{H} A 2.53 ppm and B 2.58), H-9 at δ_{H} 4.54 ppm and H-2 at δ_{H} 6.24 ppm in the HMBC spectrum. In **4** the closure of the lactone ring occurred at C-9 at δ_{C} 74.4 ppm and followed from the shift of H-9 at δ_{H} 4.54 ppm and its correlation with carbonyl C-13 at δ_{C} 171.9 ppm in the HMBC spectrum. The stereochemistry at the chiral centers 9 and 11 was not determined due to the low amount of compound available. To the best of our knowledge, this is the first description of this carbon skeleton containing an aromatic ring attached to an octalactone ring. Accordingly, **4** was identified as a new natural product for which the name coryneoctalactone A is proposed.

3.1.5. Coryneoctalactone B (5, new compound)

Coryneoctalactone B	
Synonym(s)	7,9-dihydroxy-4-(2-hydroxypropyl)-4,5-dihydro-1 <i>H</i> -benzo[<i>d</i>]oxocine-2,6-dione
Sample code	Coryseph23semi 1.3
Biological source	<i>Corynespora cassiicola</i>
Sample amount	2 mg
Physical properties	Yellowish white residue
Molecular formula	C ₁₄ H ₁₆ O ₆
Molecular weight	280 g/mol
Optical rotation[α] _D ²⁰	+14 (c 0.025, MeOH)
Retention time (HPLC)	18.5 min. (standard gradient)
	
	
	

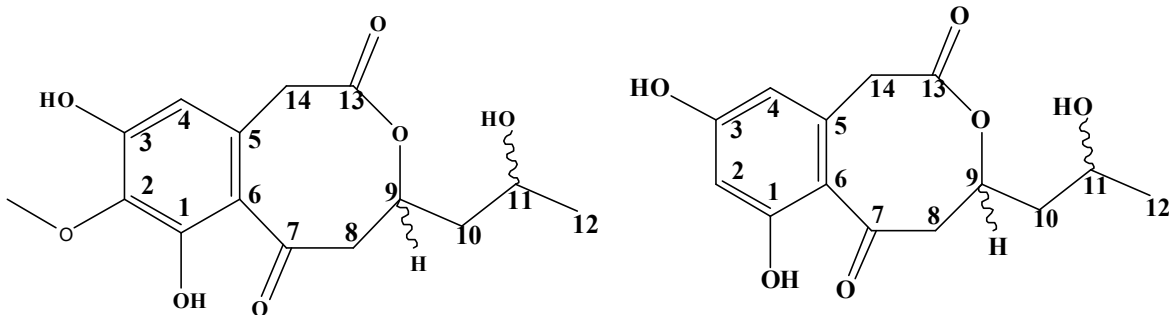
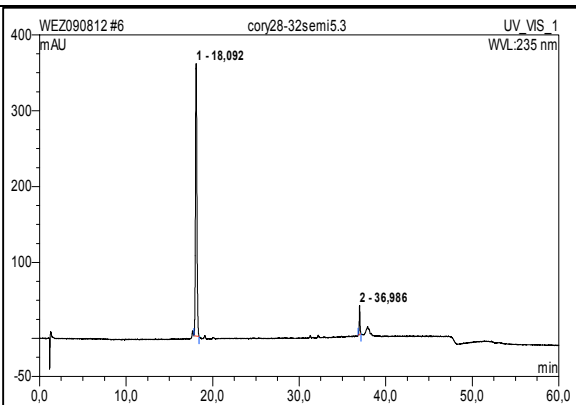
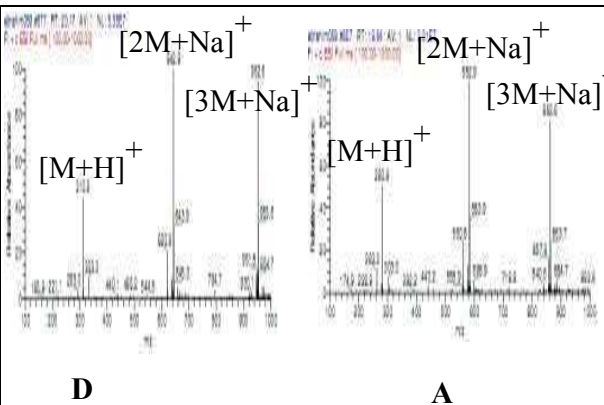
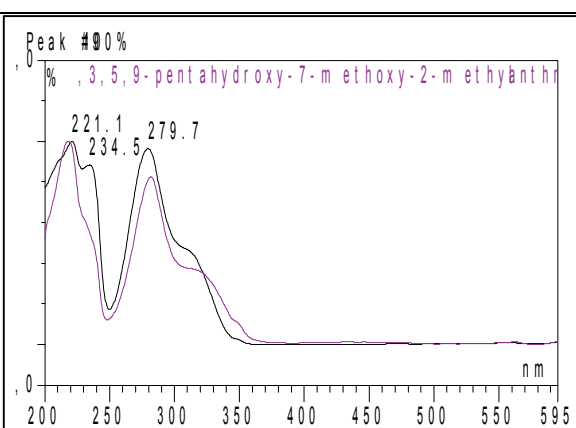
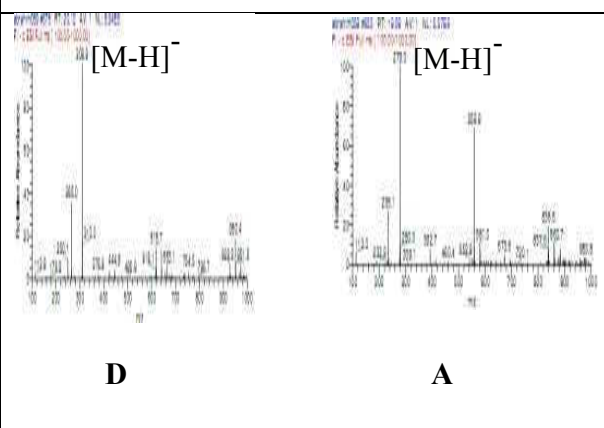
Coryneoctalactone B **5** was isolated from the EtOAc extract of rice cultures of *Corynespora cassiicola* as a yellowish white residue (2 mg). It showed UV absorbances at λ_{max} (MeOH) 218.8, 234.0, 278.5 nm. Positive and negative ESI-MS showed molecular ion peaks at m/z 281 $[\text{M}+\text{H}]^+$ (base peak) and m/z 279 $[\text{M}-\text{H}]^-$ (base peak), respectively, indicating a molecular weight of 280 g/mol. The HRESI-MS exhibited a strong peak at m/z 281.1025 $[\text{M}+\text{H}]^+$ indicating a molecular formula $\text{C}_{14}\text{H}_{16}\text{O}_6$ (calculated 281.1025, Δ 0). Compound **5** was obtained as white amorphous residue and had an identical HRESI-MS with that of **4**. The UV spectra as well as ^1H and ^{13}C NMR data of **4** and **5** (Table 3.3) showed close similarity with the exception of different chemical shifts observed for H-11 (δ_{H} 3.89 ppm in **4** and 3.71 ppm in **5**) and H-9 (δ_{H} 4.54 in **4** and 4.48 in **5**) in both compounds. These differences indicated that **5** is a stereoisomer of **4** with a different relative configuration at the chiral center 9 or 11. This was further confirmed by measuring the $[\alpha]_{\text{D}}$ for both compounds which showed different values of -32 and +14 for **4** and **5**, respectively. Hence, **5** was found to be a new natural product which we named coryneoctalactone B.

3.1.6. Coryneotalactone C (6, new compound)

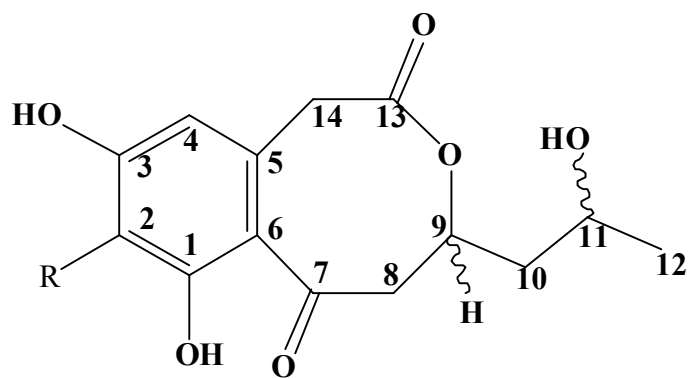
Coryneotalactone C	
Synonym(s)	7,9-dihydroxy-4-(2-hydroxypropyl)-8-methoxy-4,5-dihydro-1 <i>H</i> -benzo[d]oxocine-2,6-dione
Sample code	Corysep2832semi 4
Biological source	<i>Corynespora cassicola</i>
Sample amount	4 mg
Physical properties	yellowish white residue
Molecular formula	C ₁₅ H ₁₈ O ₇
Molecular weight	310 g/mol
Optical rotation [α] _D ²⁰	-84 (c 0.025, MeOH)
Retention time (HPLC)	17.7 min. (standard gradient)
	
	
	

Coryneoctalactone C **6** was isolated from the EtOAc extract of rice cultures of *Corynespora cassiicola* as a yellowish white residue (4 mg). It showed UV absorbances at λ_{max} (MeOH) 221, 284 nm. Positive and negative ESI-MS showed molecular ion peaks at m/z 310.9 $[\text{M}+\text{H}]^+$ (base peak) and m/z 309 $[\text{M}-\text{H}]^-$ (base peak), respectively, indicating a molecular weight of 310 g/mol. The HRESI-MS exhibited a strong peak at m/z 311.1129 $[\text{M}+\text{H}]^+$ indicating a molecular formula $\text{C}_{15}\text{H}_{18}\text{O}_7$ (calculated 311.1131, Δ 0.0002). The ^1H NMR spectrum of **6** was similar to those of **4** and **5**, except for the absence of one aromatic proton and the presence of an additional methoxyl group at δ_{H} 3.65 ppm. It further showed the same aliphatic spin system. The attachment of the methoxyl group at position 2 was confirmed by the long-range correlation of CH_2 -14 to H-4, and the HMBC correlation of OCH_3 -2 and H-4 to C-2. Thus **6** was identified as a new metabolite for which the name coryneoctalactone C is proposed.

3.1.7. Coryneotalactone D/A (7/4, new compounds)

Coryneotalactone D/A	
Synonym(s)	7,9-dihydroxy-4-(2-hydroxypropyl)-8-methoxy-4,5-dihydro-1 <i>H</i> -benzo[d]oxocine-2,6-dione (D) 7,9-dihydroxy-4-(2-hydroxypropyl)-4,5-dihydro-1 <i>H</i> -benzo[d]oxocine-2,6-dione (A)
Sample code	Corysep2832semi 5
Biological source	<i>Corynespora cassiicola</i>
Sample amount	7 mg
Physical properties	yellowish white residue
Molecular formula	C ₁₅ H ₁₈ O ₇ and C ₁₄ H ₁₆ O ₆
Molecular weight	310 g/mol(D) and 280 g/mol(A)
Retention time (HPLC)	18.1 min. (standard gradient)
	
	
	

Coryneoctalactone D **7** was isolated from the EtOAc extract of rice cultures of *Corynespora cassiicola* as a yellowish white residue (7 mg together with **4**). It showed UV absorbances at λ_{max} (MeOH) 221.1, 234.5, 279.7 nm. Positive and negative ESI-MS showed molecular ion peaks at m/z 308.9 $[\text{M}+\text{H}]^+$ (base peak) and m/z 310.9 $[\text{M}-\text{H}]^-$ (base peak), respectively, indicating a molecular weight of 310 g/mol. Compound **7** was obtained as an inseparable mixture with compound **4** forming a grayish amorphous powder. As discussed before for compounds **4** and **5**, both compounds (**6** and **7**) are stereoisomers. The COSY spectrum showed similar spin systems as in compound **6**. The HMBC confirms also the position the OMe. Confirmation of the assumption was provided by the careful analysis of COSY and HMBC spectra.



Nr.	R	Compound
4	H	Coryneoctalactone A
5	H	Coryneoctalactone B
6	OMe	Coryneoctalactone C
7	OMe	Coryneoctalactone D

Table 3.3: ^1H , ^{13}C , COSY and HMBC spectra of compounds **4** and **5**

Position	4					5			
	$\delta_{\text{C}}^{\text{a}}$	$\delta_{\text{H}}^{\text{a}}$	COSY	HMBC		$\delta_{\text{C}}^{\text{a}}$	$\delta_{\text{H}}^{\text{a}}$	COSY	HMBC
1	163.9					164.1			
2	101.8	6.24, d (2.3)	4	1, 3, 4, 6		101.8	6.23, d (2.2)	4	1, 3, 4, 6
3	162.7					162.7			
4	114.1	6.29, d (2.3)	2, 14 A, 14B	2, 3, 6, 14		114.1	6.29, d (2.3)	2, 14 A, 14B	2, 3, 6, 14
5	139.4					139.4			
6	112.3					112.2			
7	191.4					191.2			
8	43.7	A 2.53, dd (11.6, 5.2) B 2.58, dd (11.4, 5.2)	9 9	7, 9, 10 7, 9		42.9	2.58, ov. dd (9.9, 4.6)	9	7, 9, 10
9	74.4	4.54, m	8, 10A, 10B	7, 11		74.8	4.48, m	8, 10A, 10B	7, 11
10	43.8	A 1.52, ddd (13.4, 3.5, 3.8) B 1.78, ddd (13.9, 3.1, 3.1)	9, 11 9, 11	8, 9, 11, 12 8, 9, 11, 12		43.4	A 1.66, dt (12.4, 6.7) B 1.85, dt (13.7, 6.8)	9, 11 9, 11	8, 9, 11, 12 8, 9, 11, 12
11	61.9	3.89, m	10, 12			62.2	3.71, m	10, 12	9
12	24.2	1.09, d (6.2)	11	10, 11		23.6	1.11, d (6.2)	11	9, 10, 11
13	171.9					171.9			
14	40.5	3.79, br. s	4	4, 5, 6, 13		40.5	3.80, br. s	4	4, 5, 6, 13
OH-3		10.45, br. s					10.45, br. s		2, 3, 4
OH-11		4.49, d (5.0)	11	10, 11, 12			4.58, d (4.9)	11	10, 11, 12

a) Measured in DMSO- d_6

Table 3.4: ^1H , ^{13}C , COSY and HMBC spectra of compounds **6** and **7**

Position	6				7			
	$\delta_{\text{C}}^{\text{a}}$	$\delta_{\text{H}}^{\text{a}}$	COSY	HMBC	$\delta_{\text{C}}^{\text{a}}$	$\delta_{\text{H}}^{\text{a}}$	COSY	HMBC
1	156.7				156.7			
2	134.2				134.2			
3	155.2				155.2			
4	114	6.32, s	2, 14 A, 14B	2, 3, 6, 7, 14	114.2	6.36, s	2, 14 A, 14B	2, 3, 6, 7, 14
5	133.2				133.1			
6	112.8				112.9			
7	191.5				191.7			
8	43.6	A 2.58, dd (12.7, 4.2) B 2.63, dd (11.3, 5.4)	9 9	7, 9, 10 7, 9, 10	43.7	2.55, ov. dd (7.9, 4.4)	9	7, 9, 10
9	75.3	4.45, m	8, 10A, 10B		74.8	4.45, m	8, 10A, 10B	
10	43.0	A 1.56, dt (13.8, 6.9) B 1.95, dt (12.3, 6.0)	9, 11 9, 11	8, 9, 11, 12 8, 9, 11, 12	43.4	A 1.65, dt (13.8, 7.4) B 1.95, dt (13.6, 6.7)	9, 11 9, 11	8, 9, 11, 12 8, 9, 11, 12
11	62.4	3.85, m	10, 12	9	62.2	3.71, m	10, 12	
12	23.5	1.09, d (6.1)	11	10, 11	23.7	1.11, d (6.2)	11	10, 11
13	172.1				172.1			
14	40.1	3.60, br. s	4	4, 5, 6, 13	40.0	A 3.73, d (16.1) B 3.76, d (16.1)	4	4, 5, 6, 13
OMe-2	60.1	3.65, s		2	60.1	6.62, s		2
OH-3		10.20, br. s		2, 3, 4		10.19, br. s		2, 3, 4
OH-11		4.58, br. s	11			4.58, d (4.9)	11	

a) Measured in DMSO- d_6

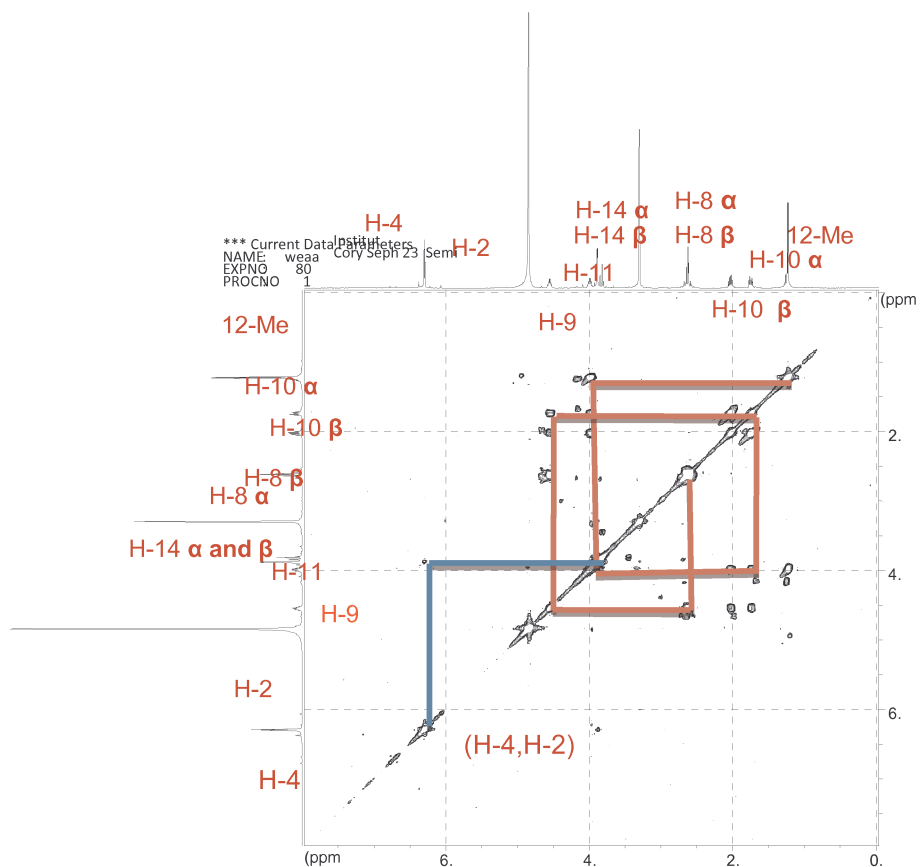


Fig. 3.3: COSY spectrum of compound 4.

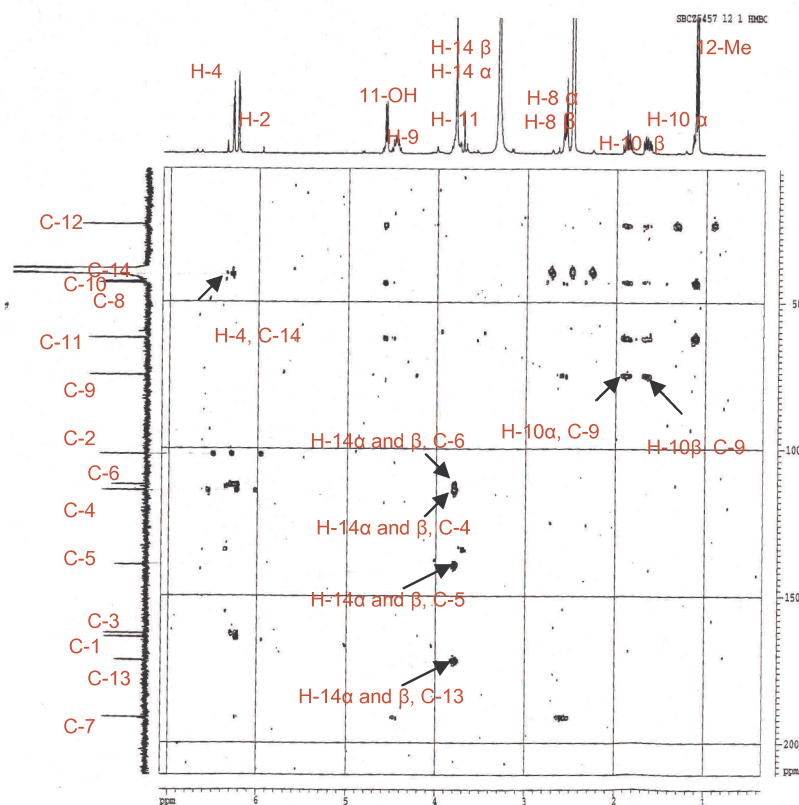


Fig. 3.4: HMBC spectrum of compound 4.

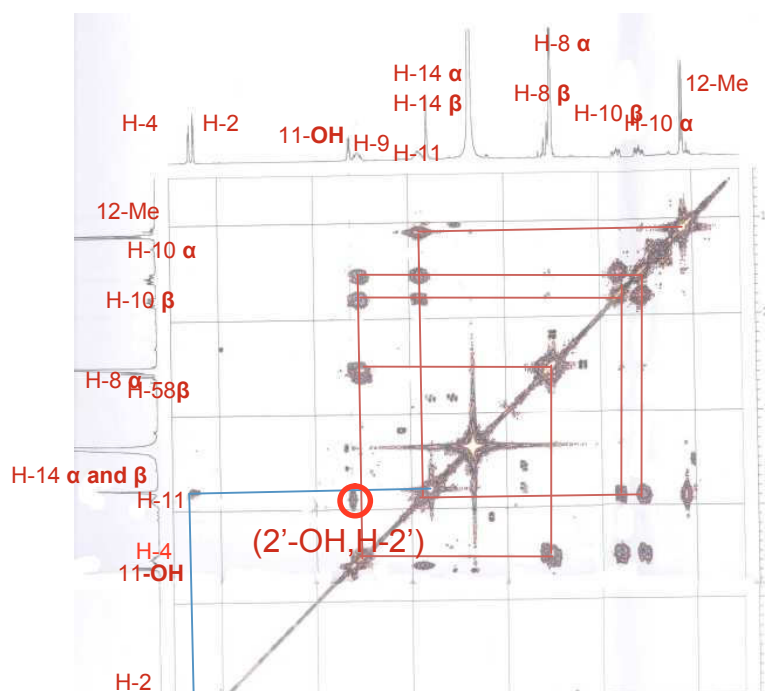


Fig. 3.5: COSY spectrum of compound 5.

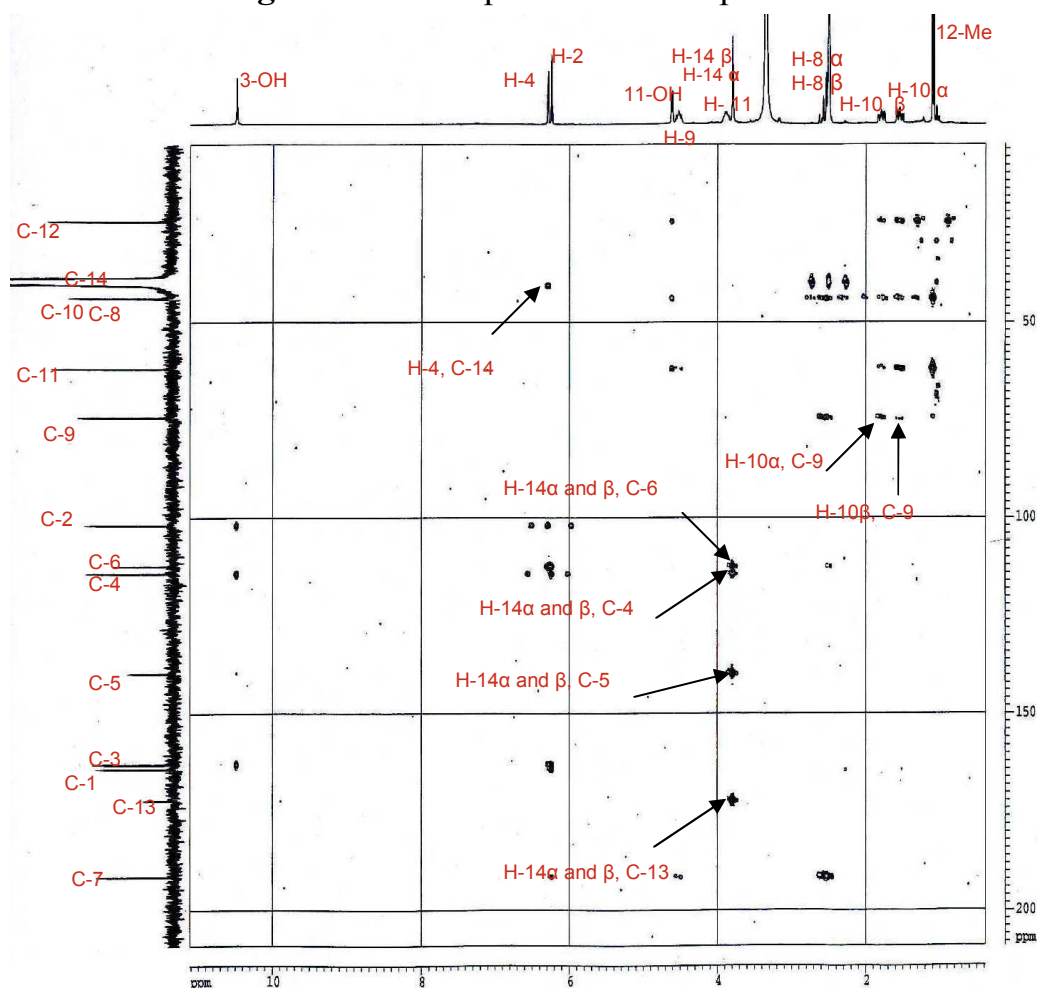


Fig. 3.6: HMBC spectrum of compound 5.

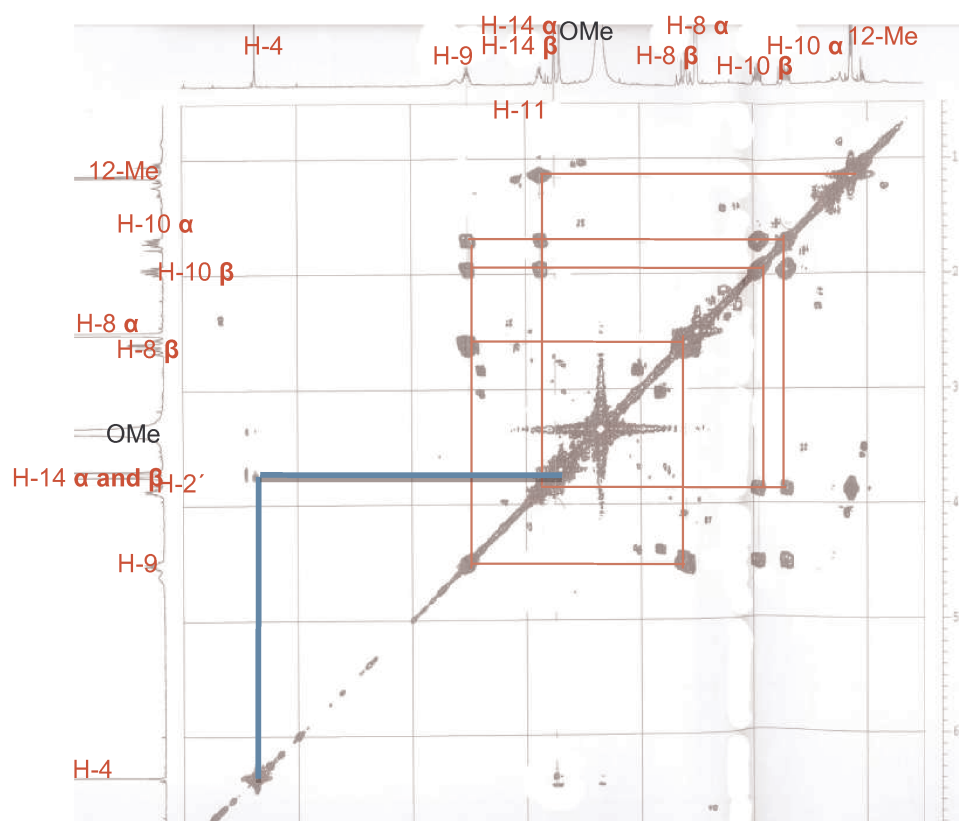


Fig. 3.7: COSY spectrum of compound 6.

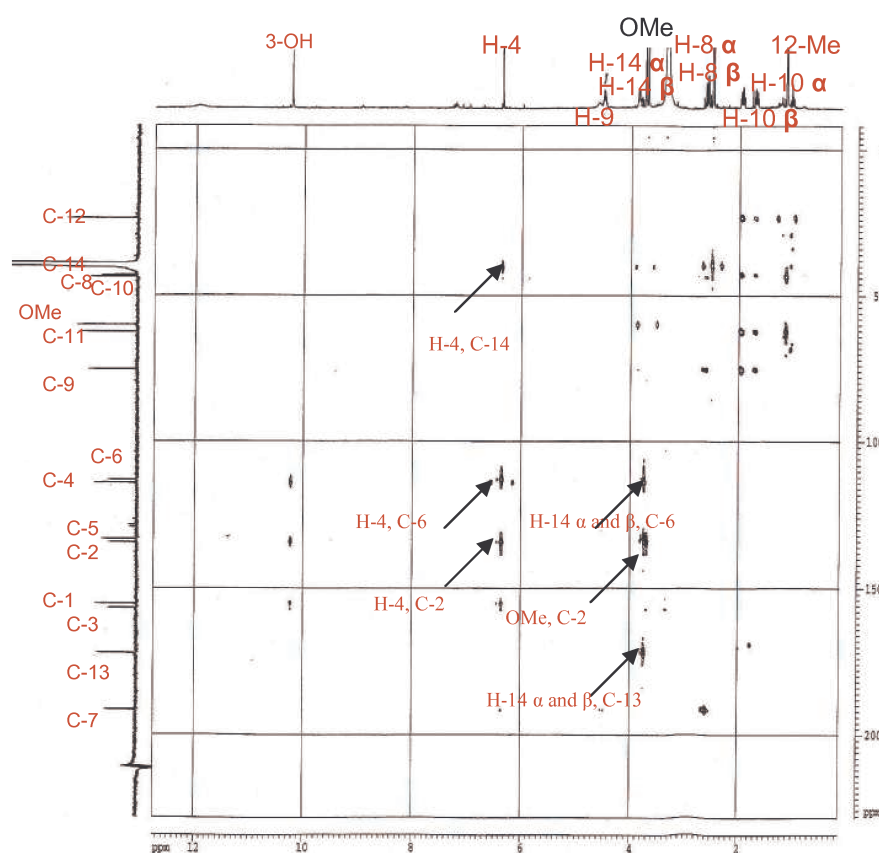


Fig. 3.8: HMBC spectrum of compound 6.

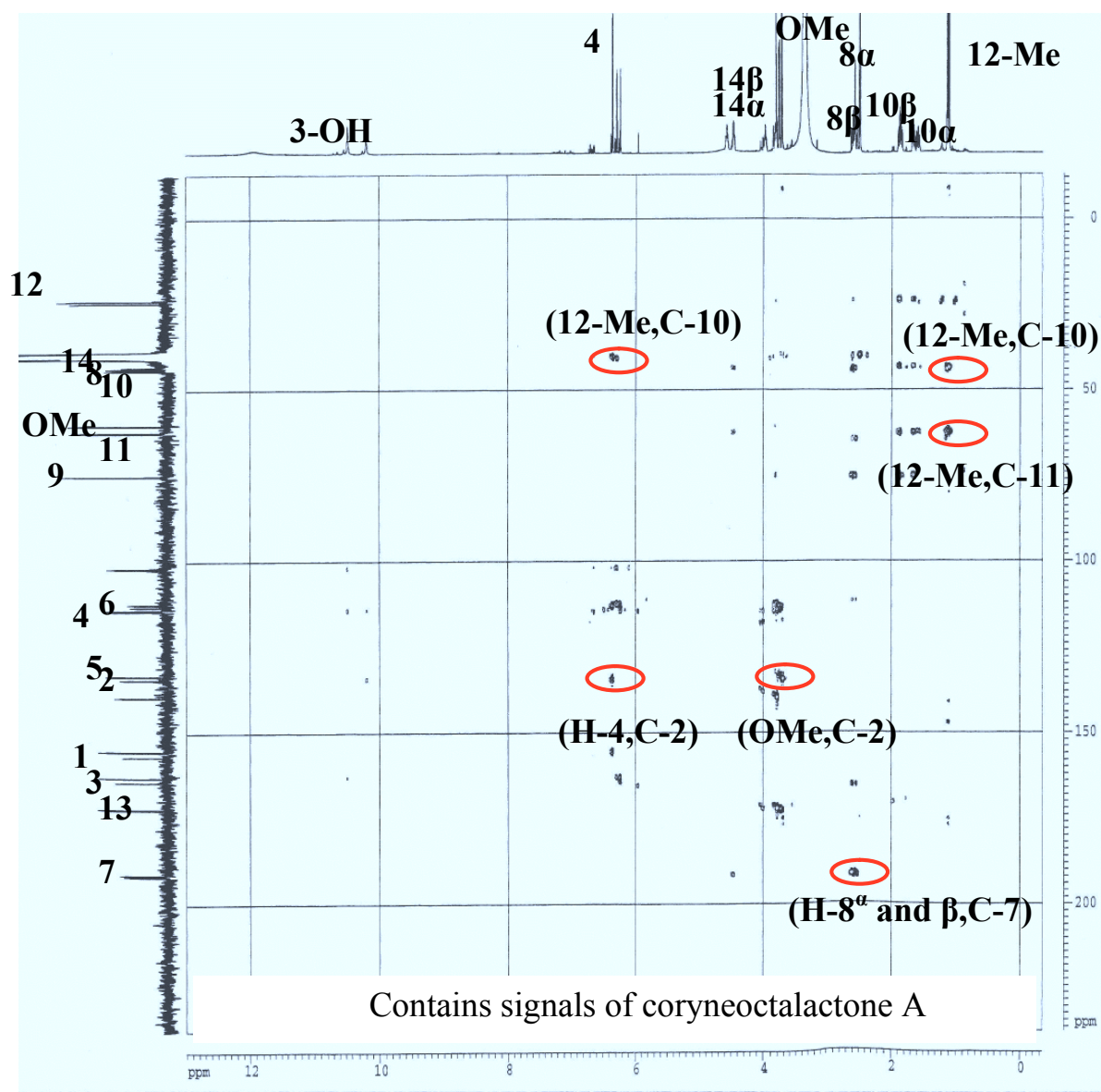
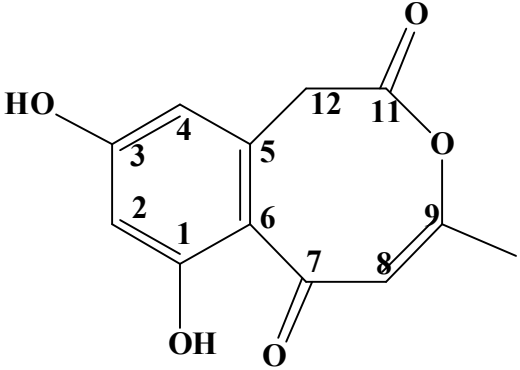
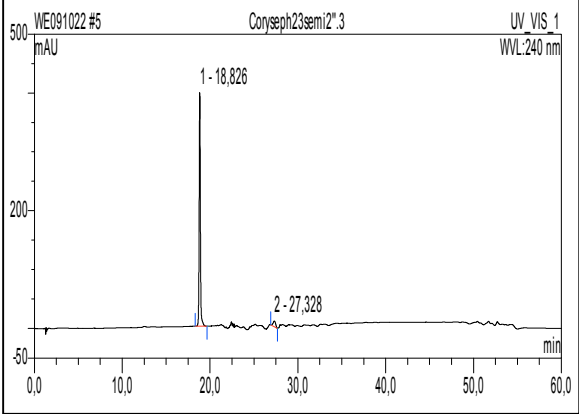
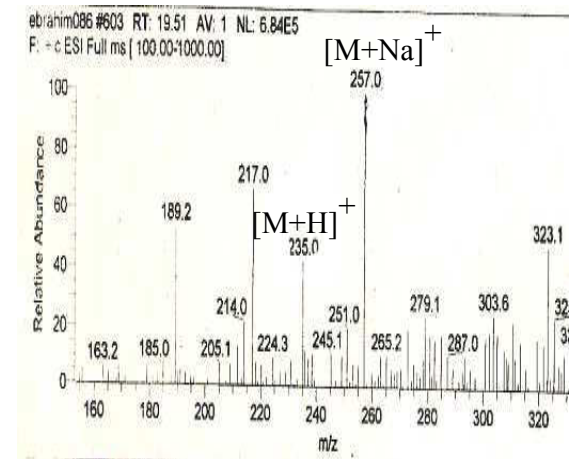
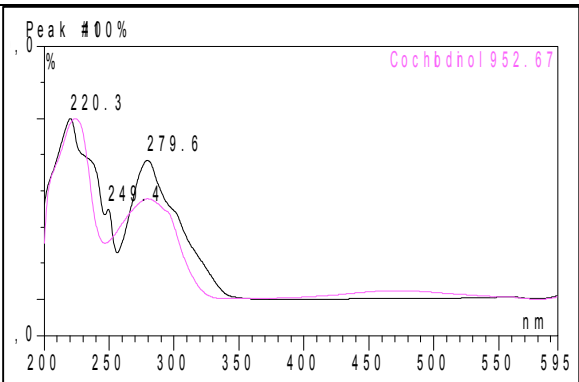
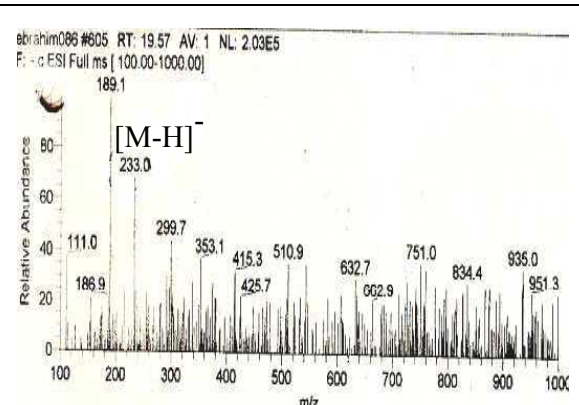


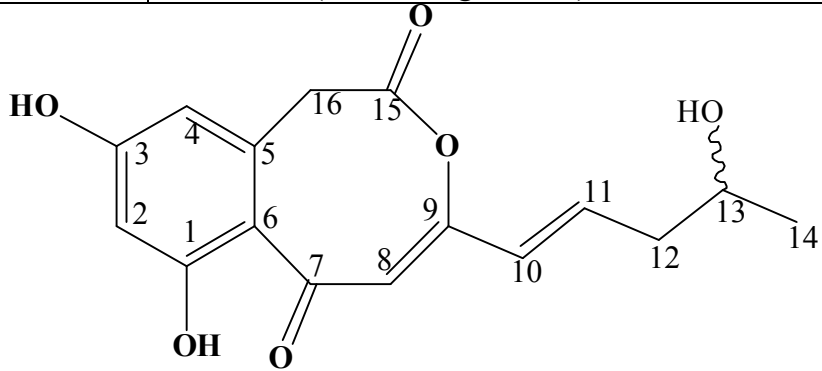
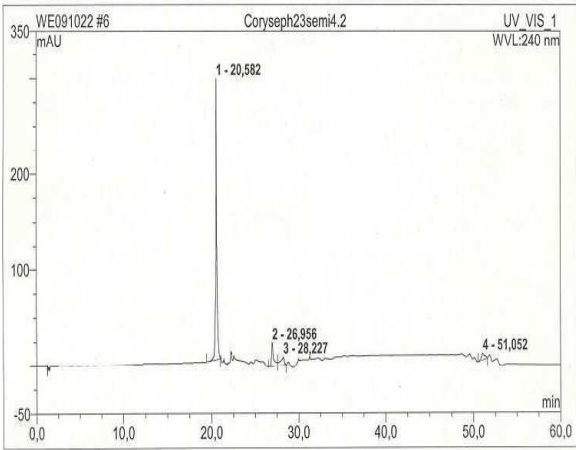
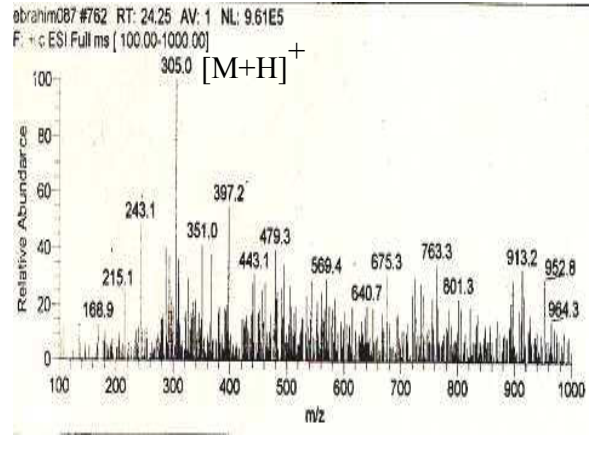
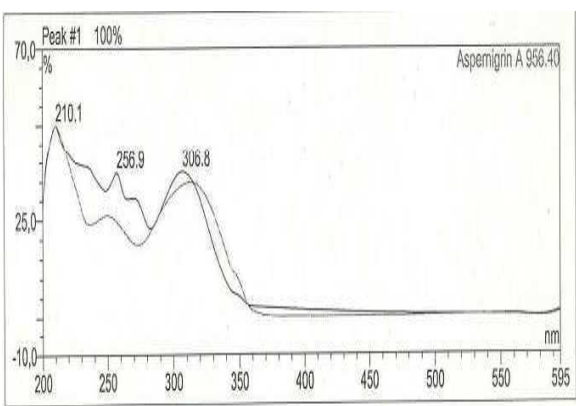
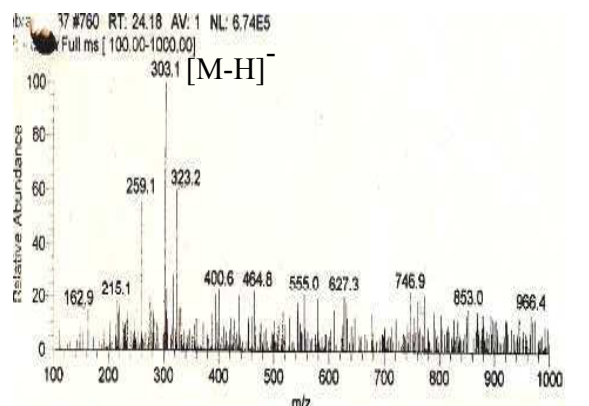
Fig. 3.9: HMBC spectrum of compound 7.

3.1.8. Coryneoctalactone E (8, new compound)

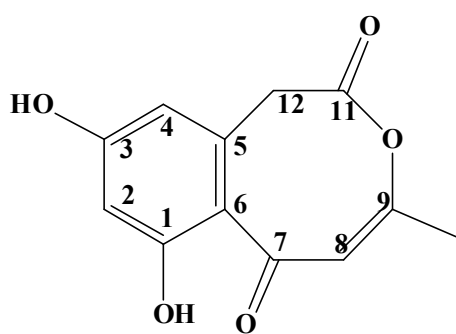
Coryneoctalactone E	
Synonym(s)	(Z)-7,9-dihydroxy-4-methyl-1 <i>H</i> -benzo[d]oxocine-2,6-dione
Sample code	Corysep23semi 2''
Biological source	<i>Corynespora cassicola</i>
Sample amount	1 mg
Physical properties	Yellowish white amorphous powder
Molecular formula	C ₁₂ H ₁₀ O ₅
Molecular weight	234 g/mol
Retention time (HPLC)	18.8 min. (standard gradient)
	
	
	

Coryneoctalactone E **8** was isolated from the EtOAc extract of rice cultures of *Corynespora cassiicola* as a yellowish white powder (1 mg). It showed UV absorbances at λ_{max} (MeOH) 220.3, 249.4, 279.6 nm. Positive and negative ESI-MS showed molecular ion peaks at m/z 235 $[\text{M}+\text{H}]^+$ and m/z 233 $[\text{M}-\text{H}]^-$, respectively, indicating a molecular weight of 310 g/mol. The HRESI-MS exhibited a strong peak at m/z 235.0595 $[\text{M}+\text{H}]^+$ indicating the molecular formula $\text{C}_{12}\text{H}_{10}\text{O}_5$ (calculated 235.0606, Δ 0.0011). Comparison of ^1H NMR (Table 3.5) and COSY spectra of **8** with those of **4** and **5** showed the same phenylacetic acid spin system consisting of one *meta*-coupled proton H-2 at δ_{H} 6.68 ppm and H-4 at δ_{H} 6.62 ppm, in which the latter further correlated with CH_2 -12 at δ_{H} 3.80 ppm. In addition to these signals, the ^1H NMR showed one methyl group (9-Me) at δ_{H} 2.25 ppm and one olefinic signal at δ_{H} 5.95 ppm (H-8), while the remaining signals observed for **4** and **5** were absent. The location of the methyl group was evident from the HMBC spectrum, where it correlated with two olefinic carbons (C-8 and C-9) but not with the carbonyl group (C-7). Furthermore, H-8 was correlated to C-6 and its chemical shift (δ_{H} 5.95 ppm) indicated its α position to the carbonyl group. For instance, attachment at β position (C-9) would have resulted in a more downfield chemical shift due to the adjacent ester group oxygen. Accordingly, **8** was identified as coryneoctalactone E representing a new natural product.

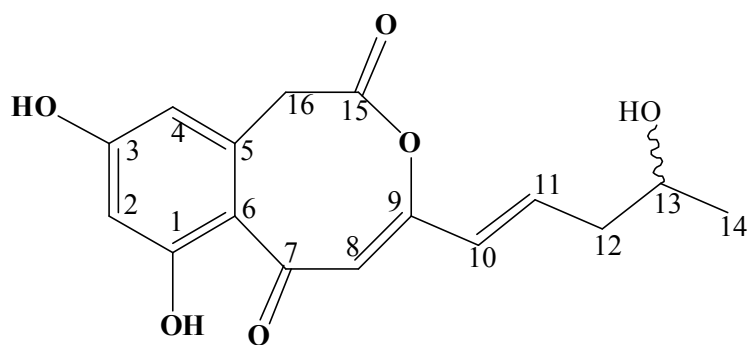
3.1.9. Coryneoctalactone F (9, new compound)

Coryneoctalactone F	
Synonym(s)	(Z)-7,9-dihydroxy-4-((E)-4-hydroxypent-1-en-1-yl)-1H-benzo[d]oxocine-2,6-dione
Sample code	Coryseph23semi 4.2
Biological source	<i>Corynespora cassiicola</i>
Sample amount	1.1 mg
Physical properties	Brown amorphous powder
Molecular formula	C ₁₆ H ₁₆ O ₆
Molecular weight	304 g/mol
Optical rotation [α] _D ²⁰	-15 (c 0.025, MeOH)
Retention time (HPLC)	20.6 min. (standard gradient)
	
	
	

Coryneoctalactone F **9** was isolated from the EtOAc extract of rice cultures of *Corynespora cassiicola* as a brown amorphous powder (1.1 mg). It showed UV absorbances at λ_{max} (MeOH) 210.1, 256.9, 306.8 nm. Positive and negative ESI-MS showed molecular ion peaks at m/z 304 $[\text{M}+\text{H}]^+$ and m/z 303.1 $[\text{M}-\text{H}]^-$, respectively, indicating a molecular weight of 310 g/mol. The HRESI-MS exhibited a strong peak at m/z 305.1031 $[\text{M}+\text{H}]^+$ indicating a molecular formula $\text{C}_{16}\text{H}_{16}\text{O}_6$ (calculated 305.1025, Δ 0.0006). ^1H NMR and COSY spectra of **9** suggested the presence of the same aromatic and lactone system observed for **8**, but with replacement of the methyl group at C-9 with a new aliphatic spin system. Its structure was readily determined from the COSY spectrum that indicated a double bond connected to C-9 with an *E*-configuration from the large vicinal coupling constant (J_{10-11} 15.7 Hz). Thus, **9** was identified as a new metabolite for which the name coryneoctalactone F is proposed.



8



9

Nr.	Compound
8	Coryneoctalactone E
9	Coryneoctalactone F

Table 5.5: ^1H , ^{13}C , COSY and HMBC spectra of compounds 8 and 9

Position	8		COSY	HMBC	9	
	$\delta_{\text{C}}^{\text{a}}$	$\delta_{\text{H}}^{\text{a}}$			$\delta_{\text{H}}^{\text{a}}$	COSY
1						
2	101.8	6.68, d (2.0)		3	6.78, d (2.3)	
3	158					
4	117.8	6.62, d (2.0)	12	6, 12	6.66, d (2.3)	16
5	138.2					
6	114.2					
7						
8	105.4	5.95, br. s		6, 9	6.04, br. s	
9	164.2					
10	19.5	2.25, s		8, 9	6.30, d (15.7)	11
11	172.4				6.79, dt (15.9, 5.7)	10, 12
12	40.0	3.80, br. s ^a	4	4, 5, 6, 11	2.33, m	11, 13
13					3.79, m	12, 14
14					1.1, d (6.1)	13
15						
16					4.02, br. s	4
OH-3		10.42, br. s			10.62, br. s	13

a) Measured in DMSO- d_6

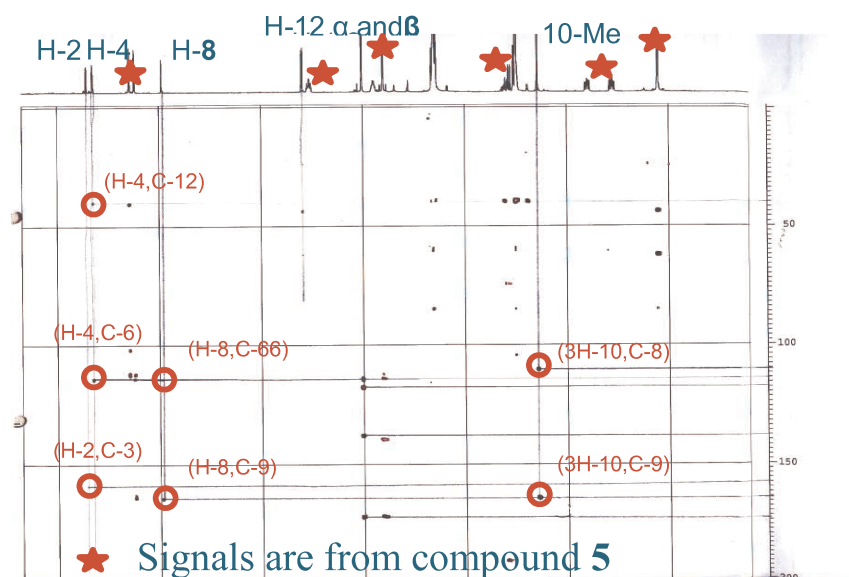


Fig. 3.10: HMBC spectrum of compound 8.

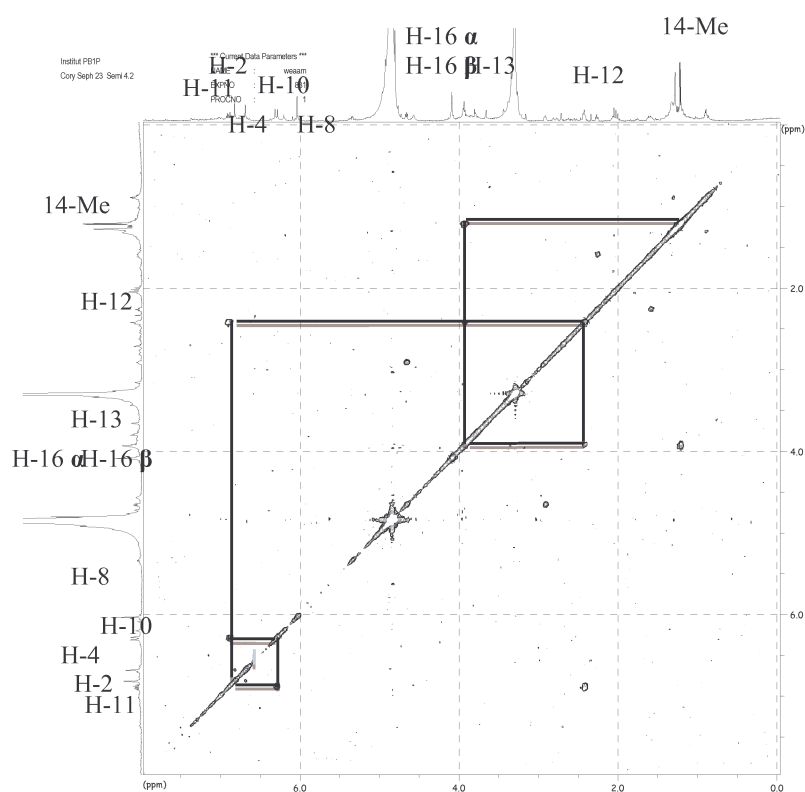
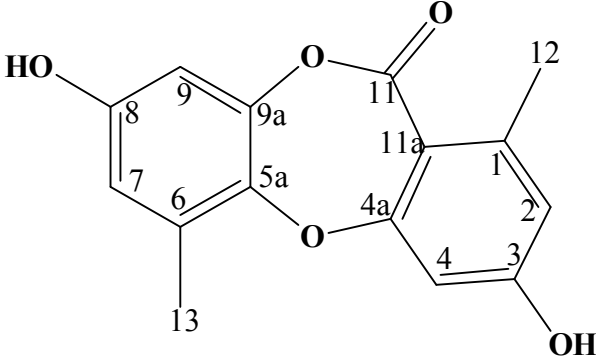
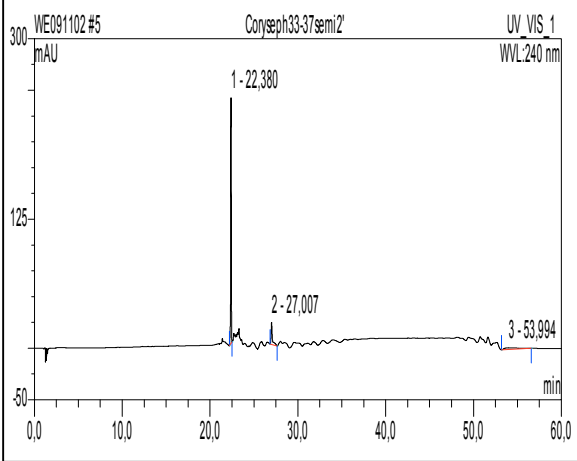
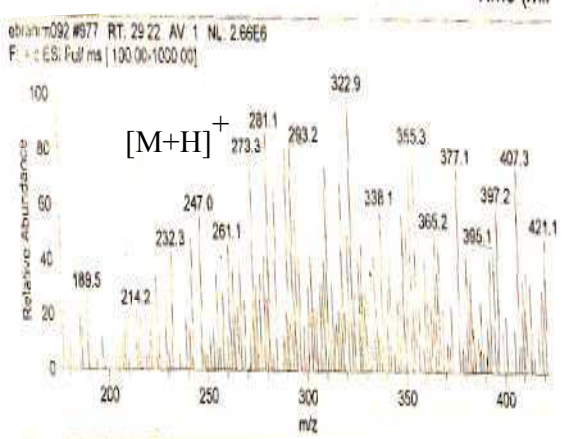
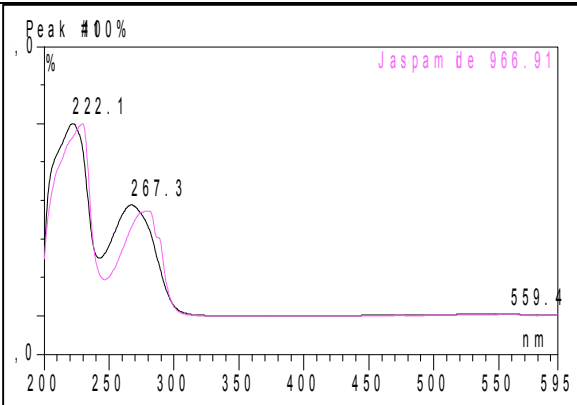
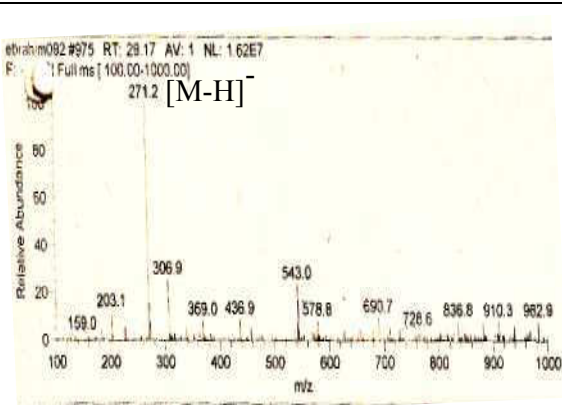


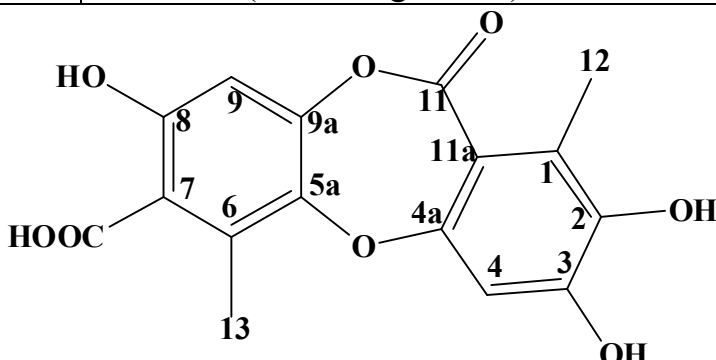
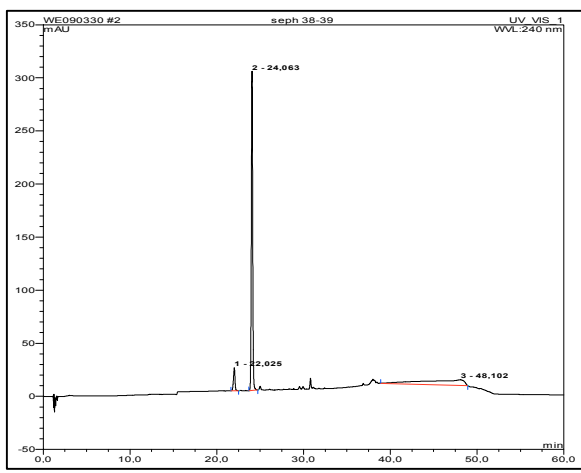
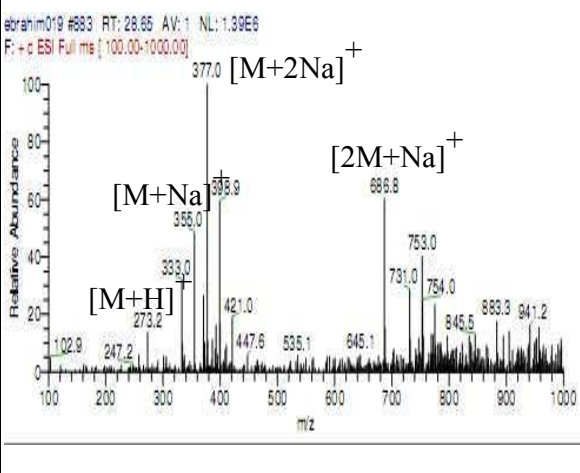
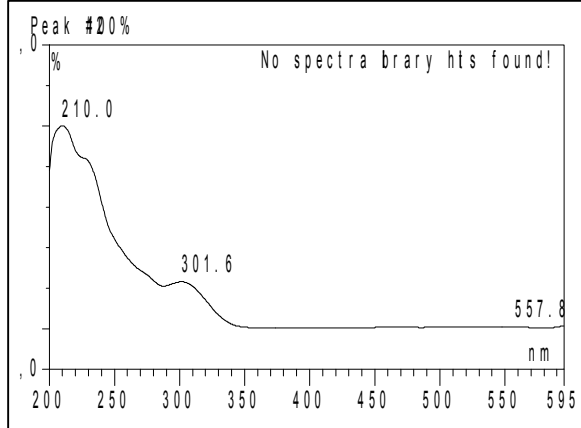
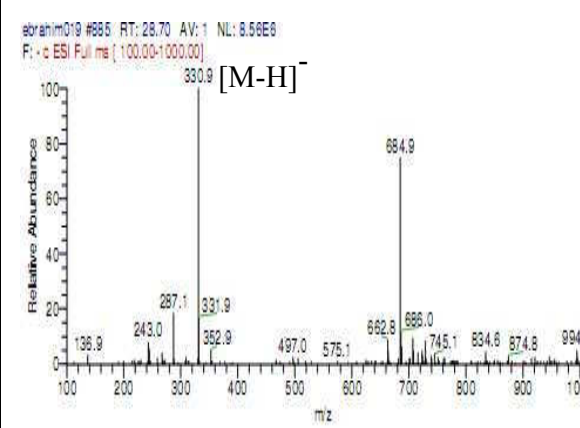
Fig. 3.11: COSY spectrum of compound 9.

3.1.10. Corynesidone A (10, known compound)

Corynesidone A	
Synonym(s)	3,8-dihydroxy-1,6-dimethyl-11 <i>H</i> -dibenzo [b,e] [1,4] dioxepin-11-one
Sample code	Corylseph3337semi 2'
Biological source	<i>Corynespora cassicola</i>
Sample amount	2 mg
Physical properties	brown amorphous solid
Molecular formula	C ₁₅ H ₁₂ O ₅
Molecular weight	272 g/mol
Retention time (HPLC)	22.3 min. (standard gradient)
	
	
	

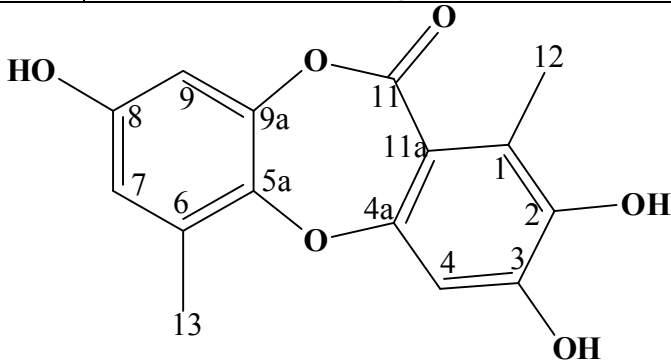
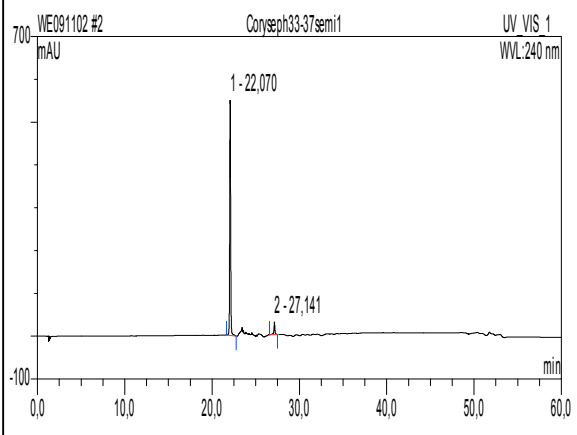
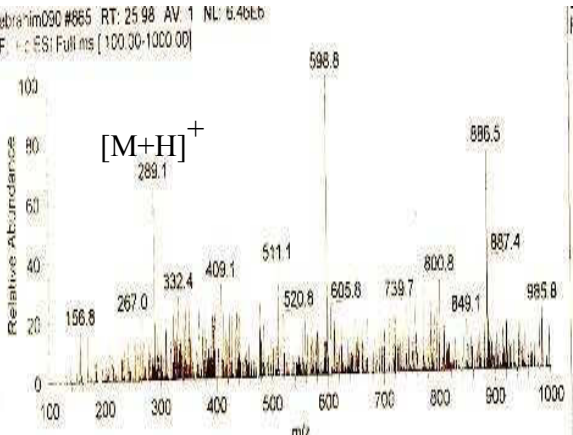
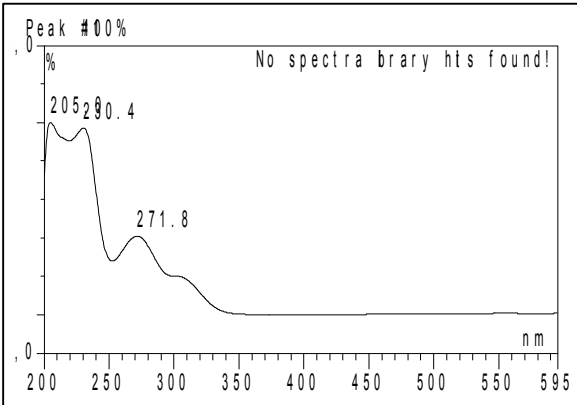
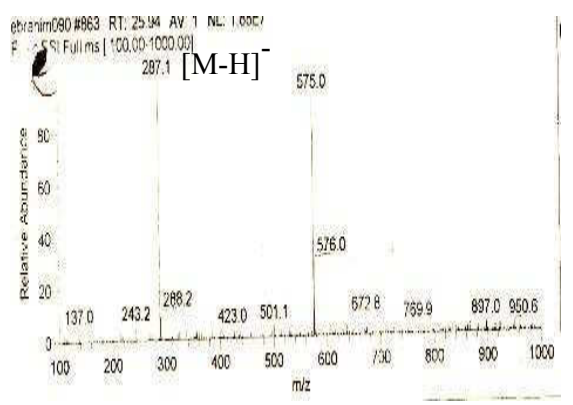
Corynesidone A **10** was isolated from the EtOAc extract of rice cultures of *Corynespora cassiicola* as a brown amorphous solid (2 mg). It showed UV absorbances at λ_{max} (MeOH) 222.1, 267.3 nm. Positive and negative ESI-MS showed molecular ion peaks at m/z 273.3 $[\text{M}+\text{H}]^+$ and m/z 271.2 $[\text{M}-\text{H}]^-$, respectively, indicating a molecular weight of 272 g/mol. The ^1H NMR spectra of **10** showed the presence of two pairs of *meta*-coupled protons (H-2 at δ_{H} 6.67 ppm, H-4 at δ_{H} 6.67 ppm, H-7 at δ_{H} 6.53 ppm and H-9 at δ_{H} 6.52 ppm) (Table 3.7). This was further confirmed by inspection of the COSY spectrum which showed two spin systems, the first one composed of H-9 at δ_{H} 6.52 ppm, H-7 at δ_{H} 6.53 ppm and 13-Me at δ_{H} 2.36 ppm, while the second one composed of H-4 at δ_{H} 6.67 ppm, H-2 at δ_{H} 6.67 ppm and 12-Me at δ_{H} 2.37 ppm. On the other hand, the HMBC spectrum confirmed attachment of the methyl group 12 to position 1 through the correlations of its proton to C-1, C-2 and C-11a. Also, the HMBC spectrum confirmed the attachment of the methyl group 13 to position 6 through the correlations to C-6, C-7 and C-5a. Further inspection of the HMBC spectrum revealed that H-2 correlates to C-3, C-11a and C-12, H-4 to C2, C-3 and C-11a, H-7 to C1, C-2 and C-11a and H-9 to C-5a, C-7, c-8 and C-9a. The structure was confirmed also by comparison with the literature (Chomcheon *et al.*, 2009).

3.1.11. Corynesidone B (11, known compound)

Corynesidone B	
Synonym(s)	3,8-dihydroxy-1,6-dimethyl-11 <i>H</i> -dibenzo [b,e] [1,4] dioxepin-11-one
Sample code	Corylseph2829
Biological source	<i>Corynespora cassiicola</i>
Sample amount	17 mg
Physical properties	brown amorphous solid
Molecular formula	C ₁₆ H ₁₂ O ₈
Molecular weight	332 g/mol
Retention time (HPLC)	24.1 min. (standard gradient)
	
	
	

Corynesidone B **11** was isolated from the EtOAc extract of rice cultures of *Corynespora cassiicola* as a brown amorphous solid (17 mg). It showed UV absorbances at λ_{max} (MeOH) 210, 301.6 nm. Positive and negative ESI-MS showed molecular ion peaks at m/z 333 $[\text{M}+\text{H}]^+$ and m/z 330.9 $[\text{M}-\text{H}]^-$, respectively, indicating a molecular weight of 332 g/mol. The ^1H NMR spectrum of **11** showed the presence of only two aromatic singlets (H-4 at δ_{H} 6.78 ppm and H-9 at δ_{H} 6.58 ppm) and two singlets attributed to two methyl groups (12-Me at δ_{H} 2.31 ppm and 13-Me at δ_{H} 2.70 ppm) (Table 3.7). On the other hand, the HMBC spectrum confirmed attachment of the methyl group 12 to position 1 through the correlations of its proton to C-1, C-2 and C-11a. Also, the HMBC spectrum confirmed the attachment of the methyl group 13 to position 6 through the correlations to C-6, C-7 and C-5a. Further inspection of HMBC spectrum revealed that H-4 correlates to C2, C-3, C-4a and C-11a and H-9 to C-5a, C-9a, C-7 and C-8. The structure was confirmed also by comparison with the literature (Chomcheon *et al.*, 2009).

3.1.12. Corynesidone D (12, new compound)

Corynesidone D	
Synonym(s)	2,3,8-trihydroxy-1,6-dimethyl-11 <i>H</i> -dibenzo [b,e] [1,4] dioxepin-11-one
Sample code	Corylseph3337semi 1
Biological source	<i>Corynespora cassiicola</i>
Sample amount	1.5 mg
Physical properties	brown amorphous solid
Molecular formula	C ₁₅ H ₁₂ O ₆
Molecular weight	288 g/mol
Retention time (HPLC)	22.1 min. (standard gradient)
	
	
	

Corynesidone B **12** was isolated from the EtOAc extract of rice cultures of *Corynespora cassiicola* as a brown amorphous solid (1.5 mg). It showed UV absorbances at λ_{max} (MeOH) 205, 230.4, 271.8 nm. Positive and negative ESI-MS showed molecular ion peaks at m/z 289.1 $[\text{M}+\text{H}]^+$ and m/z 287.1 $[\text{M}-\text{H}]^-$, respectively, indicating a molecular weight of 288 g/mol. The HRESI-MS exhibited a strong peak at m/z 289.0712 $[\text{M}+\text{H}]^+$ indicating the molecular formula $\text{C}_{15}\text{H}_{12}\text{O}_6$ (calculated 289.0712, Δ 0). The ^1H NMR spectra of both compounds were very similar, except for the presence of only one pair of *meta*-coupled protons in **12** (H-7 at δ_{H} 6.45 ppm and H-9 at δ_{H} 6.45 ppm) (Table 3.7) instead of the two pairs found for **10**. This was further confirmed by inspection of the COSY spectrum which showed only one spin system composed of H-9 at δ_{H} 6.45 ppm, H-7 at δ_{H} 6.45 ppm and 13-Me at δ_{H} 2.26 ppm. The singlet aromatic proton (H-4 at δ_{H} 6.68 ppm) showed a ω -correlation with the ester carbonyl group (C-1 at δ_{C} 128.6 ppm), and no correlation to the methyl group (12-Me) neither in the COSY nor HMBC spectra. On the other hand, the HMBC spectrum showed strong correlations (3J) of H-4 and the methyl group to carbons C-2 at δ_{C} 142.4 ppm and C-11a at δ_{C} 113.6 ppm. Thus the 16 amu increase in molecular weight and the downfield chemical shift of C-2 (δ_{C} 142.4 ppm) indicate the attachment of an additional hydroxyl group at this carbon. Hence **12** was a new natural product for which the name corynesidone D is proposed.

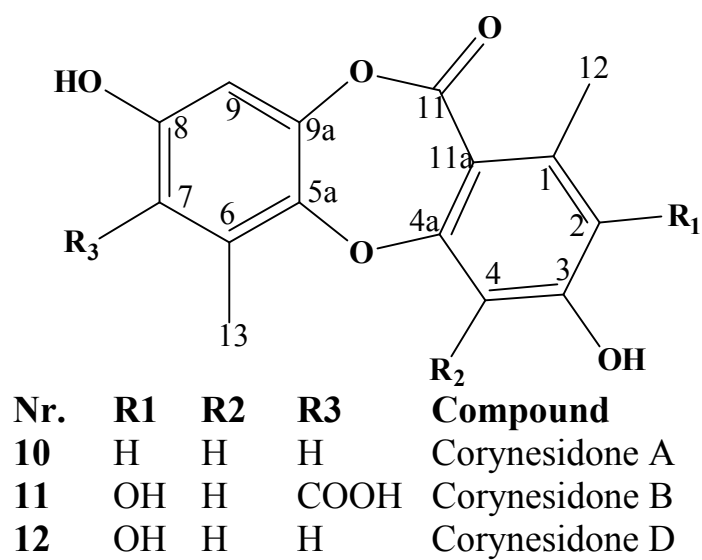


Table 3.7: ^1H , COSY and HMBC spectra of compounds **10**, **11** and **12**

Position	10				11				12		
	δ_{H}^*	$\delta_{\text{H}}^{\text{a},*}$	COSY	HMBC	δ_{H}^*	$\delta_{\text{H}}^{\text{b},*}$	COSY	HMBC	δ_{H}^*	COSY	HMBC
1											
2	6.67, br s	6.66, br s	4, 12	3, 11a, 12							
3											
4	6.67, br s	6.66, br s	2	2, 3, 11a	6.78, s	6.78, s		2, 3, 4a, 11a	6.68, s		2, 3, 4a, 11, 11a
4a											
5a											
6											
7	6.53, dd (2.8,0.7)	6.53, dd (2.8,0.7)	9, 13	5a, 8, 13					6.45, d (2.0)	9	5a, 8, 9, 13
8											
9	6.52, d (2.8)	6.52, d (2.8)	7	5a, 7, 8, 9a	6.58, s	6.64, s		5a, 9a, 7, 8	6.45, d (2.0)	7	5a, 7, 8, 9a
9a											
11											
11a			2	1, 2, 11a							
12	2.37, s	2.39, s			2.31, s	2.31, s		1, 2, 11a	2.25, s		1, 2, 11a
13	2.36, s	2.37, s	7	6, 7, 5a	2.70, s	2.70, s		6, 7 5a	2.26, s		5a, 6, 7
14											

* Measured in acetone- d_6
(a, b) (Chomcheon *et al.*, 2009)

Table 3.7a: ^{13}C NMR spectra of compounds **10**, **11** and **12**

Position	10		11		12
	$\delta_{\text{C}}^{\text{o},*}$	$\delta_{\text{C}}^{\text{a},*}$	δ_{C}^*	$\delta_{\text{C}}^{\text{b},*}$	δ_{C}^*
1	144.0	145.1	128.9	128.1	128.6
2	116.0	115.5	142.5	141.6	142.4
3	163.0	162.4	150.1	149.3	150.5
4	103.0	104.7	104.9	104.1	105.0
4a	161.0	161.5	155.8	155.0	156.6
5a	143.0	142.1	143.6	142.8	143.8
6	133.0	131.3	134.3	133.5	131.8
7	112.0	113.5	111.1	110.0	114.2
8	155.0	154.5	161.2	160.3	155.2
9	105.0	104.9	107.2	106.4	105.7
9a	143.0	144.9	150.4	149.4	146.0
11	162.0	163.3	162.6	161.6	163.6
11a	113.0	112.8	113.7	112.9	113.6
12	19.0	20.2	13.4	12.5	13.6
13	15.0	15.1	15.0	14.1	16.0
14			173.0	172.0	

* Measured in acetone- d_6

o) Extracted from HMBC

(a, b) (Chomcheon *et al.*, 2009)

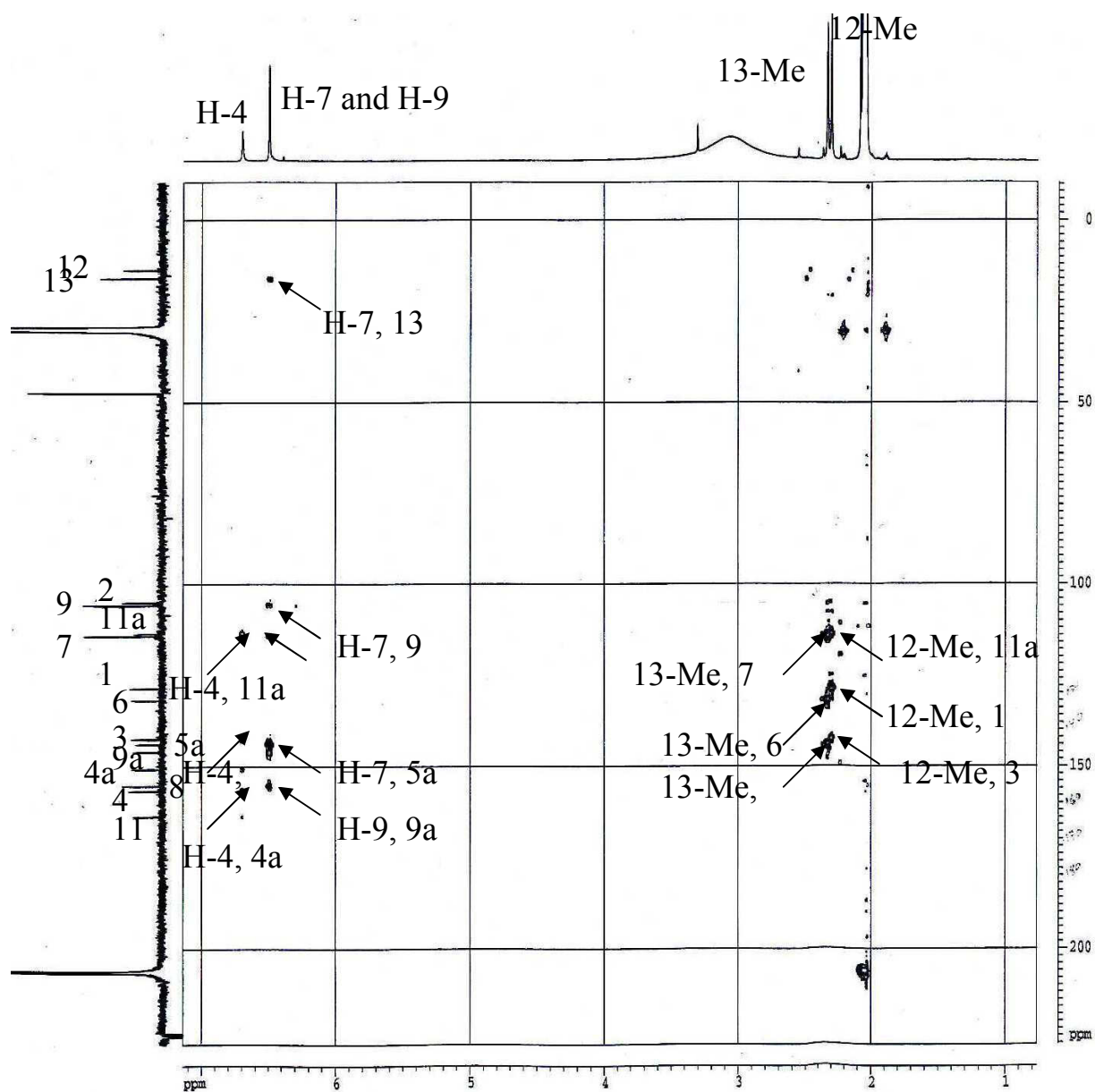
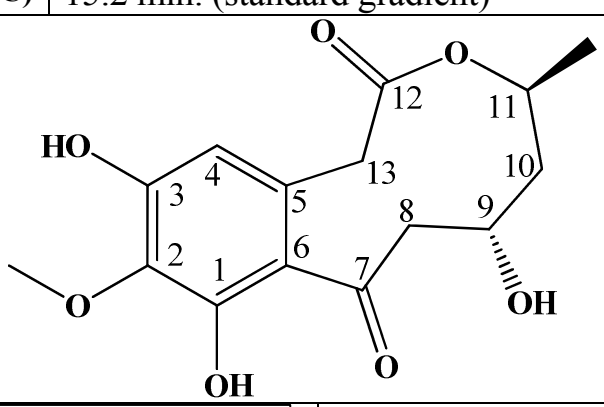
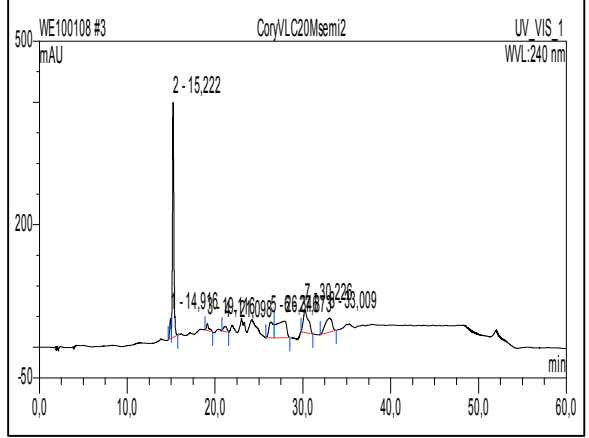
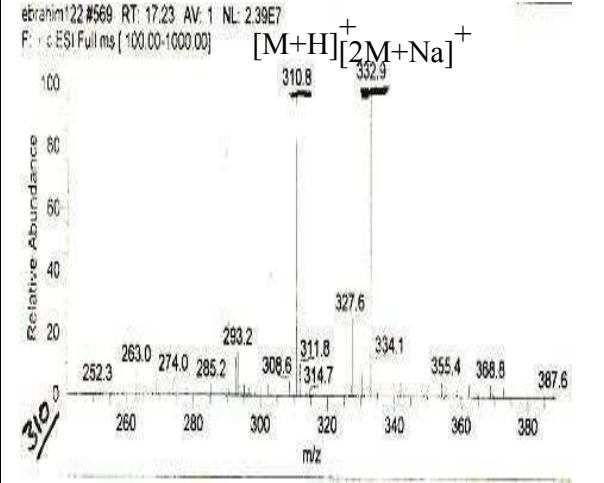
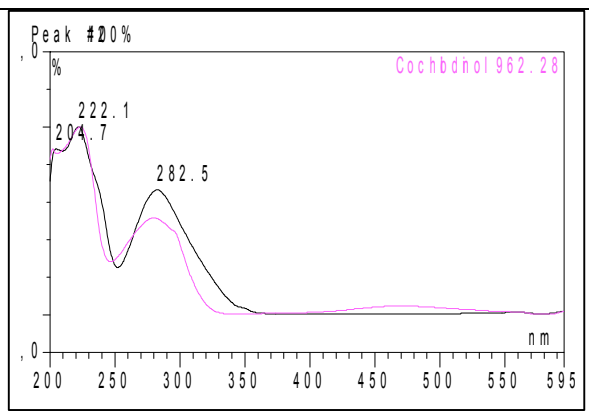
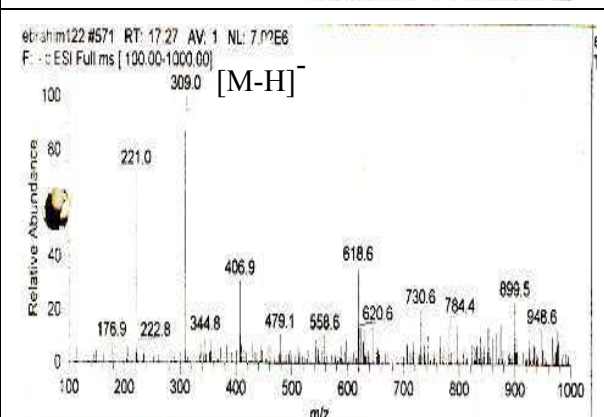


Fig. 3.12: HMBC spectrum of compound 12.

3.1.13. Xestodecalactone D (13, new compound)

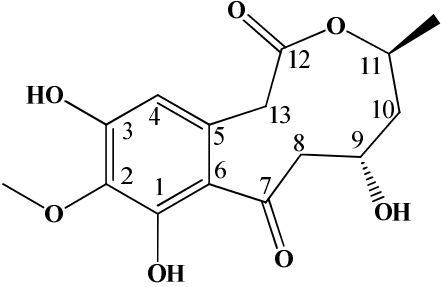
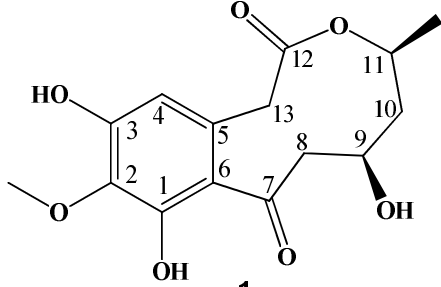
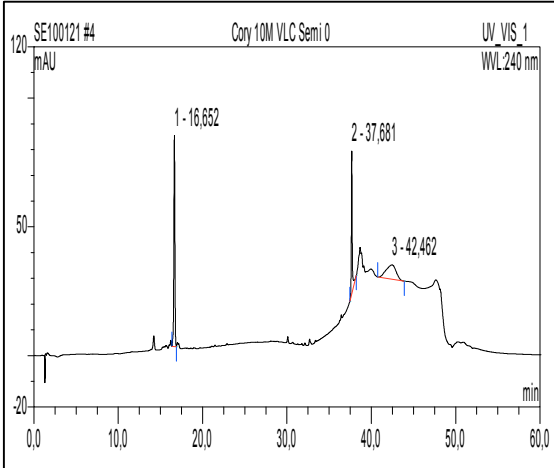
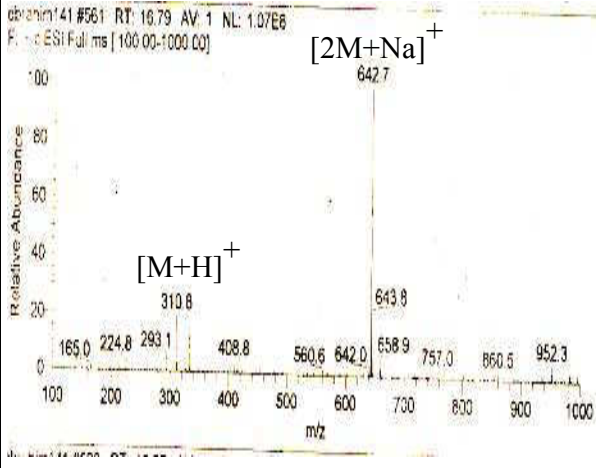
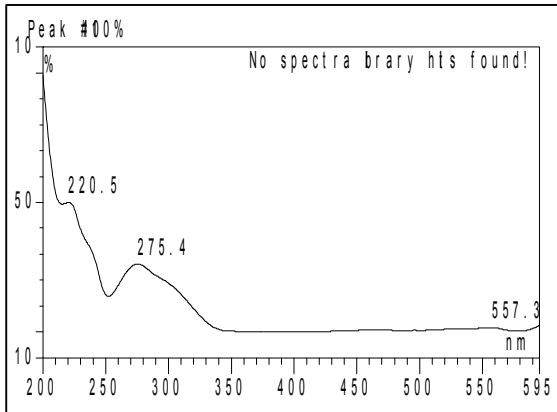
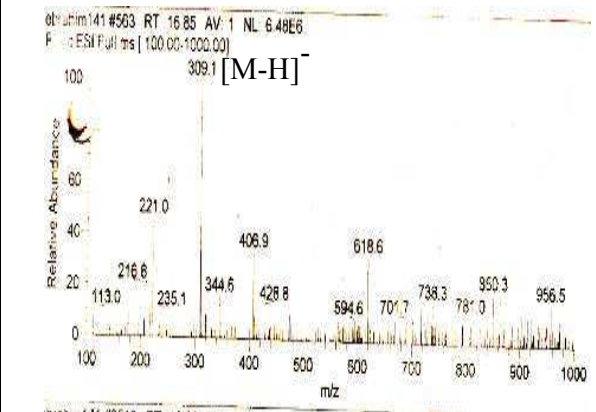
Xestodecalactone D	
Synonym(s)	(4R,6R)-6,9,11-trihydroxy-10-methoxy-4-methyl-4,5,6,7-tetrahydro-1 <i>H</i> -benzo[d]oxecine-2,8-dione
Sample code	CoryVLC10Msemi 2
Biological source	<i>Corynespora cassiicola</i>
Sample amount	2 mg
Physical properties	Yellowish white amorphous powder
Molecular formula	C ₁₅ H ₁₈ O ₇
Molecular weight	310 g/mol
Optical rotation $[\alpha]_D^{20}$	-25 (<i>c</i> 0.04, CHCl ₃)
Retention time (HPLC)	15.2 min. (standard gradient)
	
	
	

Xestodecalactone D **13** was isolated from the EtOAc extract of rice cultures of *Corynespora cassiicola* as a yellowish white amorphous powder (2 mg). It showed UV absorbances at λ_{\max} (MeOH) 204.7, 222.1, 282.5 nm. Positive and negative ESI-MS showed molecular ion peaks at m/z 310.8 $[M+H]^+$ and m/z 309.1 $[M-H]^-$, respectively, indicating a molecular weight of 310 g/mol. The HRESI-MS exhibited a strong peak at m/z 311.1134 $[M+H]^+$ indicating a molecular formula $C_{15}H_{18}O_7$ (calculated 311.1131, Δ 0.0003). Comparison of the NMR data of **13** with those reported for xestodecalactones B and C, previously isolated from *Penicillium cf. montanense* (Edrada *et al.*, 2002) indicated close structural relationship of the compounds. However, in comparison to xestodecalactones B and C (Edrada *et al.*, 2002) the 1H NMR spectrum of **13** showed an additional aromatic methoxyl group (δ_H 3.68 ppm) and absence of one aromatic proton. Inspection of the COSY correlations revealed the presence of a continuous spin system from CH_2 -8 (δ_H 3.45 and 2.66 ppm) to 11- CH_3 (δ_H 1.16 ppm) in analogy to known xestodecalactones (Edrada *et al.*, 2002). Moreover, a homonuclear long-range correlation was observed for CH_2 -13 (δ_H 3.54 ppm) to H-4 (δ_H 6.22 ppm) suggesting their neighboring positions. The attachment of the methoxyl group to the aromatic ring at C-2 (δ_C 134.1 ppm) was established based on their HMBC correlation. Moreover, diagnostic HMBC correlations of CH_2 -13 to C-4, C-5, C-6 and C-12, as well as of H-4 to C-2, C-3, C-6 and C-13 revealed the phenylacetic acid substructure of **13**. The observed downfield chemical shift of CH_2 -8 and its HMBC correlation to the carbonyl carbon appearing at δ_C 204.5 ppm (C-7) indicated its α -position to C-7. Additional correlations were observed for CH_2 -8 with C-9, CH_2 -10 (δ_H 1.76 and 1.87 ppm) with C-8 and C-9, H-11 (δ_H 4.81 ppm) with C-9, and 11- CH_3 with C-10 and C-11, thus establishing the fragment $CH_2(8)CH(9)OHCH_2(10)CH(11)CH_3$. The connection of C-7 to the aromatic ring was evident from the four bond long-range ω -correlation of H-4 to C-7. Furthermore, correlation of H-11 to the ester carbonyl group at δ_C 169.1 ppm

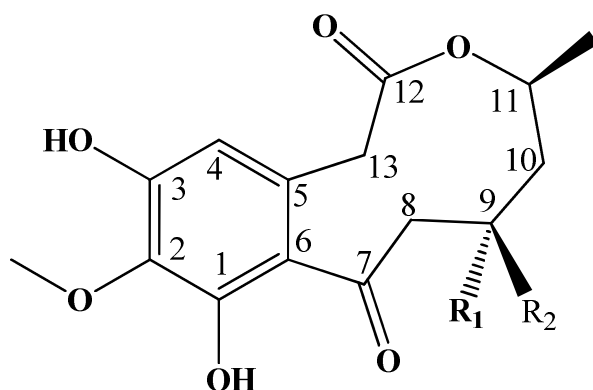
(C-12) indicated the linkage between C-12 and the oxygenated methine group CH-11 via an ester bond.

The relative configuration of **13** was obtained from a careful analysis of the coupling constants observed in the well resolved 1D ^1H NMR spectrum as well as from ROESY correlations (**13** in Fig. 3.21g). The coupling constants of H-8, 9, 10 were in accord with the lowest-energy computed conformation. The axial orientation of H-11 was evident from the large $^3J_{\text{H-11ax},\text{H-10ax}}$ value (6.7 Hz) showing the *trans diaxial* relationships of H-11_{ax} and H-10_{ax}. The three ROESY correlations of **13** shown in Fig. 3.21g and the coupling constants of H-9_{ax} in DMSO ($^3J_{\text{H-8ax},\text{H-9ax}} = 9.4$ Hz, $^3J_{\text{H-10ax},\text{H-9ax}} = 6.7$ Hz) agree well with the computed conformation, indicating the axial arrangement. For the determination of the absolute configuration, ECD calculation of the solution conformers and comparison with the solution experimental ECD curve were carried out, which was found earlier to be a powerful and reliable tool for this purpose. The measured solution ECD spectrum of **13** exhibited three Cotton effects (CEs) above 225 nm; a negative one at 316 and positive ones at 268 and 238 nm. The initial MMFF conformational search of **13** afforded 49 conformers, the DFT reoptimization of which at the B3LYP/6-31G (d) level reduced them to three above 1% population (Fig. 3.21a,b). The three conformers showed minor differences in the orientation of the phenolic hydroxyl and methoxyl groups, while the fused heterocycle adopted nearly the same conformation. Due to their similar conformations, the computed ECD spectra of the individual conformers were also quite similar. The Boltzmann-weighted average ECD spectra of (9*R*,11*R*)-**13** obtained by various functionals (B3LYP, BH&HLYP, PBE0) and TZVP basis set gave mirror image ECD curves of the experimental curve, which allowed the determination of the absolute configuration as (–)-(9*S*,11*S*)-**13** (Fig. 3.21a,b). Hence, **13** was identified as a new natural product for which the name xestodecalactone D is proposed.

3.1.14. Xestodecalactone D/E (13/14, new compounds)

Xestodecalactone D/E	
Synonym(s)	(4R,6R)-6,9,11-trihydroxy-10-methoxy-4-methyl-4,5,6,7-tetrahydro-1 <i>H</i> -benzo[d]oxecine-2,8-dione
Sample code	CoryVLC10Msemi 0
Biological source	<i>Corynespora cassiicola</i>
Sample amount	0.9 mg
Physical properties	Yellowish white amorphous powder
Molecular formula	C ₁₅ H ₁₈ O ₇
Molecular weight	310 g/mol
Retention time (HPLC)	16.7 min. (standard gradient)
<div style="display: flex; justify-content: space-around; align-items: center;"> <div style="text-align: center;">  <p>D</p> </div> <div style="text-align: center;">  <p>E</p> </div> </div>	
	
	

Compound **14** was obtained as a mixture with **13**. The ESIMS of the mixture exhibited a prominent peak at m/z 311.0 $[M+H]^+$, identical to that of **1**. The 1D and 2D COSY ^1H -NMR spectra of **14** (Table 3.8) were similar to those of **13**, except for the methylene protons CH_2 -10 (δ_{H} 1.65 and 1.75 ppm), H-8 α (δ_{H} 3.07 ppm), CH_2 -13 (δ_{H} 3.47 ppm), H-9 (δ_{H} 3.91 ppm), H-11 (δ_{H} 4.72 ppm), and H-4 (δ_{H} 6.19 ppm) that were upfield in **14** compared to **13**, whereas H-8 β (2.86 ppm) was to lower field. Even though a mixture was used, we were able to successfully determine the relative configuration of both compounds. The ROESY spectrum of **14** showed a diagnostically valuable through-space interaction between H-9 and H-11 indicating a *cis* position of these protons. Hence, **14** was identified as a diastereomer of **13** for which the name xestodecalactone E is proposed.



Nr.	R ₁	R ₂	Compound
13	OH	H	Xestodecalactone D
14	H	OH	Xestodecalactone E

Table 3.8: ^1H NMR, COSY and HMBC spectra of compounds **13** and **14**

Nr.	13				14		
	δ_{H}^*	$\delta_{\text{H}}^{\text{a},*}$	COSY	HMBC	δ_{H}^*	$\delta_{\text{H}}^{\text{b},*}$	COSY
1							
2		6.27, d (2.1)				6.27, d (2.2)	
3							
4	6.22, s	6.10, d (2.1)	13A, 13B	2, 3, 6, 13	6.19, s	6.11, d (2.2)	13A, 13B
5							
6							
7							
8	A 2.66, dd (9.4, 14.6) B 3.45, brdd (2.2, 14.6)	A 3.08, dd (10.4,15.1) B 2.81, br d (15.1)	8B, 9 8A, 9	7, 9 7, 9, 10	A 3.07, br. dd (4.7, 15.1) B 2.86, br. d (15.0)	3.48, br dd (2.6,14.5) 2.60, dd (9.5,14.4)	8B, 9 8A, 9
9	4.03, m	3.95, bt (10.0)	8A, 8B, 10A,B		3.91, m	4.02, m	8, 10
10	A 1.76, ddd (6.7, 7.3, 14.6) B 1.87, ddd (3.2, 4.0, 14.6)	A 1.65, ddd (9.8,11.4,14.5) B 1.83, br d (14.5)	10B, 9, 11 10A, 9, 11	8, 9 8, 9, 11	A 1.65, br. dd (3.2, 10.1) B 1.77, ddd (3.1, 6.8, 13.1)	1.73, ddd (3.2,6.9,14.6) 1.87, ddd (4.0,7.3,14.6)	10B, 9, 11 10A, 9, 11
11	4.81, ddq (4.0, 6.7, 6.5)	4.70, ddq (2.5,11.4,6.2)	10A, 10B, 14	9, 12	4.72, ddq (3.2, 11.5, 7.5)	4.81, ddq (4.3,6.4,6.4)	10, 14
12							
13	3.54, brs	A 3.48, d (18.7) B 3.82, d (19.0)	4	4, 5, 6, 12	3.47, br. s	3.53, d (17.3) 3.63, d (17.3)	4
11-Me	1.16, d (6.5)	1.08, d (6.2)	11	10, 11	1.09, d (6.3)	1.15, d (6.4)	11
2-OMe	3.68, s			2	3.67, s		
1-OH	9.32, s	9.98, s		1, 2, 6	9.30, br. s	9.8, s	
3-OH	9.71, s	9.87, s		2, 3, 4	9.70, br. s	9.8, s	
9-OH	4.75, d (5.0)	4.83, d (2.9)			4.75, d (5.3)		

* Measured in DMSO- d_6

a, b) (Edrada *et al.*, 2002)

Table 3.8a: ^{13}C NMR spectrum of compound **13**

Position	13	
	δ_{C}^*	$\delta_{\text{C}}^{\text{a},*}$
1	148.5	157.08
2	134.1	101.26
3	151.2	159.1
4	110.5	109.25
5	128.6	134.43
6	120.5	121.15
7	204.5	204.60
8	52.4	55.29
9	63.9	67.82
10	41.8	46.03
11	68.2	70.60
12	169.1	168.85
13	38.6	38.66
14	19.5	20.77
15	60	

* Measured in DMSO- d_6

a) (Edrada *et al.*, 2002).

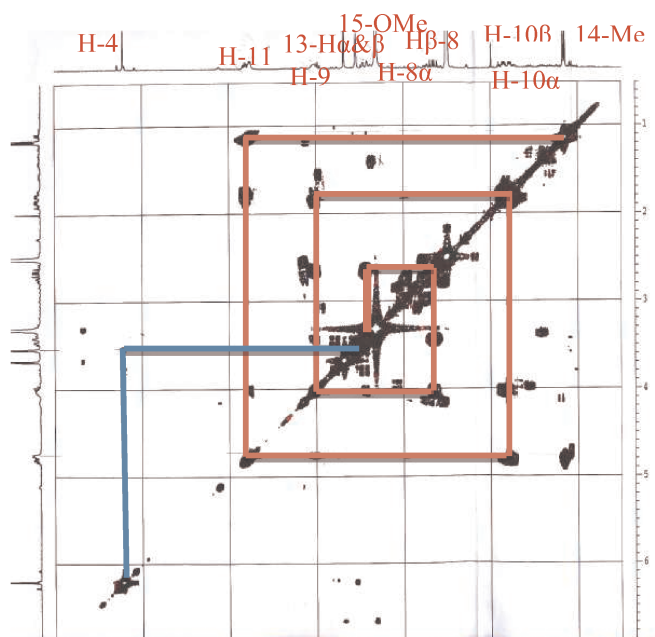


Fig. 3.13: COSY spectrum of compound 13.

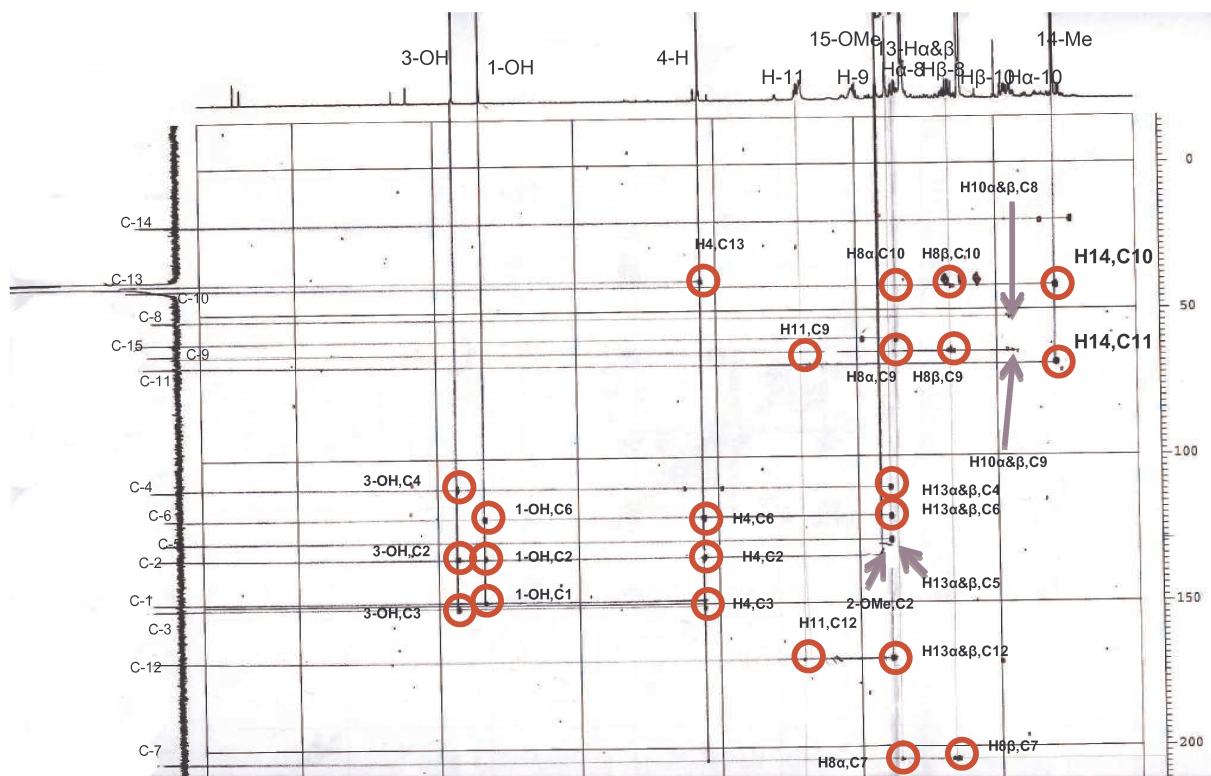


Fig. 3.14: HMBC spectrum of compound 13.

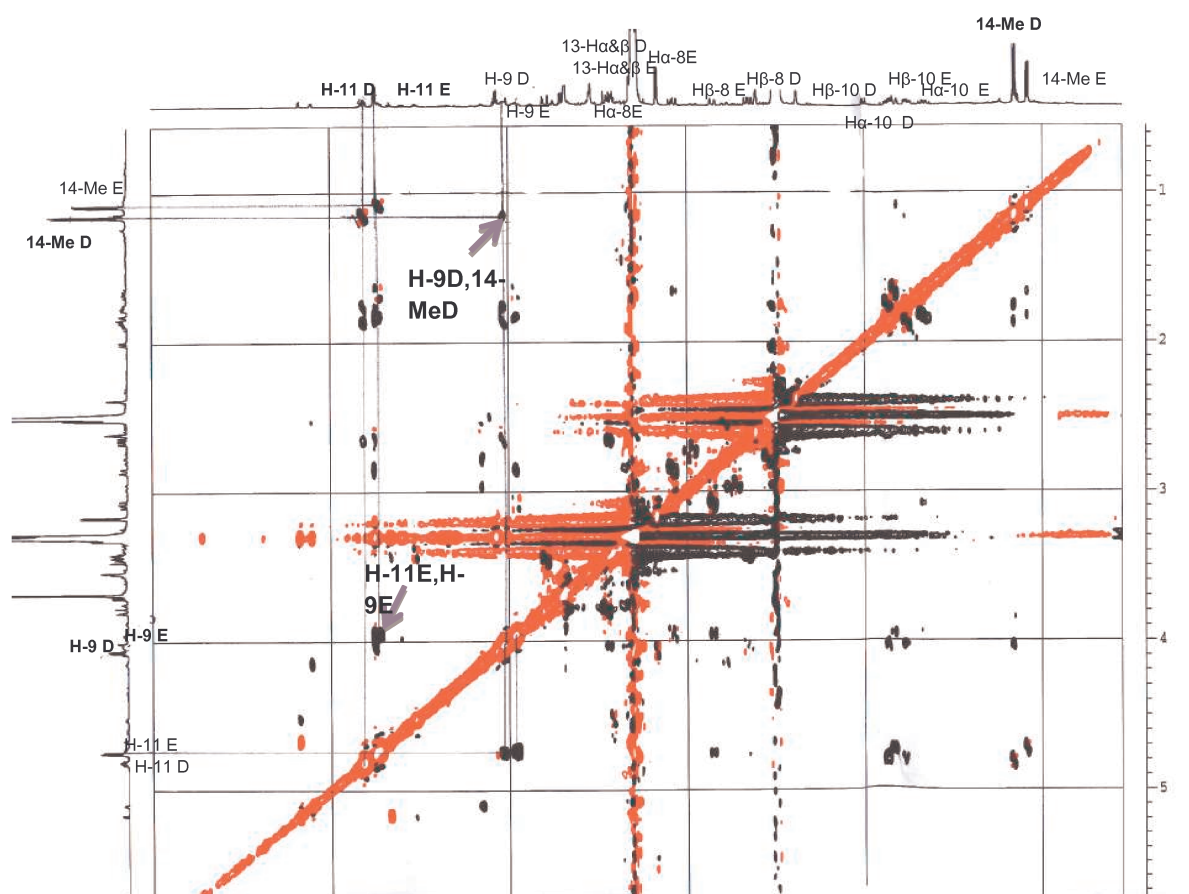
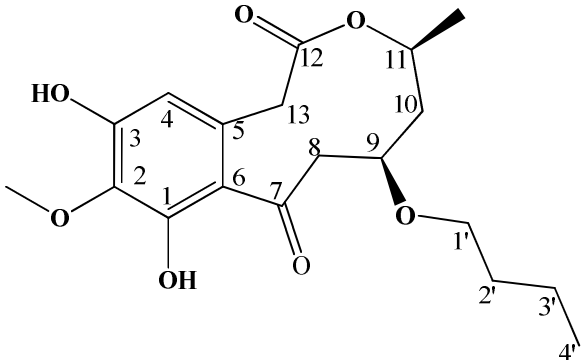
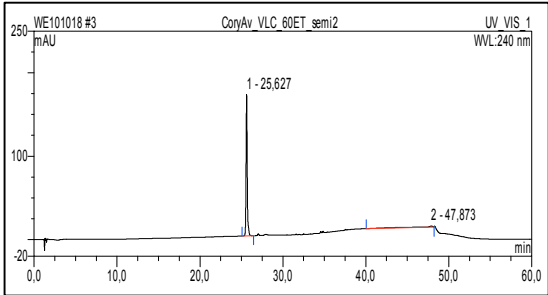
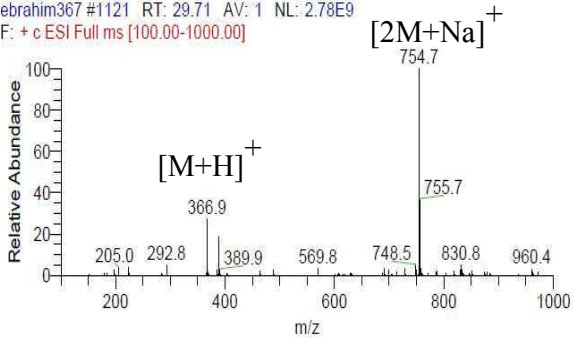
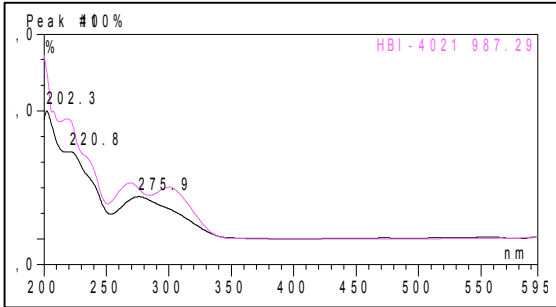
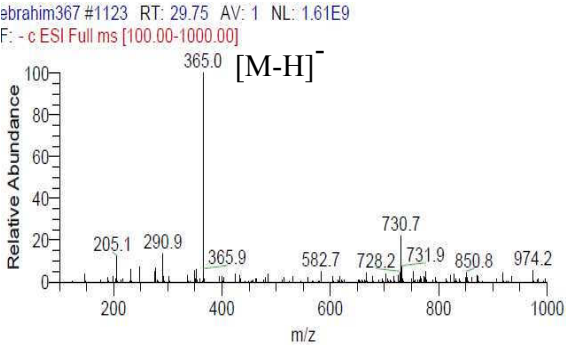


Fig. 3.15: ROESY spectrum of compounds **13** and **14**.

3.2.15. Xestodecalactone F (15, new compound)

Xestodecalactone F	
Synonym(s)	(4 <i>S</i> ,6 <i>R</i>)-6-butoxy-9,11-dihydroxy-10-methoxy-4-methyl-4,5,6,7-tetrahydro-1 <i>H</i> -benzo[d]oxecine-2,8-dione
Sample code	CoryAVVLC60ETsemi 3
Biological source	<i>Corynespora cassiicola</i>
Sample amount	3 mg
Physical properties	Brown amorphous solid
Molecular formula	C ₁₉ H ₂₆ O ₇
Molecular weight	366 g/mol
Optical rotation[α] _D ²⁰	+12 (c 0.115, CHCl ₃)
Retention time (HPLC)	25.6 min. (standard gradient)
	
	<p>ebrahim367 #1121 RT: 29.71 AV: 1 NL: 2.78E9 F: + c ESI Full ms [100.00-1000.00]</p> 
	<p>ebrahim367 #1123 RT: 29.75 AV: 1 NL: 1.61E9 F: - c ESI Full ms [100.00-1000.00]</p> 

Xestodecalactone F **15** was isolated from the EtOAc extract of rice cultures of *Corynespora cassiicola* as a brown amorphous solid (3 mg). It showed UV absorbances at λ_{max} (MeOH) 202.3, 220.8, 275.9 nm. Positive and negative ESI-MS showed molecular ion peaks at m/z 366.9 $[\text{M}+\text{H}]^+$ and m/z 365.0 $[\text{M}-\text{H}]^-$, respectively, indicating a molecular weight of 366 g/mol. The HRESI-MS exhibited a strong peak at m/z 367.1751 $[\text{M}+\text{H}]^+$ indicating the molecular formula $\text{C}_{19}\text{H}_{26}\text{O}_7$ (calculated 367.1752, Δ 0.0001) with an increase of 56 amu compared to **13**. ^1H NMR data of **2** (Table 3.9) were quite comparable to those of **13**, thus indicating a structural resemblance between both compounds. Common signals were attributed to one aromatic proton (δ_{H} 6.21 ppm, H-4), a methoxyl group (δ_{H} 3.69 ppm, 2-OCH₃), two aromatic hydroxyl groups (δ_{H} 9.36 and 9.73 ppm, assigned for 1- and 3-OH, respectively), and a methylene group (δ_{H} 3.46 and 3.78 ppm, CH₂-13). The COSY spectrum revealed the presence of a similar spin system from CH₂-8 (δ_{H} 3.04 and 2.93 ppm) to 11-CH₃ (δ_{H} 1.10 ppm) as in **1**, but lacking the signal corresponding to 9-OH. Further inspection of the COSY spectrum indicated an additional spin system extending from CH₂-1' (δ_{H} 3.41 ppm) to CH₃-4' (δ_{H} 0.88 ppm), which was attributed to a *n*-butyl side chain accounting for the difference in the molecular weight between **13** and **15** (56 amu). As in **13**, the homonuclear long-range correlation of CH₂-13 to H-4 was detected. The HMBC experiment confirmed the attachment of the methoxyl group at C-2, and established the phenylacetic acid substructure of **15** by diagnostic correlations of CH₂-13 and H-4 in analogy to **13**. Further inspection of the HMBC spectrum (Table 3.9) corroborated the attachment of CH₂-8 to the carbonyl carbon appearing at δ_{C} 204.1 ppm (C-7), and established the fragment CH₂(8)CH(9)CH₂(10)CH(11)CH₃ through correlations of CH₂-8 to C-9, CH-9 (δ_{H} 3.68 ppm) to C-1' and C-11, CH₂-10 (δ_{H} 1.67 and 1.94 ppm) to C-8 and C-9, H-11 (δ_{H} 4.75 ppm) to C-9, and 11-CH₃ to C-10 and C-11. The four bond long-range ω -correlation of H-4 to C-7, and the correlation of H-11 to the ester

carbonyl at C-12 (δ_{C} 168.8 ppm) established the connection of the detected substructures. Moreover, correlation of CH₂-1' (δ_{H} 3.41 ppm) to C-9 (δ_{C} 76.1 ppm) indicated that the *n*-butyl moiety was attached to C-9 through an ether linkage.

Since the coupling constants extracted from ¹H NMR spectrum of **15** and the ROESY correlations (Fig. 3.18 and 3.18a) were similar to those of xestodecalactone B (Edrada *et al.*, 2002) the relative configuration of **15** was assigned as *cis*. H-9 and H-11 were found to have an axial orientation from their large vicinal coupling constants ($^3J_{\text{H-8ax,H-9ax}} = 10.1$ Hz, $^3J_{\text{H-10ax,H-11ax}} = 11.5$ Hz). Furthermore, a diagnostic ROESY correlation was observed for H-9 to H-11 indicating their 1,3-*cis* orientation and implying the (9*R**,11*S**) relative configuration as shown for **15** in Fig. 3.18 and 3.18a. The structures of all the computed conformers are fully in accordance with the NMR data. The solution ECD spectrum of **15** was very similar to that of (9*S*,11*S*)-**13**. A solution ECD calculation protocol was pursued on the 9-methoxyl model compound of **15** which revealed the chiral center was inverted compared to those of (9*S*,11*S*)-**13**. The MMFF conformational search and DFT optimization provided five major conformers above 3% population (Fig. 3.21c,d). H-9 and H-11 adopted *pseudo-axial* orientation in all conformers, in which the conformation of the fused heterocycle was practically the same and they differed mainly in the arrangement of the hydroxyl and methoxyl groups. The Boltzmann-weighted TZVP ECD spectra (B3LYP, BH&HLYP, PBE0 functionals) of the conformers of the (9*R*,11*S*) enantiomer reproduced well the experimental ECD curve with B3LYP giving the best agreement (Fig. 3.21c). Thus, the absolute configuration of **15** was determined as (+)-(9*R*,11*S*) and it was named xestodecalactone F. Apparently, the inversion of the C-9 chirality center did not have a significant effect on the ECD spectra.

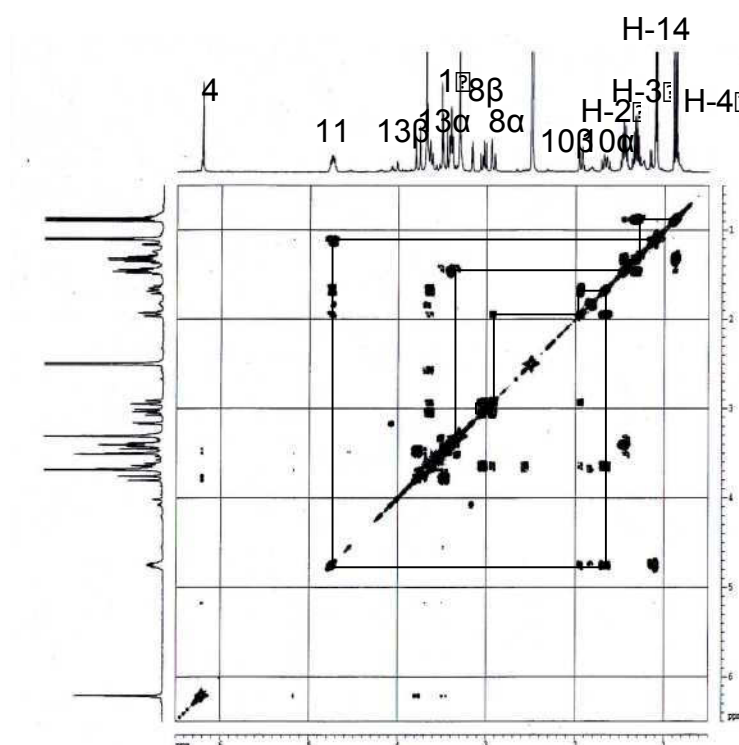


Fig. 3.16: COSY spectrum of compound 15.

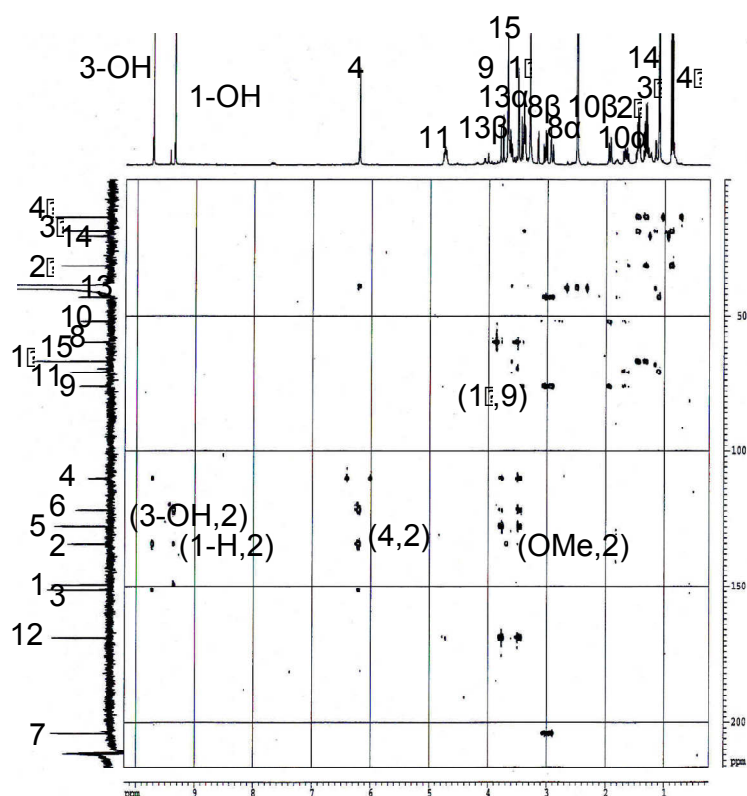


Fig. 3.17: HMBC spectrum of compound 15.

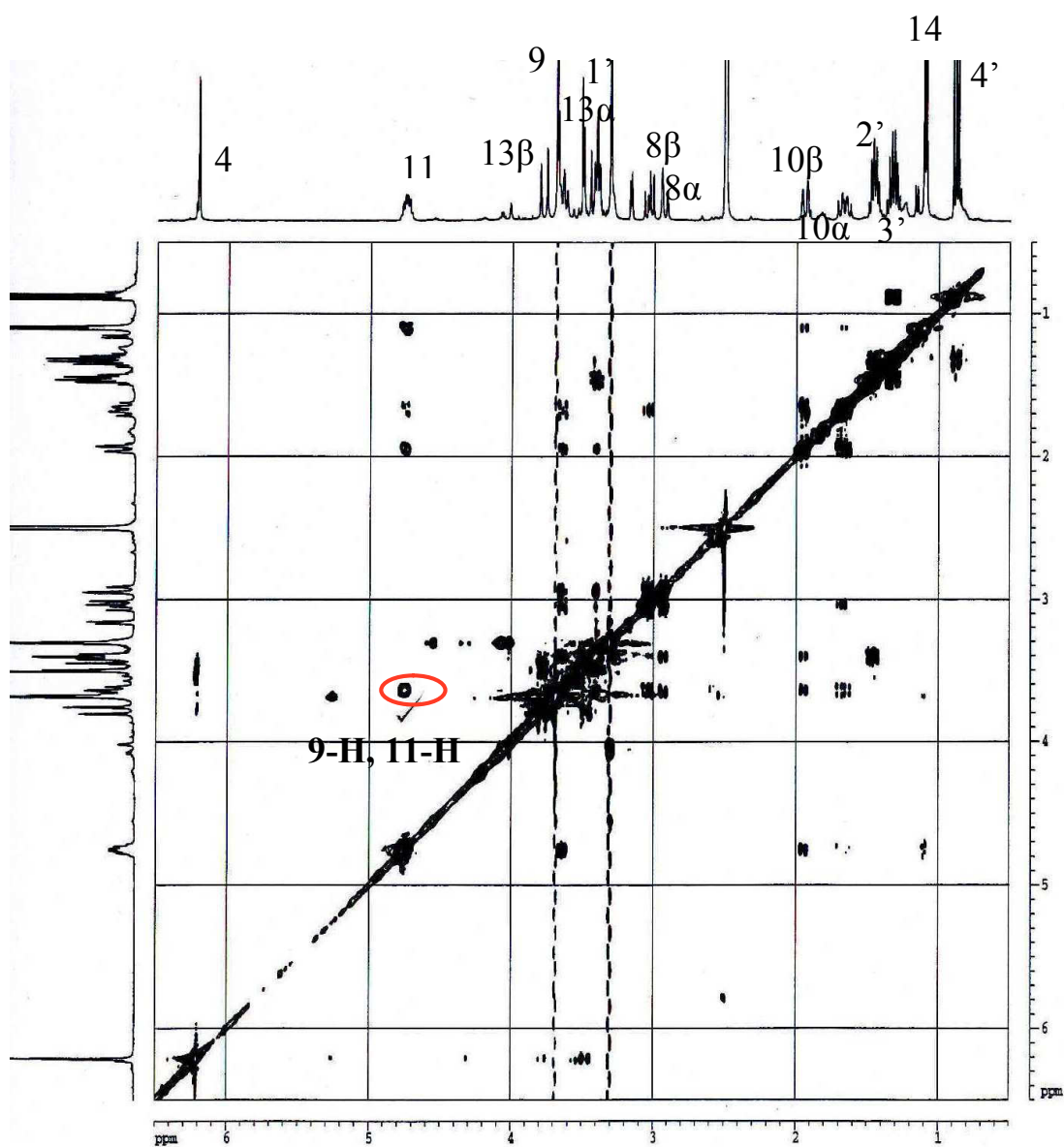


Fig. 3.18: ROESY spectrum of compound 15.

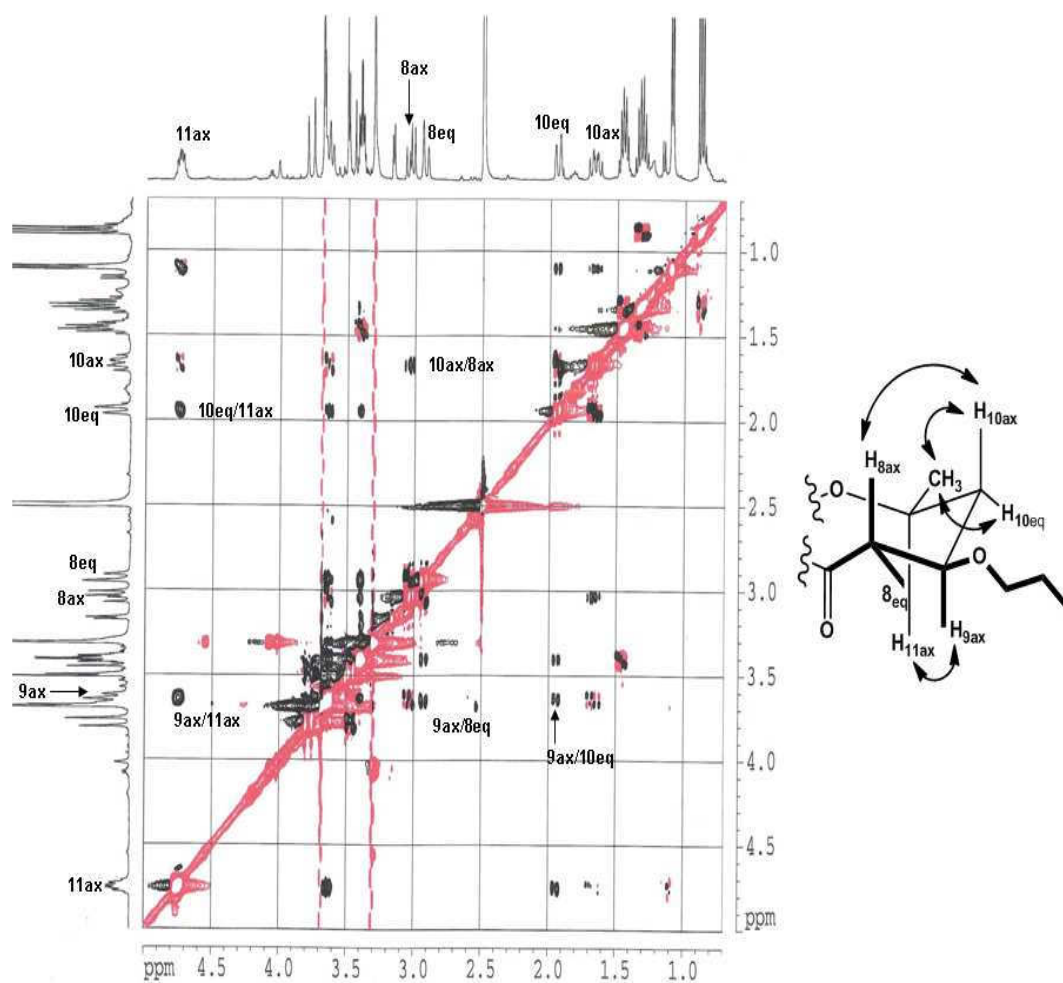
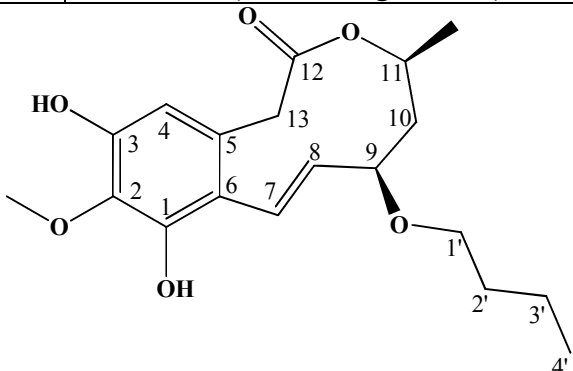
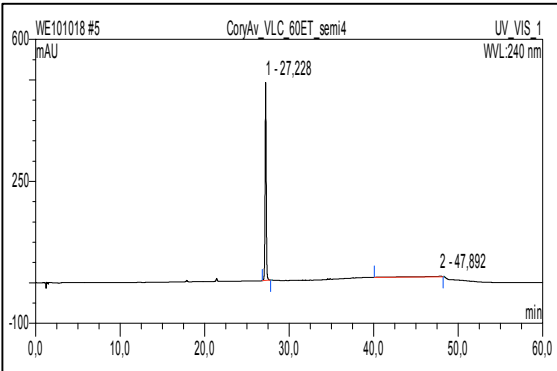
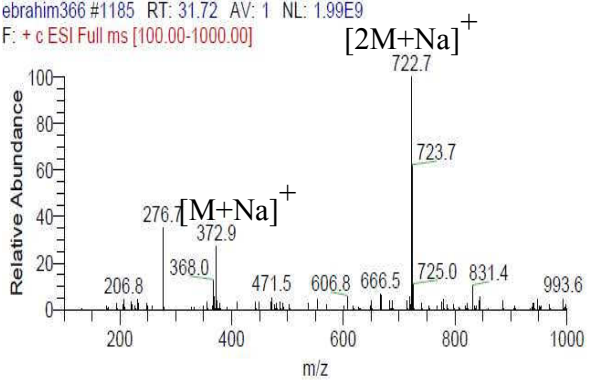
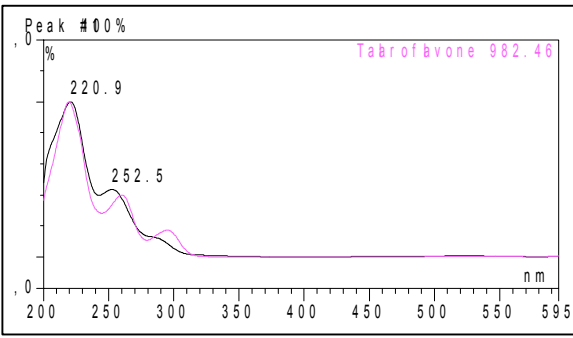
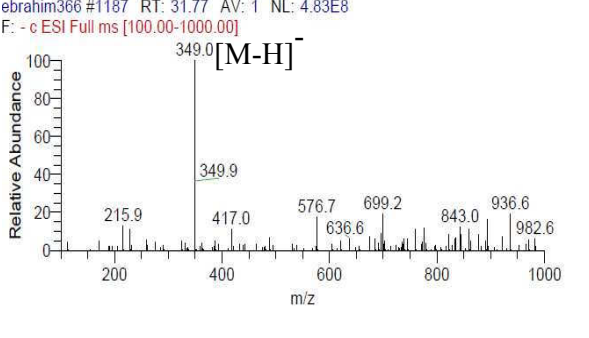


Fig. 3.18a: Important ROESY correlations showing the relative configuration of **15**.

3.2.16. Xestodecalactone G (16, new compound)

Xestodecalactone G	
Synonym(s)	(4 <i>S</i> ,6 <i>R</i> , <i>E</i>)-6-butoxy-9,11-dihydroxy-10-methoxy-4-methyl-5,6-dihydro-1 <i>H</i> -benzo[d]oxecin-2(4 <i>H</i>)-one
Sample code	CoryAVVLC60ETsemi 4
Biological source	<i>Corynespora cassiicola</i>
Sample amount	2.5 mg
Physical properties	Brown amorphous solid
Molecular formula	C ₁₉ H ₂₆ O ₆
Molecular weight	350 g/mol
Optical rotation [α] _D ²⁰	−180 (<i>c</i> 0.04, CHCl ₃)
Retention time (HPLC)	27.2 min. (standard gradient)
	
	
	

Xestodecalactone **G 16** was isolated from the EtOAc extract of rice cultures of *Corynespora cassiicola* as a brown amorphous solid (2.5 mg). It showed UV absorbances at λ_{max} (MeOH) 220.9, 252.5 nm. Positive and negative ESI-MS showed molecular ion peaks at m/z 372.9 $[\text{M}+\text{Na}]^+$ and m/z 349.0 $[\text{M}-\text{H}]^-$, respectively, indicating a molecular weight of 350 g/mol. The HRESI-MS exhibited a strong peak at m/z 373.1618 $[\text{M}+\text{Na}]^+$ indicating the molecular formula $\text{C}_{19}\text{H}_{26}\text{O}_6$ (calculated 373.1627, Δ 0.0009). ^1H NMR data of **16** (Table 3.10) showed familiar features as observed for **13** and **15** including one aromatic proton (δ_{H} 6.14 ppm), a methoxyl group (δ_{H} 3.66 ppm), two aromatic hydroxyl groups (δ_{H} 8.65 and 9.22 ppm, assigned for 1- and 3-OH, respectively), a methylene group (δ_{H} 3.29 and 3.76 ppm, CH_2 -13), and signals attributed to the *n*-butyl side chain from CH_2 -1' (δ_{H} 3.27 and 3.42 ppm) to CH_3 -4' (δ_{H} 0.86 ppm). Inspection of the COSY correlations confirmed the presence of the latter spin system, and showed the diagnostic homonuclear long-range correlation of CH_2 -13 to H-4. They further revealed an additional continuous spin system from the olefinic CH-7 (δ_{H} 6.18 ppm) to 11- CH_3 (δ_{H} 1.20 ppm). In analogy to **13** and **15**, the HMBC experiment corroborated the attachment of the methoxyl group at C-2, the phenylacetic acid substructure of **16**, the ester bond linkage between C-12 (δ_{C} 172.9 ppm) and the oxygenated methine group at C-11 (δ_{H} 4.84 ppm), as well as the attachment of the *n*-butyl side chain to C-9 (δ_{C} 79.9 ppm) through an ether linkage. Further inspection of the HMBC spectrum indicated correlations of CH-7 (δ_{H} 6.18 ppm) with C-1, C-5, C-6 and C-8, CH-8 (δ_{H} 5.46 ppm) with C-7 and C-9, CH-9 (δ_{H} 3.84 ppm) with C-1', C-7 and C-10, CH_2 -10 (δ_{H} 1.77 and 2.00 ppm) with C-8 and C-9, CH-11 (δ_{H} 4.84 ppm) with C-9, and 11- CH_3 with C-10 and C-11. Accordingly, the fragment $\text{CH}(7)\text{CH}(8)\text{CH}(9)\text{CH}_2(10)\text{CH}(11)\text{CH}_3$ was established, indicating a possible reduction of the *keto*-substituent at C-7 in **15** followed by dehydration at the same bond. Attachment of the macrocycle to the aromatic ring at C-6 was deduced from correlations of CH-7 to C-6, C-1 and C-5.

As with **13** and **15**, the relative configuration of **16** was determined from an analysis of the coupling constants and ROESY correlations. The axial orientations of protons H-9 and H-11 were evident from their large 3J values ($^3J_{\text{H-8ax,H-9ax}} = 9.5$ Hz, $^3J_{\text{H-10ax,H-11ax}} = 10.8$ Hz). Moreover, H-9 showed a diagnostic through-space correlation with H-11, an indication of the *cis* orientation of H-9 and H-11 as found in **15**. In addition, the 1,3-*cis* *di*axial relationship of H-9 and H-11 was found in all of the four computed low-energy conformers. The experimental ECD spectrum of **16** was completely different from those of **13** and **15** due to a different chromophore system. There were three negative CEs at 287, 250 and 216 nm and the 316 nm band was missing. The MMFF conformational search and DFT reoptimization of the 9-OMe model compound afforded four major conformers above 2% populations (Fig. 3.21e). The Boltzmann-weighted ECD spectra of the (9*R*,11*S*) model compound showed a good agreement with the experimental solution ECD curve (Fig. 3.21e), which proved that **16** is homochiral with **15**, *i.e.* it has a (–)-(9*R*,11*S*) absolute configuration. Compound **16** was hence identified as a new natural product for which the name xestodecalactone G was proposed. The new optically active natural products **13**, **15** and **16** have the same (11*S*) absolute configuration and their stereochemistry differed in the configuration of the C-9 chiral center. The ECD spectra of **13** and **15** are mirror image compared to those of the related xestodecalactones A-C, which confirms that the former belongs to the (11*S*) series, while the latter belongs to the (11*R*) one.

In fact only compound **13** showed a *trans* configuration of H-9 and H-11, while **15** and **16** showed a *cis* relationship (Fig. 3.21g). However, the *cis*-isomer of **13** (**14**) was also detected, albeit in a mixture with **13**. Upon measuring the ROESY spectrum of the mixture of both isomers, a clear cross peak between H-9 and H-11 was observed only for the *cis* isomer **14**. This indicates the presence of both stereoisomers, as previously described for other derivatives, (Edrada *et*

al., 2002) yet the low amount of the fraction available (0.9 mg) did not permit purification of the *cis* isomer **14**.

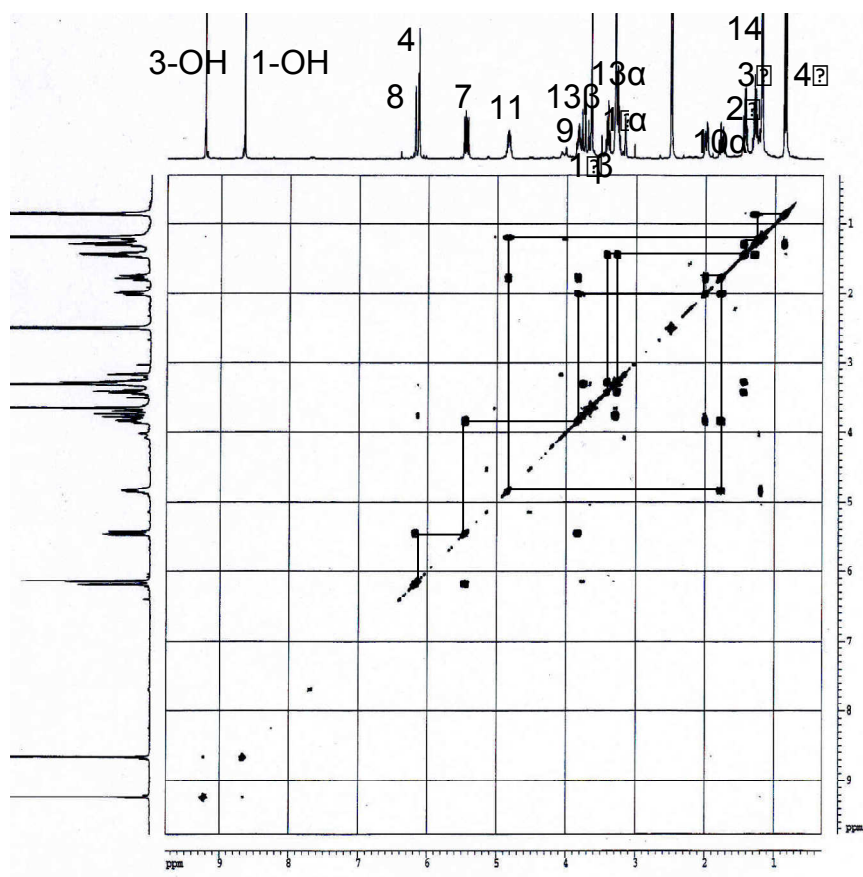


Fig. 3.19: COSY spectrum of compound 16.

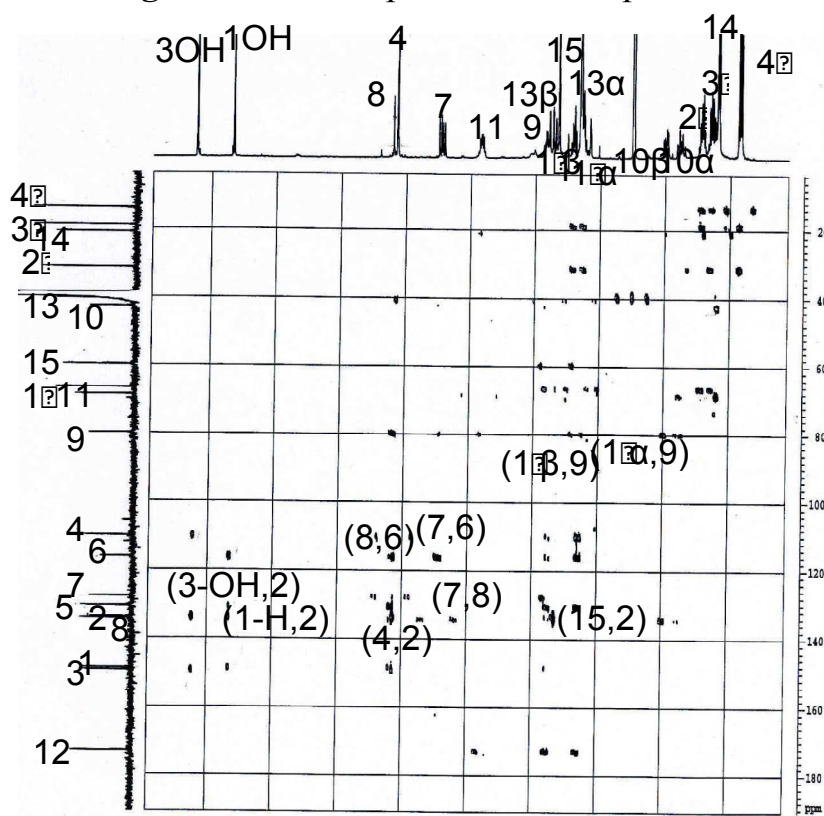


Fig. 3.20: COSY spectrum of compound 16.

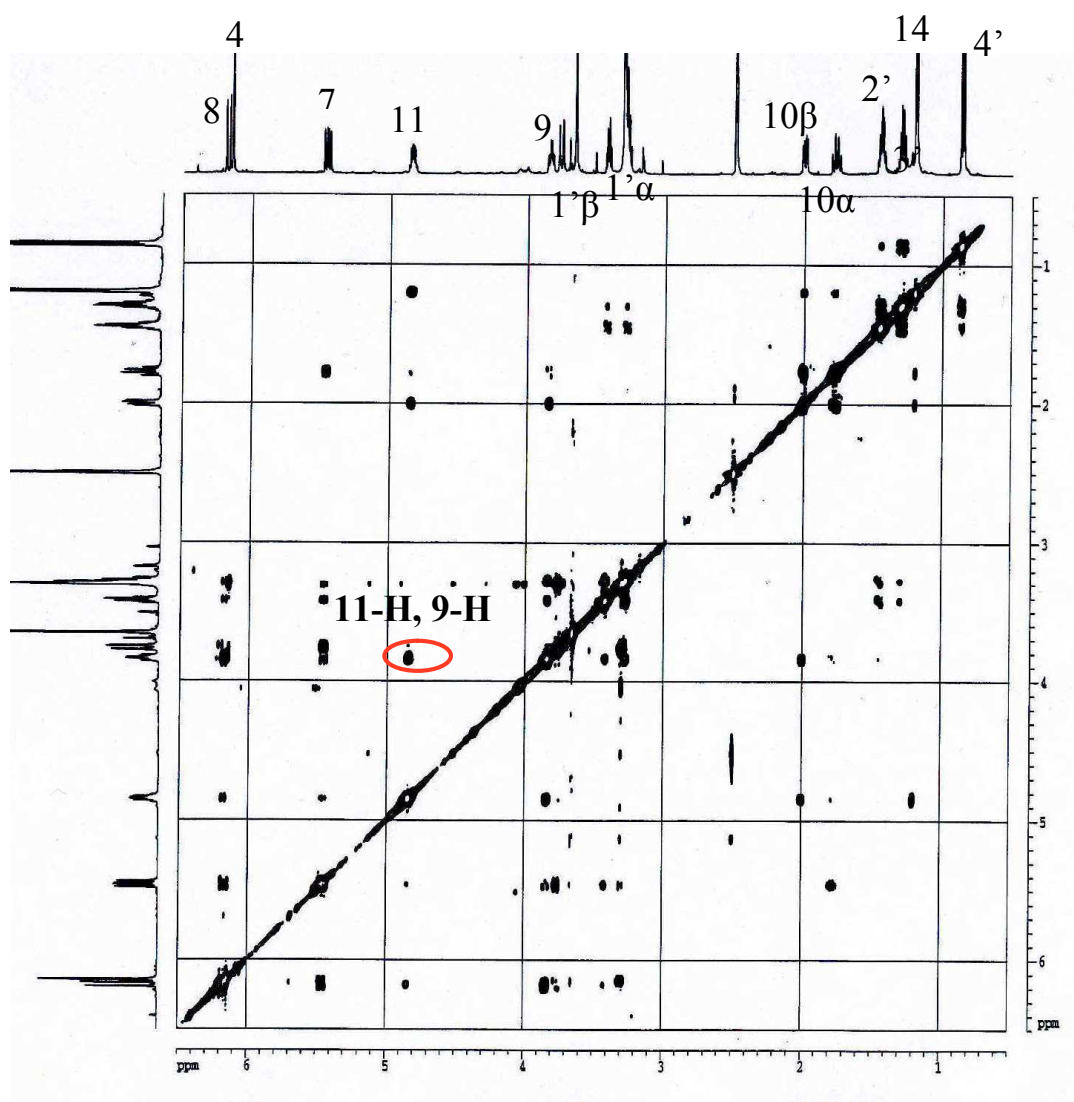


Fig. 3.21: ROESY spectrum of compound 16.

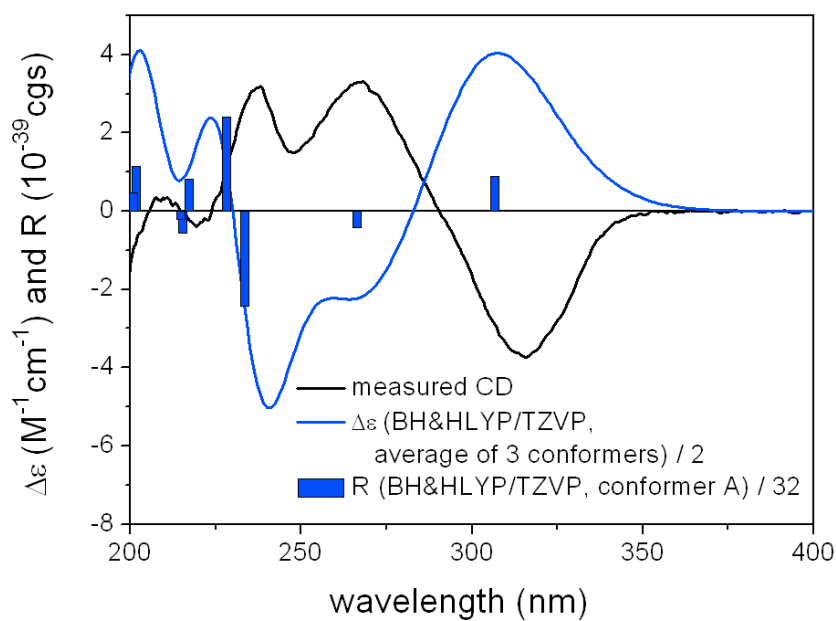


Fig. 3.21a. Experimental ECD spectrum of **13** in acetonitrile compared with the Boltzmann-weighted BH&HLYP/TZVP spectrum calculated for the three lowest-energy conformers of (9*R*,11*R*)-**13**. Bars represent rotatory strength of the lowest-energy conformer.

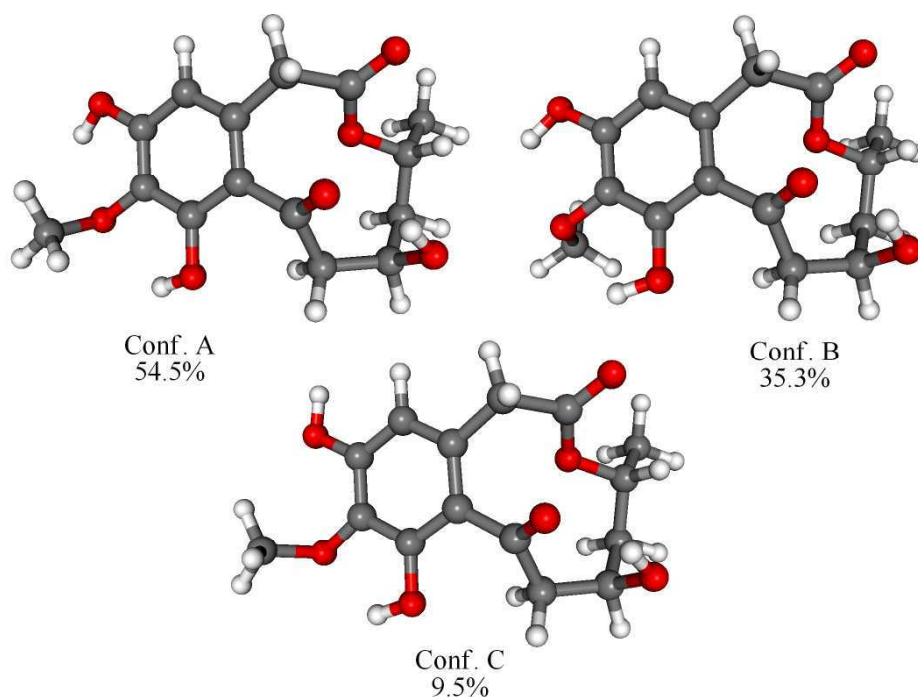


Fig. 3.21b. DFT optimized geometries of the three lowest-energy conformers of (9*R*,11*R*)-**13**.

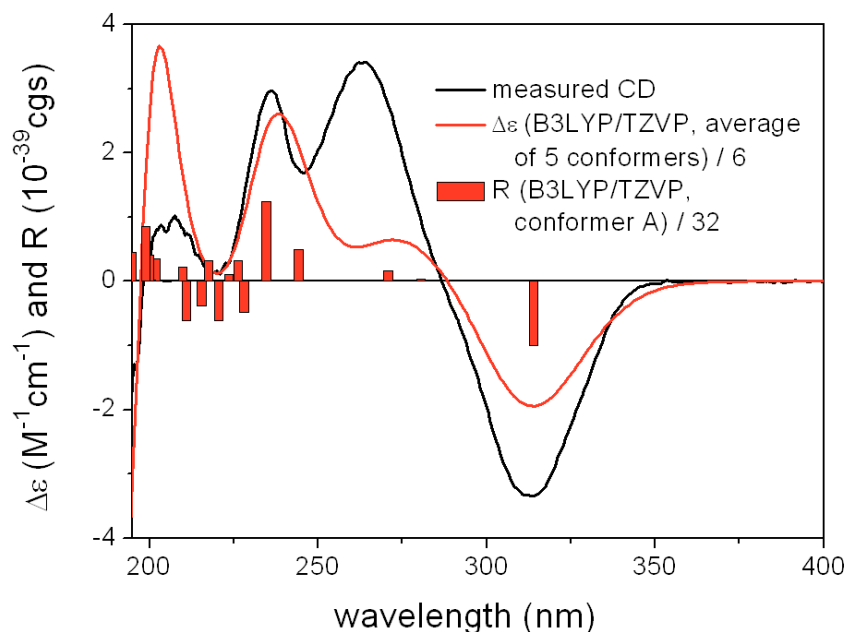


Fig. 3.21c. Experimental ECD spectrum of **15** in acetonitrile compared with the Boltzmann-weighted B3LYP/TZVP spectrum calculated for the five lowest-energy conformers of the truncated model of the (9*R*,11*S*)-enantiomer. Bars represent rotatory strength of the lowest-energy conformer.

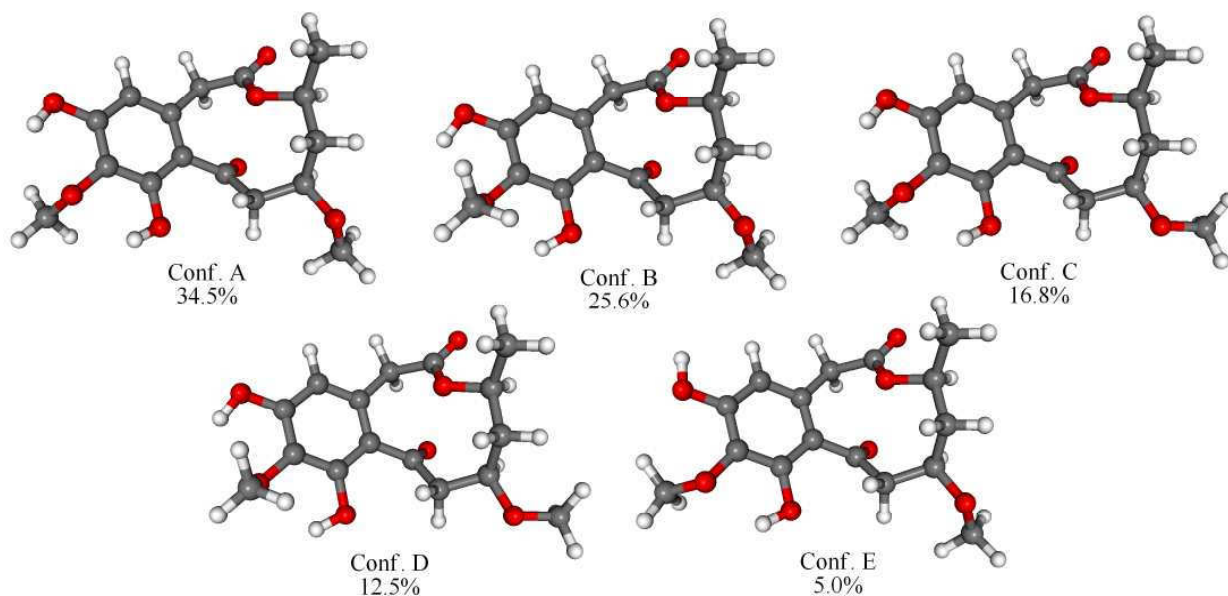


Fig. 3.21d. DFT optimized geometries of the five lowest-energy conformers of the truncated model compound of (9*R*,11*S*)-**15**.

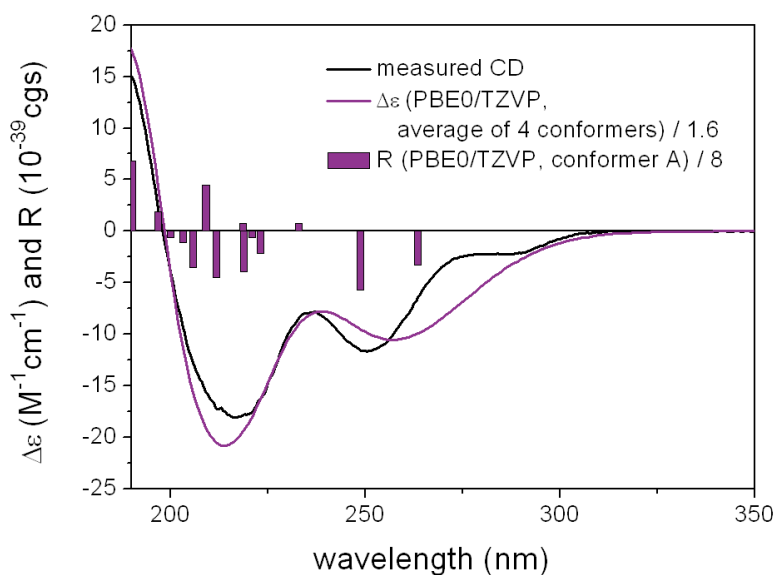


Fig. 3.21e. Experimental ECD spectrum of **16** in acetonitrile compared with the Boltzmann-weighted PBE0/TZVP spectrum calculated for the four lowest-energy conformers of the truncated model compound of the (9*R*,11*S*)-enantiomer. Bars represent rotatory strength of the lowest-energy conformer.

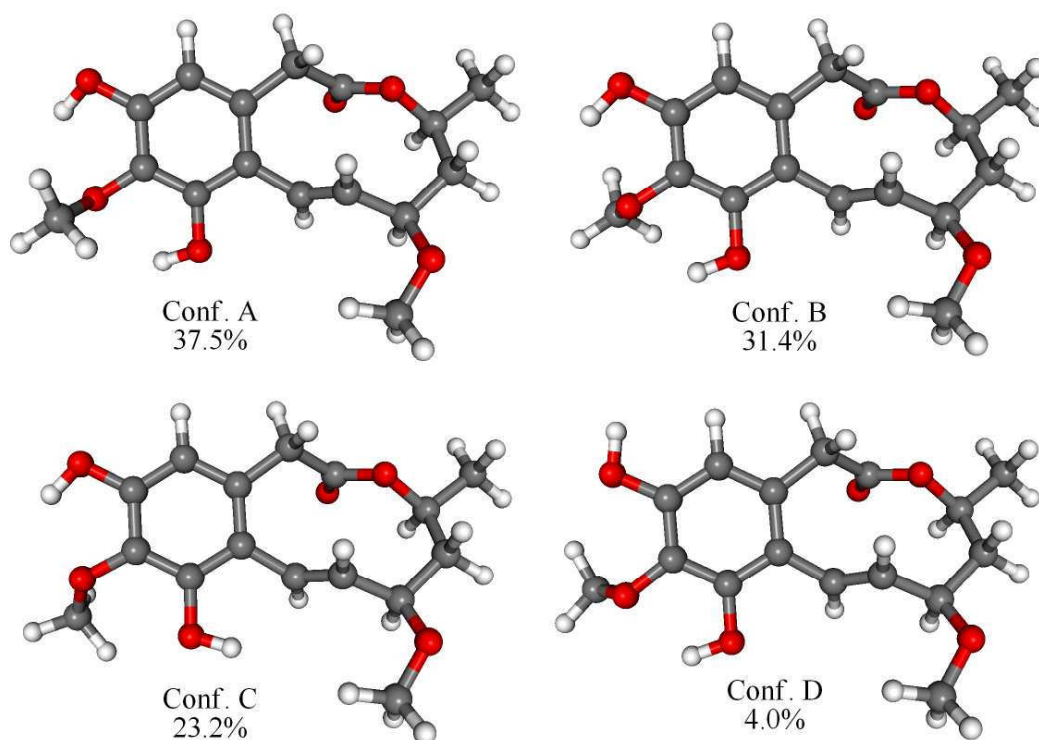


Fig. 3.21f. DFT optimized geometries of the four lowest-energy conformers of the truncated 9-OMe model compound of (9*R*,11*S*)-**16**.

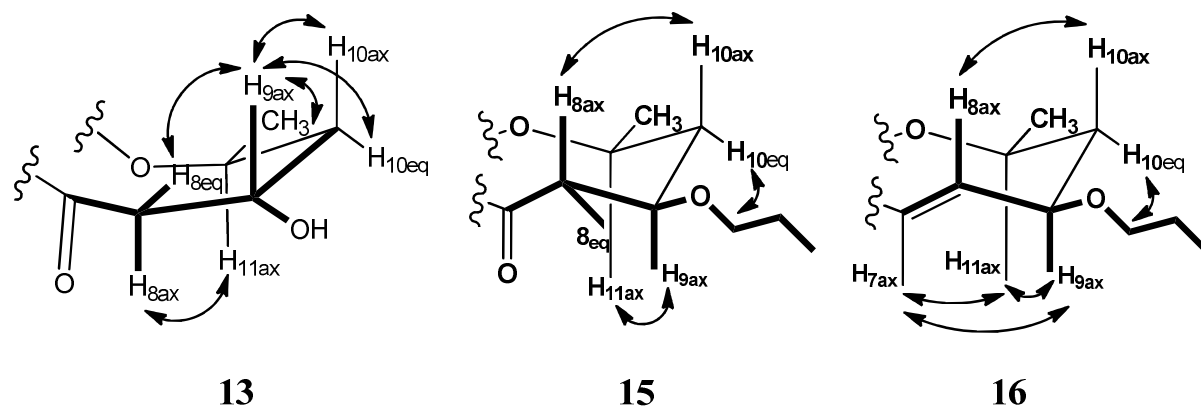
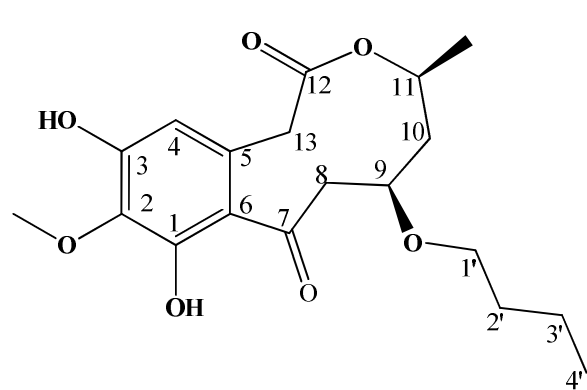
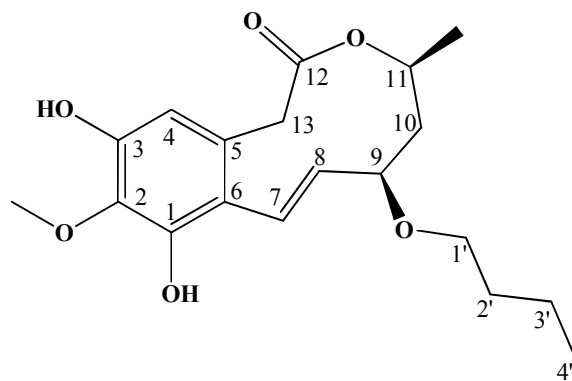


Fig. 3.21g. Key ROESY correlations of 13, 15 and 16.



15



16

15) Xestodecalactone F

16) Xestodecalactone G

Table 3.9: ^1H , ^{13}C NMR, COSY, HMBC and ROESY spectra of compound 15

Position	15*				
	δ_{C}	δ_{H}	COSY	HMBC	ROESY
1	149.4				
2	134.2				
3	151.5				
4	110.1	6.21, s	13	2, 3, 6, 13	
5	127.7				
6	121.7				
7	204.1				
8	60	A 3.04, dd (10.1, 15.3) B 2.93, brd (15.1)	8 B, 9 8 A, 9	7, 9, 10 7, 9, 10	
9	76.1	3.68, m	8 A, 8B, 10 A, 10B	1', 11	11
10	52.1	A 1.67, ddd (9.8, 11.6, 14.6) B 1.94, brd (14.6)	9, 10 B 9, 10 A	8, 9, 11 8, 9	
11	70.9	4.75, ddq (2.6, 11.5, 6.2)	10 A, 10, B	9, 12	9
12	168.8				
13	38.9	A 3.46, d (18.7) B 3.78, d (18.7)	13 B, 4 13 A, 4	4, 5, 6, 12 4, 5, 6, 12	
11-Me	20.6	1.10, d (6.2)	11	10, 11	
2-OMe	60.1	3.69, s		2	
1'	67.1	3.41, m ^a	2'	3', 9	
2'	31.5	1.46, m ^a	1', 3'	1', 3', 4'	
3'	18.9	1.32, m ^a	2', 4'	1', 2', 4'	
4'	13.7	0.88, t (7.3)	3'	2', 3'	
1-OH		9.36, s	1, 2, 6		
3-OH		9.73, s	2, 3, 4		

* Measured at 400 (^1H) and 100 (^{13}C) MHz ($\text{DMSO}-d_6$).

a Second order system.

Table 3.10: ^1H , ^{13}C NMR, COSY, HMBC and ROESY spectra of compound **16**

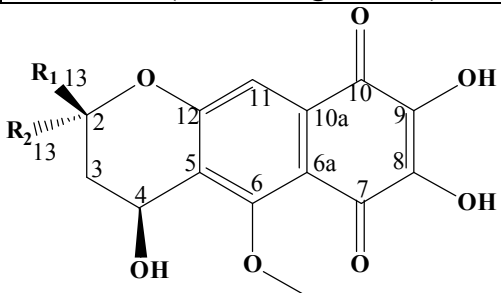
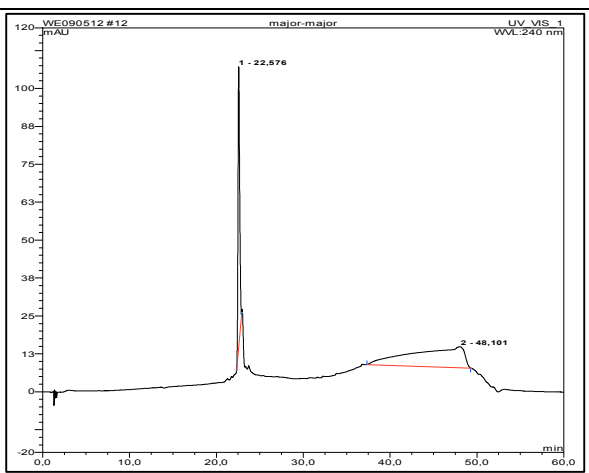
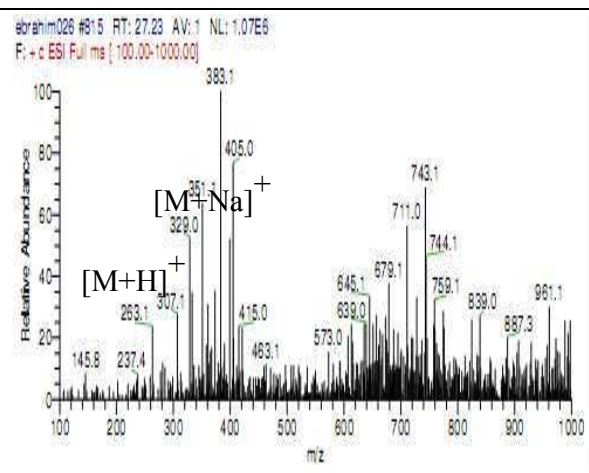
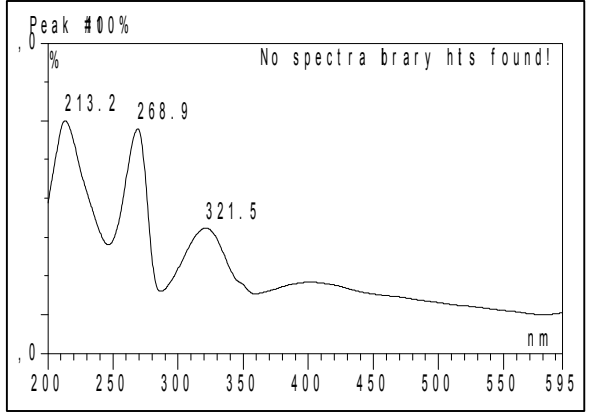
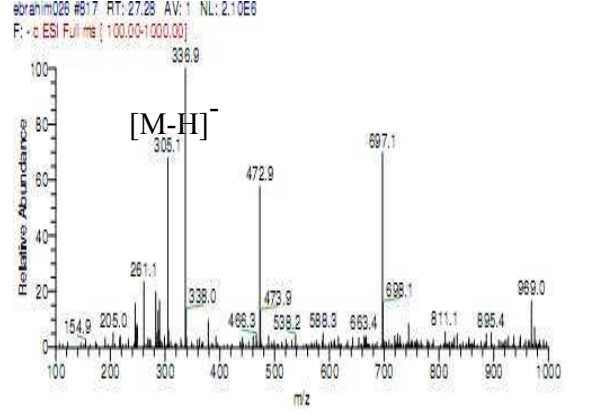
Position	^{16}O		COSY	HMBC	ROESY
	δ_{C}	δ_{H}			
1	148.7				
2	133.9				
3	149.3				
4	105.7	6.14, s	13	2, 3, 5, 6, 13	
5	130.6				
6	116.1				
7	127.8	6.18, d (16.2)	8	1, 5, 6, 8	
8	134.3	5.46, dd (9.5, 16.1)	7, 9	6, 9, 10	
9	79.9	3.84, ddd (5.1, 9.5, 10.8)	8, 10A, 10B	1', 7, 10	11
10	42.7	A 1.77, ddd (10.8, 10.8, 13.8) B 2.00, ddd (1.0, 5.1, 13.8)	9, 10 B 9, 10 A	8, 9, 11 8, 9, 14	
11	68.6	4.84, ddq (0.9, 10.8, 6.4)	10 A, 10 B	9, 12, 14	9
12	172.9				
13	40.6	A 3.29 ^b B 3.76, d (15.5)	13 B, 4 13 A, 4	4, 5, 6, 12 4, 5, 6, 12	
14	21.0	1.20, d (6.5)	11	10, 11	
15	59.8	3.66, s		2	
1'	66.6	A 3.27, m ^{a,b} B 3.42, m ^a	1' B, 2' 1' A, 2'	2', 3', 9 2', 3', 9	
2'	31.4	1.45, m ^a	1', 3'	1', 3', 4'	
3'	18.9	1.30, m ^a	2', 4'	1', 2', 4'	
4'	13.7	0.86, t (7.3)	3'	2', 3'	
1-OH		8.65, s		1, 2, 5, 6	
3-OH		9.22, s		2, 3, 4	

a Second order system.

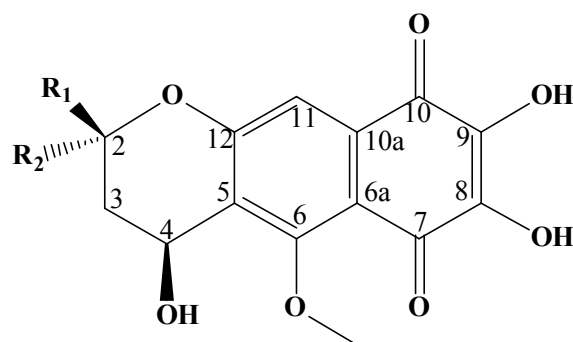
b Overlapped with water peak.

O Measured at 600 (^1H) and 75 (^{13}C) MHz (DMSO- d_6).

3.1.17. Corynecassiicol A/B (17/18, new compounds)

Corynecassiicol A/B	
Synonym(s)	4,7,8-trihydroxy-5-methoxy-2-methyl-3,4-dihydro-2 <i>H</i> -benzo[<i>g</i>]chromene-6,9-dione
Sample code	Corymajor
Biological source	<i>Corynespora cassiicola</i>
Sample amount	3 mg
Physical properties	Red amorphous powder
Molecular formula	C ₁₅ H ₁₅ O ₇
Molecular weight	306 g/mol
Optical rotation[α] _D ²⁰	-75 (c 0.025, MeOH)
Retention time (HPLC)	22.6 min. (standard gradient)
 <p>17 R₁=Me, R₂=H 18) R₁=H, R₂=Me</p>	
	
	

Corynecassiicol A/B **17/18** was isolated from the EtOAc extract of rice cultures of *Corynespora cassicola* as a red amorphous powder (3 mg). It showed UV absorbances at λ_{max} (MeOH) 213.2, 268.9, 321.5 nm. Positive and negative ESI-MS showed molecular ion peaks at m/z 307.1 $[\text{M}+\text{H}]^+$ and m/z 305.1 $[\text{M}-\text{H}]^-$, respectively, indicating a molecular weight of 306 g/mol. The HRESI-MS exhibited a strong peak at m/z 307.0816 $[\text{M}+\text{H}]^+$ indicating a molecular formula $\text{C}_{15}\text{H}_{15}\text{O}_7$ (calculated 307.0818, Δ 0.0002). The ^1H NMR spectrum showed a considerable degree of overlapping (Table 3.11), but it was possible to distinguish most signals of **17** and **18** and to assign them to either isomer on the basis of the integrals (area ratio ca. 4:3). The ^1H NMR and COSY spectra showed a spin system composed of CH_3 -13, H-2, CH_2 -3, H-4 and 4-OH. Furthermore, analysis of the HMBC spectrum indicated that CH_3 -13 was correlated to C-2 (δ_{C} 63.0 in **17**, 63.8 in **18**), which in turn was directly attached to an oxygen atom, and to C-3 (δ_{C} 42.8 in **17**, 42.4 in **18**) in both compounds. In addition, H-4 was correlated to the oxygenated aromatic carbon C-12, and H-11 to C-5, C-6a and to the *keto*-group at C-10. The attachment of the methoxyl group and the relative configuration of the aliphatic ring were both deduced from a complete set of mutual NOEs and coupling constants (measured in MeOD). The observed correlation of H-4 to the methoxyl group in the ROESY spectrum indicated their respective positions. The axial position of H-4 was confirmed from the characteristic large value for $J_{4\text{ax}-3\text{ax}}$ in both compounds (9.5 Hz in **17** and 7.9 Hz in **18**). Furthermore, the ROESY correlation of H-4 with H-2 was only detected in **17**, indicating both compounds are diastereomers with different configurations at C-2. Consequently, compounds **17** and **18** were identified as new natural isomers which we name corynecassiicol A and B, respectively.



17) $R_1=Me$, $R_2=H$

18) $R_1=H$, $R_2=Me$

Table 3.11: 1H , ^{13}C NMR, COSY and HMBC spectra of compounds **17** and **18**

Position	17				18			
	δ_C^a	δ_H^a	COSY	HMBC	δ_C^a	δ_H^a	COSY	HMBC
2	63	3.59, m	3A, 3B, 13		63.8	3.56, m	3A, 3B, 13	
3	42.8	A 2.14, m B 1.61, m	3B, 2, 4 3A, 2, 4		42.4	A 2.18, m B 1.82, m	3B, 2, 4 3A, 2, 4	
4	71.4	4.97, m	3A, 3B	12	72.1	4.81, m	3A, 3B	12
5	119.5				119.3			
6	140.5				140.5			
6a	105.7				105.7			
7	181.3				180.9			
8	148.7				148.7			
9	148.7				148.7			
10	185.4				185.4			
10a	130.2				130.3			
11	107.6	7.00, s		5, 6a, 10	107.6	7.01, s		5, 6a, 10
12	162				162.2			
13	24.2	1.05, d (6.3)	2	2, 3	23.6	1.04, d (6.3)	2	2, 3
OMe-6	60.2	3.83, s		6	60.2	3.83, s		6

a) Measured in DMSO- d_6

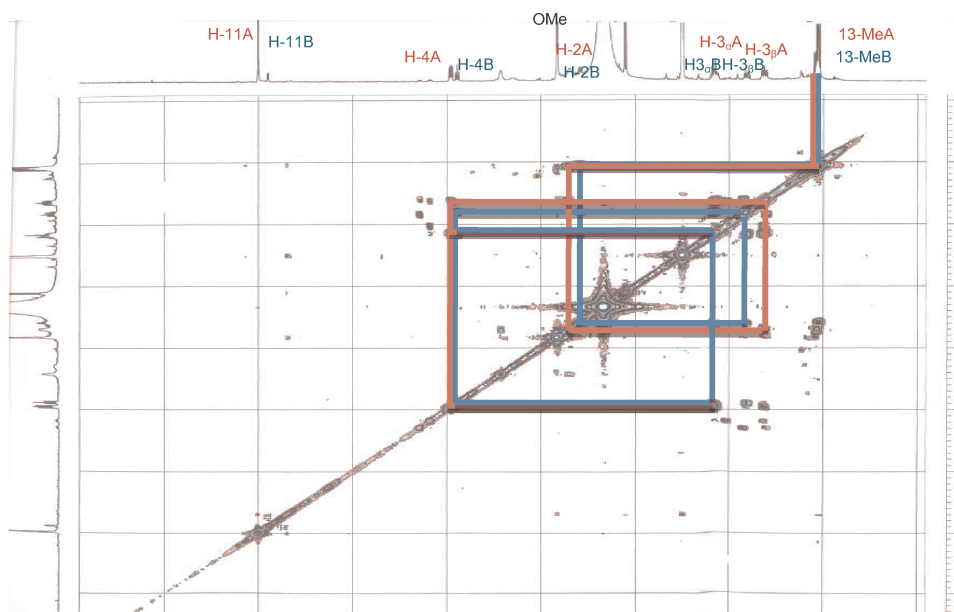


Fig. 3.22: COSY spectrum of compounds 17/18.

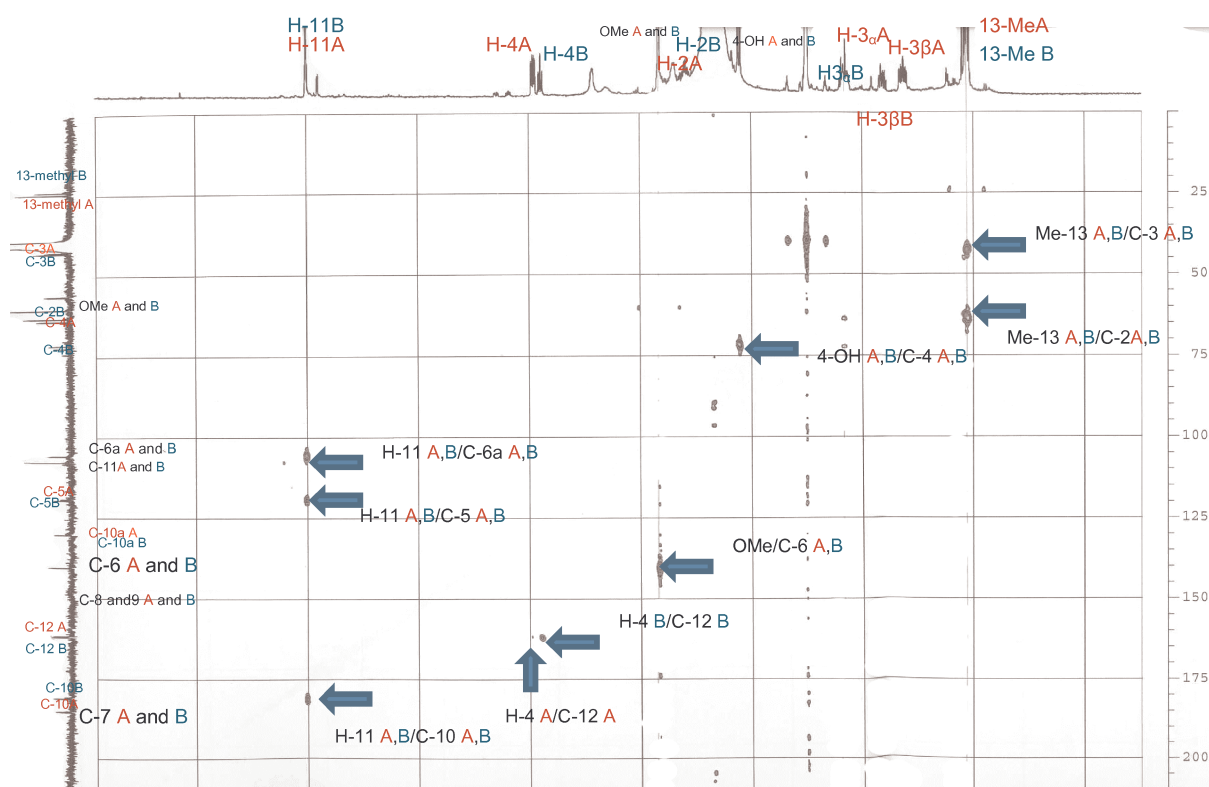


Fig. 3.23: HMBC spectrum of compounds 17/18.

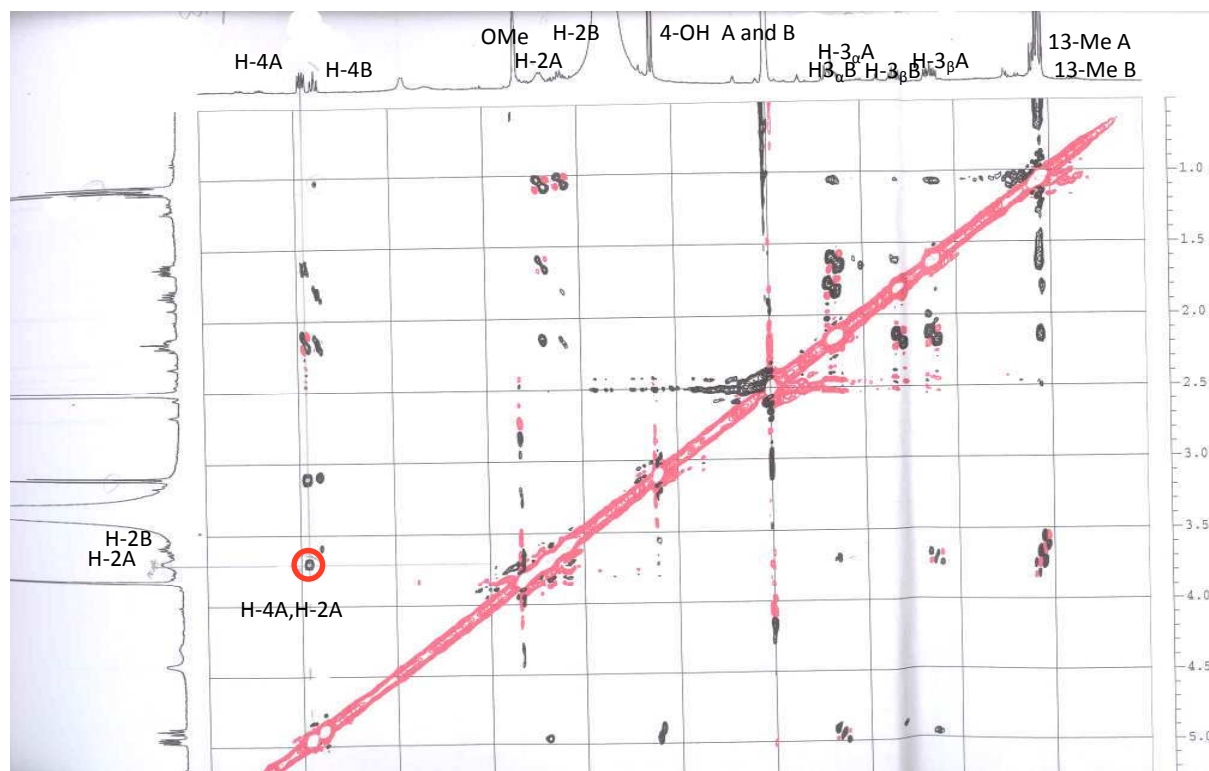


Fig. 3.24: ROESY spectrum of compounds 17/18.

Table 3.12: Bioactivity test results for compounds isolated from the endophytic fungus *Corynespora cassiicola*

Compound tested	L5178Y growth in %• (Conc. 10µg/mL)
Corynecassiidiol (1)	70
6-(3'-hydroxy-n-butyl)-7-O-methyl spinochrome B (2)	57.9
7-O-methyl spinochrome B (3)	96.2
Coryneoctalactone A (4)	80.4
Coryneoctalactone C (6)	97.1
Coryneoctalactone D/A (7)	103.4
Corynesidone A (10)	96.8
Corynesidone B (11)	68
Corynesidone D (12)	68.4
Xestodecalactone D (13)	65.6
Xestodecalactone F (15)	81.8
Xestodecalactone G (16)	93.8
CorynecassiicolA/B (17/18)	95.0

• Data provided by Prof. W. E. G. Müller, Mainz.

Looking to the cytotoxic activity of the isolated compounds from the fungus *Corynespora cassiicola*, indicates that 6-(3'-hydroxy-n-butyl)-7-O-methyl spinochrome B (**2**) showed moderate activity while all other compounds showed only weak cytotoxic activity.

Table 3.12a: IC₅₀ values of compounds **2** and **11** against different protein kinases.

Cpd	AKT1	ALK	ARK5	Aurora-B	AXL	FAK	IGF1-R	MEK1 wt
2	7.18 E-05	5.65 E-06	6.96 E-05	2.83 E-05	9.15 E-06	1.73 E-05	3.51 E-06	> 1 E-04
11	5.28E-05	4.26 E-06	4.92 E-05	1.57 E-06	9.13 E-06	2.21 E-05	4.87 E-06	> 1 E-04
Cpd	MET wt	NEK2	NEK6	PIM1	PLK1	PRK1	SRC	VEGF-R2
2	1.69 E-05	6.46 E-05	4.17 E-05	2.54 E-06	> 1 E-04	9.89 E-05	2.39 E-06	4.48 E-06
11	8.15 E-06	5.22 E-05	2.34 E-05	3.52 E-07	2.79 E-05	4.90 E-05	3.56 E-06	5.12 E-06

Inhibitory potentials of compounds at various concentrations were determined in biochemical protein kinase activity assays. Listed are IC₅₀ values in M.

The isolated compounds of *Corynespora cassiicola* also were subjected to biochemical protein kinase activity assay using 16 different human protein kinases. Only compounds **2** and **11** inhibited several of the tested kinases (Table 3.12a). The IC₅₀ values observed for both compounds were in the low micromolar range against some protein kinases such as ALK, VEGF-R2, SRC, IGF1-R, and PIM1 of which inhibition is known to confer antitumoral effects.

Of special interest is the fact that **11** inhibited PIM1 with an IC_{50} value of 3.5×10^{-7} M, indicating a tenfold higher specificity of this naturally occurring inhibitor against this particular protein kinase in comparison to most of the other kinases investigated in this study (Table 3.12a).

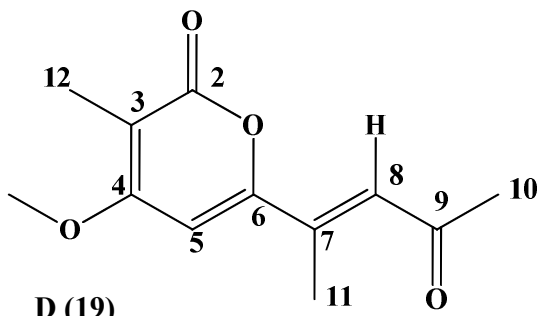
3.2. Compounds isolated from the endophytic fungus *Stemphylium botryosum*

The pure fungal strain of the endophytic fungus *Stemphylium botryosum* was cultivated in liquid Wickerham medium and on rice solid medium. Interestingly, chemical screening studies indicated a clear difference between *Stemphylium botryosum* extracts obtained from liquid (Wickerham) and rice cultures. Comparison of the HPLC chromatograms of the EtOAc extracts of both cultures showed that extracts of liquid cultures had a very complex chemical pattern compared to that obtained from rice cultures. Eight compounds were isolated from the solid rice culture of endophytic fungus *Stemphylium botryosum* including, phomapyrone D/H (**19/20**), stemphpyrone (**21**), infectopyrone (**22**), stemphbotrydione (**23**), stemphyperlenol (**24**), macrosporin (**25**) and indole-3-carbaldehyde (**26**). The yield of rice cultures was higher than that of liquid cultures with a ratio of 5:1 of dried extract, respectively. Due to the complex chemical pattern, low yield and low activity of extract obtained from liquid cultures, rice culture extracts were chosen for further investigation.

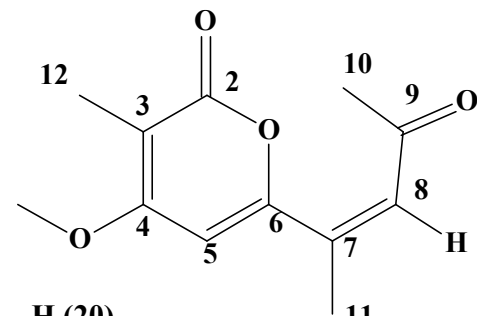
In this part of the thesis results of investigation of the natural products produced by *Stemphylium botryosum* when grown on solid rice medium are presented.

3.2.1. Phomapyrone D/H (19/20, D (known compound), H(new compound))

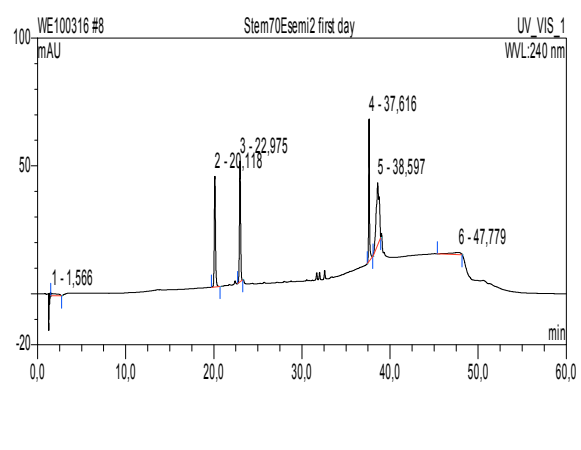
Phomapyrone D/H	
Synonym(s)	4-methoxy-3-methyl-6-(4-oxopent-2-en-2-yl)-2 <i>H</i> -pyran-2-one
Sample code	Stem70E semi2
Biological source	<i>Stemphylium botryosum</i>
Sample amount	1 mg
Physical properties	White amorphous solid
Molecular formula	C ₁₂ H ₁₄ O ₄
Molecular weight	222 g/mol
Retention time (HPLC)	20.1 min. (D), 22.9 min. (E) (standard gradient)

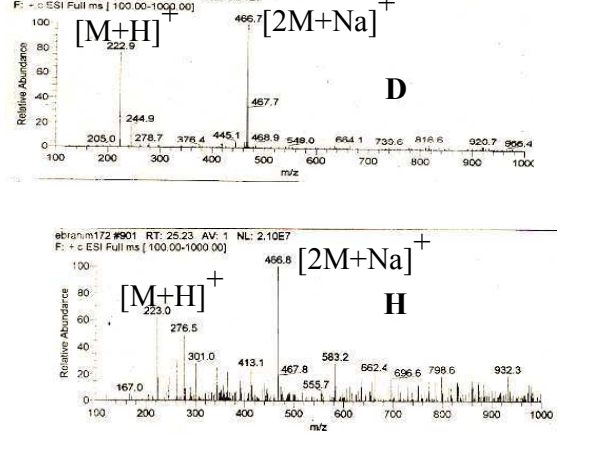


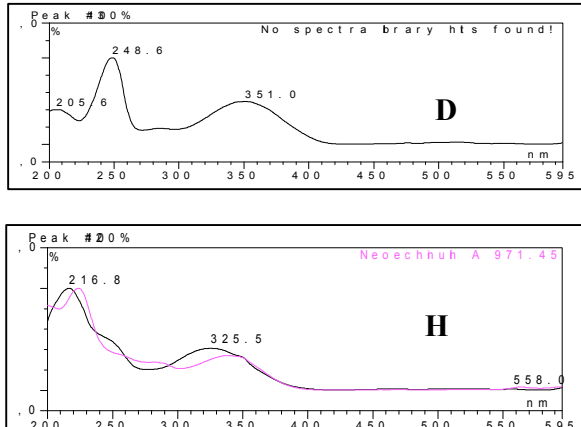
D (19)



H (20)

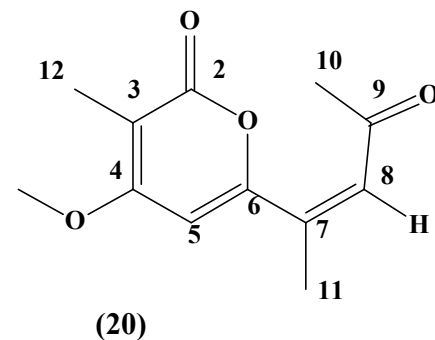
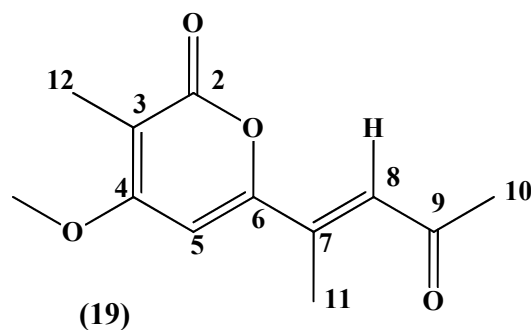






(-)-ESI-MS: no ionization

Phomapyrones D/H **19/20** were obtained as inseparable mixture and were isolated from the EtOAc extract of rice cultures of *Stemphylium botryosum* as a white amorphous solid (1 mg). They showed UV absorbances at λ_{max} (MeOH) 205.6, 248.6, 351 nm (D) and 216.8, 325.5 nm (H). Positive ESI-MS showed molecular ion peaks at m/z 223 $[\text{M}+\text{H}]^+$ (**20**) and 222.9 $[\text{M}+\text{H}]^+$ (**19**) indicating a molecular weight of 222 g/mol. The HRESI-MS exhibited a strong peak at m/z 223.0964 $[\text{M}+\text{H}]^+$ indicating the molecular formula $\text{C}_{12}\text{H}_{14}\text{O}_4$ (calculated 223.0970, Δ 0.0006). Analysis of the ^1H NMR data indicated the presence of three methyl groups 10-Me, 11-Me and 12-Me at δ_{H} 2.32, 2.13 and 1.92 ppm respectively for **19** and at δ_{H} 2.27, 2.35 and 1.88 ppm respectively for **20**, a methoxy group (4-OMe) at δ_{H} 4.01 ppm (**19**) and at δ_{H} 3.95 ppm (**20**) (Table 3.13). The ^1H - ^1H COSY spectrum shows the long range correlation of H-8 at δ_{H} 6.39 ppm (**19**) and δ_{H} 7.09 ppm (**20**) and methyl group 11 at (δ_{H} 2.13 ppm (**19**) and δ_{H} 2.35 ppm (**20**) in both isomers. Analysis of the HMBC data was instrumental for the assignment of the structures. The methyl protons (12-Me) in both isomers at δ_{H} 1.92 ppm (**19**) and δ_{H} 1.88 ppm (**20**) displayed correlations to both C-3 and C-4. The methoxy protons at δ_{H} 4.01 ppm (**19**) and δ_{H} 3.95 ppm (**20**) have correlations to C-4 allowing their attachment at C-4 in both isomers. Also, in both isomers the methyl group 10-Me at δ_{H} 2.32 ppm (**19**) and δ_{H} 2.27 ppm (**20**) correlate with the *keto*-group C-9. Furthermore, the methyl group 11-Me at δ_{H} 2.13 ppm (**19**) and δ_{H} 2.35 ppm (**20**) correlates with C-6 (allowing the complete assignment of the pyrone unit), C-7 and C-8. Hence, the structure D was confirmed to be the known compound phomapyrone D, showing a *Z*-configuration of the double bond C7-C8, which was isolated from a fungal pathogen *Leptosphaeria maculans*, by comparison to the literature (Pedras and Chumala, 2005). It is important to mention that phomapyrone H may be an artifact as the difference between **19** and **20** is only the configuration of the double bond and this could be done by the effect of light for example.



Nr.	Compound
19	Phomapyrone D
20	Phomapyrone H

Table 3.13: ^1H , COSY, HMBC spectra of compounds **19** and **20**

Position	19				20		
	δ_{H}^*	$\delta_{\text{H}}^{\text{O}}$	COSY	HMBC	δ_{H}^*	COSY	HMBC
2							
3							
4							
5	6.88, s	6.52, s		3, 6	6.69, s		
6							
7							
8	6.39, s	7.15, s	11		7.09, s	11	
9							
10	2.32, s	2.36, s		9	2.27, s		
11	2.13, s	2.36, s	8	6, 7, 8	2.35, s	8	6, 7, 8
12	1.92, s	2.05, s		3, 4	1.88, s		3, 4
OMe	4.01, s	3.95, s		4	3.95, s		4

O (Pedras and Chumala, 2005) (CDCl_3).

* Measured in ($\text{MeOH}-d_4$).

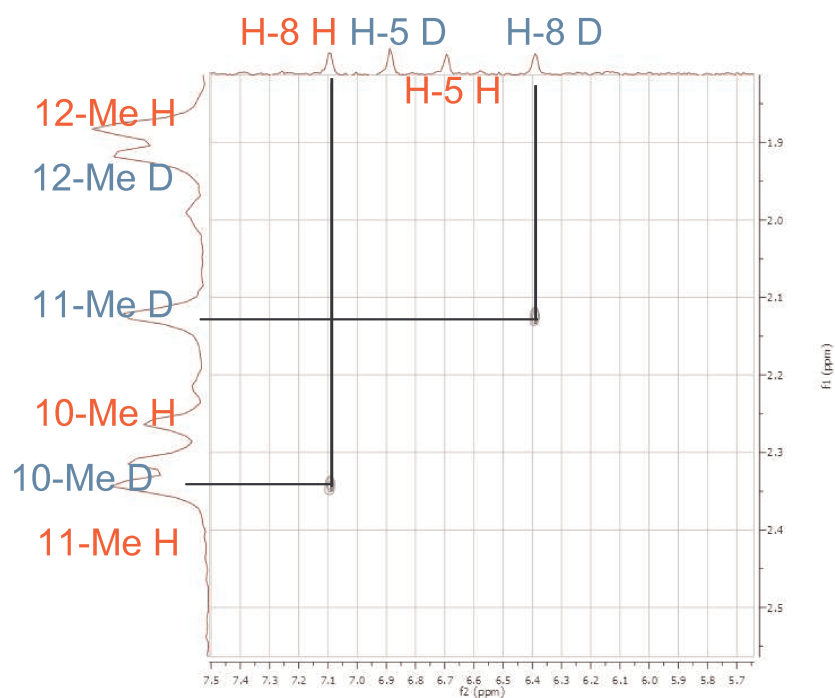


Fig. 3.25: COSY spectrum of compounds **19/20**.

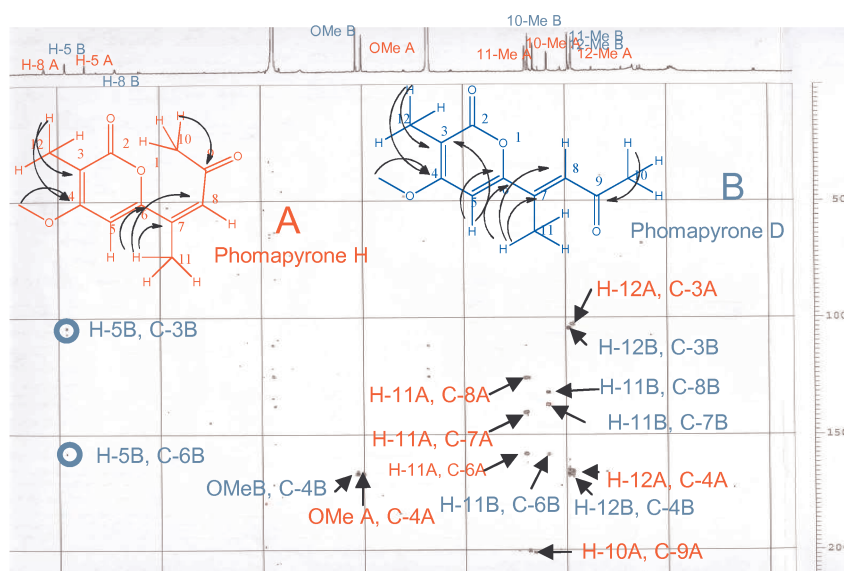


Fig. 3.26: HMBC spectrum of compounds **19/20**.

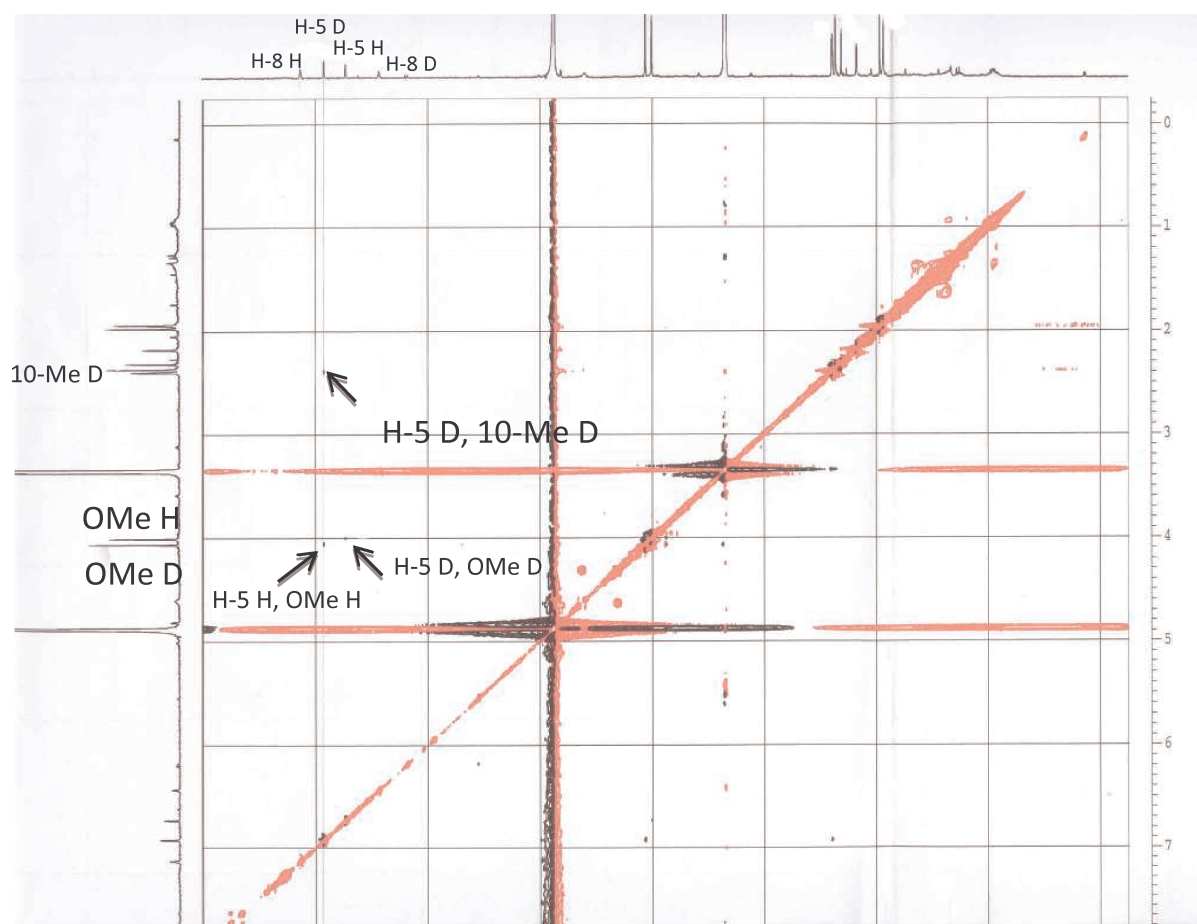
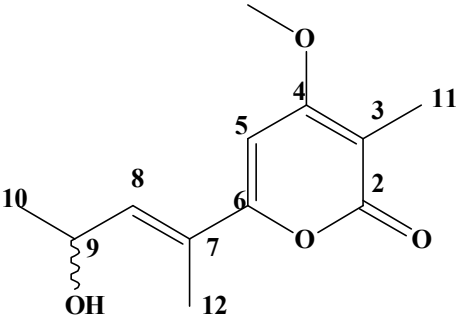
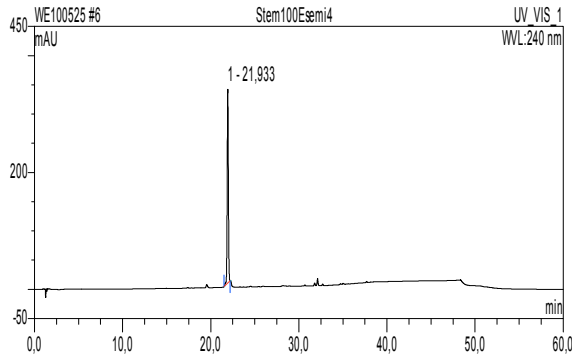
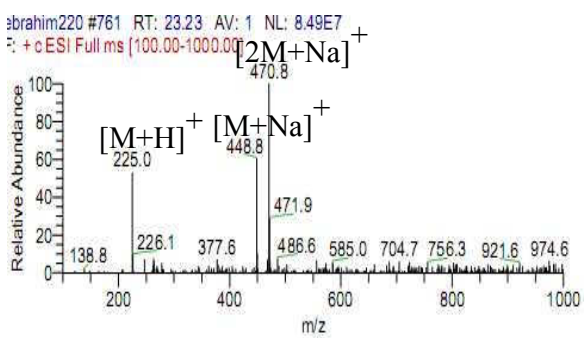
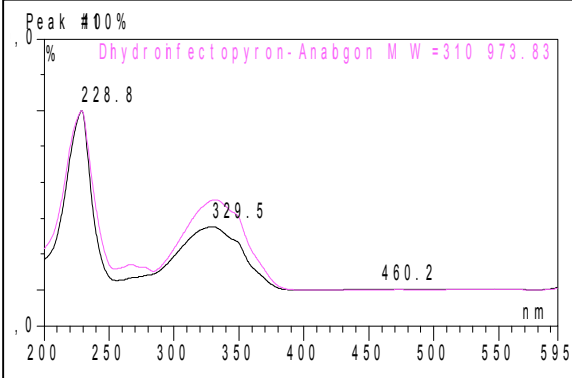
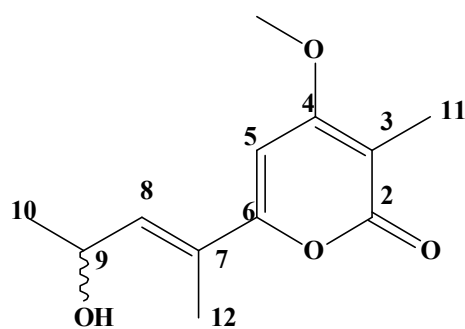


Fig. 3.27: ROESY spectrum of compounds **19/20**.

3.2.2. Stemphpyrone (21, known compound)

Stemphpyrone	
Synonym(s)	(<i>E</i>)-6-(4-hydroxypent-2-en-2-yl)-4-methoxy-3-methyl-2 <i>H</i> -pyran-2-one
Sample code	Stem100Esemi4
Biological source	<i>Stemphylium botryosum</i>
Sample amount	1 mg
Physical properties	Yellowish white solid
Molecular formula	C ₁₂ H ₁₆ O ₄
Molecular weight	224 g/mol
Optical rotation [α] _D ²²	-0.90 (<i>c</i> 0.01, MeOH)
Retention time (HPLC)	21.9 min. (standard gradient)
	
	
	(-)-ESI-MS: no ionization

Stemphpyrone **21** was isolated from the EtOAc extract of rice cultures of *Stemphylium botryosum* as a yellowish white solid (1 mg). It showed UV absorbances at λ_{max} (MeOH) 228.8, 329.5 nm. Positive ESI-MS showed molecular ion peaks at m/z 225 $[M+H]^+$ indicating a molecular weight of 224 g/mol. The ^1H NMR spectrum (Table 3.14) indicated the presence of three methyl groups (two of them are attached to olifenic bonds (11-Me and 12-Me) (at δ_{H} 1.88 and 1.98 ppm respectively) and one is attached to aliphatic bond (10-Me) (at δ_{H} 1.82 ppm), one methoxy group (4-OMe) (at δ_{H} 3.98 ppm), and three methine protons (H-5 at δ_{H} 6.35 ppm, H-8 at δ_{H} 6.47 ppm and H-9 at δ_{H} 4.69 ppm). The structure of **21** was confirmed from analysis of the COSY spectra and comparison with the literature (Debbab *et al*, 2009). In the COSY spectrum, a spin system including 10-Me (at δ_{H} 1.82 ppm), H-9 (at δ_{H} 4.69 ppm), H-8 (at δ_{H} 6.47 ppm), and 12-Me (at δ_{H} 1.98 ppm) was evident; the trans-geometry of the double bond was indicated by the upfield shift observed for 12-Me as well as the distinct allylic coupling between H-8 and 12-Me ($J=1.2$ Hz). Stemphpyrone **21** was isolated before from the endophytic fungus *Stemphylium globuliferum* (Debbab *et al.*, 2009). Unfortunately, the absolute stereochemistry of C-9 was not performed due to the small amount.



21 Stemphpyrone

Table 3.14: ^1H and COSY spectra of compound **21**

Position	21		
	δ_{H}^*	$\delta_{\text{H}}^{\text{O}}$	COSY
2			
3			
4			
5	6.53, s	6.53, s	
6			
7			
8	6.47, dd (8.2)	6.47, dd (8.2)	9, 12
9	4.69, dq (8.3, 6.4)	4.69, dq (8.3, 6.4)	8, 10
10	1.82, d (6.4)	1.82, d (6.4)	9
11	1.88, s	1.88, s	8
12	1.98, d (1.2)	1.98, d (1.2)	7
OMe	3.98, s	3.98, s	

O (Debbab *et al.*, 2009) (MeOH- d_4).

* Measured in (MeOH- d_4).

3.2.3. Infectopyrone (22, known compound)

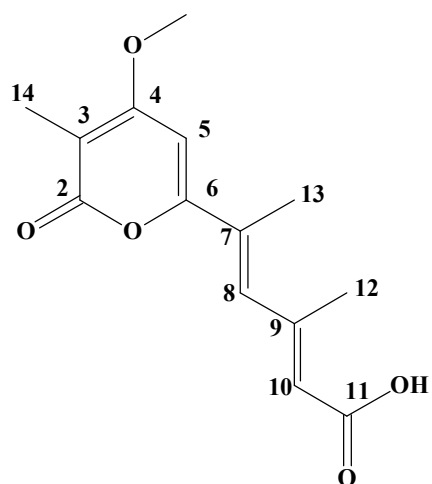
Infectopyrone	
Synonym(s)	(2E,4E)-5-(4-methoxy-3-methyl-2-oxo-2H-pyran-6-yl)-3-methylhexa-2,4-dienoic acid
Sample code	Stem20Mseph2529
Biological source	<i>Stemphylium botryosum</i>
Sample amount	7 mg
Physical properties	brown solid
Molecular formula	C ₁₄ H ₁₆ O ₅
Molecular weight	264 g/mol
Retention time (HPLC)	24.5 min. (standard gradient)

ebrahim213 #993 RT: 28.01 AV: 1 NL: 1.08E9
F: +cESI Full ms [100.00-1000.00] [2M+Na]⁺

Peak #00%

ebrahim213 #987 RT: 27.83 AV: 1 NL: 9.23E4
F: -cESI Full ms [100.00-1000.00] [M-H]⁻

Infectopyrone **22** was isolated from the EtOAc extract of rice cultures of *Stemphylium botryosum* as a brown solid (7 mg). It showed UV absorbances at λ_{max} (MeOH) 219.3, 265.2, 344.5 nm. Positive ESI-MS showed molecular ion peaks at m/z 265 $[M+H]^+$, while negative ESI-MS showed molecular ion peaks at m/z 262.7 $[M-H]^-$ indicating a molecular weight of 264 g/mol. The ^1H NMR spectra of **22** (Table 3.15) showed three methyl groups at δ_{H} 1.90, 2.12 and 2.28 ppm assigned to 14-Me, 13-Me and 12-Me respectively. In addition, one methoxy group at δ_{H} 4.0 ppm and three sp^2 hybridized CH groups at δ_{H} 6.64, 6.99 and 5.38 ppm assigned for H-5, H-8 and H-10, respectively were observed. Also, only long range couplings were present in the COSY spectra of **22**, this involving the long range correlation between 12-Me and H-8 and H-10 and that between H-8 and methyl groups 12-Me (at δ_{H} 2.28 ppm) and 13-Me (at δ_{H} 2.12 ppm). The methoxy group (at δ_{H} 4.00 ppm) was confirmed to be in position 4 by performing a NOE experiment. The structure of **22** was confirmed to be infectopyrone by comparison with the spectral data with the Literature (Ivanova *et al.*, 2010). Infectopyrone was isolated before from *Alternaria infectoria* (Larsen *et al.*, 2005).



22 Infectopyrone

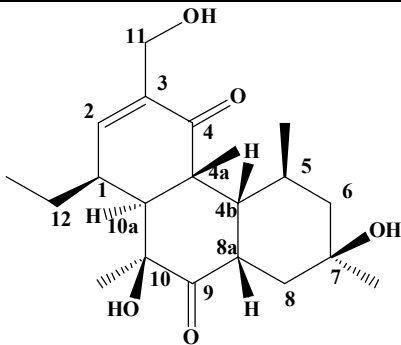
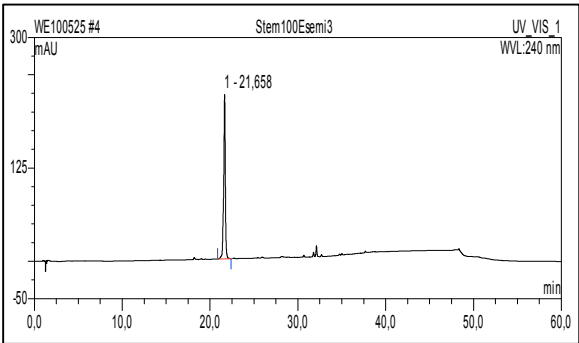
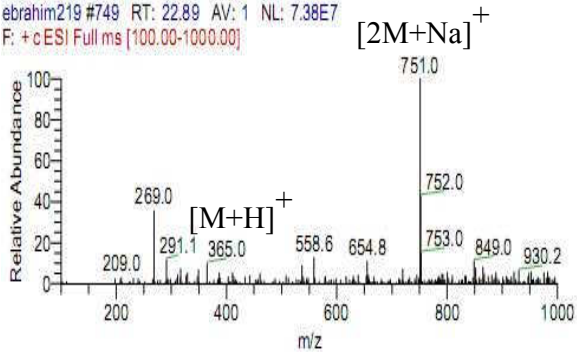
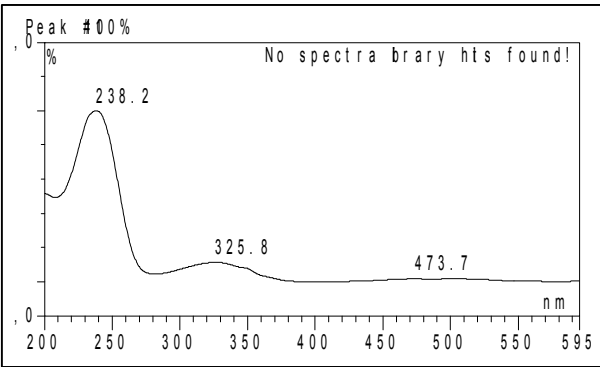
Table 3.15: ^1H and COSY spectra of compound **22**

Position	22		
	δ_{H}^*	$\delta_{\text{H}}^{\text{O}}$	COSY
2			
3			
4			
5	6.64, br. s	6.68, s	
6			
7			
8	6.99, br.s	6.84, br.s	12, 13
9			12
10	5.83, br. s	5.77, s	
11			
12	2.28, d(1.2)	2.33, d(1.1)	8, 10
13	2.12, d(0.9)	2.07, d(1.2)	8
14	1.90, s	1.81, s	
OMe	4.00, s	3.95, s	

o (Larsen *et al.*, 2005) ($\text{DMSO}-d_6$).

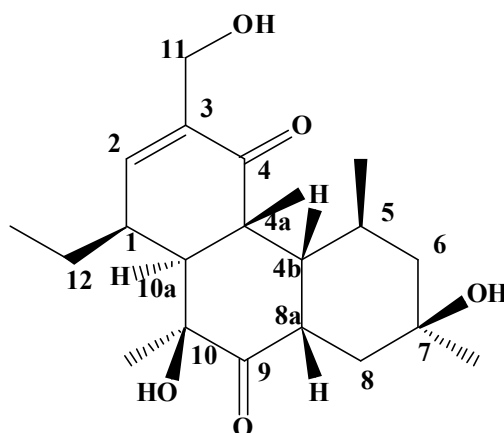
* Measured in ($\text{MeOH}-d_4$).

3.2.4. Stemphbotrydione (23, new compound)

Stemphbotrydione	
Synonym(s)	1-ethyl-7,10-dihydroxy-3-(hydroxymethyl)-4a,5,7,10-tetramethyl-4b,5,6,7,8,8a,10,10a-octahydrophenanthrene-4,9(1 <i>H</i> ,4a <i>H</i>)-dione
Sample code	Stem100Esemi3
Biological source	<i>Stemphylium botryosum</i>
Sample amount	1.3 mg
Physical properties	Yellowish white solid
Molecular formula	C ₂₁ H ₃₂ O ₅
Molecular weight	364
Optical rotation [α] _D ²⁰	+0.9 (<i>c</i> 0.0125, MeOH)
Retention time (HPLC)	21.7 min. (standard gradient)
	
	
	(-)-ESI-MS: no ionization

Stemphbotrydione **23** was isolated from the EtOAc extract of rice cultures of *Stemphylium botryosum* as a yellowish white solid (1.3 mg). It showed UV absorbance maxima at λ_{max} (MeOH) 238.2, 325.8, 473.7 nm. Positive ESI-MS showed molecular ion peaks at m/z 365 $[M+H]^+$ indicating a molecular weight of 364 g/mol. The HRESI-MS exhibited a strong peak at m/z 387.2142 $[M+Na]^+$ indicating the molecular formula $C_{21}H_{32}O_5$ (calculated 387.2142, Δ 0). The 1H -NMR spectrum of **23** (Table 3.16) shows indicative peaks attributed for 5 methyl groups 4a-Me, 5-Me, 7-Me, 10-Me and 12-Me appearing at δ_H 1.54, 0.88, 1.26, 0.98 and 1.10, respectively in addition to one olefinic proton H-2 at δ_H 6.70 ppm. Moreover, a multiplet appearing at δ_H 2.55 ppm assigned for H-1, a doublet at δ_H 2.25 ppm assigned for H-10a ($J=2.1$ Hz), a doublet of doublet at δ_H 2.08 ppm assigned for H-4b, H-8a appearing at δ_H 3.10 ppm (ddd, $J=16.1, 12.1, 4.1$ Hz), H-8 which appear at δ_H 1.30 (8A) and 2.05 (8B) and a multiplet appearing at δ_H 2.05 ppm assigned for H-5 were detected in the 1H -NMR spectrum. The 1H - 1H COSY of **23** shows two spin systems one is CH(2)CH(1)CH₂(12)CH₃(12)CH(10a) and the other one is CH₂(6)CH(5)CH₃(5)CH(4b)CH(8a)CH₂(8). The HMBC spectrum confirms the attachment of the methyl groups to the hydrophenanthrene rings through the correlations of 4a-Me to C-4a, C-4b, C-10a and C-4, 5-Me to C-4b, C-5 and C-6, 7-Me to C-6, C-7 and C-8, 10-Me to C-9, C-10 and C-10a and 12-Me to C-1 and C-12. In addition, HMBC showed the correlation of H-2 to C-1 (δ_C 37.0 ppm), C-10a (δ_C 55.0 ppm), C-11 (δ_C 62.0 ppm), and C-4 (δ_C 207.0 ppm). The position of CH₂-OH group at position 3 is evidenced from the correlation of CH₂-11 to C-2 (δ_C 143.0 ppm) and C-4 (δ_C 207.0 ppm). In addition, the position of the ethyl group at position 1 is confirmed by the correlations of the CH₂-12 to C-1 (δ_C 37.0 ppm), C-2 (δ_C 143.0 ppm) and C-10a (δ_C 55.0 ppm). The relative configuration of **23** was established by ROESY experiment through the correlations of 5-Me at δ_H 0.88 ppm to both H-4b at δ_H 2.08 ppm and 4a-Me at δ_H 1.54 ppm and H-4b at δ_H 2.08 ppm to H-8a at δ_H 3.10 ppm. In addition, the ROESY spectrum showed correlations of H-1 at δ_H 2.55 ppm to H-10a at δ_H 2.25

ppm, H-10a at δ_{H} 2.25 ppm to 10-Me at δ_{H} 0.98 ppm and CH₂-12 at δ_{H} 1.75 (A) and at δ_{H} 1.80 (B) to 4a-Me at δ_{H} 1.54 ppm. Thus, **23** is identified as a new natural product to which the name stemphbotrydione is given.



23 Stemphbotrydione

Table 3.16: ¹H, COSY, HMBC spectra of compound **23**

Positio n	²³ $\delta_{\text{C}}^{\text{O}}$	δ_{H}^*	COSY	HMBC	ROESY
1	37.0	2.55, m	12A, 12B, 2, 10a		10a, 10-Me
2	143.0	6.70, d (3.7)	1		
3	136.0				
4	207.0				
4a	48.8				
4b	44.8	2.08, dd C	5, 8a		5-Me, 4a-Me, 8
5	30.5	2.05, m	4b, 5-Me, 6A, 6B		
6	49.0	A 1.20, dd C B 1.62, dd C	5, 6B 5, 6A		
7	69.0				
8	39.5	A 1.30, dd C B 2.05, dd C	8a 8a	7, 8, 8a 7, 8, 8a	
8a	42.0	3.10, ddd (16.1, 12.1, 4.1)	8A, 8B	4b, 9	4b
9	217.5				
10	76.5				
10a	55.0	2.25, d (2.1)		9	1, 10-Me
11	60.0	A 4.15, d (13.9) B 4.27, d (13.9)	11B 11A	2, 3, 4 2, 3	
12	32.0	A 1.75, m B 1.80, m	1, 12B 1, 12A	1, 2, 10a 1, 2, 10a	4a-Me
4a-Me	22.7	1.54, s		4a, 4b, 10a, 4	4b, 12, 5-Me
5-Me	22.5	0.88, d (5.95)	5	4b, 5, 6	4b, 4a-Me, 7-Me
7-Me	28.4	1.26, s		6, 7, 8	5-Me
10-Me	21.5	0.98, s		10, 10a	1, 10a
12-Me	12.0	1.10, t (7.4)	12A, 12B	1, 12	

O Extracted from HMBC

C overlapped and not possible for calculation of *J* value

* Measured in (MeOH-*d*₄).

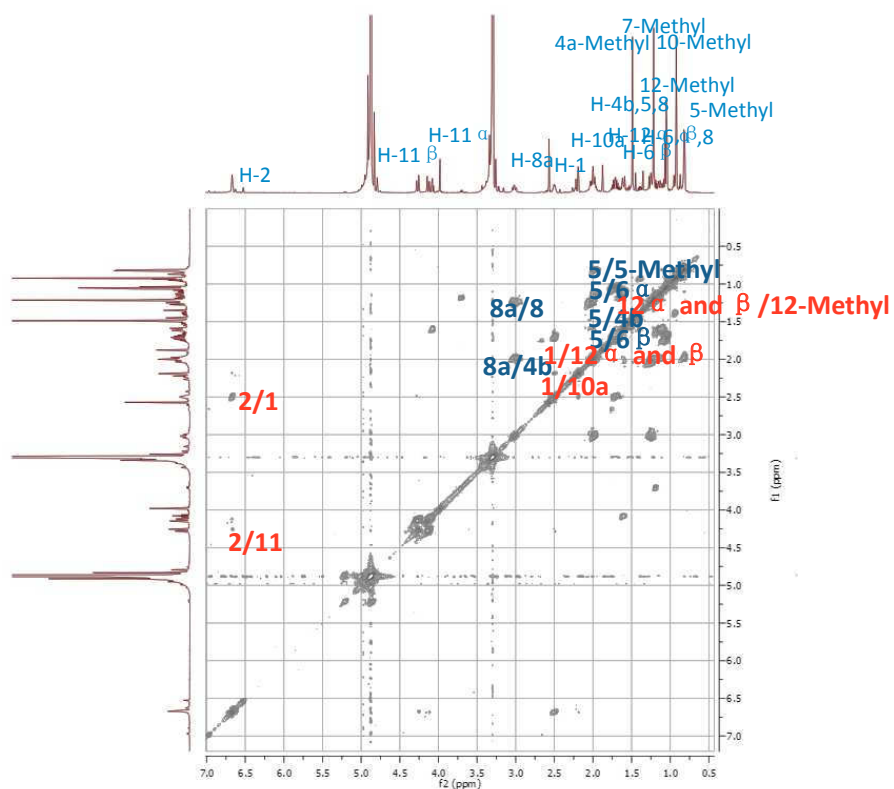


Fig. 3.28: COSY spectrum of compound 23.

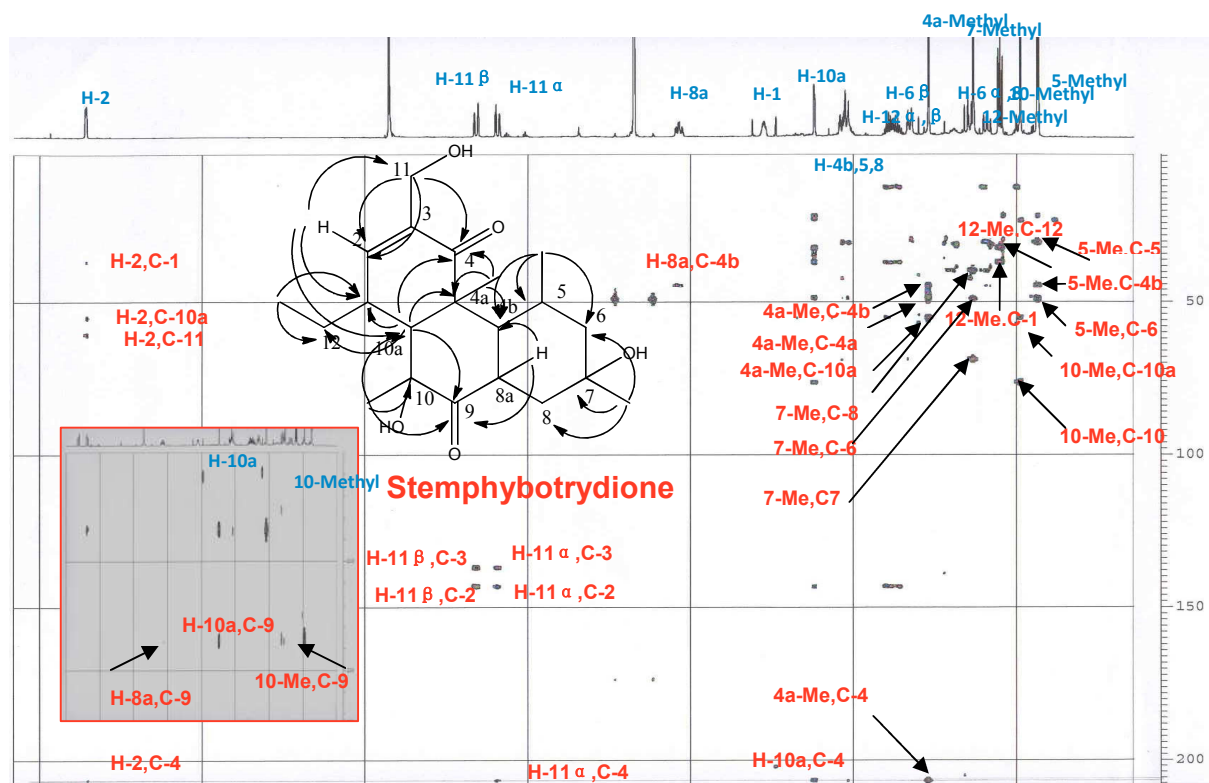


Fig. 3.29: HMBC spectrum of compound 23.

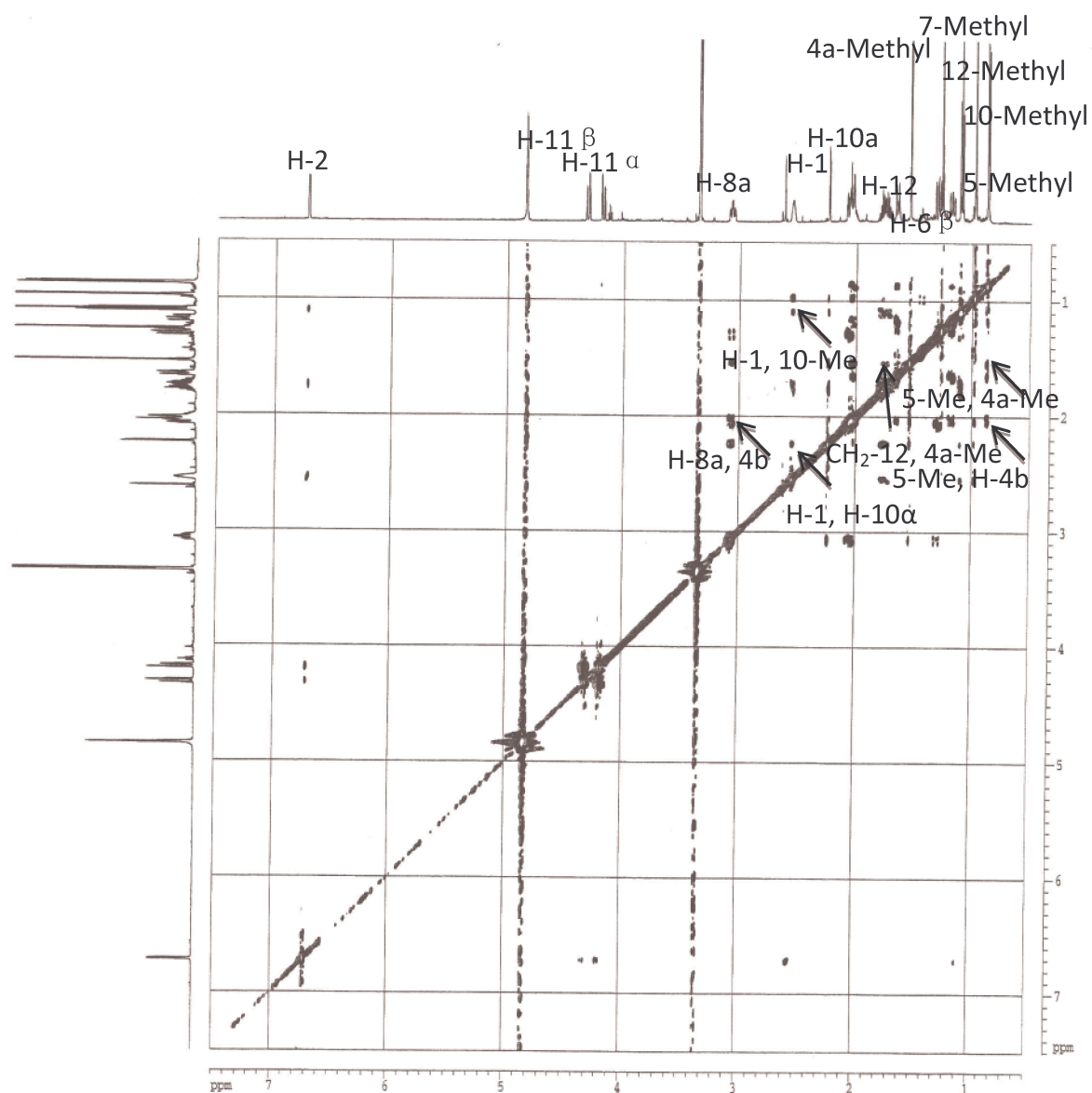
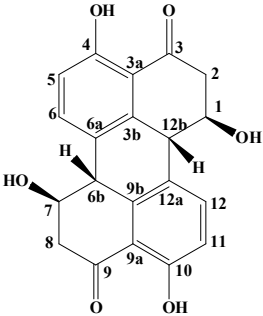
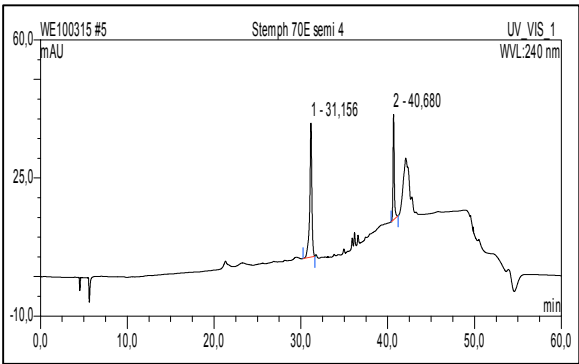
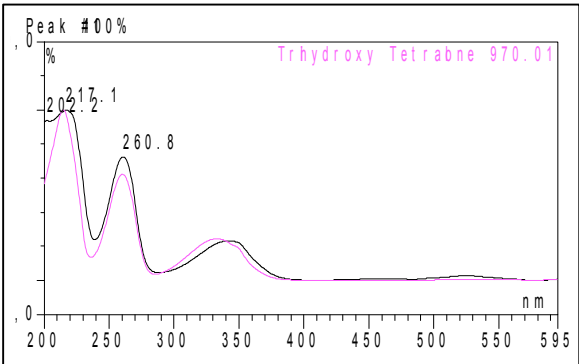
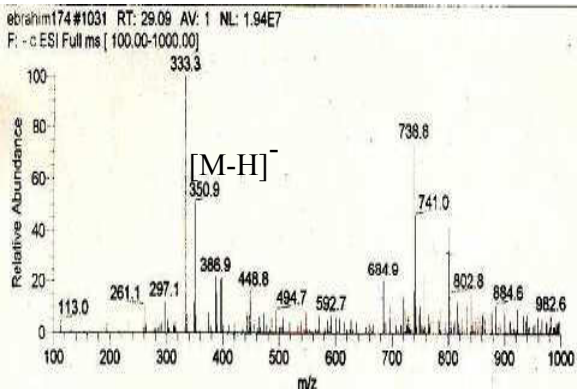


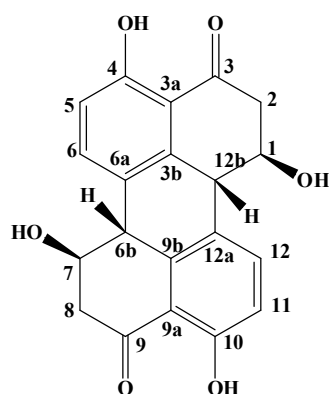
Fig. 3.30: ROESY spectrum of compound 23.

3.2.5. Stemphyperlenol (24, known compound)

Stemphyperlenol	
Synonym(s)	(1 <i>R</i> ,6 <i>bR</i> ,7 <i>R</i> ,12 <i>bR</i>)-1,4,7,10-tetrahydroxy-1,7,8,12 <i>b</i> -tetrahydroperylene-3,9(2 <i>H</i> ,6 <i>bH</i>)-dione
Sample code	Stem70Esemi4
Biological source	<i>Stemphylium botryosum</i>
Sample amount	2 mg
Physical properties	Reddish brown powder
Molecular formula	C ₂₀ H ₁₆ O ₆
Molecular weight	352 g/mol
Optical rotation $[\alpha]_D^{23}$	+411 (<i>c</i> 0.2, MeOH)
Retention time (HPLC)	31.2 min. (standard gradient)
	
	(+)-ESI-MS: no ionization
	

Stemphyperlenol **24** was isolated from the EtOAc extract of rice cultures of *Stemphylium botryosum* in the form of a reddish brown powder (2 mg). The UV spectrum showed λ_{max} (MeOH) at 217.1, 260.8 and 342.0 nm. Negative ESI-MS showed a molecular ion peak at m/z 350.9 $[\text{M-H}]^-$ (base peak) indicating a molecular weight of 352 g/mol. The ^1H NMR spectrum (Table 3.17), which contained signals due to only eight protons, indicated that the molecule is a symmetrical dimer. The ^1H NMR included signals of two *ortho*-coupled aromatic protons (H-6/H-12) and (H-5/H-11) appearing at δ_{H} 8.04 and 6.82 ppm, respectively, (H-1/H-7) at δ_{H} 4.64 ppm, (H-6b/H-12b) at δ_{H} 3.70 ppm, (H-2ax/H8ax) at δ_{H} 3.04 ppm and (H-2eq/H-8eq) at δ_{H} 3.08 ppm. The respective substructures were also assembled on basis of the COSY spectrum (Table 3.17). The HMBC spectrum showed HMBC correlations of H-5 and H-6 to C-4 indicating that the carbonyl group was located at C-3. This was confirmed by correlations of CH_2 -2/8 with C-3/9. The correlations of H-6b/12b to C-6a/12a and of H-6/12 to C-6b/12b indicated the connection of the two block units of the molecule to give the planar structure of **24**. This was further confirmed by the long-range coupling between the aromatic (H-6/12) and benzylic (H-6b/12b) protons observed in the COSY spectrum.

The obtained data were in excellent agreement with UV, ^1H -NMR, mass spectral data and $[\alpha]_{\text{D}}$ value published for stemphyperlenol (Arnone and Nasini, 1986), confirming that **24** and the latter were identical. Stemphyperlenol had previously been described from *Alternaria cassiae* (Hradil *et al.*, 1989) and *Stemphylium botryosum* var. *Lactucum* (Arnone and Nasini, 1986).



24 Stemphyperylenol

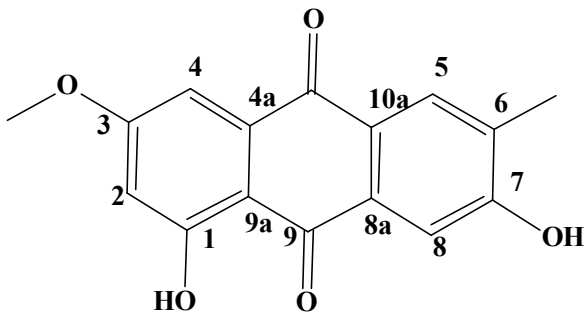
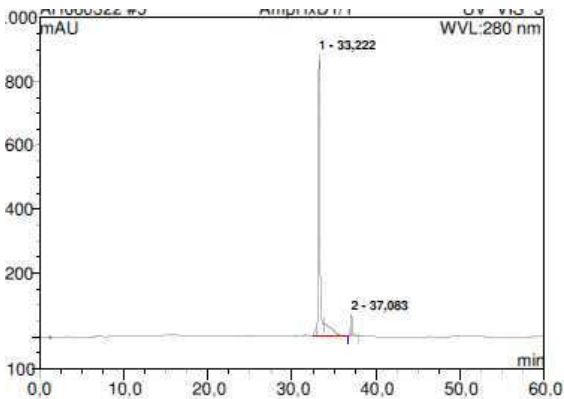
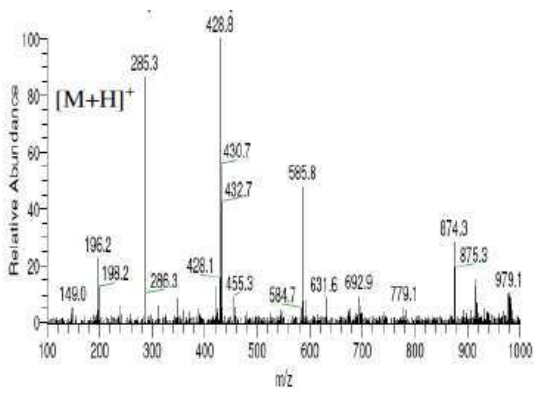
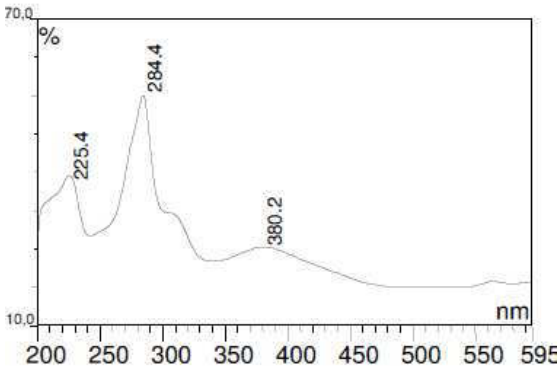
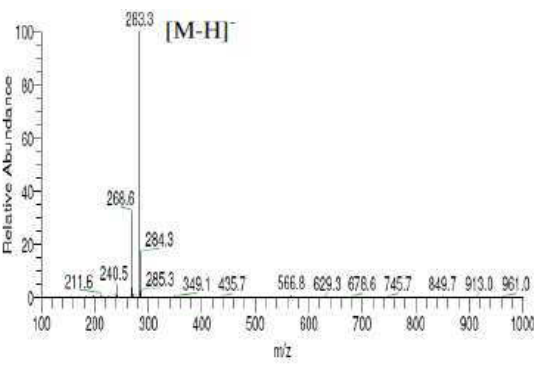
Table 3.17: ^1H NMR, COSY and HMBC spectra of compound **24**

Position	24 δ_{H}^*	$\delta_{\text{H}}^{\text{O}}$	COSY	HMBC
1, 7	4.64, m	4.77	2/8ax, 2/8eq, 6/12b	
1-, 7-OH		4.97	1/7	
2ax, 8ax	3.04, dd (15, 11)	3.17	1/7, 2/8ax	1/7, 3/9, 6/12b
2eq, 8eq	3.08, dd (15.1, 4.2)	3.07	1/7, 2/8eq	1/7, 3/9, 6/12b
3, 9				
3a, 9a				
3b, 9b				
4, 10				
5, 11	6.82, d (8)	6.81	6/12	3/9a, 4/10, 6/12a
6, 12	8.04, d (8)	8.14	5/11, 6/12b	3/9b, 4/10, 6/12b
6a, 12a				
6b, 12b	3.70, d (10)	3.75	1/7, 6/12	1/7, 3/9b, 6/12a
4-, 10-OH		12.09		

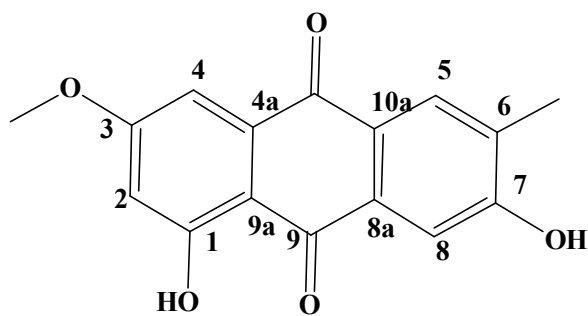
o (Arnone and Nasini, 1986) (acetone- d_6).

* Measured in (MeOH- d_4).

3.2.6. Macrosporin (25, known compound)

Macrosporin	
Synonym(s)	1,7-dihydroxy-3-methoxy-6-methylantracene-9,10-dione
Sample code	Stem70Esemi6
Biological source	<i>Stemphylium botryosum</i>
Sample amount	3 mg
Physical properties	yellow crystals
Molecular formula	C ₁₆ H ₁₂ O ₅
Molecular weight	284 g/mol
Retention time (HPLC)	33.2 min. (standard gradient)
	
	
	

Macrosporin **25** was isolated from the EtOAc extract of the rice culture of *Stemphylium botryosum* as yellow crystals (3 mg). It exhibited UV absorbances at λ_{max} (MeOH) 225.4, 284.4 and 380.2 nm suggesting an anthraquinone as the basic structure. Positive and negative ESI-MS showed molecular ion peaks at m/z 285.3 $[M+H]^+$ (base peak) and m/z 283.6 $[M-H]^-$ (base peak), respectively, indicating a molecular weight of 284 g/mol. ^1H spectrum (Table 3.18) indicated the presence of an aromatic methyl group at δ_{H} 2.34 ppm, and a methoxy singlet at δ_{H} 4.00 ppm. The ^1H NMR spectrum revealed the presence of four aromatic protons, two of which were doublets occurring at δ_{H} 7.19 ppm and 6.80 ppm with a coupling constant of 2.5 Hz, indicating their meta position in the ring system, corresponding to H-4 and H-2, respectively. The remaining two aromatic proton singlets at δ_{H} 7.95 ppm and 7.67 ppm were assigned to the para-coupled protons H-5 and H-8, respectively, of the other aromatic ring. The compound was thus identified as the known macrosporin, which was confirmed by comparison of UV, ^1H NMR and mass spectral data with published data (Suemitsu *et al.*, 1984, 1989). Macrosporin was previously reported from several *Alternaria* species (Stoessl *et al.*, 1983; Lazarovits *et al.*, 1988; Suemitsu *et al.*, 1989) as well as from *Phomopsis juniperovora* (Wheeler and Wheeler, 1975), *Dactylaria lutea* (Becker *et al.*, 1978), *Dichotomophthora lutea* (Hosoe *et al.*, 1990) and *Pleospora* sp. (Ge *et al.*, 2005).



25 Macrosporin

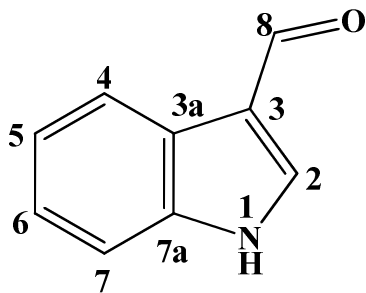
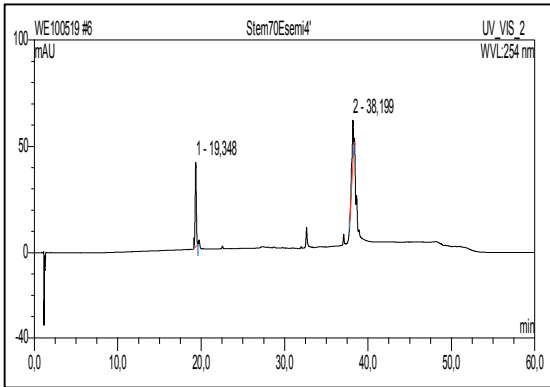
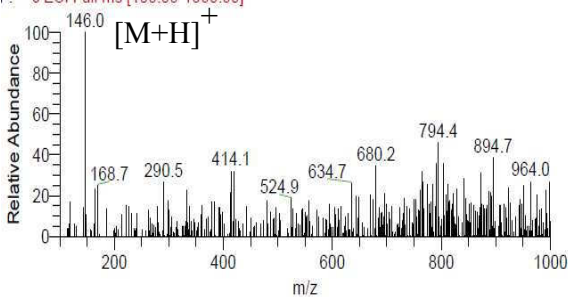
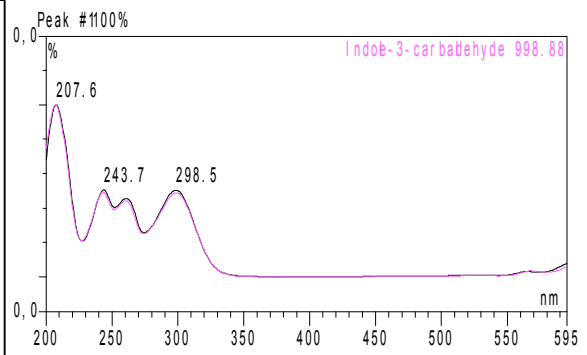
Table 3.18: ^1H NMR and COSY spectra of compound **25**

Position	25		
	δ_{H}^*	$\delta_{\text{H}}^{\text{O}}$	COSY
1			
2	6.80, d (2.5)	6.77, d (2.5)	4
3			
4	7.19, d (2.5)	7.30, d (2.5)	2
4a			
5	7.95, s	8.00, s	
6			
7			
8	7.67, s	7.54, s	
8 ^a			
9			
9 ^a			
10			
10a			
-Me	2.34, s	2.33, s	
-OMe	4.00, s	3.93, s	

o (Suemitsu *et al.*, 1984) (THF- d_8).

* Measured in (DMF- d_7).

3.2.7. Indole-3-carbaldehyde (26, known compound)

Indole-3-carbaldehyde	
Synonym(s)	1 <i>H</i> -indole-3-carbaldehyde
Sample code	Stem70E semi4'
Biological source	<i>Stemphylium botryosum</i>
Sample amount	0.3 mg
Physical properties	Yellow powder
Molecular formula	C ₉ H ₇ NO
Molecular weight	145 g/mol
Retention time (HPLC)	19.3 min. (standard gradient)
	
	<p>brahim215 #640 RT: 19.59 AV: 1 NL: 4.57E6 F: + c ESI Full ms [100.00-1000.00]</p> 
	(-)-ESI-MS: no ionization

Indole-3-carbaldehyde **26** was isolated from the EtOAc extract of rice culture of *Stemphylium botryosum* as yellow powder (0.3 mg). The compound was confirmed by comparison of the molecular weight, UV and co-injection with a reference sample (Ibrahim, 2005).

Table 3.19: Bioactivity test results for compounds isolated from the endophytic fungus *Stemphylium botryosum*

Compound tested	L5178Y growth in %• (Conc. 10µg/mL)
Phomapyrone D/H (19/20)	66.8
Infectopyrone (22)	54.3
Stemphbotrydione (23)	86.9
Stemphperyleneol (24)	44.5
Macrosporin (25)	54.5

• Data provided by Prof. W. E. G. Müller, Mainz.

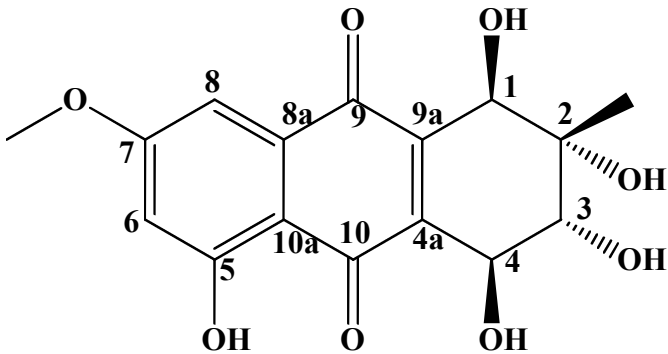
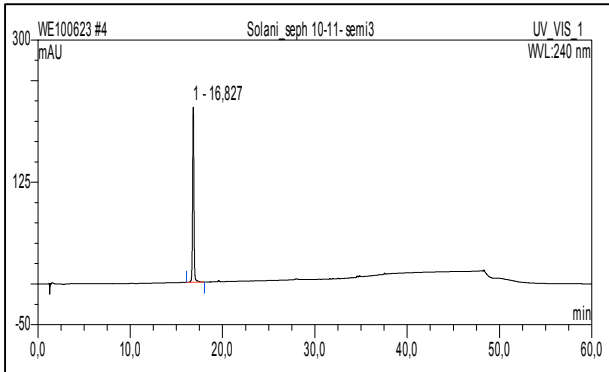
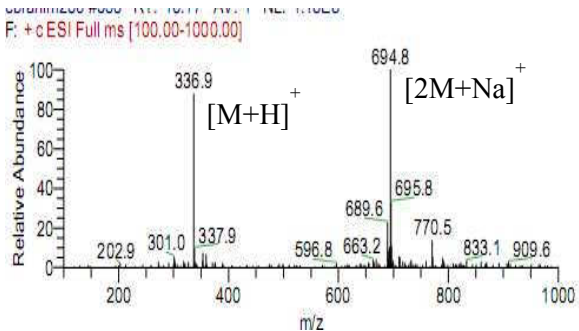
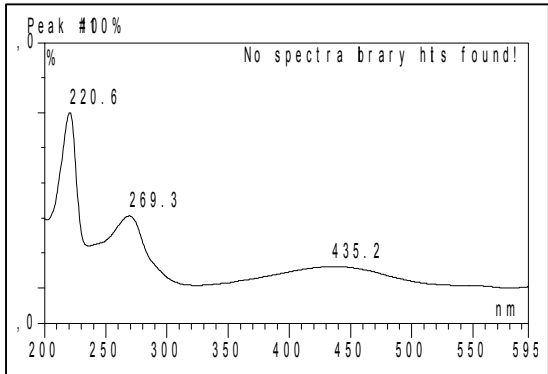
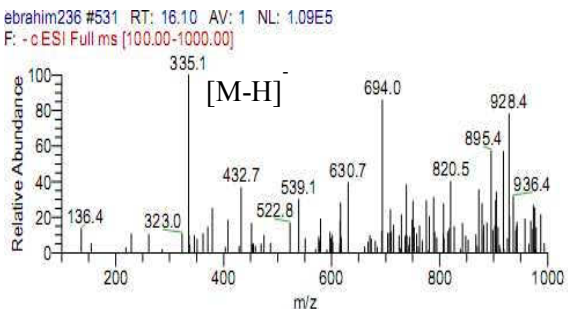
The cytotoxic activity of the isolated compounds of the fungus *Stemphylium botryosum*, indicates that phomapyrone D/H and stemphbotrydione exhibited weak activity while all the other compounds showed moderate cytotoxic activity.

3.3. Compounds isolated from the endophytic fungus *Stemphylium solani*

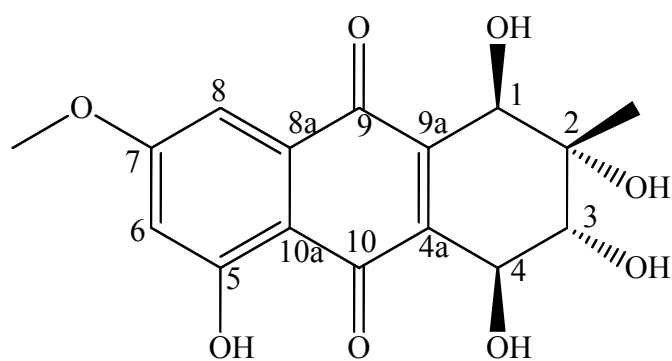
This endophytic fungal strain of the genus *Stemphylium* was isolated from stems of *Mentha pulegium* growing in Morocco. The pure fungal strain was cultivated on rice solid medium. Two compounds were isolated from the solid rice cultures; altersolanol A (**27**) and stemphsolantrione (**28**). Moreover, extracts obtained from solid cultures were subjected to some preliminary biological screening assays, i.e. cytotoxicity assays. Interestingly, extracts obtained from rice cultures showed no activity.

In this part of the investigation results on the natural products produced by *Stemphylium solani* when grown on solid rice medium are presented.

3.3.1. Altersolanol A (27, known compound)

Altersolanol A	
Synonym(s)	(1 <i>R</i> ,2 <i>S</i> ,3 <i>R</i> ,4 <i>S</i>)-1,2,3,4,5-pentahydroxy-7-methoxy-2-methyl-1,2,3,4-tetrahydroanthracene-9,10-dione
Sample code	Solaniseph89semi3
Biological source	<i>Stemphylium solani</i>
Sample amount	1.5 mg
Physical properties	Orange yellow crystals
Molecular formula	C ₁₆ H ₁₆ O ₈
Molecular weight	336
Optical rotation [α] _D ²⁰	-149 (<i>c</i> 0.12, EtOH)
Retention time (HPLC)	16.8 min. (standard gradient)
	
	
	

Altersolanol A (**27**) was isolated from the EtOAc extract of rice cultures of *Stemphylium solani* as orange yellow crystals (1.5 mg). It showed UV absorbances at λ_{max} (MeOH) 220.6, 269.3 and 435.2 nm suggesting a quinone as the basic structure. Positive and negative ESI-MS showed molecular ion peaks at m/z 336.9 $[\text{M}+\text{H}]^+$ (base peak) and m/z 335.1 $[\text{M}-\text{H}]^-$ (base peak), respectively, indicating a molecular weight of 336 g/mol. The ^1H NMR spectrum (Table 3.20) displayed two doublets at δ_{H} 3.83 ppm and 4.71 ppm ($J=5.9$ and 6.3 Hz, respectively). Furthermore, a singlet was detected at δ_{H} 1.40 ppm corresponding to an aliphatic methyl group (2-Me), together with a singlet also at δ_{H} 4.51 ppm assigned for H-1. The pair of *meta*-coupled aromatic protons at δ_{H} 7.14 ppm (H-8) and 6.74 ppm (H-6) and the aromatic methoxy group δ_{H} 3.91 ppm were also observed. The nature of the non-aromatic carbocycle was evident from the COSY spectrum (Table 3.20), establishing the planar structure of **27** as identical to altersolanol A (**27a**) (Stoessl, 1969). This assignment was further corroborated by the very similar experimental UV, ^1H , ^{13}C NMR, mass spectral data and $[\alpha]_{\text{D}}$ value obtained for **27a** in comparison to published data for altersolanol A (Yagi *et al.*, 1993; Okamura *et al.*, 1993, 1996). Also, co-injection of **27** with that of pure altersolanol A showed one and the same peak in HPLC. Altersolanol A was previously isolated from several *Alternaria* species (Stoessl *et al.*, 1983; Lazarovits *et al.*, 1988; Yagi *et al.*, 1993; Okamura *et al.*, 1993, 1996).



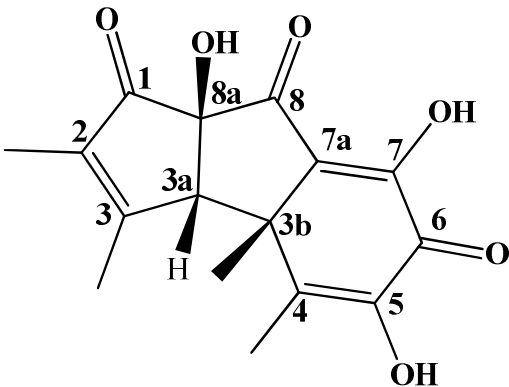
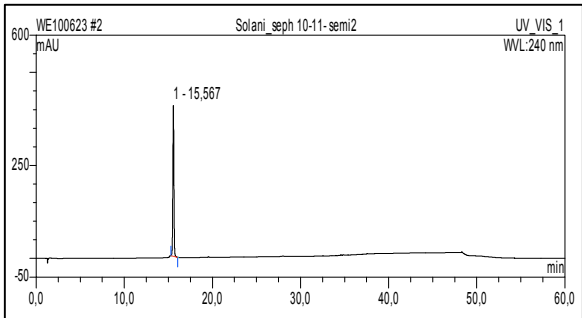
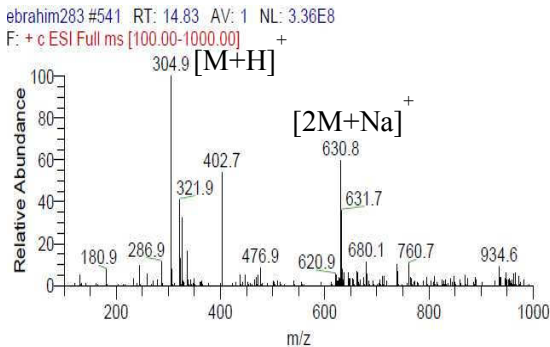
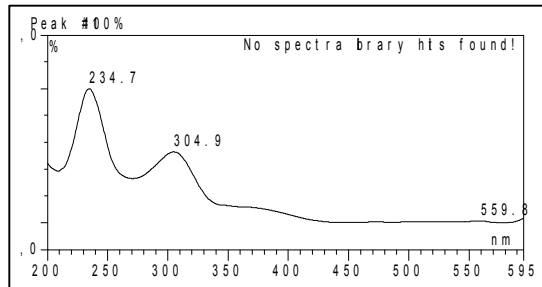
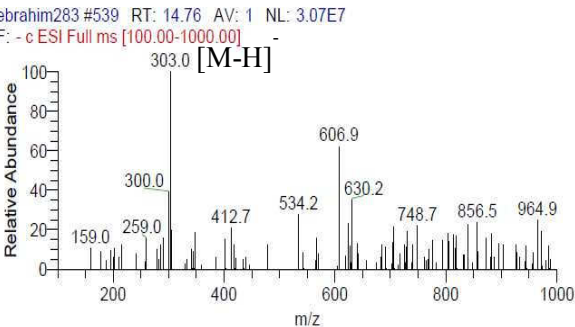
27 Altersolanol A

Table 3.20: ^1H NMR and COSY spectra of compound **27** at 500 MHz

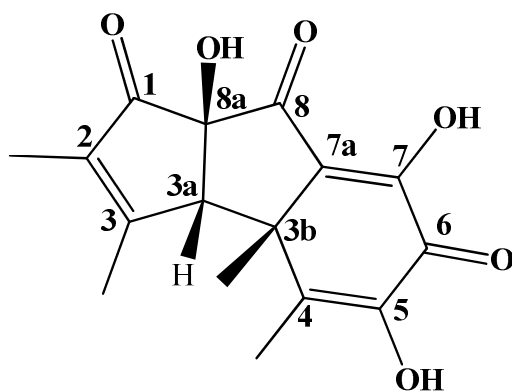
Nr.	27		27a
	δ_{H} (MeOD)	COSY	δ_{H} (DMSO)
1	4.51, s		4.38, d (4.0)
1-OH			5.30, s
2			
2-OH			4.48, br s
3	3.83, d (5.9)	4	3.64, m (7.0)
3-OH			5.00, d (7.0)
4	4.71, d (6.3)	3	4.54, m (7.0)
4-OH			5.71, d (7.0)
4a			
5			
5-OH			
6	6.74, d (2.0)	8	6.72, d (2.0)
7			
8	7.14, d (2.0)	6	6.93, d (2.0)
9			
9-OH			
9a			
10			
10a			
CH ₃	1.40, s		1.24, s
OCH ₃	3.91, s		3.90, s

a) (Yagi, *et al.*, 1993)

3.1.2. Stempholantrione (28, new compound)

Stempholantrione	
Synonym(s)	5,7,8a-trihydroxy-2,3,3b,4-tetramethylcyclopenta[α]indene-1,6,8(3aH,3bH,8aH)-trione
Sample code	Solaniseph89semi2
Biological source	<i>Stemphylium solani</i>
Sample amount	6 mg
Physical properties	Brown amorphous solid
Molecular formula	C ₁₆ H ₁₆ O ₆
Molecular weight	304
Optical rotation $[\alpha]_D^{20}$	+21 (c 0.05, MeOH)
Retention time (HPLC)	15.6 min. (standard gradient)
	
	
	

Stemphsolantrione (**28**) was isolated from the EtOAc extract of the solid rice culture of *Stemphylium solani* as brown amorphous solid (6 mg). It showed UV absorbances at λ_{max} (MeOH) 234.7 and 304.9 nm. Positive and negative ESI-MS showed molecular ion peaks at m/z 304.9 $[M+H]^+$ (base peak) and m/z 303 $[M-H]^-$ (base peak), respectively, indicating the molecular weight of 304 g/mol. The HRESI-MS exhibited a strong peak at m/z 305.1015 $[M+H]^+$ indicating the molecular formula $C_{16}H_{16}O_6$ (calculated 305.1025, Δ 0.001). Structural elucidation of **28** was based on results of 1D and 2D NMR spectral analysis including 1H NMR, 1H - 1H COSY and HMBC spectra (Table 3.21). This indicated the presence of four methyl groups, one of them is attached to an aliphatic system (3b-Me) at δ_H 1.49 and the other three are attached to an olifenic system (2-Me, 3-Me and 4-Me at δ_H 1.53, 1.88 and 2.11, respectively). Moreover there is a singlet at δ_H 3.45 ppm attributed to H-3a. In addition, to three hydroxyls 8a-OH, 5-OH and 7-OH at δ_H 6.76 ppm, 8.97 ppm and 10.75 ppm, respectively, were also observed. The HMBC spectrum confirms the attachment of methyl groups by correlation of 2-Me (at δ_H 1.53 ppm) to C-1, C-2 and C-3, 3-Me (at δ_H 1.88 ppm) to C-2, C-3 and C-3a, 4-Me (at δ_H 2.11 ppm) to C-3b, C-4 and C-5 and 3b-Me at δ_H 1.49 ppm to C-3a, C-3b, C-4 and C-7a. Furthermore, HMBC spectrum shows correlations of H-3a to C-2, C-3, C-3b, C-4, C-7a, C-8 and C-8a and correlations of 5-OH (at δ_H 8.97 ppm) to C-4, C-6 and C-7. The relative stereochemistry was established through a ROESY experiment by correlation of 3a-H to both 3b-Me and 8a-OH (at δ_H 6.76 ppm). The compound was identified as the new natural product stemphsolantrione.



28 Stemphsolantrione

Table 3.21: ^1H , ^{13}C , HMBC and ROESY spectra of compound **27**

Nr.	28			
	δ_{C} (DMSO)	δ_{H} (DMSO)	HMBC	ROESY
1	200.2			
2	136.5			
3	168.3			
3a	59.8	3.45, s	2, 3, 3b, 4, 7a, 8, 8a	8a-OH, 3b-Me
3b	47.2			
4	136.8			
5	126.4			
6	177.2			
7	145.9			
7a	147.4			
8	197.4			
8a	87.3			
5-OH		8.97, s	4, 6, 7	
7-OH		10.75, br s		
8a-OH		6.76, br s		3a
2-Me	8.6	1.53, s	1, 2, 3	
3-Me	17.1	1.88, s	2, 3, 3a	
3b-Me	29.4	1.49, s	3a, 3b, 4, 7a	3a
4-Me	14.9	2.11, s	3b, 4, 5	

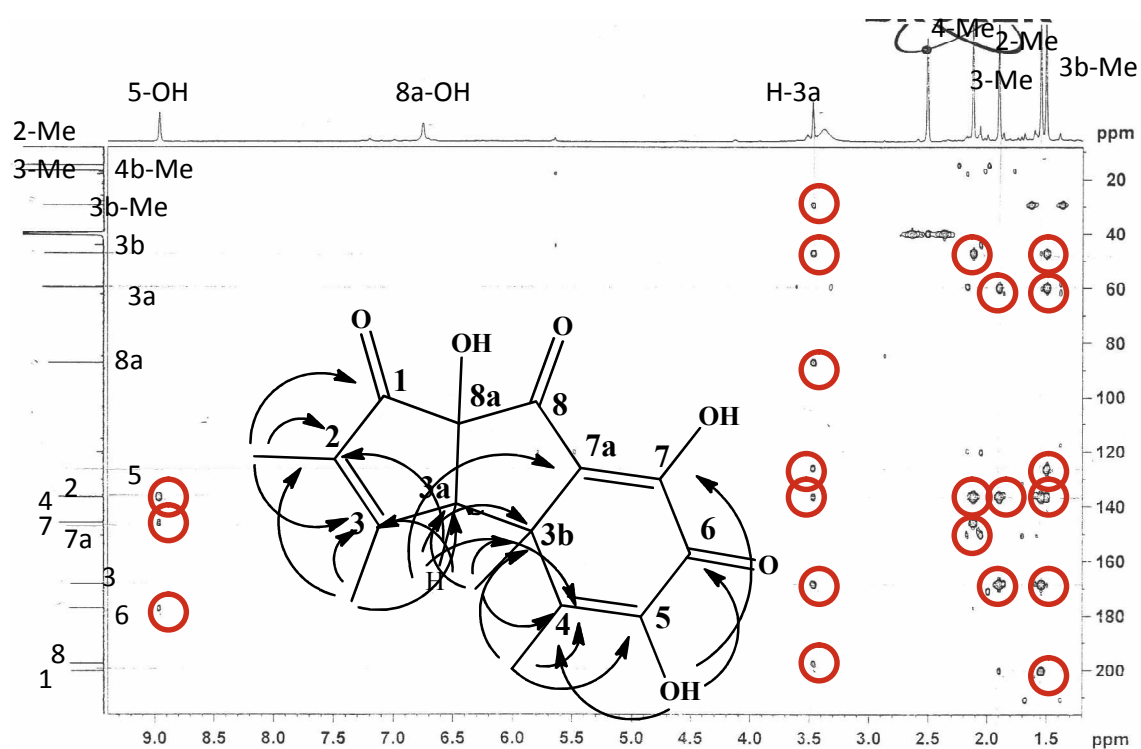


Fig. 3.31: COSY spectrum of compound **28**.

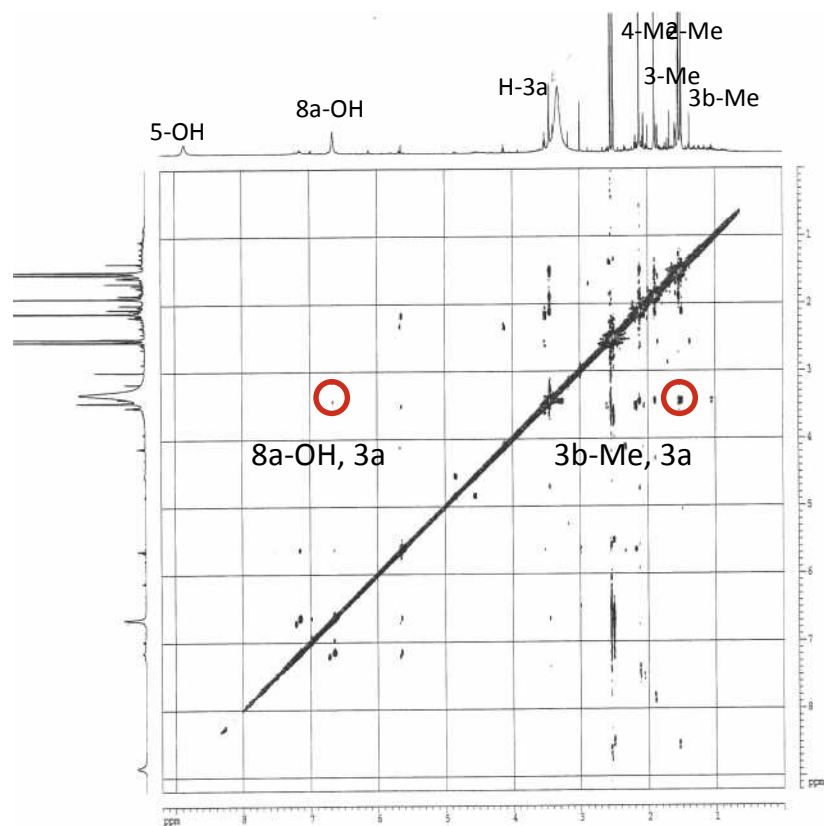


Fig. 3.32: ROESY spectrum of compound **28**.

Table 3.22: Bioactivity test results for compounds isolated from the endophytic fungus *Stemphylium solani*

Compound tested	L5178Y growth in %• (Conc. 10µg/mL)	EC ₅₀ (µg/mL)	EC ₅₀ (µmol/L)
Altersolanol A (27)	0.0	0.21	0.6
Stemphsolantrione (28)	43.8		

• Data provided by Prof. W. E. G. Müller, Mainz.

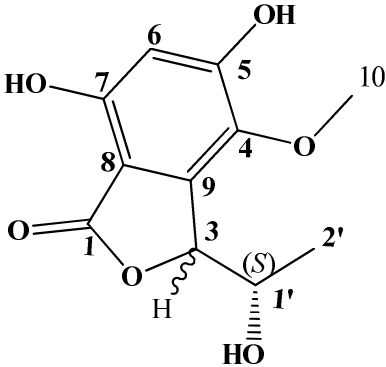
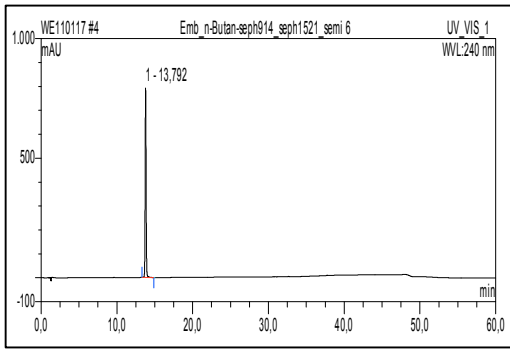
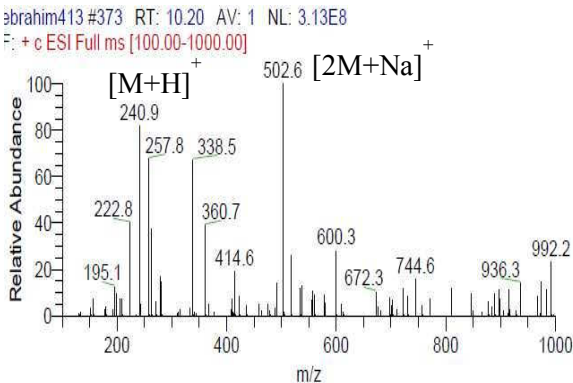
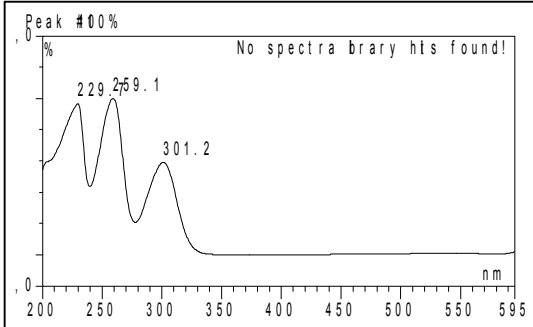
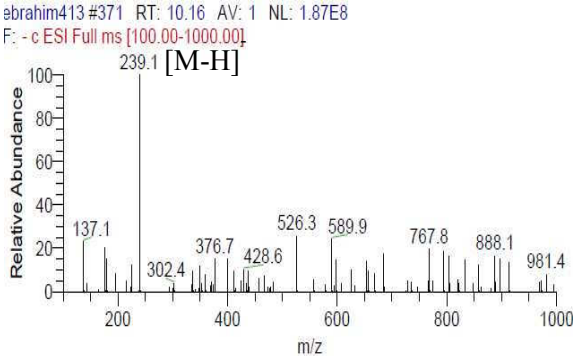
Looking to the cytotoxic activity of the isolated compounds from the fungus *Stemphylium solani* indicates that altersolanol A showed strong activity while stemphsolantrione showed only moderate cytotoxic activity.

3.4. Compounds isolated from the endophytic fungus *Embellisia eureka*

This endophytic fungal strain of the genus *Embellisia* was isolated from fresh stems of *Cladanthus arabicus* growing in Morocco. The pure fungal strain was cultivated on rice solid medium. Thirteen compounds were isolated from the solid rice cultures; embepthalide A (**29**), embepthalide B (**30**), embepthalide C (**31**), embepthalide D (**32**), embepthalide E (**33**), embeurekol A (**34**), embeurekol B (**35**), embeurekol C (**36**), P-hydroxy benzaldehyde (**37**), 2-anhydromevalonic acid (**38**), endocrocin (**39**), pyrrocidine D (**40**) and pyrrocidine E (**41**). Moreover, extracts obtained from solid cultures were subjected to some preliminary biological screening assays, i.e. cytotoxicity assays. Interestingly, extracts obtained from rice cultures showed cytotoxic activity.

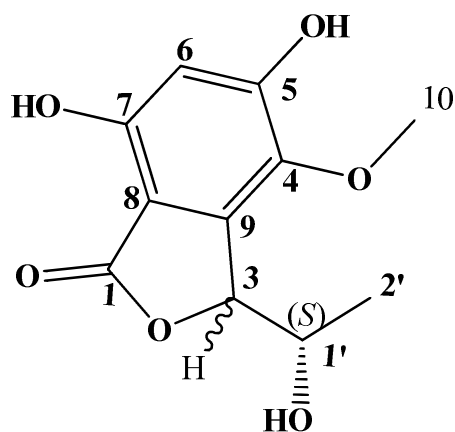
In this part of the investigation results on the natural products produced by *Embellisia eureka* when grown on solid rice medium are presented.

3.4.1. Embepthalide A (29, new compound)

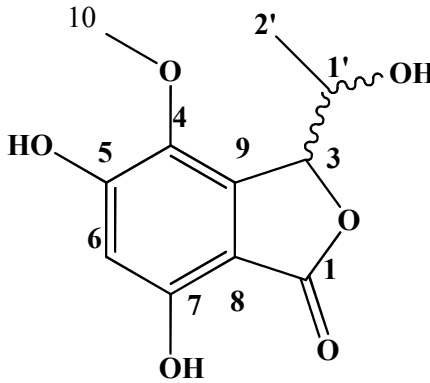
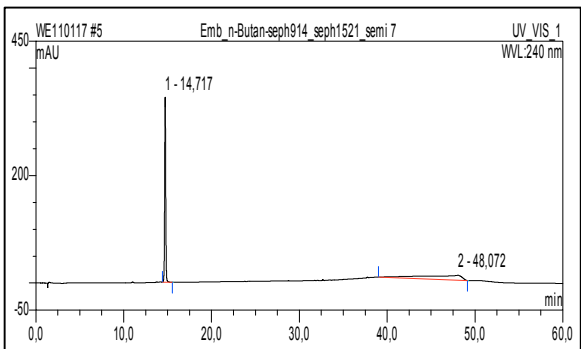
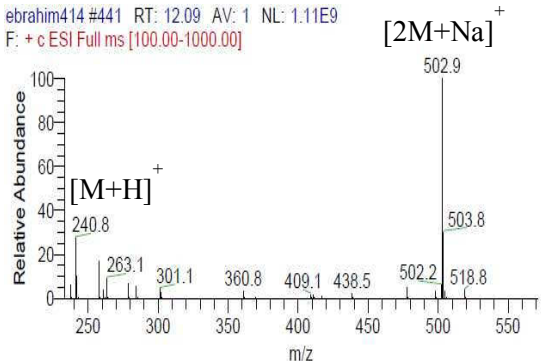
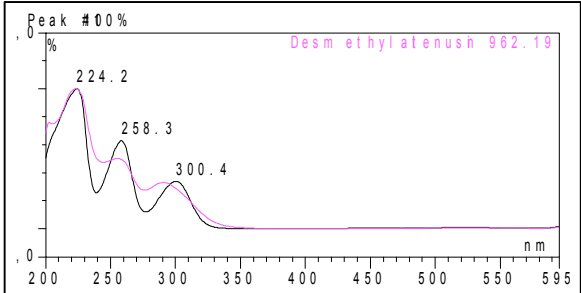
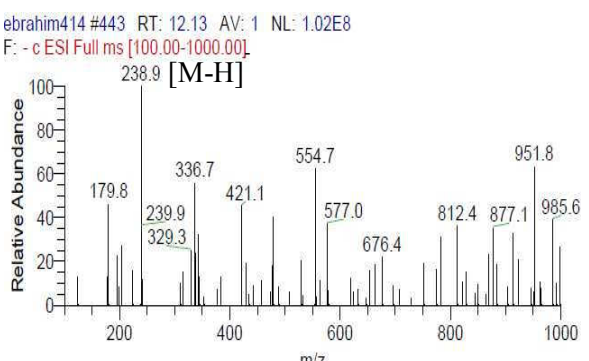
Embepthalide A	
Synonym(s)	5,7-dihydroxy-3-(1-hydroxyethyl)-4-methoxyisobenzo furan-1(3 <i>H</i>)-one
Sample code	Emb_nBut_seph914_seph1521_semi6
Biological source	<i>Embellisia eureka</i>
Sample amount	5 mg
Physical properties	yellowish amorphous solid
Molecular formula	C ₁₁ H ₁₂ O ₆
Molecular weight	240 g/mol
Optical rotation [α] _D ²⁰	-17 (<i>c</i> 0.05, MeOH)
Retention time (HPLC)	13.8 min. (standard gradient)
	
	
	

Embeppthalide A (**29**) was isolated from the EtOAc extract of solid rice cultures of *Embellisia eureka* as yellowish amorphous solid (5 mg). It showed UV absorbances at λ_{max} (MeOH) 229.7, 259.1 and 301.2 nm. Positive and negative ESI-MS showed molecular ion peaks at m/z 240.9 $[\text{M}+\text{H}]^+$ (base peak) and m/z 239.1 $[\text{M}-\text{H}]^-$ (base peak), respectively, indicating a molecular weight of 240 g/mol. The HRESI-MS exhibited a strong peak at m/z 241.0688 $[\text{M}+\text{H}]^+$ indicating the molecular formula $\text{C}_{11}\text{H}_{12}\text{O}_6$ (calculated 241.0707, Δ 0.0019). Structural elucidation of **29** was based on results of 1D and 2D NMR spectral analysis including ^1H NMR, ^1H - ^1H COSY, ROESY and HMBC spectra (Table 3.23). The ^1H NMR spectrum showed a doublet at δ_{H} 0.73 ppm ($J=6.3$ Hz) interpreted for 2'-Me, a multiplet at δ_{H} 4.24 ppm for H-1', a doublet at δ_{H} 5.45 ppm ($J=2.3$ Hz) for H-3, a singlet at δ_{H} 3.69 ppm for 4-OMe, an aromatic singlet at δ_{H} 6.45 ppm for H-6 and two singlets at δ_{H} 10.21 ppm and 10.46 ppm for the aromatic hydroxyl groups, 7-OH and 5-OH, respectively. ^1H - ^1H COSY showed one distinct spin system from 2'-Me at δ_{H} 0.73 ppm (d, $J=6.3$) to H-3 at δ_{H} 5.45 ppm (d, $J=2.3$). The aromatic proton H-6 resonating at δ_{H} 6.45 ppm showed a strong ROESY correlation to the two aromatic hydroxyl groups at δ_{H} 10.21 ppm and 10.46 ppm, indicating that the aromatic proton must be between both hydroxyls. In addition, 4-OMe at δ_{H} 3.69 ppm showed a strong ROESY correlation to both H-1' at δ_{H} 4.24 ppm, H-3 at δ_{H} 5.45 ppm and 2'-Me at δ_{H} 0.73 ppm. Furthermore, the aromatic proton H-6 showed 2J - 3J and 4J HMBC correlations, an ω -correlation to C-1 (at δ_{C} 167.9), to C-4, to C-5, to C-7 and to C-8, which secures its position at C-6. Correlations of 2'-Me at δ_{H} 0.73 ppm to C-1' and C-3, H-1' at δ_{H} 4.24 ppm to C-2' and C-3 and H-3 at δ_{H} 5.45 ppm to C-1, C-4, C-5, C-7, C-8, C-9, C-1' and C-2' were also detected. Moreover, the HMBC correlation of 4-OMe at δ_{H} 3.69 ppm to C-4 confirms the attachment of the methoxy group to position 4. Furthermore, for the determination of the absolute stereochemistry at the chiral center C-1' the modified Mosher procedure was applied. The difference between the (*S*)-ester derivative and the (*R*)-ester

derivative allow to assign the chiral center C-1' to have (*S*) configuration (Table 3.23a). From the previous data compound **29** was found to be a new natural product to which the name embepthalide A is given.



3.4.2. Embepthalide B (30, new compound)

Embepthalide B	
Synonym(s)	5,7-dihydroxy-3-(1-hydroxyethyl)-4-methoxyisobenzofuran-1(3 <i>H</i>)-one
Sample code	Emb_nBut_seph914_seph1521_semi7
Biological source	<i>Embellisia eureka</i>
Sample amount	4 mg
Physical properties	yellowish amorphous solid
Molecular formula	C ₁₁ H ₁₂ O ₆
Molecular weight	240 g/mol
Optical rotation $[\alpha]_D^{20}$	+96 (<i>c</i> 0.05, MeOH)
Retention time (HPLC)	14.7 min. (standard gradient)
	
	<p>ebrahim414 #441 RT: 12.09 AV: 1 NL: 1.11E9 F: + c ESI Full ms [100.00-1000.00]</p> 
	<p>ebrahim414 #443 RT: 12.13 AV: 1 NL: 1.02E8 F: - c ESI Full ms [100.00-1000.00]</p> 

Embeophthalide B (**30**) was isolated from the EtOAc extract of solid rice cultures of *Embellisia eureka* as yellowish amorphous solid (4 mg). It showed UV absorbances at λ_{max} (MeOH) 224.2, 258.3 and 300.4 nm. Positive and negative ESI-MS showed quasi-molecular ion peaks at m/z 240.8 $[\text{M}+\text{H}]^+$ (base peak) and m/z 238.9 $[\text{M}-\text{H}]^-$ (base peak), respectively, indicating a molecular weight of 240 g/mol. The HRESI-MS exhibited a strong peak at m/z 241.0691 $[\text{M}+\text{H}]^+$ indicating the molecular formula $\text{C}_{11}\text{H}_{12}\text{O}_6$ (calculated 241.0707, Δ 0.0016). The NMR data of **30** are similar to those of **29** with only small differences in chemical shifts. Structural elucidation of **30** was based on results of 1D and 2D NMR spectral analysis including ^1H NMR, ^1H - ^1H COSY, ROESY and HMBC spectra (Table 3.23). The ^1H NMR spectrum showed a doublet at δ_{H} 1.52 ppm ($J=6.2$ Hz) interpreted for 2'-Me, a multiplet at δ_{H} 4.15 ppm for H-1', a broad singlet at δ_{H} 5.25 ppm for H-3, a singlet at δ_{H} 3.69 ppm for 4-OMe, an aromatic singlet at δ_{H} 6.41 ppm for H-6 and two singlets at δ_{H} 10.09 ppm and 10.31 ppm for the aromatic hydroxyl groups 7-OH and 5-OH, respectively. The ^1H - ^1H COSY spectrum showed also one distinct spin system from 2'-Me at δ_{H} 1.52 ppm (d, $J=6.2$) to H-3 at δ_{H} 5.25 ppm (br. s). The aromatic proton H-6 resonating at δ_{H} 6.41 ppm showed strong ROESY correlations to both aromatic hydroxyl groups at δ_{H} 10.09 ppm and 10.31 ppm indicating its position between both hydroxyls. In addition, 4-OMe at δ_{H} 3.69 ppm showed strong ROESY correlations to H-1' at δ_{H} 4.15 ppm, H-3 at δ_{H} 5.25 ppm and 2'-Me at δ_{H} 1.52 ppm. Furthermore, the aromatic proton H-6 showed 2J - 3J and 4J HMBC correlations, an ω -correlation to C-1 (at δ_{C} 167.9), to C-4, to C-5, to C-7 and to C-8, which secures its position at C-6. Correlations of 2'-Me at δ_{H} 1.52 ppm to C-1' and C-3, H-1' at δ_{H} 4.15 ppm to C-2' and C-3 and H-3 at δ_{H} 5.25 ppm to C-1, C-4, C-7, C-8, C-9 and C-2' were also detected. Moreover, the HMBC correlation of 4-OMe at δ_{H} 3.69 ppm to C-4 confirms its attachment to carbon C-4. For the determination of the absolute stereochemistry at the chiral center C-1' modified Mosher procedure was applied but unfortunately, the differences between the (*S*)-ester derivative and the (*R*)-

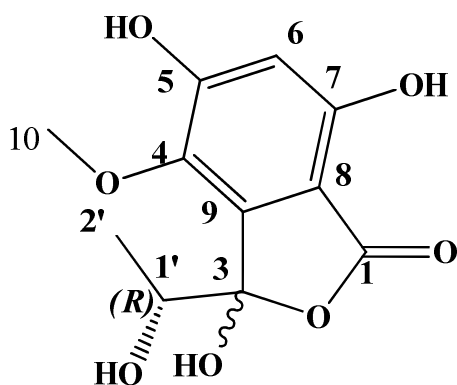
ester derivative was insignificant. We noticed that compound **29** and **30** are isomers since they share the same UV and molecular weights but different retention times. From the previous data compound **30** was found to be a new natural product to which the name embepthalide B is given.

3.4.3. Embepthalide C (31, new compound)

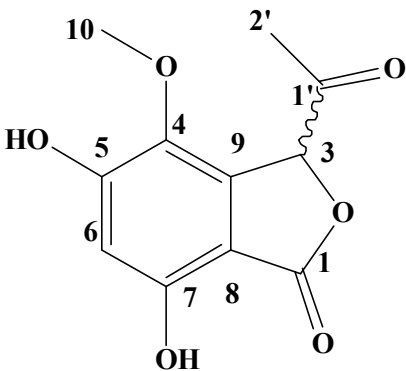
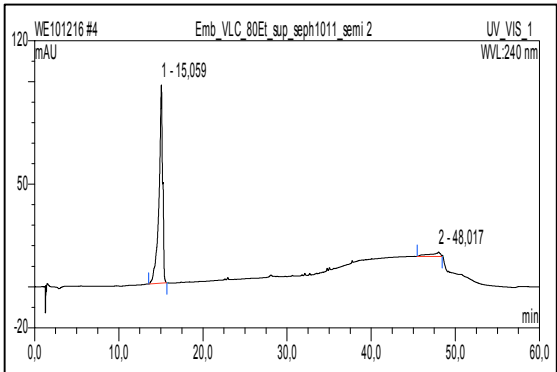
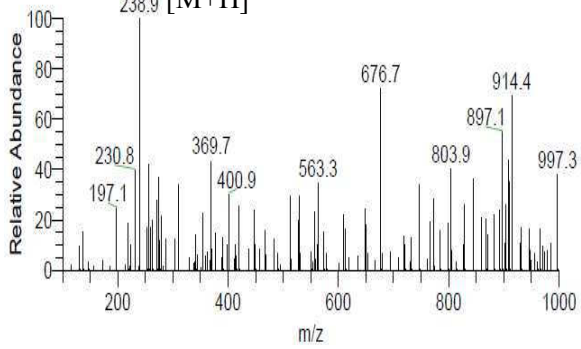
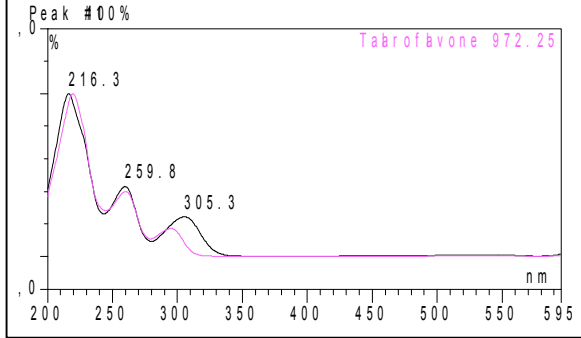
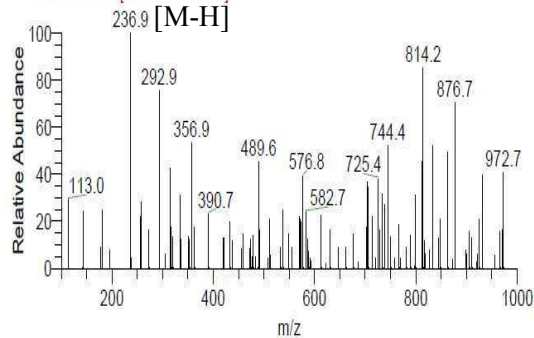
Embepthalide C	
Synonym(s)	3,5,7-trihydroxy-3-(1-hydroxyethyl)-4-methoxyisobenzofuran-1(3H)-one
Sample code	Emb_VLC_80Et_sup_seph914_semi4
Biological source	<i>Embellisia eureka</i>
Sample amount	3 mg
Physical properties	yellowish amorphous solid
Molecular formula	C ₁₁ H ₁₂ O ₇
Molecular weight	256 g/mol
Optical rotation [α] _D ²⁰	+12 (<i>c</i> 0.05, MeOH)
Retention time (HPLC)	8.0 min. (standard gradient)
	<p>ebrahim410 #133 RT: 3.63 AV: 1 NL: 2.14E8 F: + c ESI Full ms [100.00-1000.00] +</p>
	<p>ebrahim410 #131 RT: 3.59 AV: 1 NL: 1.56E8 F: - c ESI Full ms [100.00-1000.00] -</p>

Embeophthalide C (**31**) was isolated from the EtOAc extract of solid rice cultures of *Embellisia eureka* as yellowish amorphous solid (3 mg). It showed UV absorbance maxima at λ_{max} (MeOH) 213.7, 260.8 and 304.2 nm, similar to those of **29** and **30** which indicate that all three compounds have the same chromophore. Positive and negative ESI-MS showed molecular ion peaks at m/z 256.9 $[\text{M}+\text{H}]^+$ (base peak) and m/z 255.1 $[\text{M}-\text{H}]^-$ (base peak), respectively, indicating a molecular weight of 256 g/mol. The molecular formula $\text{C}_{11}\text{H}_{12}\text{O}_7$ was obtained from HRESI-MS which exhibited a strong peak at m/z 257.0636 $[\text{M}+\text{H}]^+$ (calculated 257.0656, Δ 0.002). The difference in the molecular weight between **31** and those of **29** and **30** is 16 amu suggesting an extra hydroxyl group in **31**. The NMR data of **31** is very similar to those of **29** and **30** (Table 3.24). The ^1H NMR spectrum showed a doublet at δ_{H} 1.22 ppm ($J=6.3$ Hz) interpreted for 2'-Me, a quartet at δ_{H} 4.11 ppm ($J=6.18, 12.6$) for H-1' instead of multiplet in both **29** and **30**, the presence of a broad singlet at δ_{H} 7.40 ppm interpreted for 3-OH (which together with absence of H-3 confirm that a hydroxyl group is attached to C-3), a singlet at δ_{H} 3.69 ppm for 4-OMe, an aromatic singlet at δ_{H} 6.43 ppm for H-6 and two singlets at δ_{H} 9.98 ppm and 10.29 ppm for the aromatic hydroxyl groups, 7-OH and 5-OH, respectively. The ^1H - ^1H COSY spectrum showed also one distinct spin system from 2'-Me at δ_{H} 1.22 ppm (d, $J=6.2$) to H-1' at δ_{H} 4.11 ppm (q, $J=6.18, 12.6$ Hz). The aromatic proton H-6 resonating at δ_{H} 6.43 ppm showed also the same strong ROESY correlation to both aromatic hydroxyl groups at δ_{H} 9.98 ppm and 10.29 ppm as in **29** and **30** indicating that the aromatic proton is located between both hydroxyls. In addition, 4-OMe at δ_{H} 3.69 ppm showed a strong ROESY correlation to both H-1' at δ_{H} 4.11 ppm and 2'-Me at δ_{H} 1.22 ppm. Furthermore, the aromatic proton H-6 showed 2J - 3J and 4J HMBC correlations, an ω -correlation to C-1 (at δ_{C} 166.3), to C-4, to C-5, to C-7, to C-8 and to C-9, which secures its position at C-6. Correlations of 2'-Me at δ_{H} 1.22 ppm to C-1' and C-3, H-1' at δ_{H} 4.11 ppm to C-2', C-3 and C-9, 3-OH at δ_{H} 7.40 ppm to C-1', C-3, and C-4 were also detected. Moreover, the HMBC correlation

of 4-OMe at δ_{H} 3.69 ppm to C-4 confirms its attachment to carbon C-4. Furthermore, for the determination of the absolute stereochemistry at the chiral center C-1' the modified Mosher procedure was applied. The difference between the (*S*)-ester derivative and the (*R*)-ester derivative allow to assign the chiral center C-1' to have (*R*) configuration (Table 3.24). From the previous data compound **31** was found to be a new natural product to which the name embephtalide C is given.



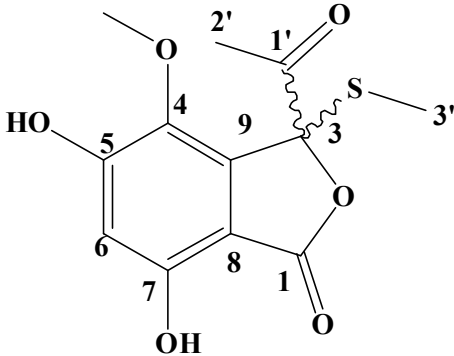
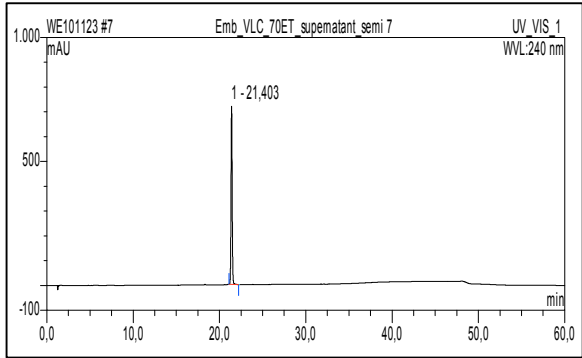
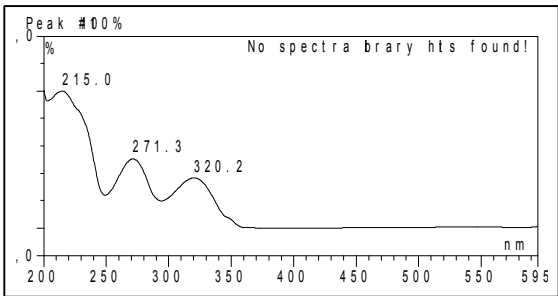
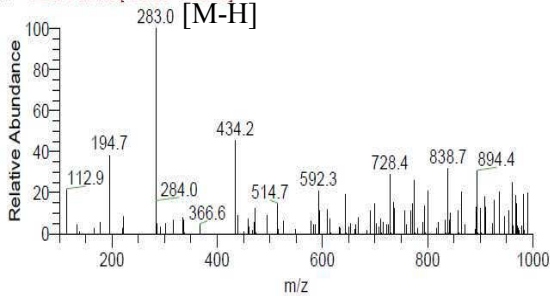
3.4.4. Embepthalide D (32, new compound)

Embepthalide D	
Synonym(s)	3-acetyl-5,7-dihydroxy-4-methoxyisobenzofuran-1(3H)-one
Sample code	Emb_VLC_80Et_sup_seph914_semi2
Biological source	<i>Embellisia eureka</i>
Sample amount	2 mg
Physical properties	yellowish amorphous solid
Molecular formula	C ₁₁ H ₁₀ O ₆
Molecular weight	238 g/mol
Optical rotation $[\alpha]_D^{20}$	+25 (<i>c</i> 0.05, MeOH)
Retention time (HPLC)	15.1 min. (standard gradient)
	
	<p>brahim397 #481 RT: 12.80 AV: 1 NL: 1.23E8 F: + c ESI Full ms [100.00-1000.00]+</p> 
<p>Peak #100%</p>  <p>Tabrofivone 972.25</p>	<p>brahim397 #479 RT: 12.75 AV: 1 NL: 6.46E7 F: - c ESI Full ms [100.00-1000.00]-</p> 

Embeophthalide D (**32**) was isolated from the EtOAc extract of solid rice cultures of *Embellisia eureka* as yellowish amorphous solid (2 mg). It showed UV absorbance maxima at λ_{max} (MeOH) 216.3, 259.8 and 305.3 nm. Positive and negative ESI-MS showed molecular ion peaks at m/z 238.9 $[\text{M}+\text{H}]^+$ (base peak) and m/z 236.9 $[\text{M}-\text{H}]^-$ (base peak), respectively, indicating a molecular weight of 238 g/mol. The molecular formula $\text{C}_{11}\text{H}_{10}\text{O}_6$ was obtained from HRESI-MS which exhibited a strong peak at m/z 239.0534 $[\text{M}+\text{H}]^+$ (calculated 239.0550, Δ 0.0006). The difference in the molecular weight between **32** and both **29** and **30** is 2 amu. The NMR data of **32** are very similar to those of **29** and **30**. Structural elucidation of **32** was based on results of 1D and 2D NMR spectral analysis including ^1H NMR, ^1H - ^1H COSY, ROESY and HMBC spectra (Table 3.25). The ^1H NMR spectrum of **32** showed only one aliphatic singlet at δ_{H} 5.45 ppm instead of a doublet in both **29** and **30**. In addition, the methyl group 2'-Me appears as a singlet at 2.19 ppm and showed strong HMBC correlation to a *keto*-group resonating at δ_{C} 201.3 ppm, which indicated the loss of protons located at C-1' and OH-1' in compound **30**, confirming the difference in their molecular weights. The ^1H NMR spectrum showed also a broad singlet at δ_{H} 5.45 ppm for H-3, a singlet at δ_{H} 3.69 ppm for 4-OMe, an aromatic singlet at δ_{H} 6.51 ppm for H-6 and two singlets at δ_{H} 10.48 ppm and 10.66 ppm for the aromatic hydroxyl groups, 7-OH and 5-OH, respectively. The aromatic proton H-6 resonating at δ_{H} 6.51 ppm showed strong ROESY correlations to the two aromatic hydroxyl groups at δ_{H} 10.48 ppm and 10.66 ppm indicating that the aromatic proton must be between both hydroxyls. In addition, 4-OMe at δ_{H} 3.69 ppm showed a strong ROESY correlation to both H-3 at δ_{H} 5.45 ppm and 2'-Me at δ_{H} 2.19 ppm. Furthermore, the aromatic proton H-6 showed 2J - 3J and 4J HMBC correlations, an ω -correlation to C-1 (at δ_{C} 167.9), to C-4, to C-5, to C-7 and to C-8, which secures its position at C-6. Correlations of 2'-Me at δ_{H} 2.19 ppm to C-1' (at δ_{C} 201.3) and C-3 were also detected. Further inspection of the HMBC spectrum revealed that H-3 at δ_{H} 5.45 ppm is correlated to C-1, C-4, C-5, C-8, C-9 and C-1'. Moreover, the HMBC

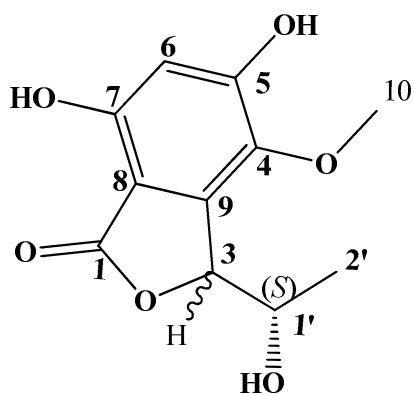
correlation of 4-OMe at δ_{H} 3.69 ppm to C-4 confirm its attachment to position 4. From the previous data compound **32** was found to be a new natural product to which the name embepthalide D is given.

3.4.5. Embepthalide E (33, new compound)

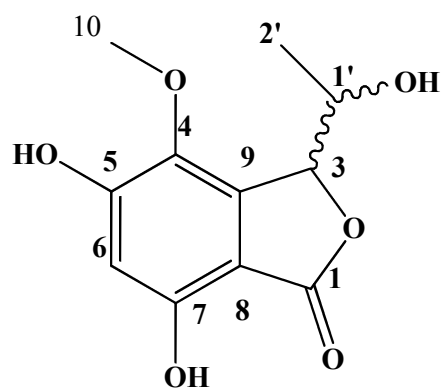
Embepthalide E	
Synonym(s)	3-acetyl-5,7-dihydroxy-4-methoxy-3-(methylthio)isobenzofuran-1(3H)-one
Sample code	Emb_VLC_70Et_sup_semi5
Biological source	<i>Embellisia eureka</i>
Sample amount	2 mg
Physical properties	yellowish amorphous mass
Molecular formula	C ₁₂ H ₁₂ O ₆ S
Molecular weight	284 g/mol
Optical rotation $[\alpha]_D^{20}$	-8 (c 0.05, MeOH)
Retention time (HPLC)	21.4 min. (standard gradient)
	
	No ionization
	<p>ebrahim379 #743 RT: 20.14 AV: 1 NL: 1.05E8 F: - c ESI Full ms [100.00-1000.00] -</p> 

Embeppthalide E (**33**) was isolated from the EtOAc extract of solid rice cultures of *Embellisia eureka* as yellowish amorphous solid (2 mg). It showed UV absorbances at λ_{max} (MeOH) 215.0, 271.3 and 320.2 nm. Negative ESI-MS showed molecular ion peaks at m/z 283.0 $[\text{M}-\text{H}]^-$ (base peak), respectively, indicating a molecular weight of 284 g/mol. The molecular formula $\text{C}_{12}\text{H}_{12}\text{O}_6\text{S}$ which was obtained from HRESI-MS which exhibited a strong peak at m/z 285.0423 $[\text{M}+\text{H}]^+$ (calculated 285.0433, Δ 0.001). The difference in the molecular weight between **33** and **32** is 47 amu. Structural elucidation of **33** was based on results of 1D and 2D NMR spectral analysis including ^1H NMR and HMBC spectra (Table 3.25). The ^1H NMR spectrum also showed a singlet at δ_{H} 2.13 ppm for 2'-Me, a singlet at δ_{H} 1.80 ppm for 3'-Me, the absence of H-1' as in **32**, the absence of H-3, a singlet at δ_{H} 3.69 ppm for 4-OMe, an aromatic singlet at δ_{H} 6.61 ppm for H-6 and two singlets at δ_{H} 10.81 ppm and 11.00 ppm for the aromatic hydroxyl groups, 7-OH and 5-OH, respectively. The ^{13}C chemical shift of the two methyls 2'-Me (at δ_{C} 24.9 ppm) and 3'-Me (at δ_{C} 11.2 ppm) was characteristic to indicate that 2'-Me is attached to a *keto*-group and 3'-Me is attached to a sulfur atom (which is also confirmed by HRMS). Similar to the previously isolated phthalides the aromatic proton H-6 resonating at δ_{H} 6.61 ppm in the ROESY spectrum showed also a strong correlation to the two aromatic hydroxyl groups at δ_{H} 10.81 ppm and 11.00 ppm indicating its position between both hydroxyls. In addition, in the HMBC the aromatic proton showed ω -correlation to C-1 (at δ_{C} 165.9), to C-4, C-5, to C-7 and to C-8, which secures its position at C-6. Further inspection of the HMBC spectrum revealed the correlation of 2'-Me at δ_{H} 2.13 ppm to C-1' (at δ_{C} 197.9) and C-3, and of 3'-Me at δ_{H} 1.80 ppm only to C-3 (which confirms the attachment of the methylthio group to C-3). The attachment of methylthio substituent to C-3 in **33** confirms also the difference in the molecular weight by 47 amu. Moreover, the HMBC correlation of 4-OMe at δ_{H} 3.69 ppm to C-4 confirms the attachment of the methoxy group to position 4.

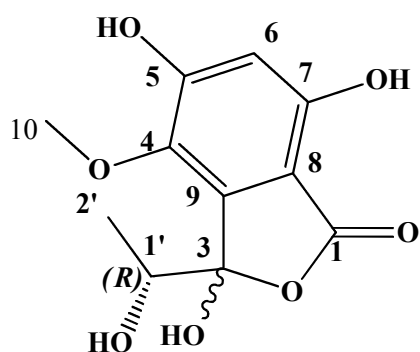
From the previous data compound **33** was found to be a new natural product to which the name embepthalide E is given.



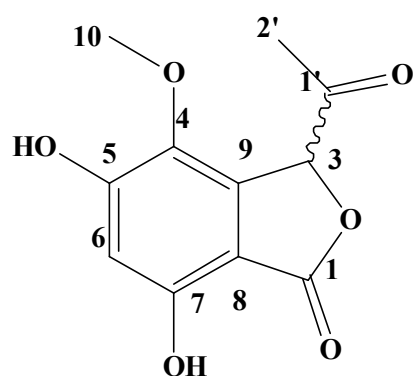
29



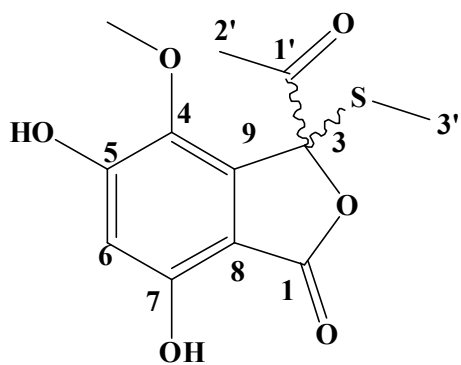
30



31



32



33

Nr.	Compound
29	Embepthalide A
30	Embepthalide B
31	Embepthalide C
32	Embepthalide D
33	Embepthalide E

Table 3.23: ^1H , ^{13}C , COSY, HMBC and ROESY spectra of compounds **29** and **30**

Position	29 (DMSO- d_6)		COSY	HMBC	ROESY	30 (DMSO- d_6)		COSY	HMBC	ROESY
	δ_{C}	δ_{H}				δ_{C}	δ_{H}			
1	167.9					167.9				
2										
3	82.0	5.45, d (2.3)	1'	1, 4, 5, 7, 8, 9, 1', 2'	10, 2'	81.4	5.25, br. s	1'	1, 4, 8, 9, 2'	10, 2'
4	134.2					134.3				
5	156.7					156.6				
6	104.4	6.45, s		1, 4, 5, 7, 8, 9	5-OH, 7-OH	104.0	6.41, s		1, 4, 5, 7, 8	5-OH, 7-OH
7	153.6					153.2				
8	102.8					103.8				
9	140.4					141.7				
10	59.8	3.69, s		4	3, 1', 2'	59.7	3.69, s		4	3, 1', 2'
1'	66.1	4.24, m	2', 3	2', 3	10	64.9	4.15, m	2', 3	2', 3	10
2'	15.1	0.73, d (6.3)	1'	1', 3	3, 10	20.5	1.52, d (6.2)	1'	1', 3	3, 10
5-OH		10.46, s		4, 5	6		10.31, s		5, 6	6
7-OH		10.21, br. s			6		10.09, br. s			6

Table 3.23a: Chemical shift differences between the (*S*)-MTPA and (*R*)-MTPA esters of **29**.

Proton no.	Chemical shift (δ_{H} , in $\text{C}_5\text{D}_5\text{N}$, at 500 MHz)			
	29	(<i>S</i>)-MTPA ester	(<i>R</i>)-MTPA ester	$\Delta \delta S - \delta R$
2'	1.03047	1.2948	1.2954	-0.0006
3	6.0673	6.0593	6.0583	+0.001
6	6.9355	7.0739	7.0547	+0.0192

Table 3.24: ^1H , ^{13}C , COSY, HMBC and ROESY spectra of compound **31**

Position	31 (DMSO-d_6)		COSY	HMBC	ROESY
	δ_{C}	δ_{H}			
1	166.3				
2					
3	104.8				
4	134.8				
5	157.3				
6	103.9	6.43, s		1, 4, 5, 7, 8, 9	5-OH, 7-OH
7	152.8				
8	104.4				
9	142.5				
10	60.7	3.69, s		6	1', 2'
1'	67.6	4.11, q (6.18, 12.6)	2'	2', 3, 9	10
2'	17.0	1.22, d (6.3)	1'	1', 3	10
3-OH		7.40, br s		1', 3, 4	
5-OH		10.29, s		4, 5, 6	6
7-OH		9.98 br. s			6

Table 3.24a: Chemical shift differences between the (*S*)-MTPA and (*R*)-MTPA esters of **31**.

Proton no.	Chemical shift (δ_{H} , in $\text{C}_5\text{D}_5\text{N}$, at 500 MHz)			
	31	(<i>S</i>)-MTPA ester	(<i>R</i>)-MTPA ester	$\Delta \delta_{\text{S}} - \delta_{\text{R}}$
2'	1.8762	1.8676	1.8649	+0.0027
6	6.9286	6.9031	6.9103	-0.0072

Table 3.25: ^1H , ^{13}C , COSY, HMBC and ROESY spectra of compounds **32** and **33**

Position	32 (DMSO- d_6)				33 (DMSO- d_6)			
	δ_{C}	δ_{H}	HMBC	ROESY	δ_{C}	δ_{H}	HMBC	ROESY
1	167.9				165.9			
2								
3	80.2	5.45, br. s	1, 4, 5, 8, 9, 1'	10, 2'	94.7			
4	134.6				135.3			
5	156.7				159.2			
6	105.0	6.51, s	1, 4, 5, 7, 8	5-OH, 7-OH	106.6	6.61, s	1, 4, 5, 7, 8	5-OH, 7-OH
7	153.6				154.5			
8	101.2				101.5			
9	137.6				137.6			
10	59.7	3.69, s	4	3, 2'	60.6	3.69, s	4	
1'	201.3				197.9			
2'	25.9	2.19, s	1', 3	3, 10	24.9	2.13, s	3, 1'	
3'					11.2	1.80, s	3	
5-OH		10.66, s	4, 5, 6	6		11.00, s	4, 5, 6	6
7-OH		10.48, s	4, 5, 6	6		10.81, s	7, 8	6

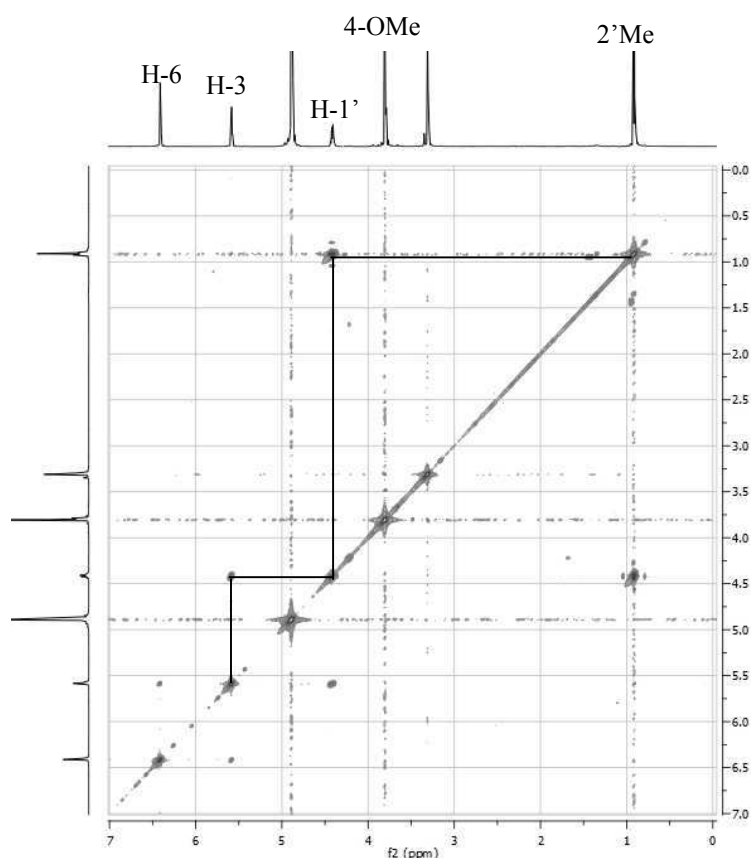


Fig. 3.32: COSY spectrum of compound 29.

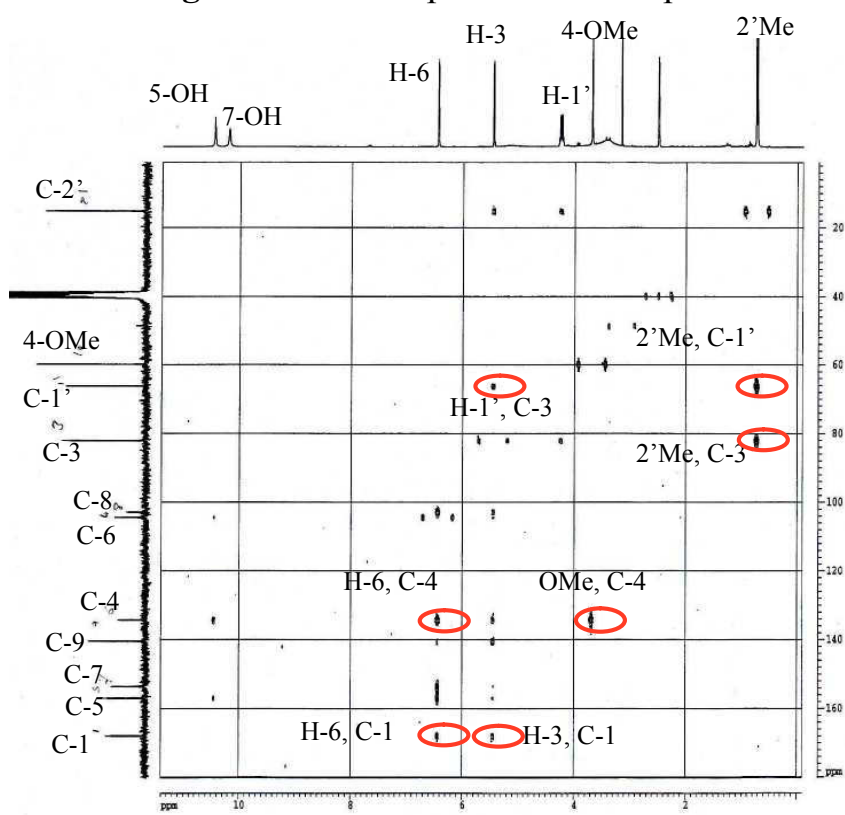


Fig. 3.33: HMBC spectrum of compound 29.

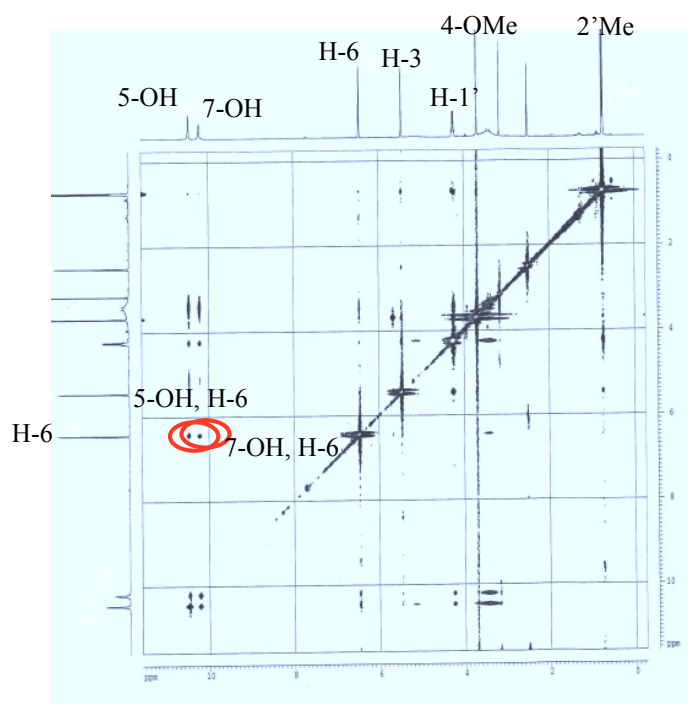


Fig. 3.34: ROESY spectrum of compound 29.

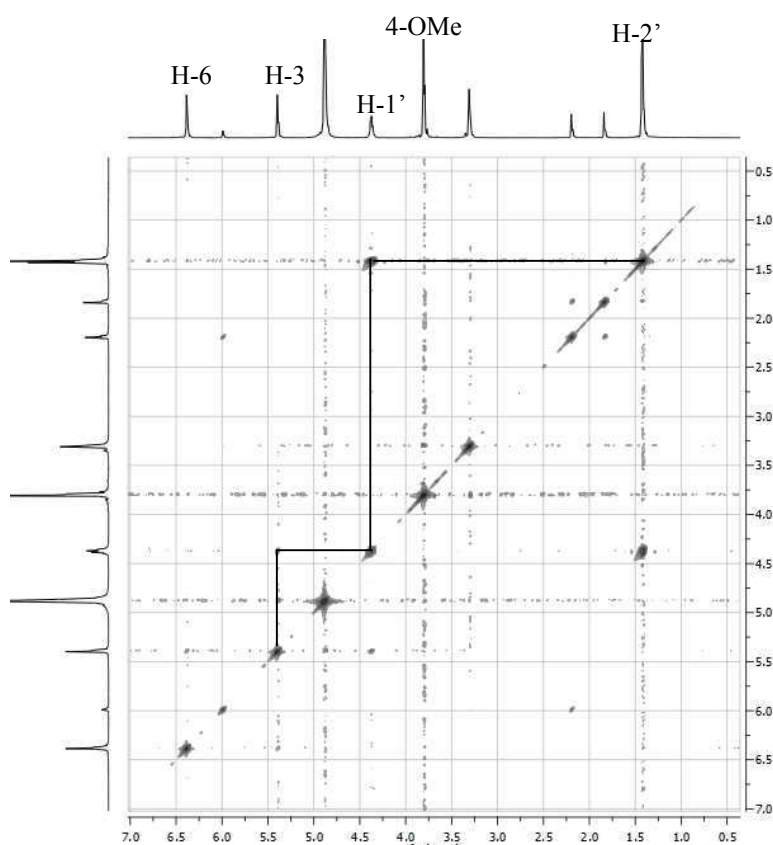


Fig.3.35: COSY spectrum of compound 30.

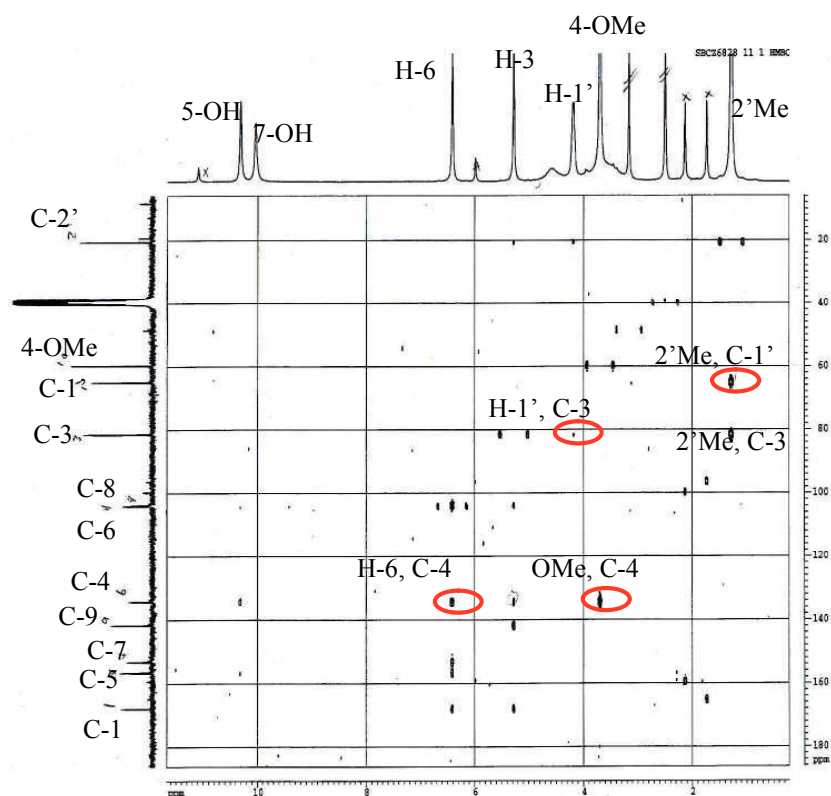


Fig. 3.36: HMBC spectrum of compound **30**.

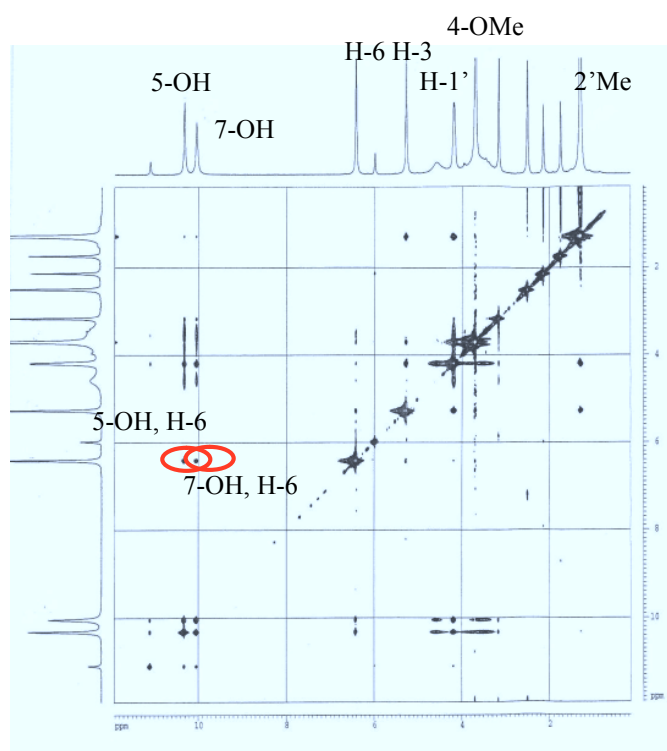


Fig. 3.37: ROESY spectrum of compound **30**.

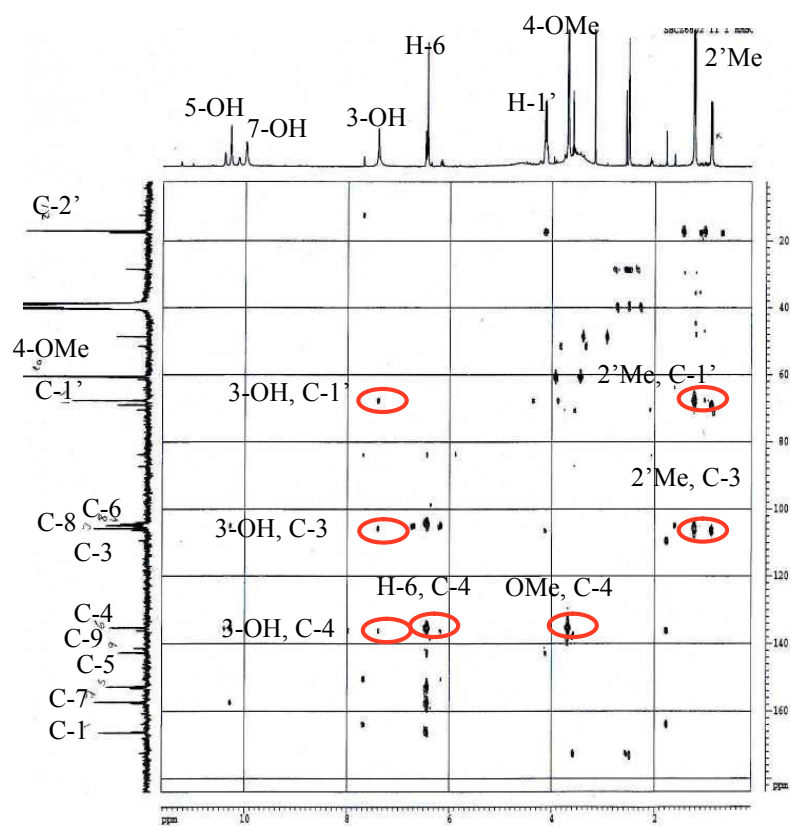


Fig. 3.38: HMBC spectrum of compound **31**.

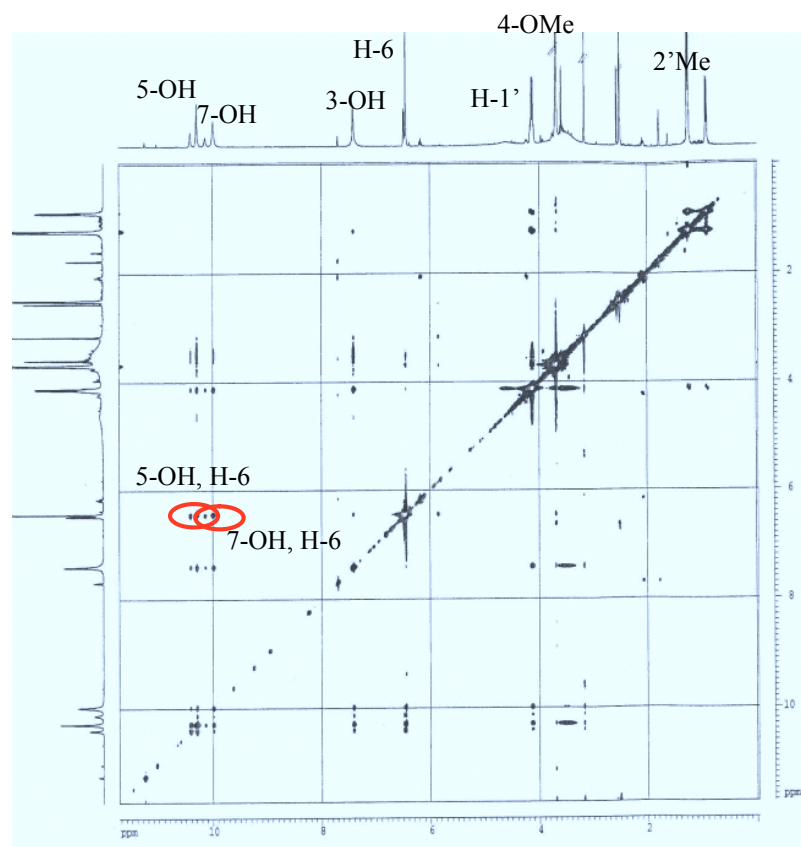


Fig. 3.39: ROESY spectrum of compound **31**.

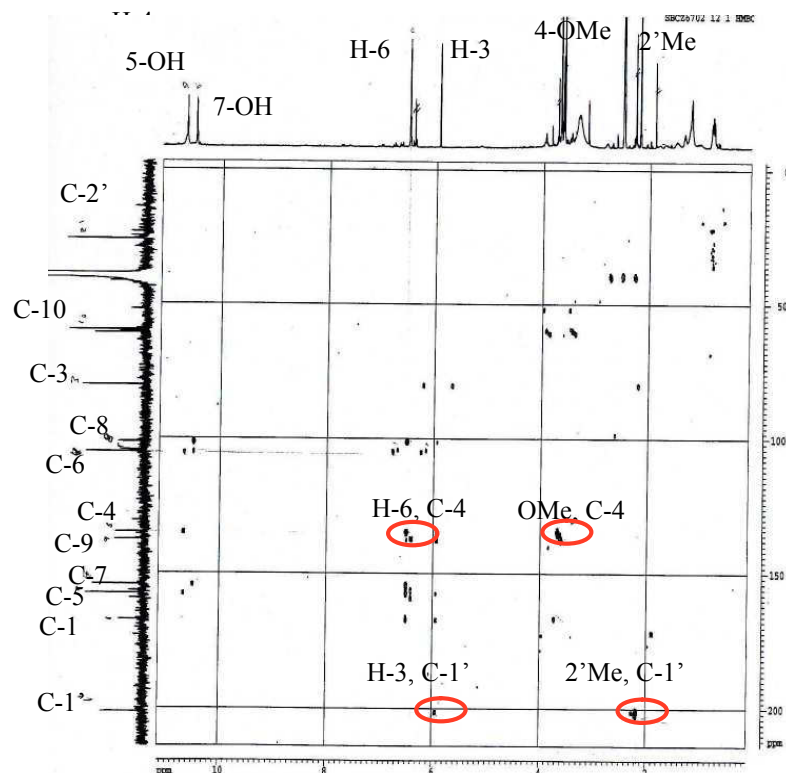


Fig. 3.40: HMBC spectrum of compound 32.

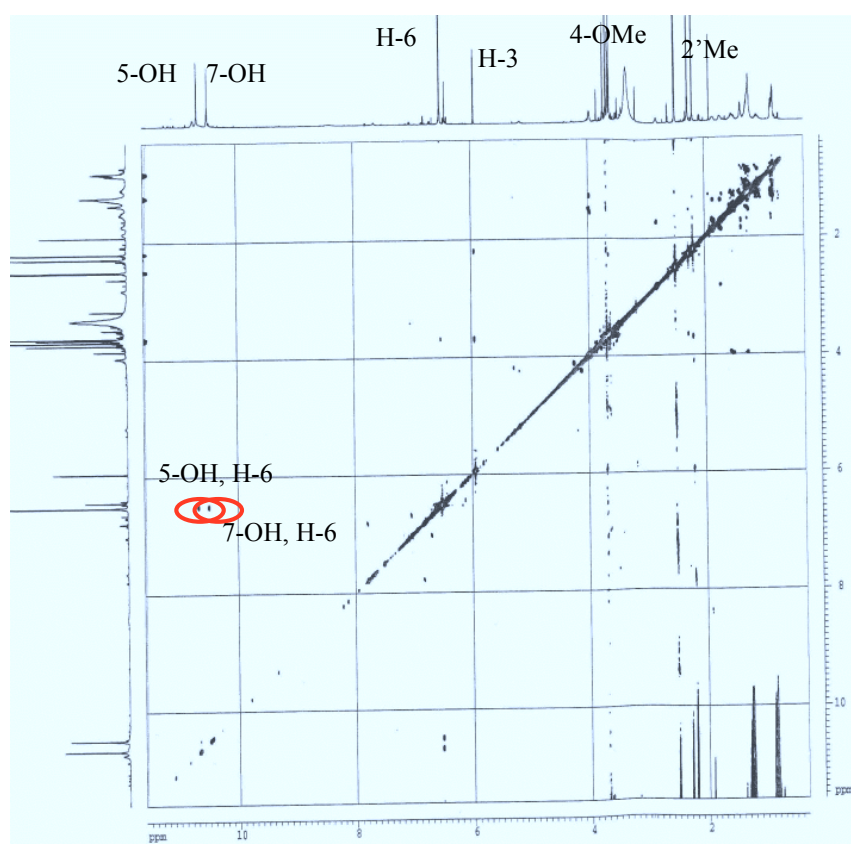


Fig. 3.41: ROESY spectrum of compound 32.

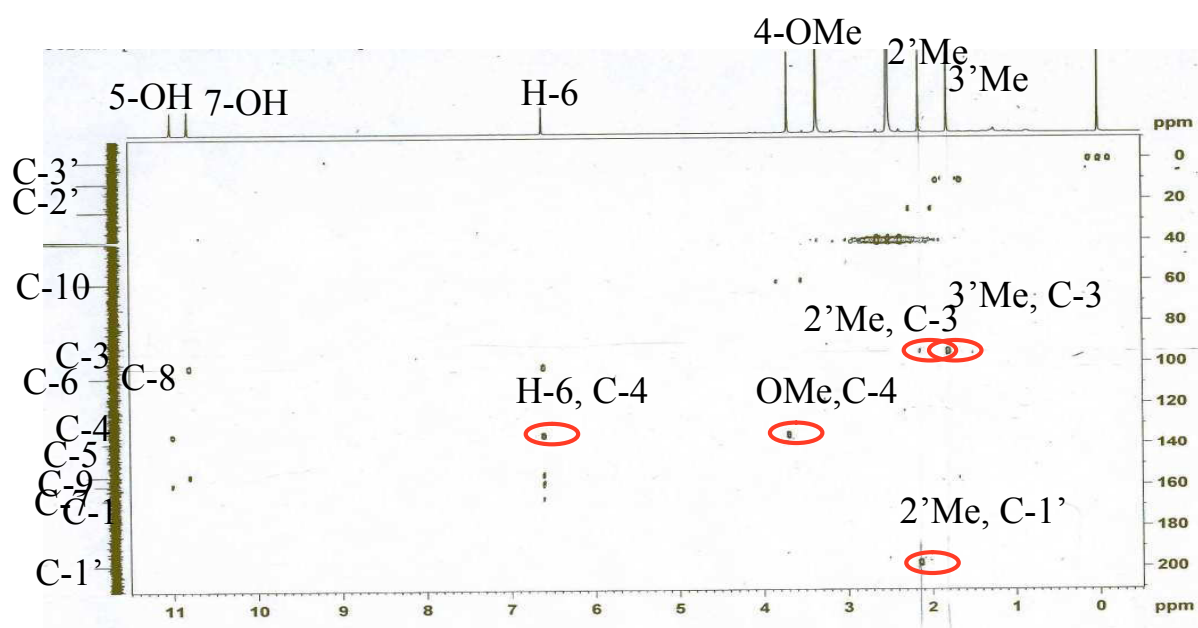


Fig. 3.42: HMBC spectrum of compound 33.

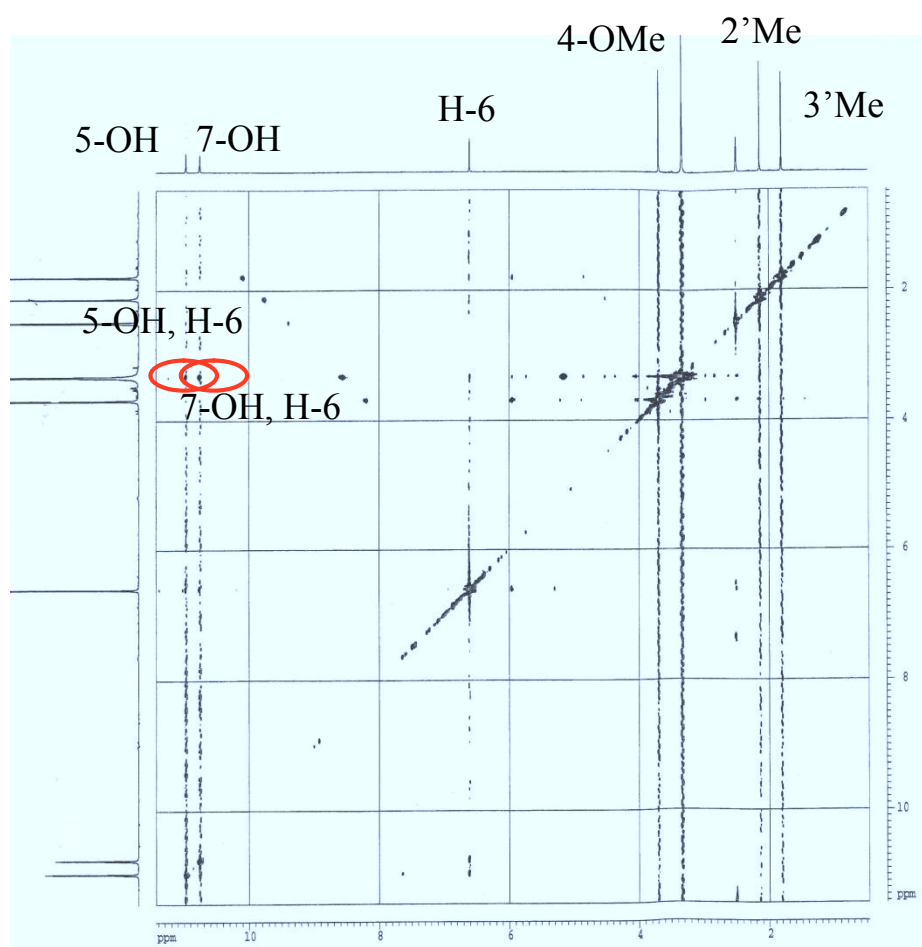
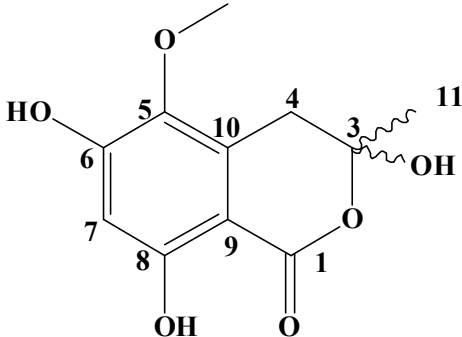
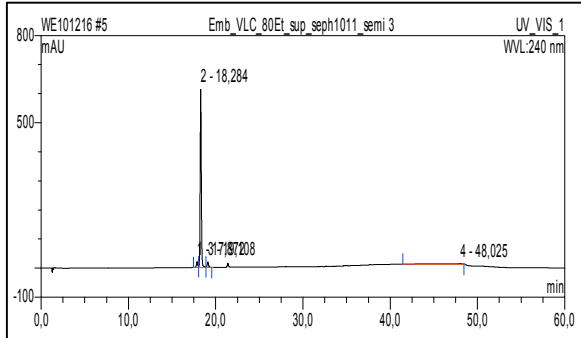
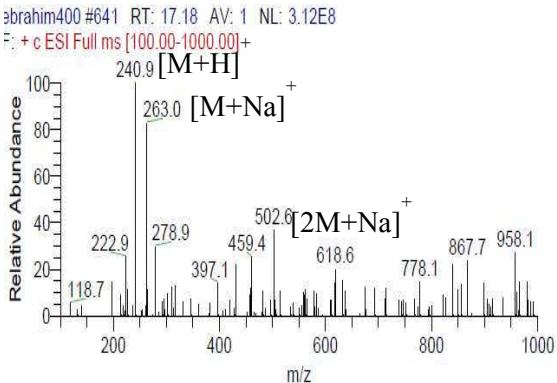
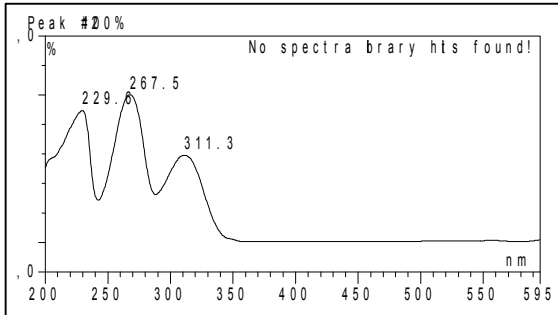
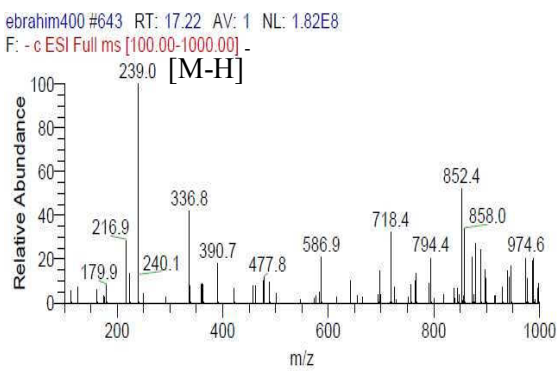


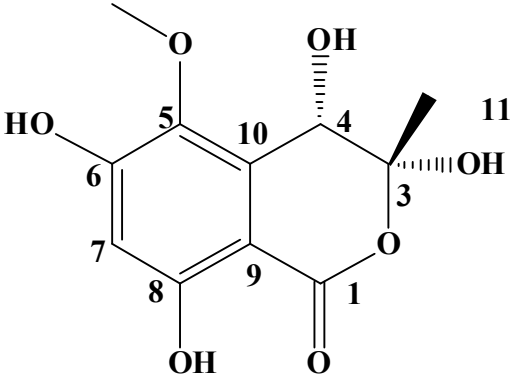
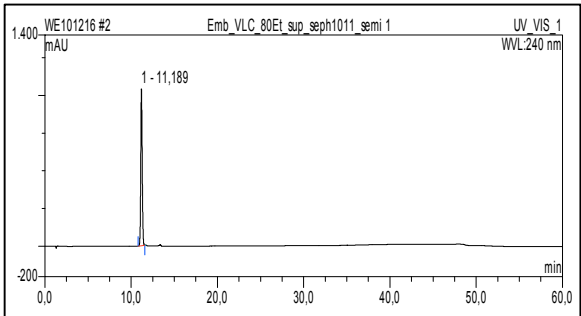
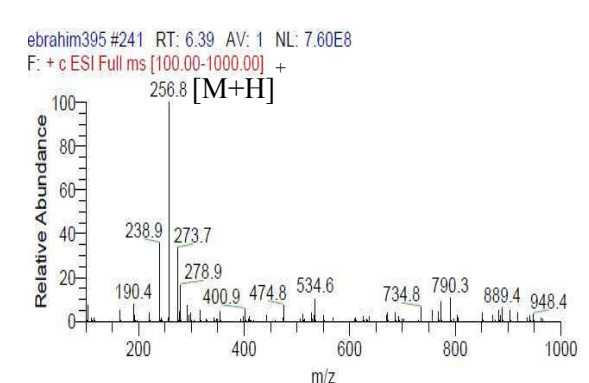
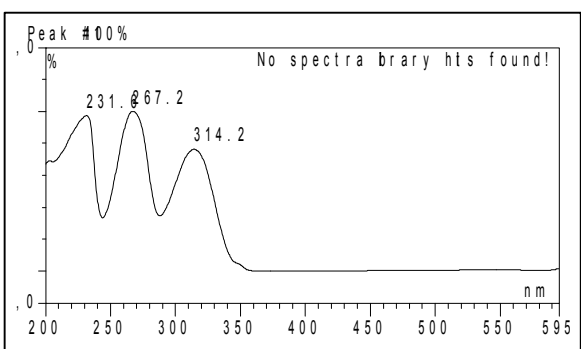
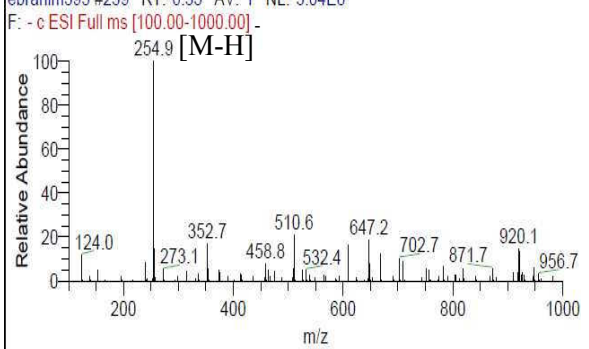
Fig. 3.43: ROESY spectrum of compound 33.

3.4.6. Embeurekol A (34, new compound)

Embeurekol A	
Synonym(s)	3,6,8-trihydroxy-5-methoxy-3-methylisochroman-1-one
Sample code	Emb_VLC_80Et_sup_seph914_semi3
Biological source	<i>Embellisia eureka</i>
Sample amount	3 mg
Physical properties	yellowish amorphous solid
Molecular formula	C ₁₁ H ₁₂ O ₆
Molecular weight	240 g/mol
Optical rotation [α] _D ²⁰	+14 (<i>c</i> 0.05, MeOH)
Retention time (HPLC)	18.3 min. (standard gradient)
	
	
	

Embeurekol A (**34**) was isolated from the EtOAc extract of solid rice cultures of *Embellisia eureka* as yellowish amorphous solid (3 mg). It showed UV absorbance maxima at λ_{max} (MeOH) 229.9, 267.5.9 and 311.3 nm. Positive and negative ESI-MS showed molecular ion peaks at m/z 240.9 $[M+H]^+$ (base peak) and m/z 239.0 $[M-H]^-$ (base peak), respectively, indicating a molecular weight of 240 g/mol. The molecular formula $C_{11}H_{12}O_6$ which was obtained from HRESI-MS which exhibited a strong peak at m/z 241.0707 $[M+H]^+$ (calculated 241.0707, Δ 0). Structural elucidation of **34** was based on results of 1D and 2D NMR spectral analysis including 1H NMR, 1H - 1H COSY, ROESY and HMBC spectra (Table 3.26). The 1H NMR spectrum showed a singlet at δ_H 1.62 ppm interpreted for 11-Me, two doublets at δ_H 3.10 and 3.18 ppm, d ($J=16.9$) for the two geminally coupled protons CH_2 -4, an aromatic singlet at δ_H 6.29 ppm for H-7, a singlet at δ_H 3.63 ppm for 5-OMe, a broad singlet at δ_H 7.42 ppm for 3-OH, and two singlets at δ_H 10.70 ppm and 10.90 ppm for the aromatic hydroxyl groups, 6-OH and 8-OH respectively. The aromatic proton H-7 resonating at δ_H 6.29 ppm showed a strong ROESY correlation with the two aromatic hydroxyl groups at δ_H 10.70 ppm and 10.90 ppm indicating that the aromatic proton must be between both hydroxyls. In addition, 5-OMe at δ_H 3.63 ppm showed a strong ROESY correlation to CH_2 -4 at δ_H 3.10 and 3.18 ppm. Furthermore, the aromatic proton H-7 showed 2J - 3J and 4J HMBC correlations, an ω -correlation to C-1 (at δ_C 168.2), to C-5, to C-6, to C-8 and to C-9, which secures its position at C-7. Further inspection of the HMBC spectrum revealed the correlation of 11-Me at δ_H 1.62 ppm to C-3 and C-4, CH_2 -4 at δ_H 3.10 and 3.18 ppm to C-3, C-5, C-9, C-10 and C-11. Moreover, the HMBC correlation of 5-OMe at δ_H 3.63 ppm to C-5 confirmed the attachment of the methoxy group to position 5. From the previous data compound **34** was found to be a new natural product to which the name embeurekol A is given.

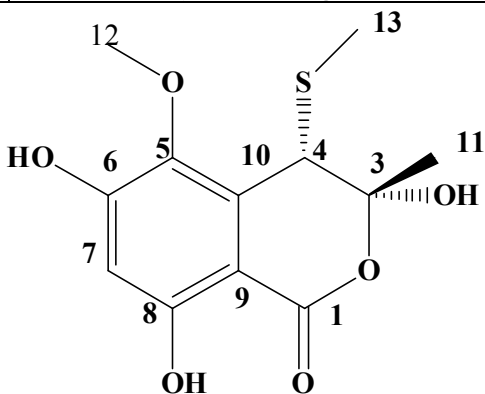
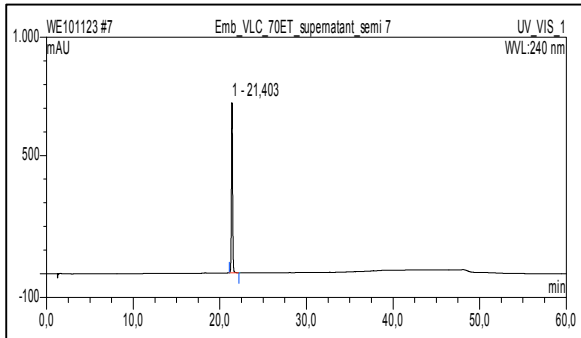
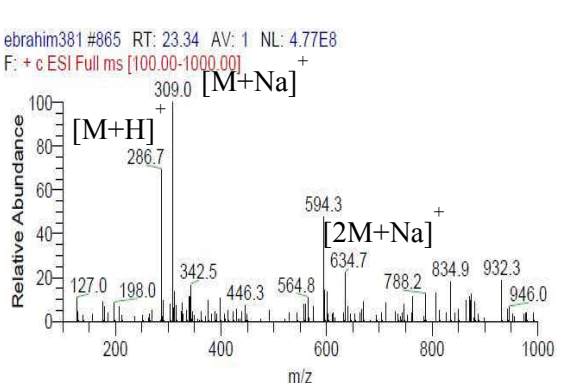
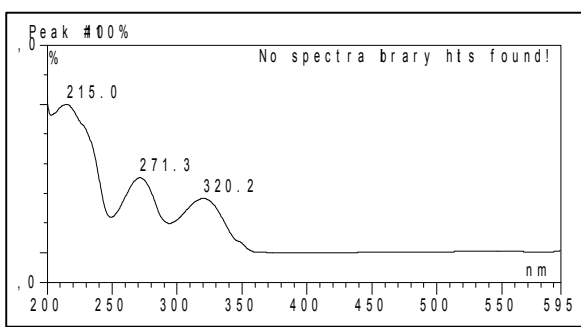
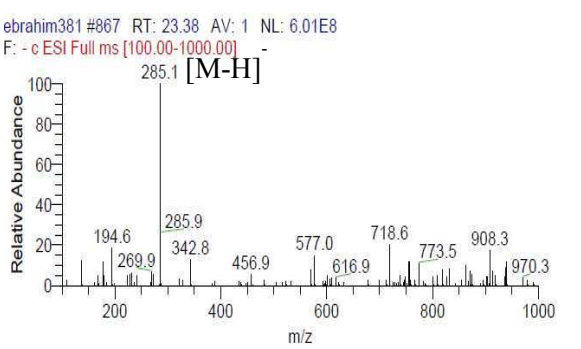
3.4.7. Embeurekol B (35, new compound)

Embeurekol B	
Synonym(s)	(3S,4R)-3,4,6,8-tetrahydroxy-5-methoxy-3-methylisochroman-1-one
Sample code	Emb_VLC_80Et_sup_seph914_semi1
Biological source	<i>Embellisia eureka</i>
Sample amount	100 mg
Physical properties	yellowish amorphous solid
Molecular formula	C ₁₁ H ₁₂ O ₇
Molecular weight	256 g/mol
Optical rotation $[\alpha]_D^{20}$	-2 (c 0.05, MeOH)
Retention time (HPLC)	11.2 min. (standard gradient)
	
	
	

Embeurekol B (**35**) was isolated from the EtOAc extract of solid rice cultures of *Embellisia eureka* as yellowish amorphous solid (100 mg). It showed UV absorbances at λ_{max} (MeOH) 231.0, 267.2 and 314.2 nm. Positive and negative ESI-MS showed molecular ion peaks at m/z 256.8 $[\text{M}+\text{H}]^+$ (base peak) and m/z 254.9 $[\text{M}-\text{H}]^-$ (base peak), respectively, indicating a molecular weight of 256 g/mol. The molecular formula $\text{C}_{11}\text{H}_{12}\text{O}_7$ is obtained from HRESI-MS which exhibited a strong peak at m/z 257.0636 $[\text{M}+\text{H}]^+$ (calculated 257.0656, Δ 0.002). The difference in the molecular weight between **35** and **34** is 16 amu which indicates the possible presence of an extra hydroxyl group in **35**. The NMR data of **35** is closely similar to those of **34**, indicating that they are related to each other. Structural elucidation of **35** was based on results of 1D and 2D NMR spectral analysis including ^1H NMR, ^1H - ^1H COSY, ROESY and HMBC spectra (Table 3.26). The ^1H NMR spectrum showed a singlet at δ_{H} 1.62 ppm interpreted for 11-Me, a singlet at δ_{H} 4.50 ppm for H-4 (instead of a doublet in **34**) confirming that the extra hydroxyl group is attached to C-4, an aromatic singlet resonating at δ_{H} 6.37 ppm for H-7, a singlet at δ_{H} 3.71 ppm for 5-OMe, a singlet at δ_{H} 7.53 ppm for 3-OH, and two singlets at δ_{H} 10.70 ppm and 11.04 ppm for the aromatic hydroxyl groups, 6-OH and 8-OH, respectively. The aromatic proton H-7 resonating at δ_{H} 6.37 ppm showed strong ROESY correlations with both aromatic hydroxyl groups at δ_{H} 10.70 ppm and 11.04 ppm, indicating its position between both hydroxyls. In addition, 5-OMe at δ_{H} 3.71 ppm showed a strong ROESY correlation to H-4 at δ_{H} 4.50 ppm. Furthermore, the aromatic proton H-7 showed 2J - 3J and 4J HMBC correlations, a ω -correlation to C-1 (at δ_{C} 169.1), to C-5, to C-6, to C-8 and to C-9, which secures its position at C-7. Further inspection of the HMBC spectrum revealed the correlation of 11-Me at δ_{H} 1.62 ppm to C-1, C-3 and C-4, H-4 at δ_{H} 4.50 ppm to C-5, C-9 and C-10. Moreover, the HMBC correlation of 5-OMe at δ_{H} 3.71 ppm to C-5 confirmed its attachment to position 5. The relative stereochemistry of **35** was established by a ROESY experiment. H-4 at δ_{H} 4.50 ppm showed a strong correlation to 11-Me at δ_{H} 1.62 ppm confirming

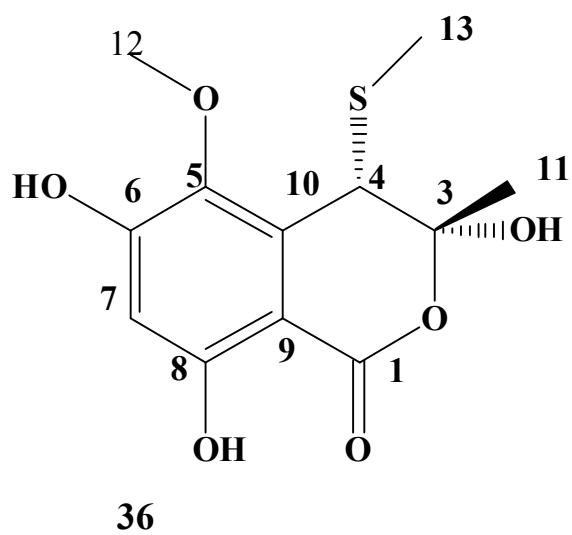
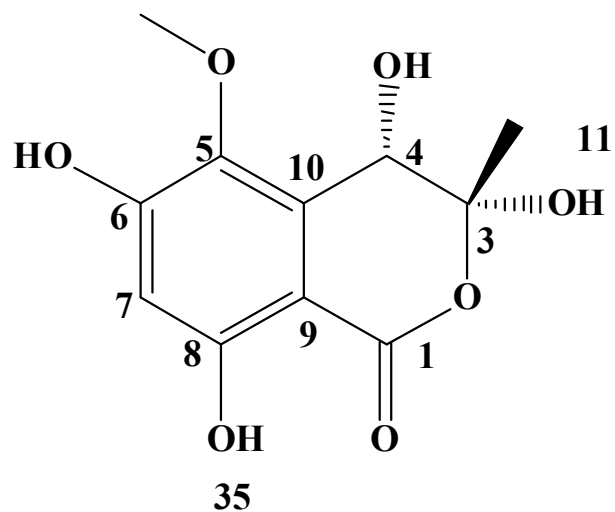
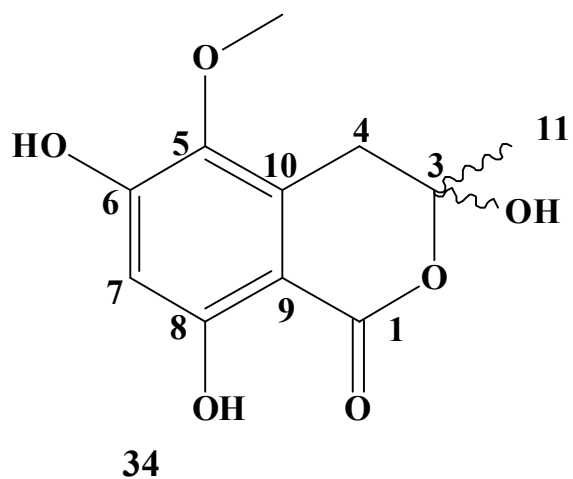
their *cis* configuration. From the previous data compound **35** was found to be a new natural product to which the name embeurekol B is proposed.

3.4.8. Embeurekol C (36, new compound)

Embeurekol C	
Synonym(s)	3,6,8-trihydroxy-5-methoxy-3-methyl-4-(methylthio)isochroman-1-one
Sample code	Emb_VLC_70Et_sup_seph914_semi7
Biological source	<i>Embellisia eureka</i>
Sample amount	3 mg
Physical properties	yellowish amorphous solid
Molecular formula	C ₁₂ H ₁₄ O ₆ S
Molecular weight	286 g/mol
Optical rotation $[\alpha]_D^{20}$	+5 (c 0.05, MeOH)
Retention time (HPLC)	21.4 min. (standard gradient)
	
	
	

Embeurekol C (**36**) was isolated from the EtOAc extract of solid rice cultures of *Embellisia eureka* as yellowish amorphous solid (3 mg). It showed UV absorbances at λ_{max} (MeOH) 215.0, 271.3 and 320.2 nm. Positive and negative ESI-MS showed molecular ion peaks at m/z 286.7 $[\text{M}+\text{H}]^+$ (base peak) and m/z 285.1 $[\text{M}-\text{H}]^-$ (base peak), respectively, indicating a molecular weight of 286 g/mol. The HRESI-MS exhibited a strong peak at m/z 287.0581 $[\text{M}+\text{H}]^+$ indicating the molecular formula $\text{C}_{12}\text{H}_{14}\text{O}_6\text{S}$ (calculated 287.0589, Δ 0.0008). Structural elucidation of **36** was based on results of 1D and 2D NMR spectral analysis including ^1H NMR, ^1H - ^1H COSY and HMBC spectra (Table 3.26). The NMR data of **36** are very similar to those of **34** and **35** indicating that these compounds are related to each other. Structural elucidation of **36** was based on results of 1D and 2D NMR spectral analysis including ^1H NMR, ^1H - ^1H COSY, ROESY and HMBC spectra (Table 3.26). The ^1H NMR spectrum showed a singlet at δ_{H} 1.79 ppm interpreted for 11-Me, an extra methyl singlet at δ_{H} 2.01 ppm for 13-Me, a singlet at δ_{H} 4.17 ppm for H-4, an aromatic singlet at δ_{H} 6.35 ppm for H-7, a singlet at δ_{H} 3.75 ppm for 5-OMe, a singlet at δ_{H} 7.71 ppm for 3-OH, and two singlets at δ_{H} 10.89 ppm and 10.91 ppm for the aromatic hydroxyl groups 6-OH and 8-OH, respectively. The resonance of the extra methyl group at δ_{C} 14.5 ppm is characteristic for the methylthio-group which is also confirmed by HRMS. In the ROESY spectrum, the aromatic proton H-7 at δ_{H} 6.35 ppm showed strong correlations with two aromatic hydroxyl groups at δ_{H} 10.89 ppm and 11.91 ppm indicating its localization between both hydroxyls. In addition, 5-OMe at δ_{H} 3.75 ppm showed a strong ROESY correlation to H-4 at δ_{H} 4.17 ppm. In addition, the aromatic proton H-7 showed HMBC correlations to C-1 (at δ_{C} 168.9 ppm), C-5, C-6, C-8 and C-9, which secures its position at C-7. Further inspection of the HMBC spectrum revealed the correlation of 11-Me at δ_{H} 1.79 ppm to C-1, C-3 and C-4, 13-Me at δ_{H} 2.01 ppm to C-4 and H-4 at δ_{H} 4.17 ppm to C-5, C-9 and C-10. Moreover, the HMBC correlation of 5-OMe at δ_{H} 3.75 ppm to C-5 as well as strong ROESY correlation between 5-OMe at δ_{H} 3.75 ppm and H-4 at δ_{H} 4.17

ppm confirm the attachment of the methoxy group to position 5. The relative stereochemistry of **36** was established by ROESY experiment. H-4 at δ_{H} 4.17 ppm showed a strong correlation to 11-Me at δ_{H} 1.79 ppm confirming the *cis* configuration. From the previous data compound **36** was found to be a new natural product to which the name embeurekol C is given.



Nr.	Compound
34	Embeurekol A
35	Embeurekol B
36	Embeurekol C

Table 3.26: ^1H , ^{13}C , COSY and HMBC spectra of compounds **34**, **35** and **36**

Nr.	34 (DMSO- d_6)					35 (DMSO- d_6)				36 (DMSO- d_6)			
	δ_{C}	δ_{H}	COSY	HMBC	ROESY	δ_{C}	δ_{H}	HMBC	ROESY	δ_{C}	δ_{H}	HMBC	ROESY
1	168.2					169.1				168.9			
3	105.1					105.2				105.4			
4	32.2	A 3.10, d (16.9) B 3.18, d (16.9)	4B 4A	3, 5, 9, 10, 11 3, 7, 9, 10, 11	11, 12 11, 12	64.0	4.50, s	5, 9, 10	11, 12	45.4	4.17, s	5, 9, 10, 13	11, 12, 13
5	137.8					140.1				138.3			
6	158.3					158.3				158.6			
7	101.6	6.29, s		1, 5, 6, 8, 9	6-OH, 8-OH	103.8	6.37, s	1, 5, 6, 8, 9	6-OH, 8-OH	102.7	6.35, s	1, 5, 7, 8, 9	6-OH, 8-OH
8	159.1					159.5				159.0			
9	98.5					98.7				98.9			
10	130.9					130.8				133.6			
11	22.3	1.62, s		3, 4	4A, 4B	24.3	1.62, s	1, 3, 4	4, 3-OH	14.5	1.79, s	1, 3, 4	4
12	60.2	3.63, s		7	4A, 4B	61.5	3.71, s	5	4	60.8	3.75, s	5	4
13										26.0	2.01, s	4	4
3-OH		7.42, br. s					7.53, s	3, 4, 11	11		7.71, br. s	5, 9, 10, 13	11, 12, 13
6-OH		10.70, s		5, 6, 7	7		10.70, s	5, 6, 7	7		10.89, s		7
8-OH		10.90, s		7, 8, 9	7		11.04, s	7, 8, 9	7		10.91, s		7

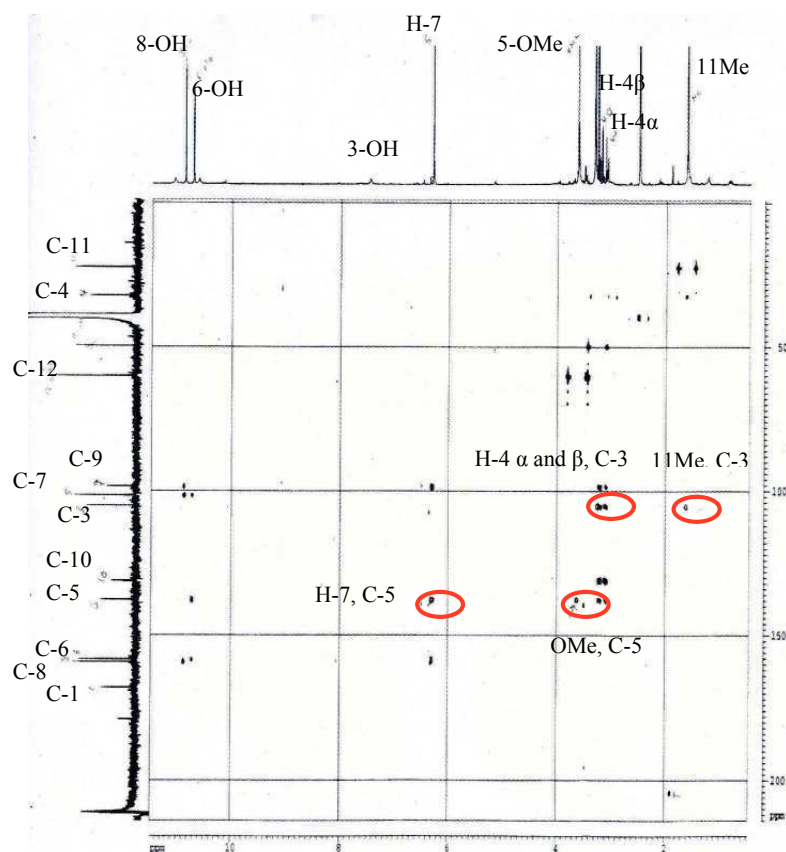


Fig. 3.44: HMBC spectrum of compound **34**.

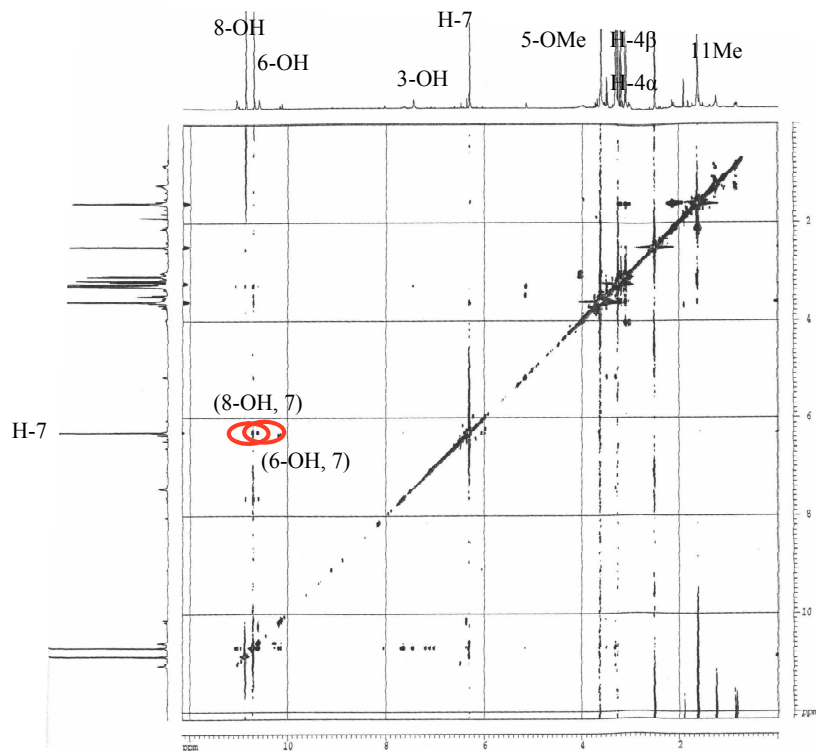


Fig. 3.45: ROESY spectrum of compound **34**.

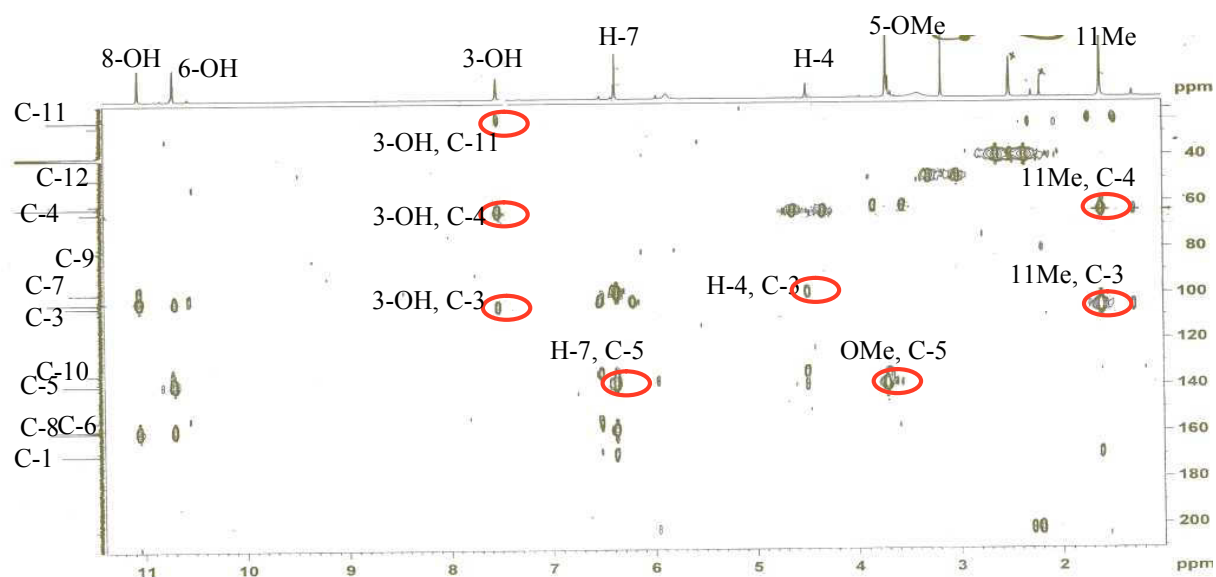


Fig. 3.46: HMBC spectrum of compound 35.

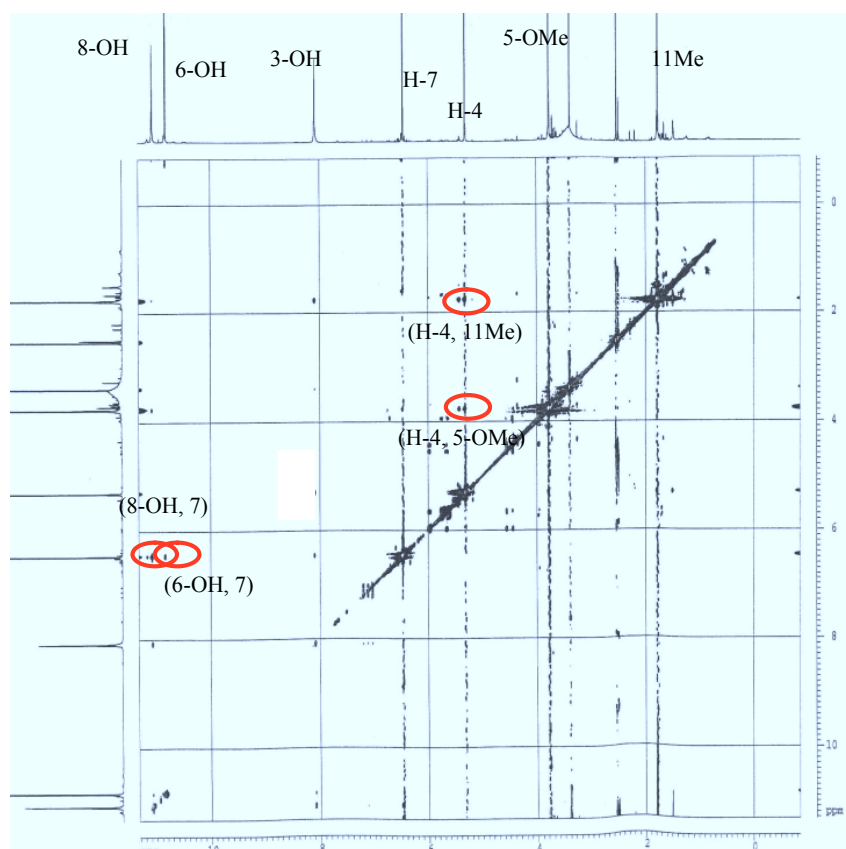


Fig. 3.47: ROESY spectrum of compound 35.

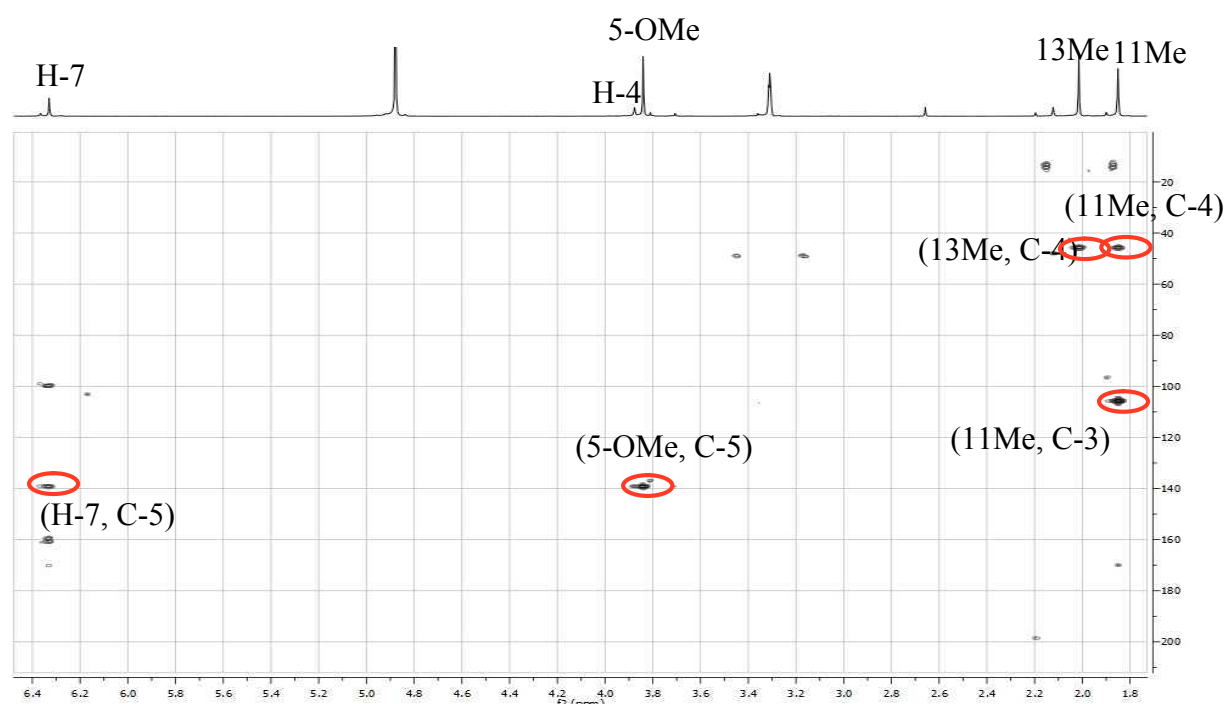


Fig. 3.48: HMBC spectrum of compound **36**.

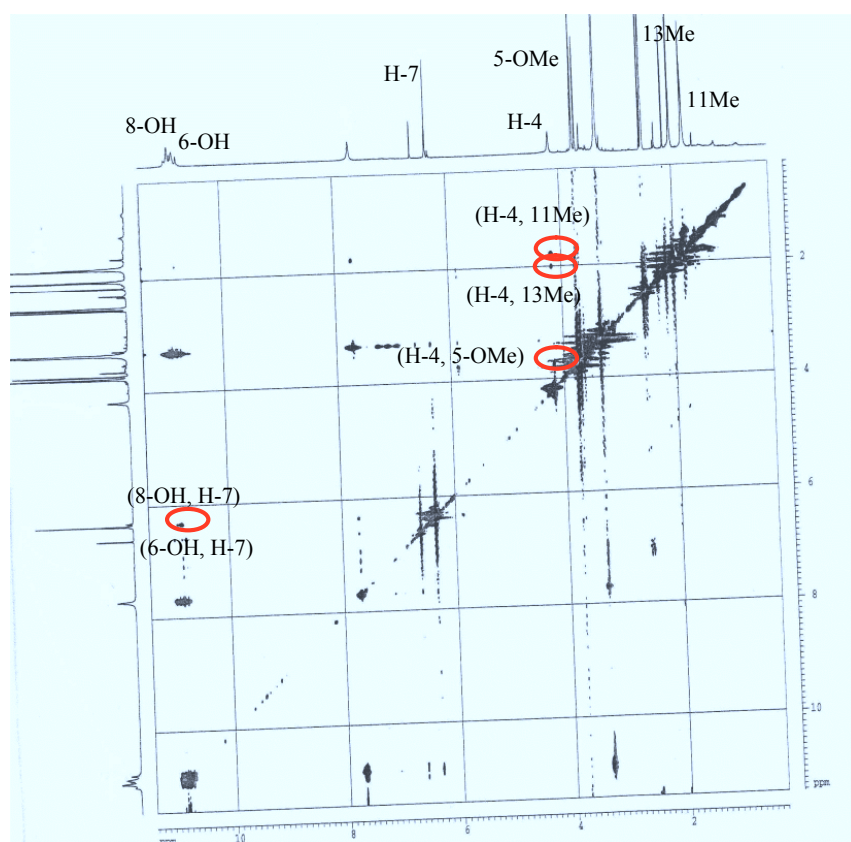
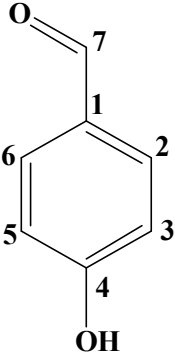
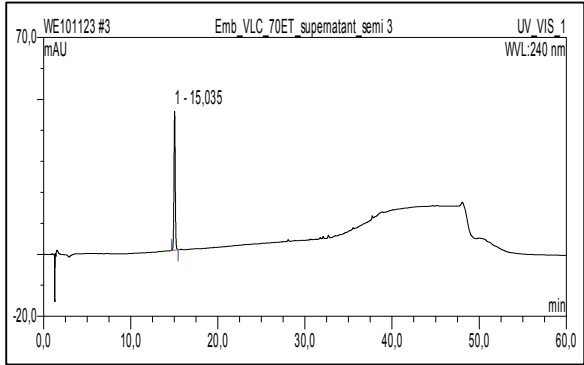
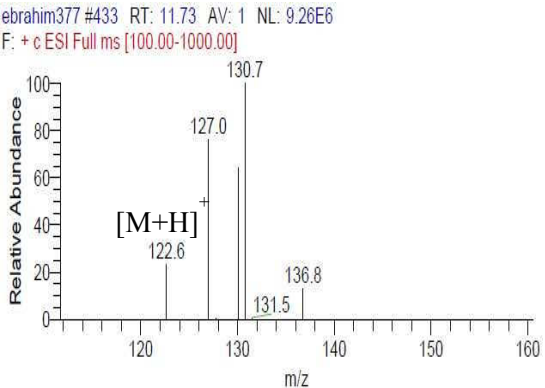
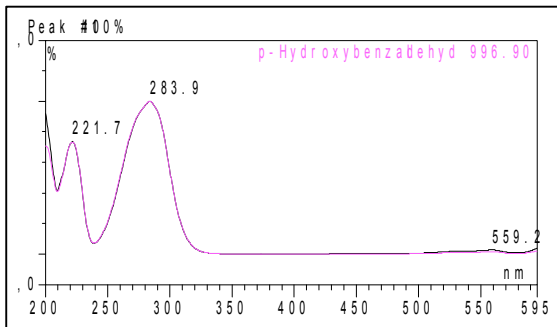
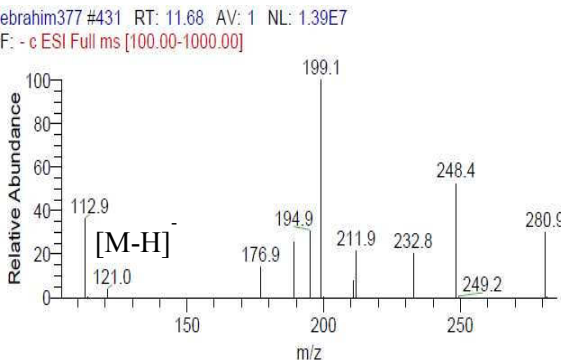


Fig. 3.49: ROESY spectrum of compound **36**.

3.4.9. *p*-hydroxybenzaldehyde (37, known compound)

<i>p</i> -hydroxybenzaldehyde	
Synonym(s)	4-hydroxybenzaldehyde
Sample code	Emb_VLC_70Et_sup_semi3
Biological source	<i>Embellisia eureka</i>
Sample amount	1 mg
Physical properties	White powder
Molecular formula	C ₇ H ₆ O ₂
Molecular weight	122 g/mol.
Retention time (HPLC)	15.0 min. (standard gradient)
	
	<p>ebrahim377 #433 RT: 11.73 AV: 1 NL: 9.26E6 F: + c ESI Full ms [100.00-1000.00]</p> 
<p>Peak #00%</p> 	<p>ebrahim377 #431 RT: 11.68 AV: 1 NL: 1.39E7 F: - c ESI Full ms [100.00-1000.00]</p> 

p-hydroxybenzaldehyde (**37**) was isolated from the EtOAc extract of solid rice cultures of *Embellisia eureka* as white powder (1 mg). It showed UV absorbances at λ_{max} (MeOH) 221.7 and 283.9 nm. Positive and negative ESI-MS showed molecular ion peaks at m/z 122.6 $[\text{M}+\text{H}]^+$ (base peak) and m/z 121.0 $[\text{M}-\text{H}]^-$ (base peak), respectively, indicating a molecular weight of 122 g/mol. Structural elucidation of **37** was based on results of 1D and 2D NMR spectral analysis including ^1H NMR and ^1H - ^1H COSY spectra (Table 3.27). This is indicated by the presence of an aldehyde group proton (H-7) (δ_{H} 9.79, s) and an AA'BB' spin system appearing at 7.76 ppm (for H-2/6) and 6.73 ppm (for H-3/5). Compound **37** was identified as p-hydroxybenzaldehyde by comparison of its spectroscopic data with those of the literature (Beistel *et al*, 1976).

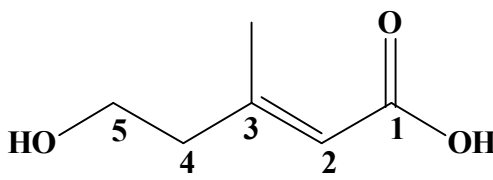
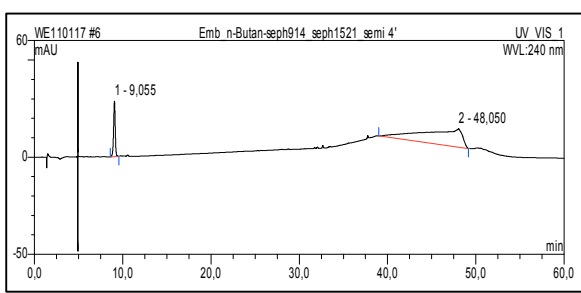
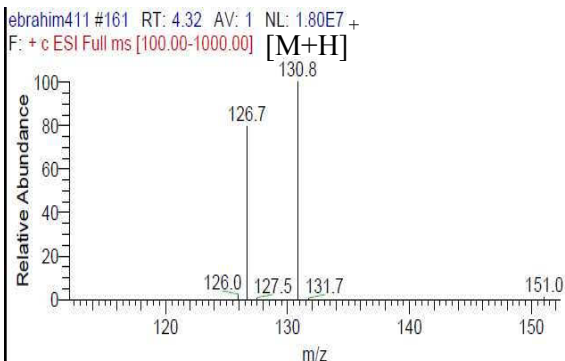
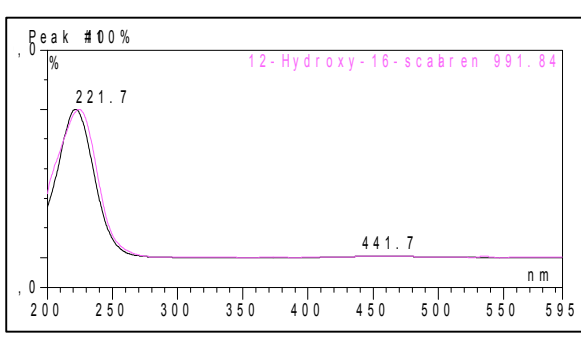
Table 3.27: ^1H NMR and COSY spectra of compound **37**

Position	37		COSY
	δ_{H}^*	$\delta_{\text{H}}^{\text{o}}$	
1			
2	7.76, d (8.85)	7.82, d (9.2)	3
3	6.73, d (8.85)	6.98, d (9.2)	2
4			
5	6.73, d (8.85)	6.98, d (9.2)	6
6	7.76, d (8.85)	7.82, d (9.2)	5
7	9.79, s		

* Measured in (DMSO- d_6)

o (Beistel *et al*, 1976)

3.4.10. 2-Anhydromevalonic acid (38, known compound)

2-anhydromevalonic	
Synonym(s)	(<i>E</i>)-5-hydroxy-3-methylpent-2-enoic acid
Sample code	Emb_VLC_70Et_sup_semi3
Biological source	<i>Embellisia eureka</i>
Sample amount	1.2 mg
Physical properties	Yellow solid
Molecular formula	C ₆ H ₁₀ O ₃
Molecular weight	130 g/mol.
Retention time (HPLC)	9.01 min. (standard gradient)
	
	 <p>brahim411 #161 RT: 4.32 AV: 1 NL: 1.80E7 + F: + c ESI Full ms [100.00-1000.00] [M+H]⁺</p>
	No ionization

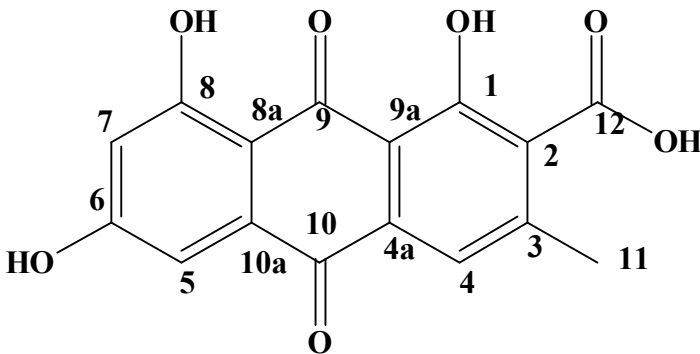
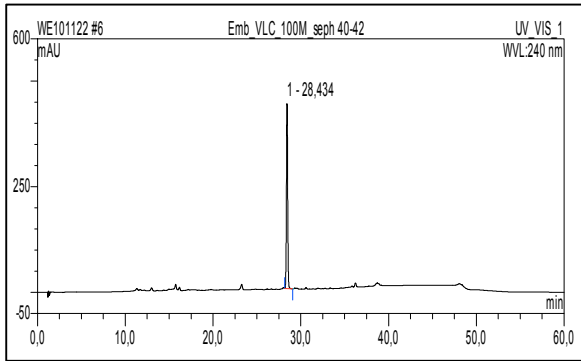
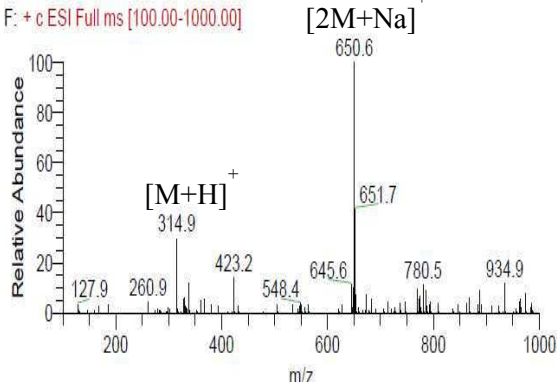
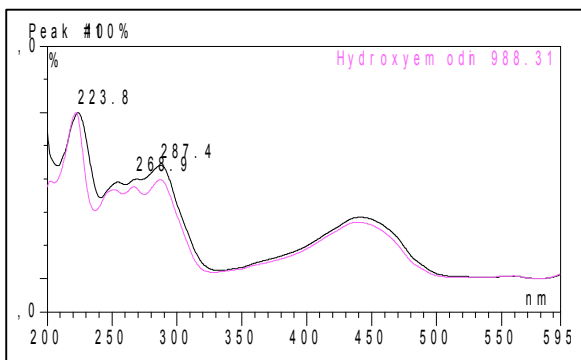
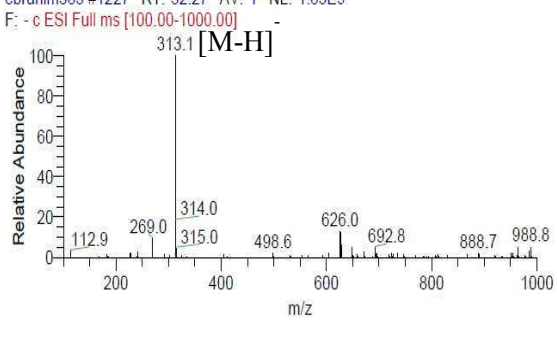
2-Anhydromevalonic acid (**38**) was isolated from the EtOAc extract of solid rice cultures of *Embellisia eureka* as yellow solid (1.2 mg). It showed UV absorbances at λ_{max} (MeOH) 221.7 nm. Positive ESI-MS showed a molecular ion peak at m/z 131.0 $[M+H]^+$ (base peak) indicating a molecular weight of 130 g/mol. Structural elucidation of **38** was based on results of 1D and 2D NMR spectral analysis including ^1H NMR, ^1H - ^1H COSY and HMBC spectra (Table 3.28) as well as comparison with the literature (Dieckmann, 1968). This is indicated by the presence of an olefinic methine group CH-2 (δ_{H} 5.61, br. s), a 1, 2 disubstituted ethoxy groups CH₂-4 (δ_{H} 2.25, t, $J=6.2$) and CH₂-5 (δ_{H} 3.55, dt, $J=7, 6.2$), hydroxyl group 5-OH (δ_{H} 4.55, t, $J=6.2$), a methyl group 3-Me (δ_{H} 2.18, s) and a carboxylic group proton (δ_{H} 11.81, br.s). Comparison of the NMR data with those of 2-anhydromevalonic acid with its synonym (*E*)-5-hydroxy-3-methylpent-2-enoic acid which was isolated from endophytic fungus *Fusarium* sp. and other fungi (Dieckmann, 1968) revealed that they are identical.

Table 3.28: ^1H , COSY and HMBC spectra of compound **38**

Position	38	COSY	HMBC
	δ_{H}^*		
1			
2	5.61, br. s	3-Me	4, 3-Me
3			
4	2.25, t (6.2)	5	2, 3, 5
5	3.55, dt (7, 6.2)	4, 5-OH	3, 4
3-Me	2.18, s	2	2, 3, 4
5-OH	4.55, t (6.2)		4,5
-COOH	11.81, br.s		

* Measured in ($\text{DMSO}-d_6$)

3.4.11. Endocrocin (39, known compound)

Endocrocin	
Synonym(s)	1,6,8-trihydroxy-3-methyl-9,10-dioxo-9,10-dihydroanthracene-2-carboxylic acid
Sample code	Emb_VLC_100M_seph4042
Biological source	<i>Embellisia eureka</i>
Sample amount	2.5 mg
Physical properties	Brick red amorphous powder
Molecular formula	C ₁₆ H ₁₀ O ₇
Molecular weight	314 g/mol.
Retention time (HPLC)	28.4 min. (standard gradient)
	
	<p>ebrahim383 #1229 RT: 32.31 AV: 1 NL: 6.45E8 F: + c ESI Full ms [100.00-1000.00]</p> 
	<p>ebrahim383 #1227 RT: 32.27 AV: 1 NL: 1.83E9 F: - c ESI Full ms [100.00-1000.00]</p> 

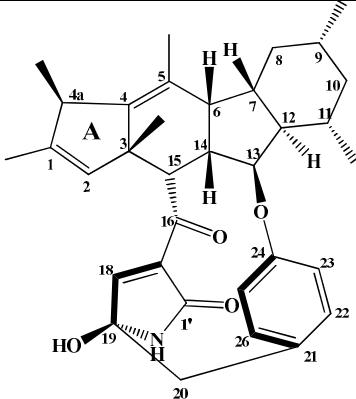
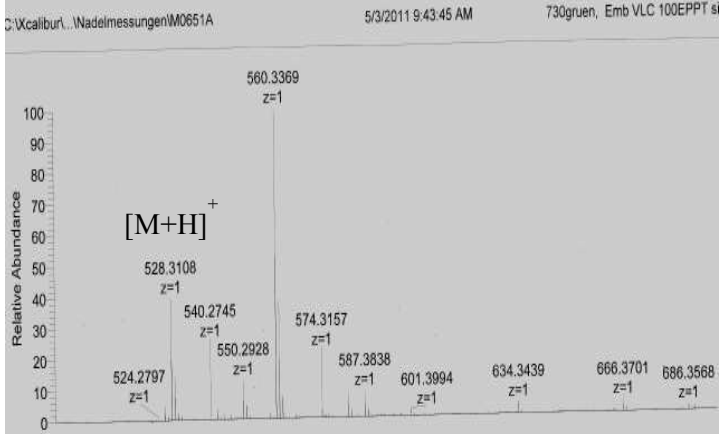
Endocrocin (**39**) was isolated from the EtOAc extract of solid rice cultures of *Embellisia eureka* as brick red amorphous powder (2.5 mg). It showed UV absorbances at λ_{max} (MeOH) 223.8, 268.9 and 287.4 nm. Positive and negative ESI-MS showed molecular ion peaks at m/z 313.1 $[\text{M}+\text{H}]^+$ (base peak) and m/z 314.9 $[\text{M}-\text{H}]^-$ (base peak), respectively, indicating a molecular weight of 314 g/mol. Structural elucidation of **39** was based on results of 1D and 2D NMR spectral analysis including ^1H NMR and HMBC spectra (Table 3.29) and comparison with the spectroscopic data of endocrocin (Kurobane and Vinng, 1979). The ^1H NMR indicated the presence of two *meta*-coupled protons H-5 and H-7 (δ_{H} 5.68, d, $J=2.5$ and 6.49, d, $J=2.5$ respectively), one aromatic proton H-4 (δ_{H} 7.19, s), an aromatic methyl group (3-Me) (δ_{H} 2.50, s) and a hydroxyl group (δ_{H} 13.39, s). Comparison of the NMR data with those of endocrocin isolated from the fungi *Pyrenochaeta terrestris* and *Aspergillus aculeatus* (Kurobane and Vinng, 1979) revealed that they are identical. It is important to note that some differences in the δ_{H} values with reported literature values might be due to the C-1 hydroxy-assisted tautomerization of the carboxylic acid.

Table 3.29: ^1H NMR and HMBC spectra of compound **39**

Position	39		
	δ_{H}^*	$\delta_{\text{H}}^{\text{O}}$	HMBC
1			
2			
3			
4	7.19, s	7.37, s	2, 3, 4a
4a			
5	6.49, br. d (2.5)	6.99, d (2.4)	10, 10a
6			
7	5.68, br. d (2.5)	6.48, d (2.4)	
8			
8a			
9			
9a			
10			
10a			
11	2.50, s	2.37, s	2, 3, 4
12			
1-OH	13.39, s		

* Measured in (DMSO- d_6)
o (Kurobane and Vinng, 1979)

3.4.12. Pyrrocidine D (40, new compound)

Pyrrocidine D	
Sample code	Emb_VLC_1000Et_PPT of PPT_sil1520
Biological source	<i>Embellisia eureka</i>
Sample amount	6 mg
Physical properties	yellowish amorphous solid
Molecular formula	C ₃₄ H ₄₁ NO ₄
Molecular weight	527 g/mol
Optical rotation $[\alpha]_D^{20}$	-8 (c 0.004, DMSO)
Retention time (HPLC)	No peak in HPLC detectable (detected only by TLC)
	
	

Pyrrocidine D (**40**) was isolated from the EtOAc extract of solid rice cultures of *Embellisia eureka* as yellowish amorphous solid (6 mg). The HRESI-MS exhibited a strong peak at m/z 528.3108 $[M+H]^+$ indicating a molecular formula $C_{34}H_{41}NO_4$ (calculated 528.3108, Δ 0). Comparison of 1H and ^{13}C NMR data of **40** with those of related known pyrrocidines A, B and C (He et al, 2002; Wicklow et al, 2005; Bigelis et al, 2006) showed a close relationship except for the presence of an extra five membered ring (ring A) and two methyl groups (CH₃-3 and CH₃-4a) as well as the absence of CH₃-7 in **40**. The 1H NMR spectrum showed peaks indicative for an exchangeable signal at δ_H 8.26 ppm, assigned to the amide proton NH-2'. There were four double doublet signals belonging to a homonuclear spin system resonating between δ_H 6.67 and 7.30 ppm, assigned to a *para*-substituted benzene ring whose rotation was restricted. In addition, six methyl signals were observed at δ_H 0.94 (d, $J=6.2$ Hz), 0.98 (d, $J=6.8$ Hz), 1.05 (s), 1.05 (d, $J=7.3$ Hz), 1.45 (s) and 1.75 (s) ppm signal for CH₃-9, CH₃-4a, CH₃-3, CH₃-11, CH₃-1 and CH₃-5 respectively.

Detailed analysis of 2D 1H - 1H COSY, 1H - ^{13}C HMBC, and 1H - ^{13}C HMQC data of **40** revealed a tetra-cyclic system from C-1 to C-4a. The 1H - 1H COSY spectrum delineated five spin systems, including CH(6)CH(7)CH₂(8)CH(9)CH₃(9)CH₂(10)CH(11)CH₃(11)CH(12)CH(13)CH(14)CH(15), a spin system between CH₃-4a and 4a-H, a homonuclear long range correlation between 1-Me and H-2, another homonuclear long range correlation between -NH and H-18 and the last spin system including the aromatic protons H-22, H-23, H-25 and H-26. The 2J or 3J HMBC correlations between 1-Me (δ_H 1.45 ppm) and C-1 (δ_C 140.9 ppm), C-2 (δ_C 129.5 ppm), and C-4a (δ_C 44.4 ppm), between 3-Me (δ_H 1.05 ppm) and C-2 (δ_C 129.5 ppm), C-3 (δ_C 51.8 ppm), C-4 (δ_C 145.7 ppm), and C-15 (δ_C 52.6 ppm), between 4a-Me (δ_H 0.98 ppm) and C-1 (δ_C 140.9 ppm), C-4 (δ_C 145.7 ppm) and C-4a (δ_C 44.4 ppm), between 5-Me (δ_H 1.75 ppm) and C-4 (δ_C 145.7 ppm), C-5 (δ_C 127.0 ppm), and C-6 (δ_C 43.5 ppm), between 9-Me (δ_H 0.94 ppm) and C-8 (δ_C 38.8 ppm), C-9 (δ_C 33.3 ppm) and C-10 (δ_C 43.8 ppm) and 11-Me (δ_H

1.05 ppm) and C-10 (δ_C 43.7 ppm), C-11 (δ_C 31.1 ppm), and C-12 (δ_C 51.6 ppm) established the substituted dodecahydrocyclopentafluorene moiety.

This tetra-cyclic system was fused to an unusual 12-membered macrocycle through ether and *ketone*-linkages. In the HMBC spectrum, the weak correlation from H-13 to C-24 and their chemical shifts (3.59 ppm for H-13, 159.4 for C-24) implied that C-13 and C-24 were connected through an ether linkage. On the other hand, the evidence for the ketone linkage was found by examination of 2^2J or $3J$ HMBC correlations from H-14 (δ_H 2.81 ppm), H-15 (δ_H 3.08 ppm), and H-18 (δ_H 7.11 ppm) to the *keto*-group C-16 appearing at δ_C 195.4 ppm. The 5-membered pyrrolidinone ring was identified based on the chemical shift data, COSY through the spin system CH(18)OH(19)NH and HMBC correlations from the amide proton resonating at δ_H 8.26 ppm to carbons C-1' (δ_C 167.2 ppm), C-17 (δ_C 131.1 ppm) and C-18 (δ_C 157.7 ppm) and from H-18 to C-16 (δ_C 195.4 ppm), C-19 (δ_C 86.2 ppm), and C-1' (δ_C 167.2 ppm). The correlations from CH₂-20 appearing at δ_H 3.10 and 3.14 ppm to C-19 (δ_C 86.2 ppm) and C-21 (δ_C 131.9 ppm) indicated that the phenyl and pyrrolidinone functions were connected through a methylene group. Thus, the elucidation of the planar structure of pyrrocidine D **40** was completed.

The relative stereochemistry of **40** was established through ROESY experiment. H-7 (δ_H 1.91 ppm) showed cross peaks with both H-9 (δ_H 1.34 ppm) and H-6 (δ_H 2.88 ppm). Moreover, CH₃-4a (δ_H 0.98 ppm) correlates with CH₃-3 (δ_H 1.05 ppm). Further inspection of ROESY spectrum revealed that H-12 (δ_H 0.94 ppm) showed cross peaks with both CH₃-11 (δ_H 1.05 ppm) and H-13 (δ_H 3.59 ppm) while the latter did not correlate with H-14 (δ_H 2.81 ppm). Furthermore H-14 (δ_H 2.81 ppm) correlated with H-15 (δ_H 3.08 ppm). H-18 (δ_H 7.11 ppm) showed correlations to both H-26 (δ_H 7.30 ppm), H-25 (δ_H 7.07 ppm) and H-15 (δ_H 3.08 ppm) and this defines the stereochemistry of the pyrrolidinone ring with respect to the dodecahydrocyclopentafluorene moiety and the benzene ring. In

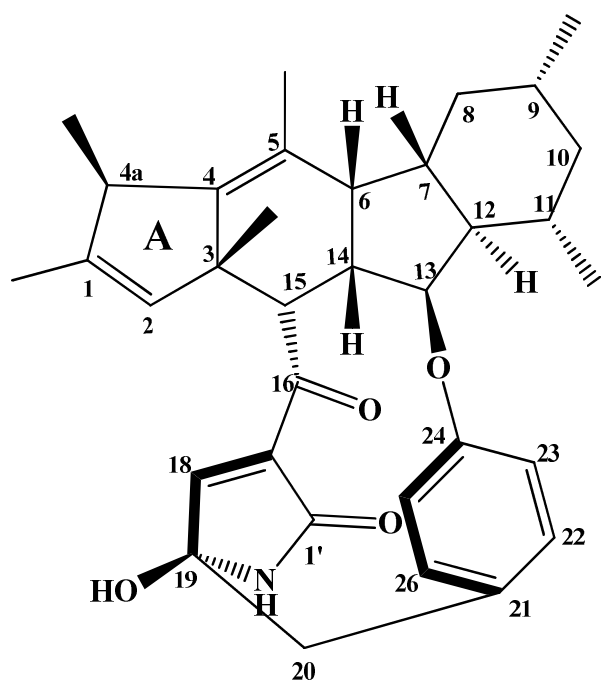
order to obtain the configuration of the rest of the molecule, a 3D model was built. The built 3D model showed a rigid molecule which is in agreement with the configuration of rings A, B, C and D. Furthermore, H-18 was correlated to only H-26 and H-25, confirming that the benzene ring is not freely rotating and was found to be more or less parallel to the pyrrolidinone ring. Thus, the relative configuration of compound **40** is defined.

3.4.13. Pyrrocidine E (41, new compound)

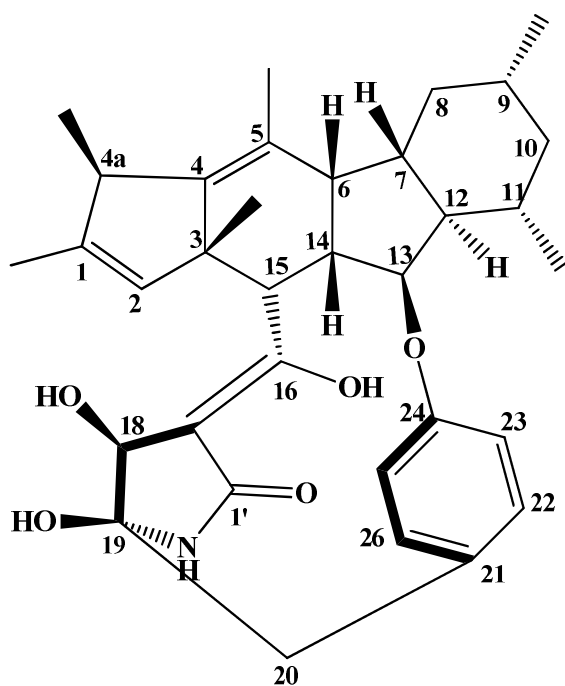
Pyrrocidine E	
Sample code	Emb_VLC_1000Et_PPT of PPT_sil3348
Biological source	<i>Embellisia eureka</i>
Sample amount	20 mg
Physical properties	yellowish amorphous solid
Molecular formula	C ₃₄ H ₄₂ NO ₅
Molecular weight	545 g/mol
Optical rotation $[\alpha]_D^{20}$	-10 (c 0.004, DMSO)
Retention time (HPLC)	No peak in HPLC detectable (detected only by TLC)

Pyrrrocidine E (**41**) was isolated from the EtOAc extract of solid rice cultures of *Embellisia eureka* as yellowish amorphous solid (20 mg). The HRESI-MS exhibited a strong peak at m/z 546.3212 $[M+H]^+$ indicating the molecular formula $C_{34}H_{42}NO_5$ (calculated 546.3219, Δ 0.0007). Structural elucidation of **41** was established based on comparison of the results of NMR spectral analysis including 1H NMR, 1H - 1H COSY and HMBC spectra (Table 3.30) as well as mass spectrometry with **40**. The molecular weight of **41** is increased by 18 amu, suggesting that **41** contains an extra H_2O in the structure compared to **40**. The 1H NMR spectrum of **41** showed the same signals appearing in the spectrum of **40** except for two extra peaks, appearing at δ_H 5.18 ppm ($J=6.2$ Hz) assigned for 18-OH, and one singlet at 11.97 ppm assigned to 16-OH, replacing the *keto*-group in **40**. Furthermore, a doublet signal at 3.75 ppm which correlated to 18-OH, and support the idea of the saturation of the olifenic bond in the *N*-containing ring in **40**. Further inspection of the HMBC spectrum confirmed the presence of correlations of 18-OH resonating at δ_H 5.18 ppm to C-17 (δ_C 105.9 ppm) and C-18 (δ_C 69.2 ppm), correlations of H-18 to C-1' (δ_C 174.1 ppm), C-17 (δ_C 105.9 ppm) and C-20 (δ_C 45.2 ppm) and correlations of 16-OH to C-15 (δ_C 46.9 ppm), C-16 (δ_C 167.4 ppm), C-17 (δ_C 105.9 ppm).

The relative stereochemistry of **41** was established based on ROESY correlations, a 3D model and comparison with that of **40**. Comparison of ROESY spectrum of **40** and **41** showed an identical configuration of rings A, B, C and D, including both chiral centers C-13 and C-15. The relative stereochemistry of the extra chiral center C-18 of compound **41** was established based on correlation of 18-OH appearing at δ_H 5.18 ppm to 19-OH resonating at δ_H 5.37 ppm. Thus the relative configuration of **41** is established.



40



41

Nr.	Compound
40	Pyrrocidine D
41	Pyrrocidine E

Table 3.30: ^1H , ^{13}C NMR, ROESY and HMBC spectra of compounds **40** and **41** in (DMSO- d_6)

No.	40				41			
	δ_{C}	δ_{H}	HMBC	ROESY	δ_{C}	δ_{H}	HMBC	ROESY
1	140.9				137.8			
1-Me	14.8	1.45, s	1, 2, 4a	13	14.7	1.46, s	1, 2, 4a	
2	129.5	4.90, s	1-Me, 3-Me, 1,3, 4, 4a		132.1	5.26, s	1-Me, 3-Me, 1,3, 4, 4a	
3	51.8				50.2			
3-Me	24.1	1.05, s	2, 3, 4, 15	6, 11, 14, 15, 10B, 4a-Me	26.0	0.96, s	1, 2, 3, 4	
4	145.7				147.9			
4a	44.4	2.99, m	4a-Me, 1, 4	8A, 12, 11-Me	44.1	2.97, m	4a-Me, 1, 4	
4a-Me	16.7	0.98, d (6.8)	1, 4, 4a	6, 11, 14, 3-Me	18.0	0.98, d (6.9)	1, 4, 4a	
5	127.0				126.3			
5-Me	19.6	1.75, s	4, 5, 6		19.7	1.76, s	4, 5, 6	
6	43.5	2.88, m	5, 7, 12, 13	7, 8B, 11, 15, 4a-Me, 3-Me	43.7	2.86, m	4, 5, 7, 12, 13	
7	45.8	1.91, m	5, 6, 8, 9, 12	6, 9, 11, 13, 14	45.5	1.91, m	6, 9, 11, 12	
8	38.8	A 1.38, t (11.4) B 1.95, br d (10.6)	9-Me, 9, 10, 12 5, 9, 10, 12	9-Me, 11-Me, 10 ^a , 4a 6, 14	38.0	A 1.45-1.49, m B 1.91, br d (10.8)	6, 7 5, 5-Me	
9	33.3	1.34, m	10	7, 10B, 11	33.2	1.35, m	7	
9-Me	22.5	0.94, d (6.2)	8, 9, 10	11-Me, 8A, 10A	22.5	0.94, d (6.4)	8, 9, 10	
10	43.8	A 0.71, ddd (12.0, 12.0, 12.0) B 1.66, m	11-Me, 9-Me, 9, 11, 12 9, 11, 12	8A, 12, 9-Me, 11-Me 9, 11, 3-Me	43.7	A 0.72, ddd (12.1, 12.1, 12.1) B 1.66, m	9-Me, 11-Me, 8, 9, 11, 12 8	
11	31.1	1.77, m	11-Me, 10, 12	6, 7, 9, 10B, 3-Me, 4a-Me	31.2	1.81, m	11-Me, 10, 12	
11-Me	20.4	1.05, d (7.3)	10, 11, 12	9-Me, 8A, 4a, 10A, 12	20.4	1.06, d (6.3)	10, 11, 12	
12	51.6	0.96, m	7	4a, 10A, 13, 11-Me	50.2	1.05-1.10, m	11-Me, 7, 11	
13	91.6	3.59, dd (3.5, 7.4)	7, 12, 15, 24	7, 12, 1-Me	90.1	4.63, dd (3.7, 7.3)	7, 12, 24	
14	50.1	2.81, ddd (3.6, 8.6, 10.6)	5, 6, 13, 15, 16	7, 8B, 25, 3-Me, 4a-Me	51.3	2.69, ddd (3.8, 7.7, 10.6)	5, 6, 15, 16	
15	52.6	3.08, d (10.8)	3-Me, 3, 4, 6, 13, 14, 16	3-Me, 6, 18, 26	46.9	2.41, d (10.9)	3-Me, 3, 4, 12, 16	
16	195.4				167.4			
17	131.1				105.9			
18	157.7	7.11, d (1.7)	1', 16, 19	15, 26	69.2	3.75, d (6.1)	1', 17, 20	
19	86.2				87.7			
20	44.7	A 3.14, d (12.2) B 3.10, d (12.2)	18, 19, 26 18, 19, 21, 26	22 22	45.2	A 2.75, d (12.7) B 3.07, d (12.7)	19, 21, 22 19, 21, 22	
21	131.9				130.2			
22	129.4	6.91, dd (8.4, 2.2)	18, 21, 24	20A, 20B	130.4	6.99, dd (8.5, 1.3)	20, 21, 24	
23	122.8	6.67, dd (8.3, 2.5)	21, 24, 25		121.8	6.72, dd (8.3, 2.1)	22, 24, 25	
24	159.4				159.3			
25	123.5	7.07, dd (8.2, 2.5)	21, 23, 21	14	122.4	7.01, dd (8.2, 2.1)	23, 25, 26	
26	131.5	7.30, dd (8.2, 2.2)	20, 22, 24	15, 18	132.1	7.12, dd (8.1, 1.5)	20, 22, 24	
1'	167.2				174.1			
NH		8.26, d (1.7)	1', 17, 18			8.15, s	1', 17, 18, 19	
16-OH						11.97, s	15, 16, 17	
18-OH						5.18, d (6.2)	17, 18	19-OH
19-OH		6.26, s	1', 18, 19, 20			5.37, s	18, 19, 20, 21	18-OH

Table 3.31: NMR data comparison of compounds **40** and **pyrrocidine A**

Position	40			* Pyrrocidine A		
	δ_C	δ_H	HMBC	δ_C	δ_H	HMBC
1	140.9			114.7	4.95, d (9.5) 4.98, d (16.5)	2, 3 2, 3
1-Me	14.8	1.45, s	1,2, 4a			
2	129.5	4.90, s	1-Me, 3-Me, 1,3, 4, 4a	141.6	5.86, m	3, 4, 15
3	51.8			37.2	2.68, m	2, 4, 5, 14, 15, 16
3-Me	24.1	1.05, s	2, 3, 4, 15			
4	145.7			122.7	5.42, d (6.4)	3, 5-Me, 6
4a	44.4	2.99, m	4a-Me, 1, 4			
4a-Me	16.7	0.98, d (6.8)	1, 4, 4a			
5	127.0			135.4		
5-Me	19.6	1.75, s	4, 5, 6	25.0	1.74, s	4, 5, 6
6	43.5	2.88, m	5, 7, 12, 13	51.7	2.11, m	4, 5, 7, 7-Me, 12, 13, 14
7	45.8	1.91, m	5, 6, 8, 9, 12	46.9		
7-Me				23.5	1.15, s	6, 7, 8, 12
8	38.8	A 1.38, t (11.4) B 1.95, br d (10.6)	9-Me, 9, 10, 12 5, 9, 10, 12	47.8	0.88, m 1.69, m	8, 7-Me, 9 7, 9, 10, 12
9	33.3	1.34, m	10	27.7	1.70, m	10
9-Me	22.5	0.94, d (6.2)	8, 9, 10	22.8	0.85, d (6.2)	8, 9, 10
10	43.8	A 0.71, ddd (12.0, 12.0, 12.0) B 1.66, m	11-Me, 9-Me, 9, 11, 12 9, 11, 12	44.3	0.43, ddd (11.7, 11.7, 11.7) 1.67, m	8, 9, 9-Me, 11, 11-Me, 12 8, 9, 12
11	31.1	1.77, m	11-Me, 10, 12	26.6	1.78, m	11-Me, 10
11-Me	20.4	1.05, d (7.3)	10, 11, 12	19.7	0.94, d (6.2)	10, 11, 12
12	51.6	0.96, m	7	52.8	1.10, dd (11.4, 6.1)	6, 7, 7-Me, 8, 11, 11-Me
13	91.6	3.59, dd (3.5, 7.4)	7, 12, 15, 24	91	4.25, dr.d (6.1)	7, 12, 15, 24
14	50.1	2.81, ddd (3.6, 8.6, 10.6)	5, 6, 13, 15, 16	41.4	2.10, m	3, 5, 6, 13, 15, 16
15	52.6	3.08, d (10.8)	3-Me, 3, 4, 6, 13, 14, 16	50.4	2.76, br.s	2, 3, 4, 6, 13, 14, 16
16	195.4			202.4		
17	131.1			138.5		
18	157.7	7.11, d (1.7)	1', 16, 19	151.3	6.67, s	1', 16, 17, 19
19	86.2			87.6		
20	44.7	A 3.14, d (12.2) B 3.10, d (12.2)	18, 19, 26 18, 19, 21, 26	43.8	3.10, d (12.5) 3.17, d (13.7)	18, 19, 21, 26 18, 19, 21, 26
21	131.9			130.9		
22	129.4	6.91, dd (8.4, 2.2)	18, 21, 24	130.0	7.15, dr.d (7.3)	19, 20, 24, 26
23	122.8	6.67, dd (8.3, 2.5)	21, 24, 25	121.4	7.02, br.d (7.9)	21, 24, 25
24	159.4			156.6		
25	123.5	7.07, dd (8.2, 2.5)	21, 23, 21	124.4	6.80, br.d (7.8)	21, 23, 24
26	131.5	7.30, dd (8.2, 2.2)	20, 22, 24	131.6	7.17, br.d (6.9)	19, 20, 22, 24
1'	167.2			168.2		
NH		8.26, d (1.7)	1', 17, 18		8.77, s	1', 17, 18, 19
19-OH		6.26, s	1', 18, 19, 20			

* (He *et al.*, 2002).

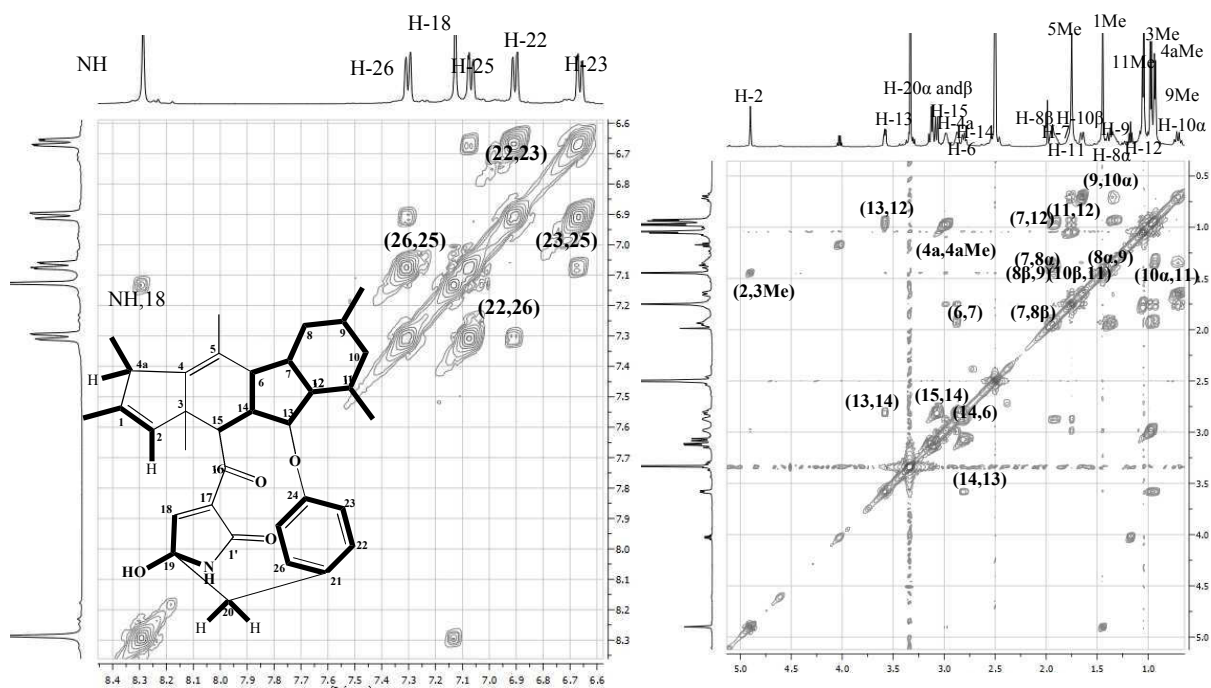


Fig. 3.50: COSY spectrum of compound **40**.

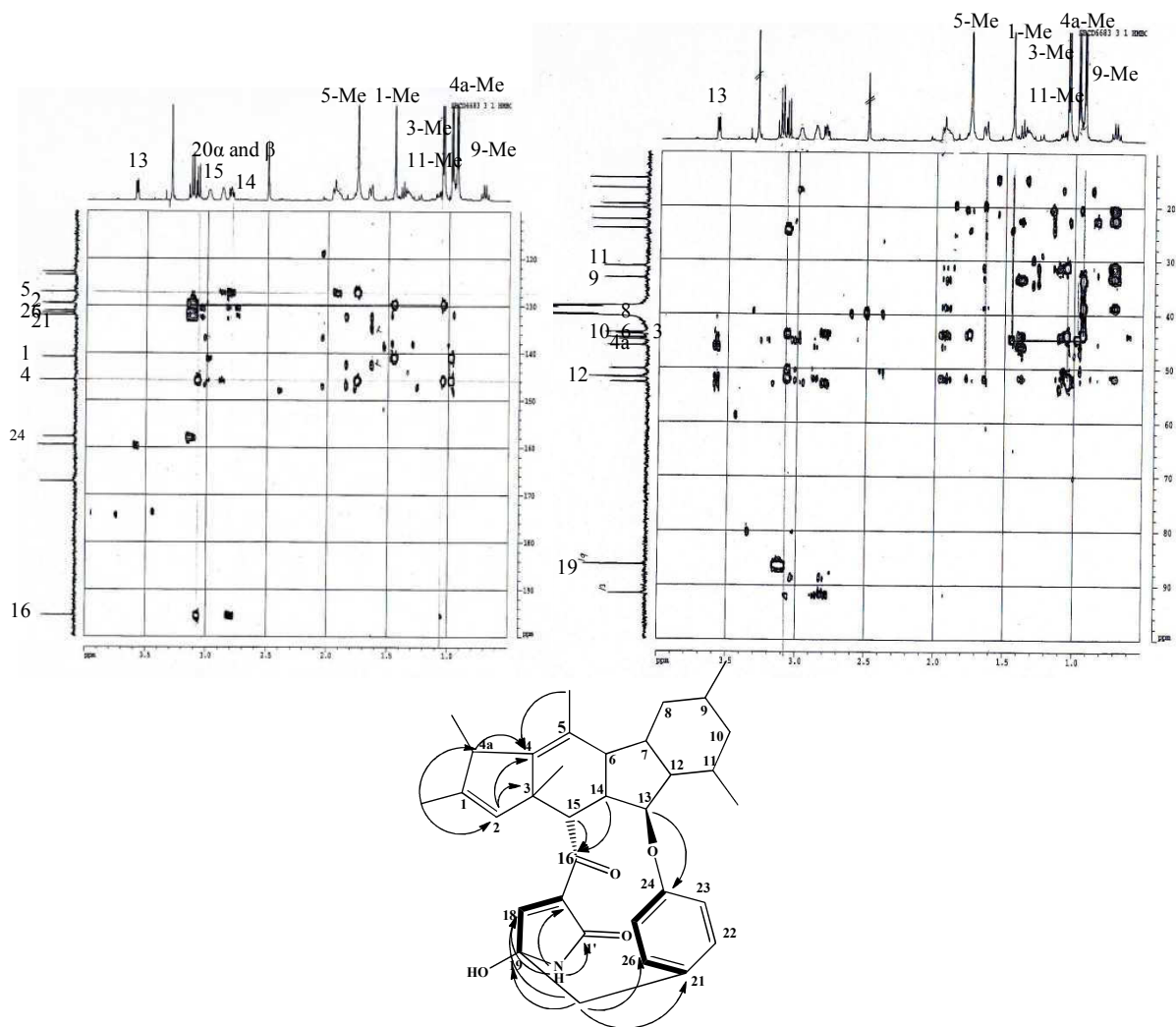


Fig. 3.51: HMBC spectrum of compound **40**.

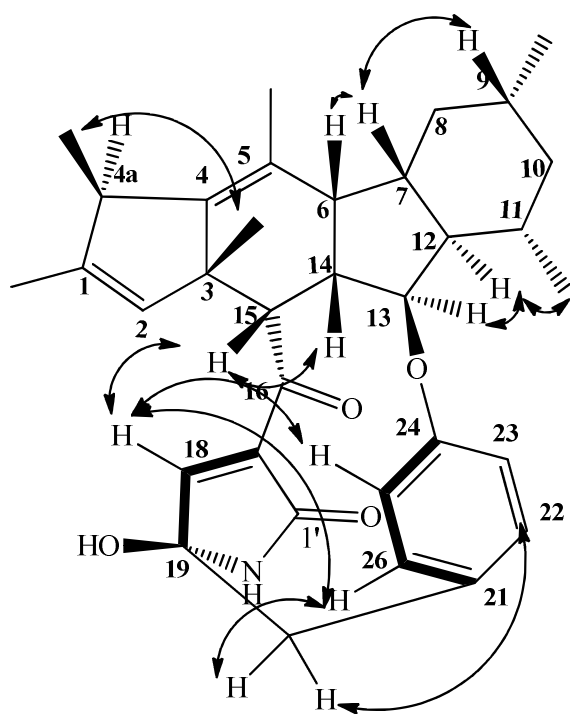
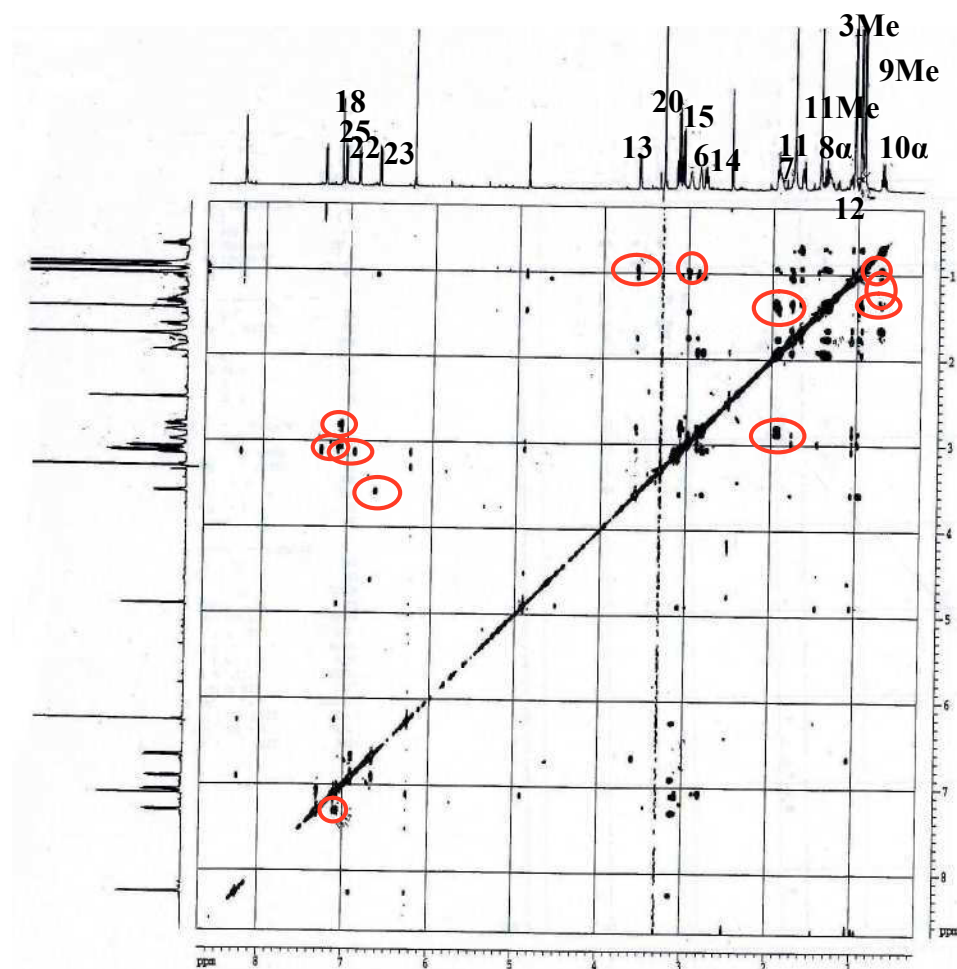


Fig.3.52: ROESY spectrum of compound 40.

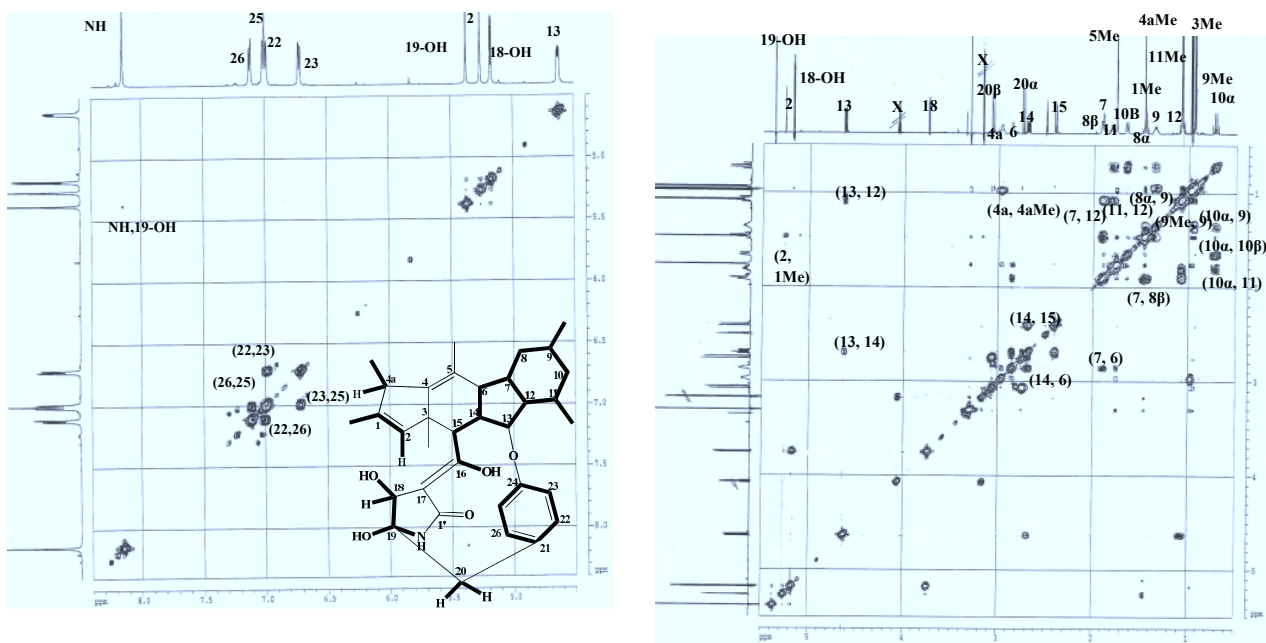


Fig. 3.53: COSY spectrum of compound **41**.

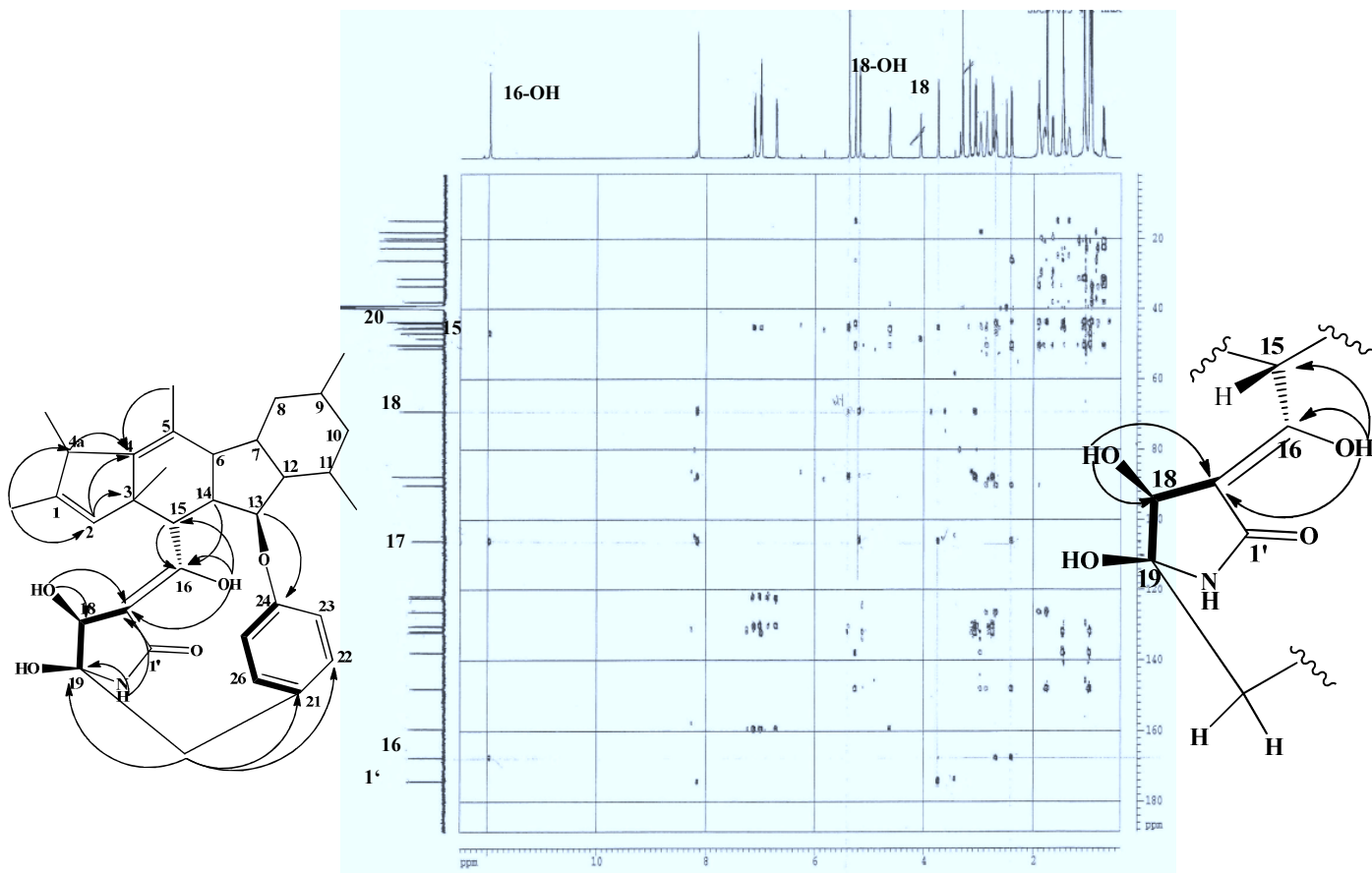


Fig. 3.54: HMBC spectrum of compound **41**.

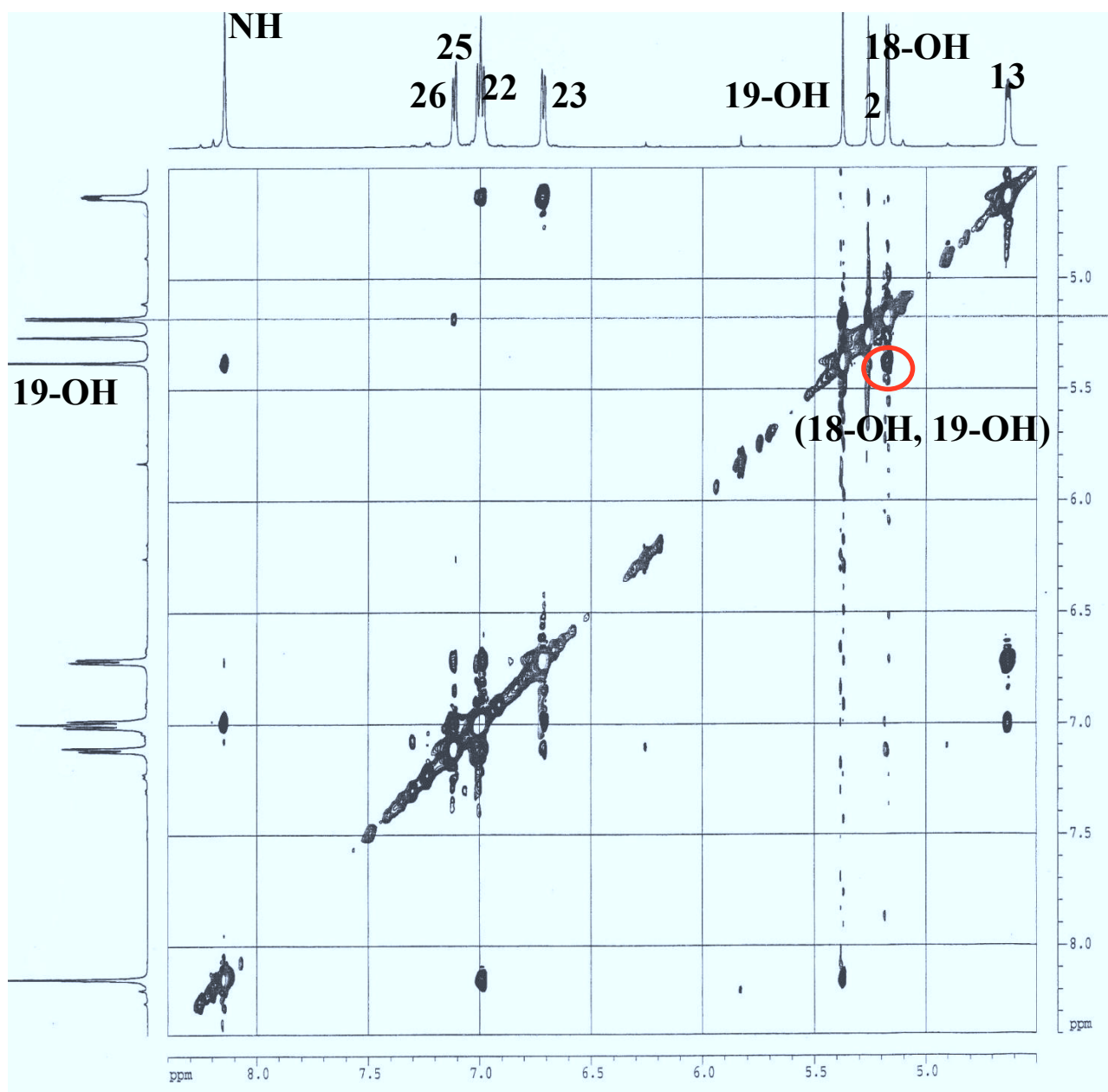


Fig. 3.55: ROESY spectrum of compound 41.

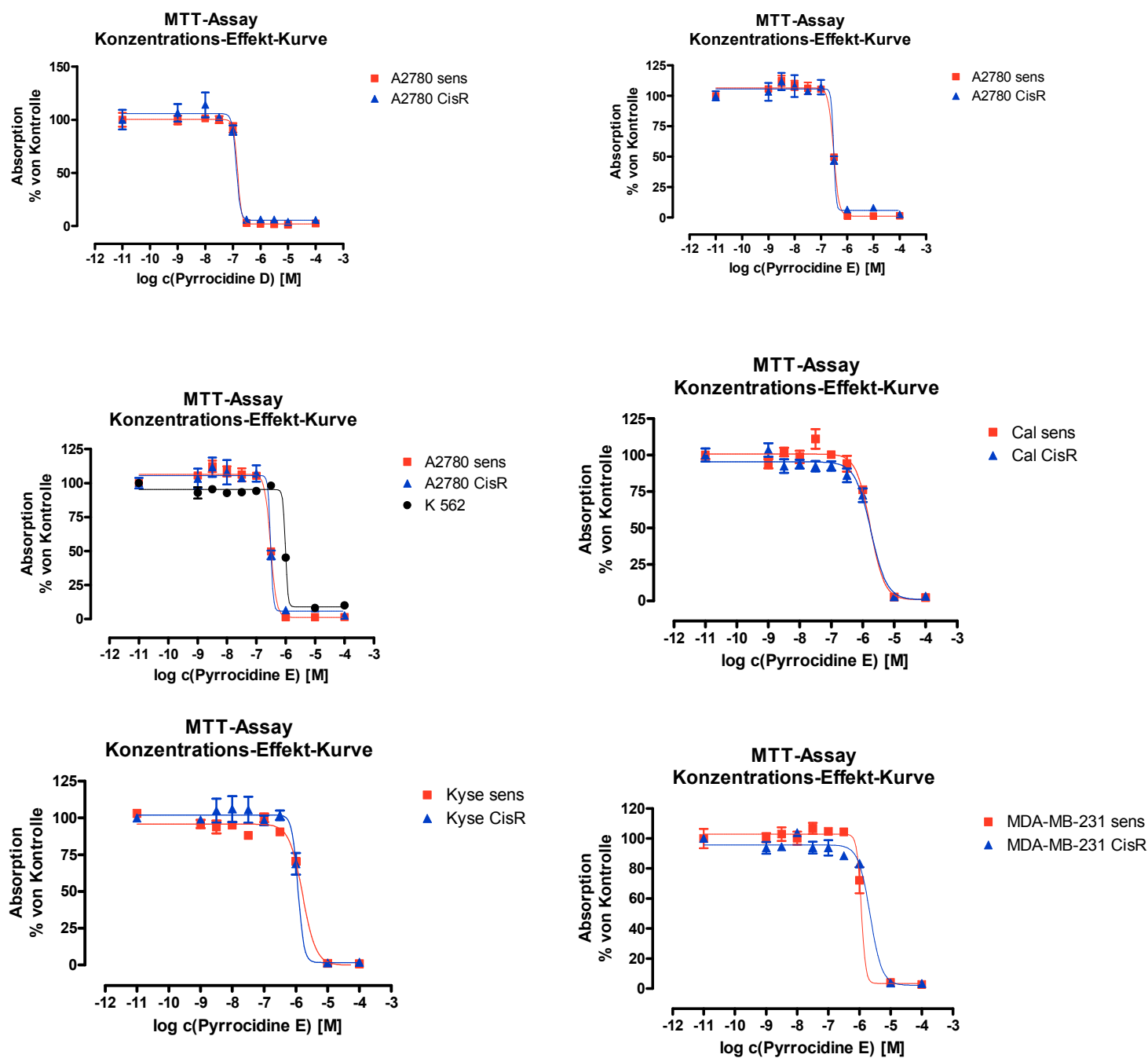
Table 3.32: IC₅₀ values of selected compounds isolated from *Embellisia eureka*.

Compound	IC ₅₀ (μ M)		
	L5178Y	A2780sens.	A2780CisR.
Embepthalide A [•] (29)		53.3	62.1
Embepthalide B [•] (30)		n.d.	68
Embepthalide C [•] (31)		70.8	67.8
Embepthalide D [•] (32)		73.1	73.1
Embeurekol A [•] (34)		67.6	85.7
Embeurekol B [•] (35)		82.2	82
Embeurekol C [•] (36)		62.7	67.3
Endocrocin [•] (39)		73.3	71.1
Pyrrocidine D (40)	0.11	0.15	0.15
Pyrrocidine E (41)	0.19	0.30	0.30
Kahalalide F (positive control)	4.30	-	-
Cisplatin CDDP (positive control)	-	0.8	8.40

n.d. Not determined

• All these substances showed only these IC₅₀ at conc. 10⁻⁴ M while at conc. 10⁻⁵ no activity observed.

The selected isolated compounds were tested in vitro for their antiproliferative activity against three different tumor cell lines including mouse lymphoma (L5178Y), human ovarian cancer (A2780sens.) and cisplatin-resistant human ovarian cancer cells (A2780CisR) by using the MTT assay with kahalalide F or cisplatin (CDDP) as positive controls. Results of the MTT assay (Table 3.32) revealed that among the tested compounds, only pyrrocidine D (40) and E (41) revealed strong antiproliferative activity.



Cell line	Pyrrocidine D (IC ₅₀ [μM])	Pyrrocidine E (IC ₅₀ [μM])	Cell line code	Cell line name
A2780 sens.	0.15	0.30	A2780	Ovarian carcinoma
A2780 CisR.	0.13	0.31	K 562	Leukemia
K 562		0.97	Cal	Head and neck carcinoma
Cal sens.		1.74	Kyse	Head and neck carcinoma
Cal CisR.		1.82	MDA-MB-231	Breast carcinoma
Kyse sens.		1.63	Sens.	Untreated cell line
Kyse CisR.		1.16	CisR.	Cisplatin-Resistant
MDA-MB-231 sens.		1.14		
MDA-MB-231 CisR.		2.21		

Fig. 3.56: Cytotoxic activity of compound **41** in different cell lines.

Pyrrocidine E (**41**) was also investigated in vitro for its antiproliferative activity against additional different tumor cell lines (Cal, Kyse and MDA-MB-231) (Fig. 3.56) and this revealed that pyrrocidine E (**41**) showed strong antiproliferative activity against these cell lines.

Table 3.32a: IC₅₀ values of pyrrocidine E (**41**) against different cell lines.

PBMC cytotoxicity (IC ₅₀ in μ M)	Inhibition of HCT116 (soft agar growth) (IC ₅₀ in μ M)	
Pyrrocidine E (41)	Pyrrocidine E (41)	
1.1	0.76	
Inhibition of A549 (soft agar growth) (IC ₅₀ in μ M)	Inhibition of A375 (IC ₅₀ in μ M)	
Pyrrocidine E (41)	Pyrrocidine E (41)	
1.04	0.598	
Inhibition of MDA MB 231 migration (IC ₅₀ in μ M)	Angiogenesis assay (IC ₅₀ in μ M)	
Pyrrocidine E (41)	Pyrrocidine E (41)	Positive Control (Sunitinib)
0.1	0.79	0.12

Pyrrocidine E (**41**) was further investigated in vitro for its antiproliferative activity against different tumor cell lines (Table 3.32a) and this revealed that pyrrocidine E (**41**) revealed strong antiproliferative activity. Further investigation of the mechanism of action of **41** was performed through conducting the in vitro angiogenesis assay against human umbilical vascular endothelial cells (HUVEC) sprouting induced by vascular endothelial growth factor A (VEGF-A) using sunitinib as a positive control. Results (Table 3.32a) revealed that **41** inhibited VEGF-A dependent endothelial cells sprouting with IC₅₀ value of 0.79 μ M, compared to sunitinib (IC₅₀ = 0.12 μ M).

- NF- κ B inhibitory activity of pyrrocidine E (41).

Pyrrocidine E (41) exhibited a potent NF- κ B inhibitory activity at IC₅₀ 250 nM which explains its cytotoxic mechanism of action.

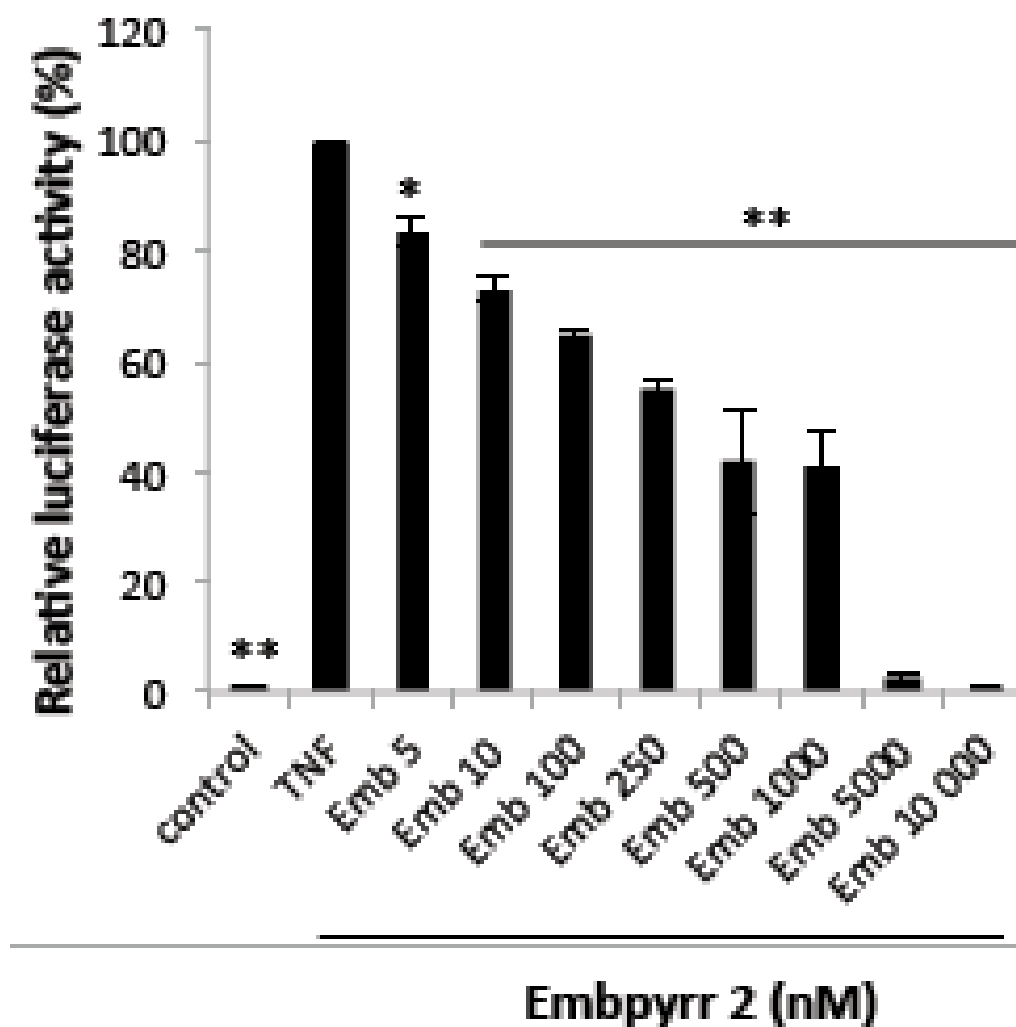


Fig. 3.57: NF- κ B inhibitory activity of compound 41.

Pyrrocidine E (41), when tested on peripheral blood mononuclear cells (PBMC) exhibited activity in μ M while on cancer cells in nM and this indicate that pyrrocidine E is more or less safe when used as anticancer agent (Fig. 3.58).

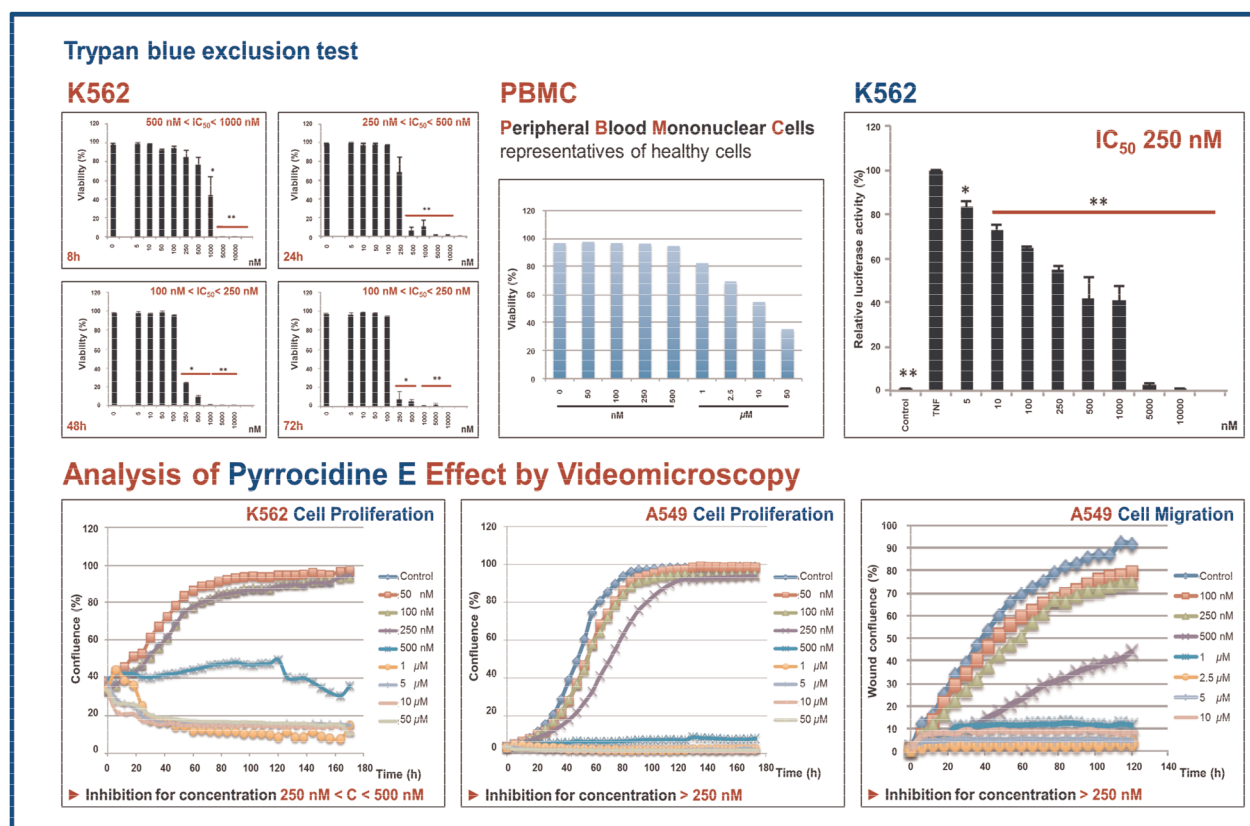


Fig. 3.58: Effect of compound **41** on cell viability.

4. Discussion

4.1. Culturing media

Culturing media and culture conditions have a great influence on the growth of microorganisms and the production of secondary metabolites (Bills, 1995). Thus it is important to grow the organism in different media in order to obtain a variety of secondary metabolites (Larsen *et al.*, 2005). Moreover, some natural products are only synthesized under certain environmental conditions and if all trace metals, phosphate and other medium cofactors are present in certain amounts (Knight *et al.*, 2003). Consequently, optimal media for good metabolite production can be varied for different genera being studied (Larsen *et al.*, 2005).

Fungi, unlike other microorganisms typically grow in nature on solid substrates such as wood, roots and leaves of plants (Nielsen *et al.*, 2004). Thus, in this study chosen fungal strains were cultured in liquid (Wickerham) medium as well as on solid rice medium. Bioactivity and chemical profiles of the obtained extracts from both cultures were compared and subjected to further investigation. HPLC chromatograms of the EtOAc extracts of liquid and rice cultures showed different chemical patterns for some of fungal strains investigated in this study. Moreover, EtOAc extracts of liquid and rice cultures showed different cytotoxic activity in preliminary biological screening tests which was in accordance with the different chemical picture.

4.2. Methodologies for profiling of the metabolites

Isolation and structure elucidation processes enrich chemistry of natural products (Butler, 2004). Hence, interesting fungal strains can be elected to be screened, which together with the use of spectroscopic methods in addition to chemoinformatics can be used as part of an effective dereplication protocol (Larsen *et al.*, 2005). Secondary metabolites profiling is not an easy task to be applied since natural products display a very diverse chemical structures. Thus, a single analytical method does not exist, which is capable of profiling

all natural products in the investigated extract (Wolfender *et al.*, 2005). However, advanced analytical and spectroscopic techniques, like the hyphenated techniques linked with HPLC, can provide a good idea about the substructures and/or functional groups in the chemical structure.

4.2.1. HPLC/UV

Combination of HPLC and UV make it easy to obtain the UV spectrum of practically every single metabolite from an extract, provided it has a suitable chromophore. Thus, the UV spectrum has turned into one of the most readily accessible data related to structure elucidation of secondary metabolites (Cannall, 1998).

In this study, a lot of natural products that share similar chromophoric functions were investigated by HPLC/UV-photodiode array detection (LC/UVDAD) which showed very often that this also interpreted into similar UV spectra, even though there were significant differences in addition of non-chromophoric functions.

4.2.2. HPLC/ESI-MS

Electrospray ionization mass spectrometry (ESI-MS) and the associated techniques about 25 years ago provided the scientific community with a highly versatile method for studies of secondary metabolites. ESI-MS is soft and sensitive ionization technique which can be adjusted to produce mainly protonated or sodiated ions (assuming positive ESI) from a wide range of natural products (Smedsgaard and Frisvad, 1996). Moreover, this method is also useful in establishing the related secondary metabolites. In the present study, this proved extremely efficient tool in detecting the octalactones and decalactones isolated from *Corynespora cassiicola*.

4.3. Isolation of natural products

4.4. Compounds isolated from purified fungal strains

4.4.1. Compounds isolated from the endophytic fungus *Corynespora cassiicola*.

Corynespora cassiicola was isolated from leaves of *Laguncularia racemosa* (Combretaceae) growing in China. The white mangrove plant *Laguncularia racemosa* (L) Gaertn. is an evergreen tree, and is a common species in mangrove forests along the Pacific and Atlantic coasts and tropical southern Asia (Eyberger *et al.*, 2006). To date the chemical constituents of fungi of the genus *Corynespora* have received only scant attention. A literature survey showed that an endolichenic *Corynespora* sp. yielded three secondary metabolites of heptaketide origin, corynesporol, herbarin, and 1-hydroxydehydroherbarin (Paranagama *et al.*, 2007). Furthermore, other metabolites of depsidone origin, including depsidones A-C and diaryl ethers (Chomcheon *et al.*, 2009), 6-(3'-hydroxy-*n*-butyl)-7-*O*-methyl spinochrome B (Chimura *et al.*, 1973), and 2,5,7-trihydroxy-3-methoxynaphthalene-1,4-dione (Assante *et al.*, 1977), were likewise reported from different *Corynespora* strains. In the present study three compounds were isolated from the liquid Wickerham medium; corynecassiidiol (**1**), 6-(3'-hydroxy-*n*-butyl)-7-*O*-methyl spinochrome B (**2**) and 7-*O*-methyl spinochrome B (**3**). Fifteen compounds were isolated from the solid rice cultures; coryneoctalactone A (**4**), coryneoctalactone B (**5**), coryneoctalactone C (**6**), coryneoctalactone D/A (**7**), coryneoctalactone E (**8**), coryneoctalactone F (**9**), corynesidone A (**10**), corynesidone B (**11**), corynesidone D (**12**), xestodecalactone D (**13**), xestodecalactone D/E (**14**), xestodecalactone F (**15**), xestodecalactone G (**16**) and corynecassiicol A/B (**17**, **18**).

4.4.1.1. Biosynthesis of octalactones and decalactones

Fungi are well known to produce a diversity of polyketide derived secondary metabolites, ranging from simple aromatic rings to complex highly modified reduced-type compounds, such as macrolides (Rawlings, 1999, Kobayashi and Kubota, 2007). This wide variety of structures is initially formed from poly- β -keto chains (poly- β -keto ester) biosynthesized through a decarboxylative condensation of malonyl-CoA units. Aromatic structures are then rationalized in terms of aldol and Claisen reactions (Dewick, 2002). The biosynthesis of small macrolides such as curvularin, an octaketide macrolide produced by some *Curvularia* (Coombe *et al.*, 1968), *Alternaria* (Robeson and Strobel, 1981) and *Penicillium* (Lai *et al.*, 1989) species, is well studied (Birch *et al.*, 1959, Liu *et al.*, 1998). To our knowledge, the biosynthesis of decalactone and octalactone derivatives was not investigated so far. We propose that the isolated lactones from *C. cassicola* and the macrolide curvularin share similar biosynthetic pathways. The only difference lies within the cyclisation step. In the case of curvularin derivatives, the macrocycle moiety includes 6 malonyl CoA units, whereas in decalactones as well as the octalactones isolated in this study, the macrocycle includes 5 and 4 malonyl CoA units, respectively (Fig. 4.1).

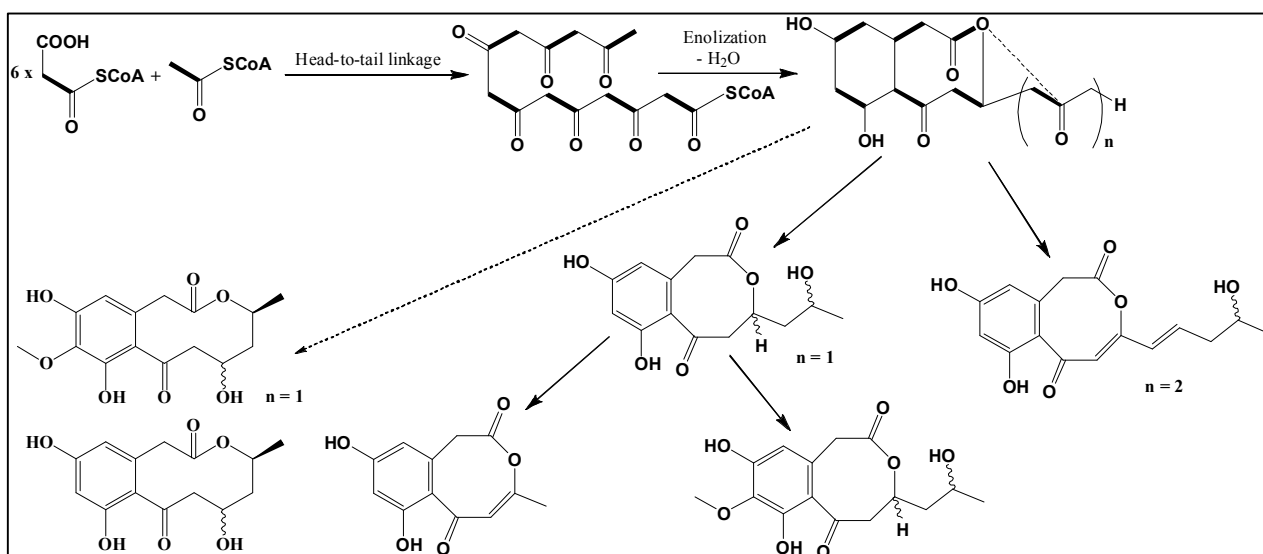


Fig. 4.1: Proposed biosynthetic pathway for isolated octalactones and decalactones derivatives.

4.4.1.2 Bioactivity of isolated compounds from *Corynespora cassicola*.

The isolated compounds of *Corynespora cassicola* also were subjected to biochemical protein kinase activity assay using 16 different human protein kinases, only compounds **2** and **11** inhibited several of the tested kinases (Table 3.12a). The IC₅₀ values observed for both compounds were in the low micromolar range against some protein kinases such as ALK, VEGF-R2, SRC, IGF1-R, and PIM1 of which inhibition is known to confer antitumoral effects. Of special interest is the fact that **11** inhibited PIM1 with an IC₅₀ value of 3.5 x 10⁻⁷ M, indicating a tenfold higher specificity of this naturally occurring inhibitor against this particular protein kinase in comparison to most of the other kinases investigated in this study (Table 3.12a).

4.4.2. Compounds isolated from the endophytic fungus *Stemphylium botryosum*.

Stemphylium botryosum is a mould which causes leaf spot of lettuce, a disease of economic importance in many countries. Both saprotrophic and pathogenic forms of *Stemphylium* occur on a wide range of plants. Many species of *Stemphylium* are economically important pathogens of agricultural crops. Usually, the toxicity of moulds is related to the production of one or

more phytotoxins, which is the case in *Stemphylium* species that are reported to produce a wide array of toxins (Arnone and Nasini, 1986, Camara *et al.*, 2002).

Eight compounds were isolated from the solid rice culture of the endophytic fungus *Stemphylium botryosum* named, phomapyrone D/H (**19/20**), stemphpyrone (**21**), infectopyrone (**22**), stemphbotrydione (**23**), stemphyperlenol (**24**), macrosporin (**25**) and indole-3-carbaldehyde (**26**).

4.4.2.1. Biosynthesis of stemphyperlenol

Stemphyperlenol (**24**) is an example of reduced perylenequinones so far identified in fungi of the morphologically closely related genera *Alternaria* and *Stemphylium*. The biosynthesis of these compounds occurs probably via oxidative coupling of two molecules of a tetralone derivative, which in turn is synthesized from a pentaketide derivative (Okuno *et al.*, 1983) by head-to-head coupling, followed by reduction and hydroxylation in different positions (Arnone *et al.*, 1986). The proposed biosynthetic pathway was confirmed by an incorporation experiment of ^{13}C -labelled sodium acetate and may be depicted as shown in Fig. 4.2 (Okuno *et al.*, 1983).

However, it is noticed that, whereas all compounds so far found appear to derive from so-called head-to-head coupling, stemphyperlenol (Fig. 4.2) seems to be an unusual example of a head-to-tail coupling of pentaketide-derived moieties (Arnone and Nasini, 1986).

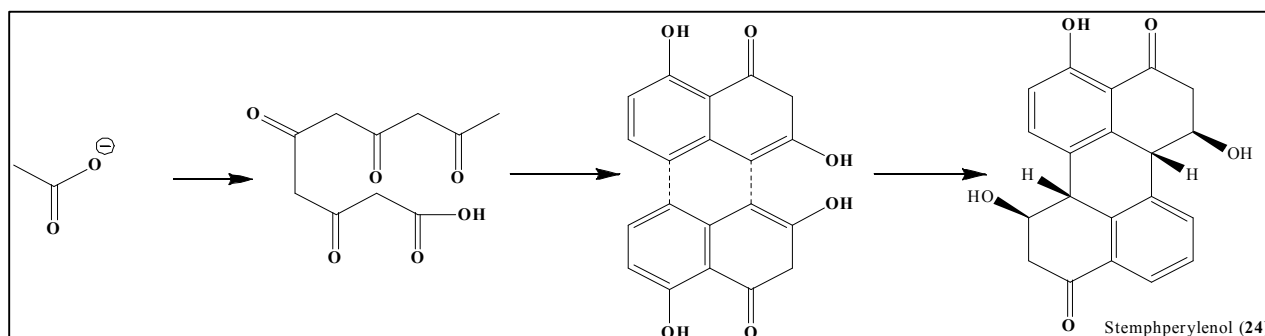


Fig. 4.2: Proposed biosynthetic pathway for stemphyperlenol.

4.4.2.2. Biosynthesis of pyrones

From a biogenetic point of view, 18-polyketo carboxylic acids are expected to convert into both the corresponding pyrones and phenolic compounds according to the mode of enzymatic cyclization as shown in Figure 4.10 (Lai *et al.*, 1991).

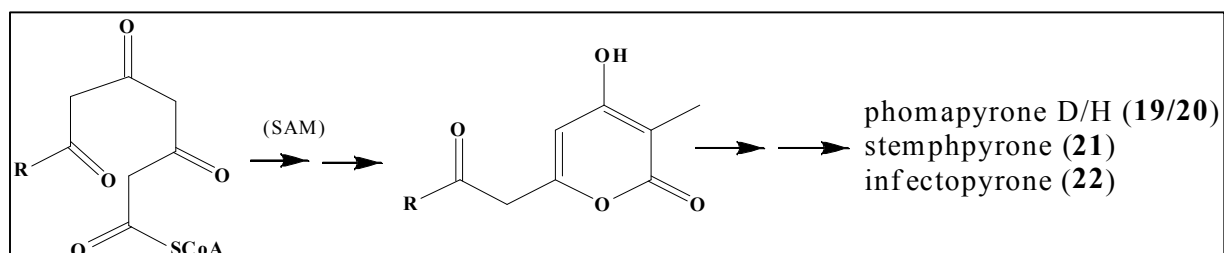


Fig. 4.3: Proposed biosynthetic pathway for pyrones.

4.4.3. Compounds isolated from the endophytic fungus *Stemphylium solani*.

Stemphylium solani was isolated from stem tissues of the traditional medicinal plant *Mentha pulegium* (Lamiaceae) growing in Morocco. Teas brewed from the leaves of *M. pulegium* are used traditionally to treat common colds and disorders of the liver and gall-bladder, as a carminative, as a diuretic, and to stimulate digestive action (Stahl-Biskup and Schultz, 2006). The essential oil has been reported to have antifungal (Bouchra *et al.*, 2006), larvicidal (Cetin *et al.*, 2006), acaricidal (Rim and Jee, 2006) and cytotoxic activities (Badisa *et al.*, 2003). This was the stimulus that prompted our investigation.

Two compounds were isolated from the solid rice cultures; altersolanol A (27) and stemphsolantrione (28).

Looking to the cytotoxic activity of the isolated compounds from the fungus *Stemphylium solani*, indicates that altersolanol A showed strong activity with IC_{50} of 0.6 μ M, while stemphsolantrione showed only moderate cytotoxic activity.

4.4.3.1. Biosynthesis of altersolanol A

Fungi are known to synthesize anthraquinones by linear head-to-tail combination of acetate and malonate, namely, octaketide chains, catalyzed by a fungal polyketide synthase, followed by the loss of carboxylic acid carbon from the terminal unit at C-3, but the details of the sequence of condensation, dehydration and hydroxylation steps is not well known (Figure 4.4). The periphery of the carbon skeleton is constructed by folding the octaketide chain, and then the ring at the centre of the fold is formed first, followed by the next two rings (Ohnishi *et al.*, 1991, Dewick, 2006).

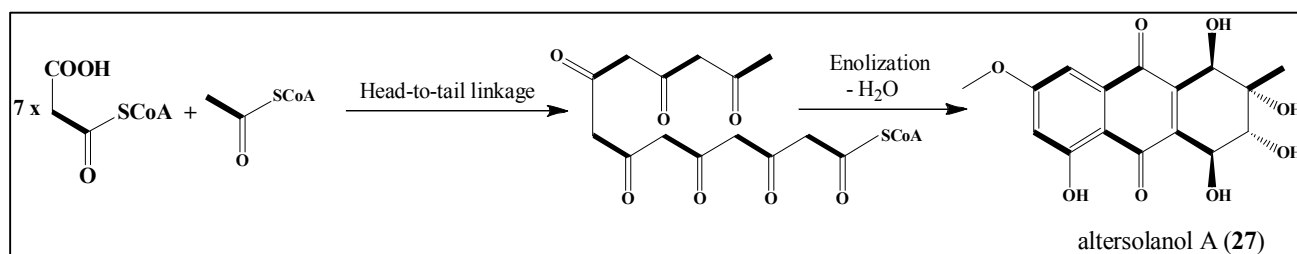


Fig. 4.4: Proposed biosynthetic pathway for altersolanol A.

4.4.4. Compounds isolated from the endophytic fungus *Embellisia eureka*.

Embellisia eureka was isolated from stem tissues of the plant *Cladanthus arabicus* (Asteraceae) growing in Morocco. Embellestatin (Kwon *et al.*, 2005) and terpestacin (Jung *et al.*, 2003) were isolated from *Embellisia chlamydospora*. Moreover, hydroxyl substituted indolizidine alkaloids were also isolated from *Embellisia oxytropis* (Shi *et al.*, 2009).

Thirteen compounds were isolated from the solid rice cultures; embphthalide A (29), embphthalide B (30), embphthalide C (31), embphthalide D (32), embphthalide E (33), embeurekol A (34), embeurekol B (35), embeurekol C (36), *P*-hydroxy benzaldehyde (37), 2-anhydromevalonic acid (38), endocrocin (39), pyrrocidine D (40) and pyrrocidine E (41).

4.4.4.1 Biosynthesis pathway of pyrrocidines.

The biosynthesis of pyrrocidines has been investigated by administration

of isotopically labeled (^{13}C and ^2H) precursors to *Penicillium* sp. GKK1032. These studies showed that the backbone of pyrrolicidines is constructed from L-tyrosine and a nonaketide chain flanked with five methyl groups probably by a polyketide synthase and a nonribosomal peptide synthetase hybrid. On the basis of the oxidation level of the starter unit and unusual 13-membered macroether formation between the tyrosine hydroxy group and the polyketide chain, novel cyclization mechanisms on the formation of a tricarboxylic system and a macroether have been proposed. Involvement of a similar type of cyclization in the biosynthesis of structurally related metabolites is discussed (Oikawa, 2003).

Discussion

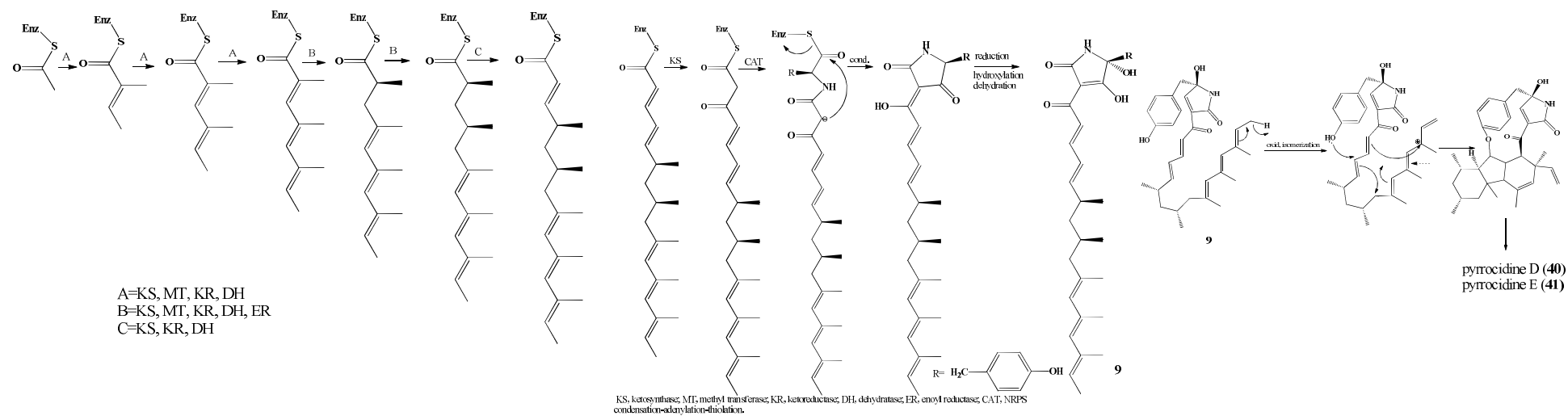


Fig. 4.5: Proposed biosynthetic pathway for pyrrocidines.

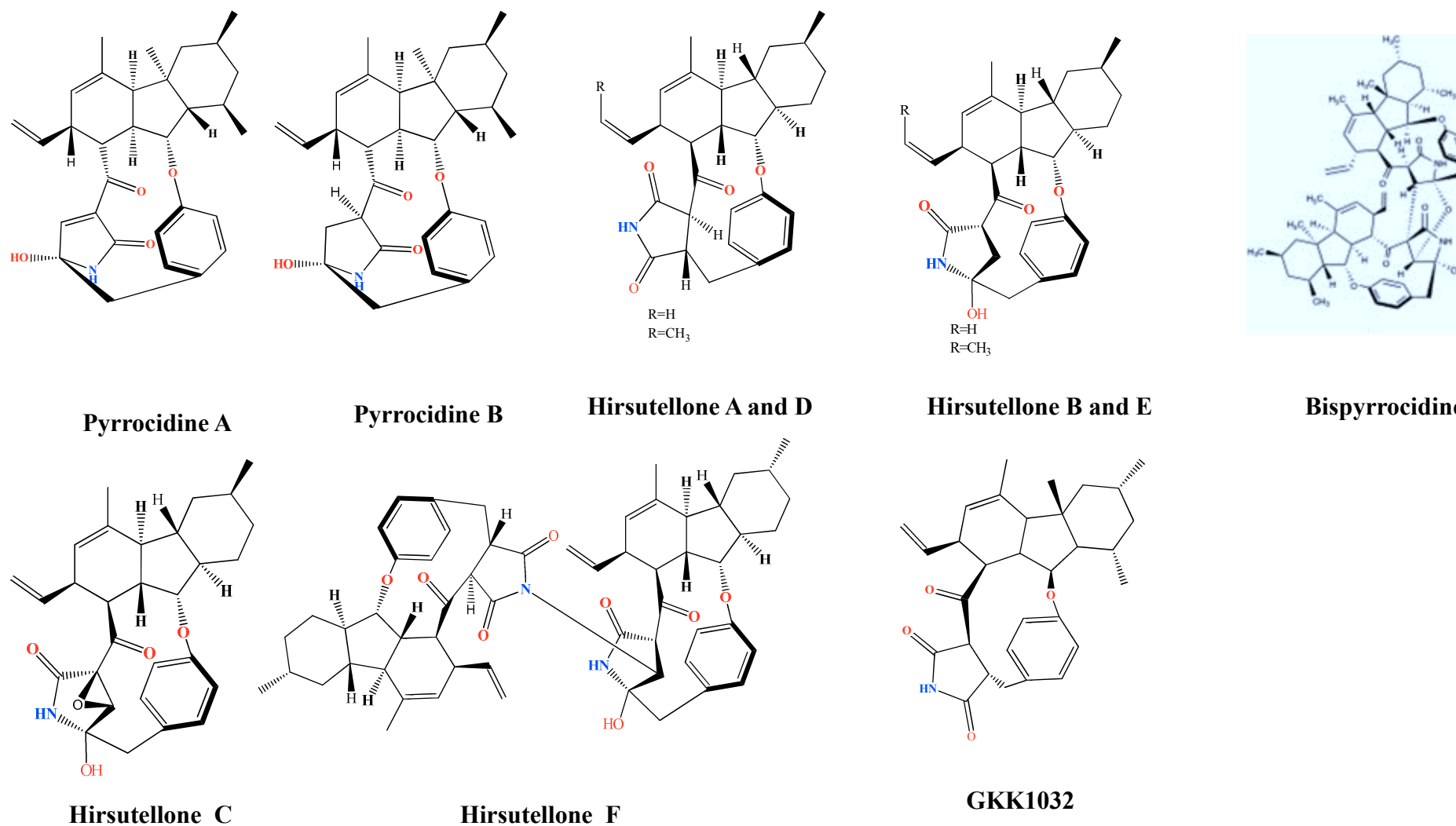


Fig. 4.5a: Structures of known pyrrocidine derivatives (He *et al.*, 2002; Pastre *et al.*, 2007; Isaka *et al.*, 2005; Shiono *et al.*, 2012).

4.4.4.2 Biosynthesis pathway of phthalides and isocoumarines.

From a biogenetic point of view, 18-polyketo carboxylic acids are expected to convert into both the corresponding pyrones and phenolic compounds according to the mode of enzymatic cyclization as shown in Figure 4.10 (Lai *et al.*, 1991).

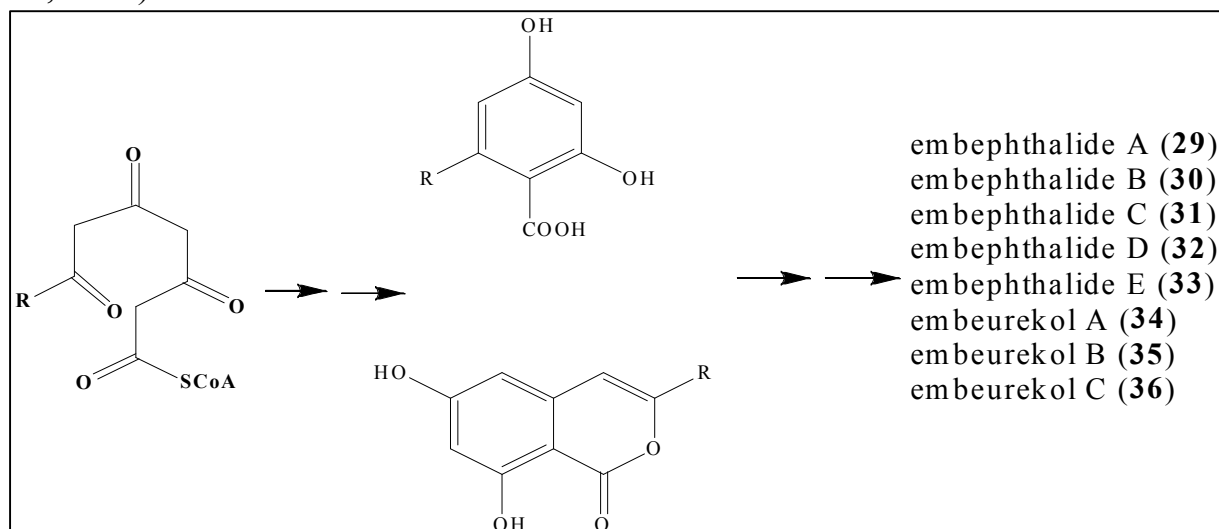


Fig. 4.6: Proposed biosynthetic pathway for phthalides and isocoumarines.

The isocoumarin derivatives **34-36** are typical heptaketide compounds with oxygen atoms located at alternate carbons. The carbonyl carbons in the side chain (R) might be reduced by fungal reductases to hydroxyl groups (Watanabe *et al.*, 1998).

4.4.4.3 Bioactivity of isolated compounds from *Embellisia eureka*.

The selected isolated compounds were tested *in vitro* for their antiproliferative activity against three different tumor cell lines including mouse lymphoma (L5178Y), human ovarian cancer (A2780sens.) and cisplatin-resistant human ovarian cancer cells (A2780CisR) by using the MTT assay with kahalalide F or cisplatin (CDDP) as positive controls. Results of the MTT assay (Table 3.32) revealed that of the tested compounds, only pyrrocidine D (**40**) and E (**41**) revealed a strong antiproliferative activity.

Pyrrocidine E (**41**) was further investigated *in vitro* for its antiproliferative activity against different tumor cell lines (Table 3.32a) and this

revealed that pyrrocidine E (**41**) exhibited strong antiproliferative activity. Further investigation of the mechanism of action of **41** was performed through conducting the in vitro angiogenesis assay against human umbilical vascular endothelial cells (HUVEC) sprouting induced by vascular endothelial growth factor A (VEGF-A) using sunitinib as a positive control. Results (Table 3.32a) revealed that **41** inhibited VEGF-A dependent endothelial cells sprouting with IC_{50} value of 0.79 μ M, compared to sunitinib ($IC_{50} = 0.12 \mu$ M).

Pyrrocidine E (**41**) was also investigated in vitro for its antiproliferative activity against additional different tumor cell lines (Cal, Kyse and MDA-MB-231) (Fig. 3.56) and this revealed that pyrrocidine E (**41**) showed strong antiproliferative activity against these cell lines.

Pyrrocidine E (**41**) exhibited a potent NF- κ B inhibitory activity at IC_{50} 250 nM which explains its cytotoxic mechanism of action is due to NF- κ B inhibition (Fig. 3.57).

4.4.4.4. What is NF- κ B?

The nuclear factor kappa B (NF- κ B) transcription factors control many vital biological operations in the cell through specific genes (Pahl, 1999). These physiological operations include immune and acute phase inflammatory response and apoptosis. NF- κ B transcription complexes could be one of a various homo- and heterodimers which developed from the subunits P50, P52, c-Rel, RelA (P65) and RelB (Gilmore, 2006). DNA-regulating-sites binding ability of these subunits activates certain gene expression (Gilmore, 2006).

Normally NF- κ B dimers are located in the cytosol of the cell as an inactive form by the linkage of I κ B inhibitor proteins (I κ B α , - β , - ϵ , - γ , P105 and P100) (Gilmore, 2006). As a reflex to external wide range of environmental factors (Pahl, 1999), such as proinflammatory substances, I κ B is easily phosphorylated and its complex with NF- κ B is cleaved liberating NF- κ B dimer which in turn is

translocated into the nucleus catalyzing specific gene expression (Gilmore, 2006).

It was found that regulation of the phosphorylation and degradation of I κ B are considered as key steps in the regulation of NF- κ B complexes (Scheidereit, 2006). I κ B kinase enzyme (IKK) complex contains two subunits (IKK α and IKK β) and an associated scaffold-like protein called MEMO (akka IKK α) (Gilmore, 2006). Other proteins namely immunophilins, ELKS and heat-shock proteins are also present but the role of them is not well defined (Gilmore, 2006).

After stimulation of the cell by several arrays such as tumor necrosis factor α (TNF α), interleukin-1 (IL1) or several pathogens, the IKK complex is activated by phosphorylation of specific serine units (Scheidereit, 2006). The activated IKK complex phosphorylate I κ B by IKK signals it at specific lysine residues by SCF- β -TrCP E3 ligase complex which activates I κ B degradation and liberates NF- κ B that can enter the nucleus (Gilmore, 2006).

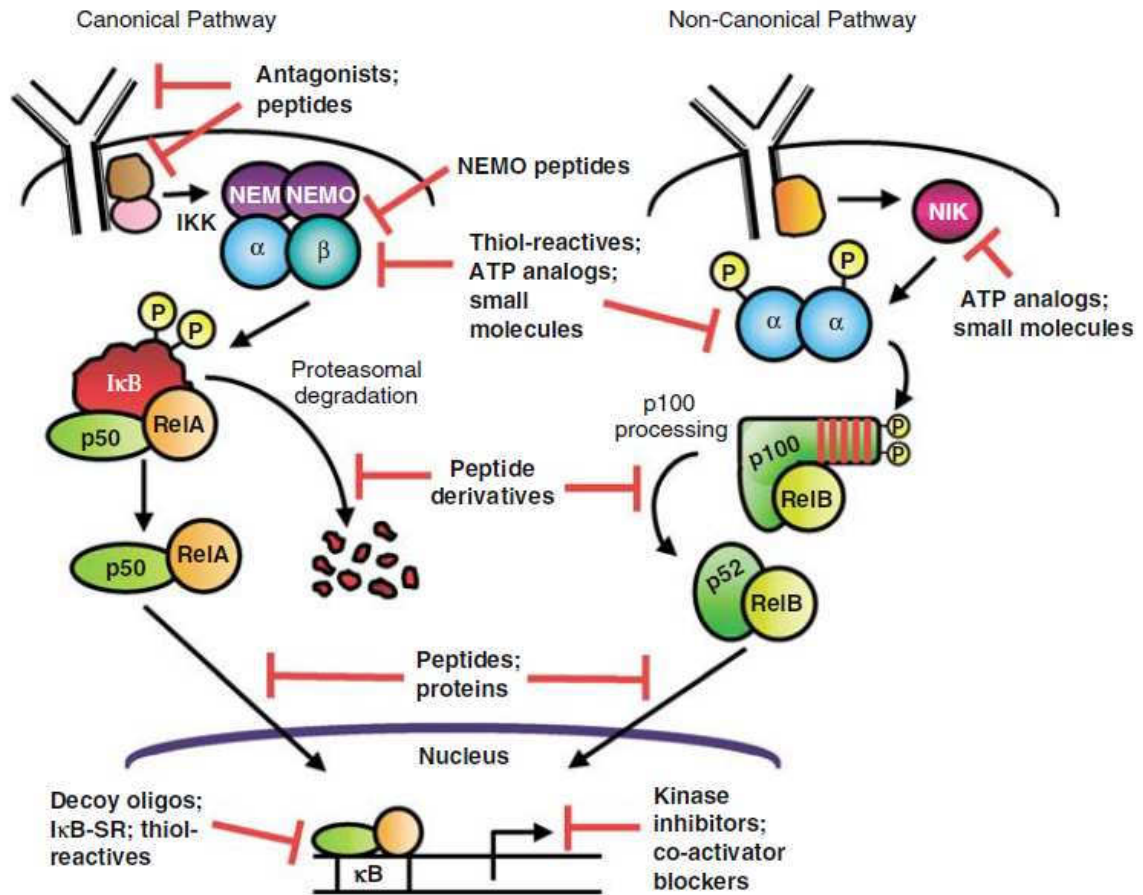


Fig. 4.7: Schematic representation of NF-κB activation and translocation into the nucleus (Gilmore and Herscovitch 2006).

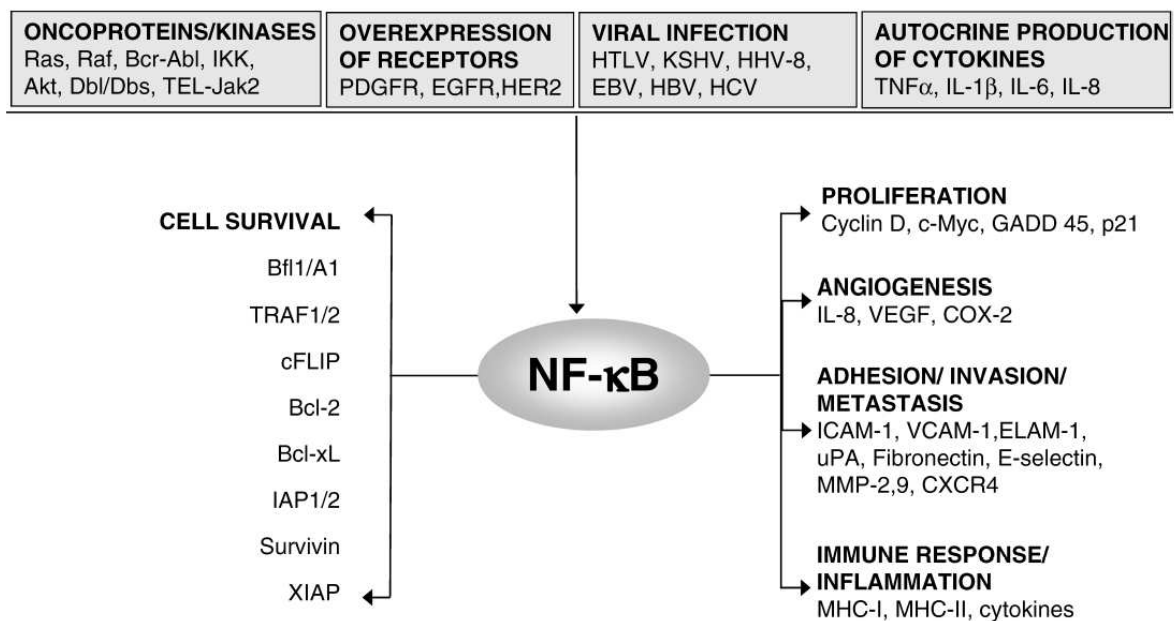


Fig. 4.8: Constitutive activation of NF-κB (Sethi *et al.*, 2008).

There are many pathways for NF- κ B activation. The two most common pathways are the canonical (classical) and the non-canonical (alternative) pathways (Scheidereit, 2006). In the canonical pathway, a complex like (P50-RelA/I κ B α) is activated by IKK complex containing I κ B α /I κ B β /MEMO, with I κ B β being the primary kinase of I κ B α (Gerondakis *et al.*, 2006). In the non-canonical pathway, the latent cytoplasmic NF- κ B complex is P100/RelB. Upon activation by certain stimuli, I κ B α homodimer is activated and phosphorylates P100 at two C-terminal serine units (Gerondakis *et al.*, 2006).

4.4.4.5. NF- κ B in cancer.

Many studies showed and confirmed that NF- κ B is one of the key-factors that regulate the development of many types of cancer like lymphoid and myeloid malignancies (Braun *et al.*, 2006; Pikarsky and Ben-Neriah, 2006). It was found that NF- κ B can play a tumor controlling role and that it is important in promoting apoptosis (Calzado *et al.*, 2007). On the other hand, NF- κ B plays an important role in the anti-inflammatory/apoptotic effect of tumor development and so in cancer prevention and cancer therapy. Therefore it is important to use NF- κ B inhibitors as adjuvants during cancer therapy (Calzado *et al.*, 2007).

Mechanism of NF- κ B activation in cancer.

Several studies investigated the role of NF- κ B in cancer (Karin *et al.*, 2002; Kim *et al.*, 2006; Rayet and Gelinas, 1999). Some of the reasons for sustained NF- κ B activity are IKK activity and the shorter half-life of I κ B α and B-cells, lymphoma, mutated I κ B α in Hodgkin's lymphoma, IL-1 β production in acute myelogenous leukemia, and TNF production in cutaneous T-cell lymphoma and Brukitti's lymphoma (Garg and Aggarwal, 2002).

NF- κ B activation is essential for transforming the ability of several cellular and viral oncoproteins. The viral homologue of c-Rel (v-Rel) was discovered as translocating gene of avian retroviruses, which cause aggressive lymphoma and leukemia in chickens (Gilmore, 1999). In rat fibroblasts

transformation by HTL-I Tax protein, NF- κ B played an essential role (Yamaoka *et al.*, 1996). In addition, in human T-cell leukemia virus-I (HTLV-I) NF- κ B is the key-factor (Yamaoka *et al.*, 1996).

It was found also that NF- κ B suppresses apoptosis by inducing the expression of many anti-apoptotic proteins and by interfering with the expression or activity of pro apoptotic proteins (Lee *et al.*, 2007). The analysis of inflammatory cells (Loch *et al.*, 2001) was the first evidence for the inhibitory effect of NF- κ B on apoptosis.

NF- κ B and its role in cell proliferation.

In fact NF- κ B regulates and mediates several genes of cell proliferation in cancer (Ahn and Aggarwal, 2005). These genes include TNF α , IL-1 β and IL-6 (Ahn and Aggarwal, 2005). TNF α plays an important role in glioblastoma (Ahn and Aggarwal, 2005; Aggarwal *et al.*, 1996) and cutaneous T-cell lymphoma (Giri and Aggarwal, 1998), while, IL-1 β in acute myelogenous leukemia (Estrov *et al.*, 1998), IL-6 which the regulatory factor of multiple myeloma (Bharti *et al.*, 2003) and head and neck squamous cell carcinoma (Kato *et al.*, 2000). Also, NF- κ B regulates certain cell cycle-regulating proteins (Mukhopadhyay *et al.*, 2002).

NF- κ B promotes survival of tumor cells.

NF- κ B controls many gene products that negatively regulate apoptosis (Sethi *et al.*, 2008). These include IAP-1, IAP-2, XIAP, cFLIP, TRAF1, TRAF2, Bcl-2, Bcl-XL, A1 and survivin (Ahn and Aggarwal, 2005). NF- κ B is found to be linked to anti-apoptotic function in tumors such as T-cell lymphoma, melanoma, pancreatic cancer, bladder cancer and breast cancer.

NF- κ B and tumor cell invasion.

Tumor invasion is controlled by many proteases (Novak *et al.*, 1991; Bond *et al.*, 1998). Matrix metallo proteases (MMPs) promote growth of cancer cells through the interaction of extracellular matrix (ECM) molecules and integrins, cleaving insulin-like growth factor and shedding trans membrane

precursor of growth factors, including transforming growth factors- β (TGF- β) (Novak *et al.*, 1991; Bond *et al.*, 1998). All of these factors are controlled by NF- κ B which suggests a potential strategy to block the invasion of tumors is by targeting NF- κ B (Novak *et al.*, 1991).

NF- κ B and angiogenesis.

Angiogenesis is critical for tumor progression and this process is dependant mainly on chemokines (MCP-1, IL-8) and growth factors (vascular endothelial growth factor [VEGF]) (Aggarwal *et al.*, 2006). These angiogenic factors are found to be controlled mainly by NF- κ B activation (Aggarwal *et al.*, 2006) through the upregulation of IL-8 and VEGF expression (Levine *et al.*, 2003). These studies further established the role of NF- κ B activation in angiogenesis (Sethi *et al.*, 2008).

NF- κ B and tumor metastasis.

Migration of cancerous cells into and out of the vessels is required for cancer metastasis (Sethi *et al.*, 2008). Penetration through vessel walls is mediated by specific molecules in the endothelial cells of blood vessels in response to a number of arrays from inflammatory cells and tumor cells (van de Stolpe *et al.*, 1994). ICAM-1, CLAM-1 and VCAM-1 are these special molecules (van de Stolpe *et al.*, 1994). All these molecules are found to be expressed in response to NF- κ B (van de Stolpe *et al.*, 1994). The suppression of NF- κ B activation is very important in controlling cancer cell metastasis (Sethi *et al.*, 2008).

NF- κ B and chemo/radio resistance.

NF- κ B inhibits apoptosis induced by a variety of DNA-damaging chemotherapeutic agents and ionizing radiation in addition to suppression of TNF α -induced apoptosis (Lee *et al.*, 2007). In many types of tumors, cells which are exposed to chemotherapeutic drugs or radiation showed enhanced NF- κ B activation and resistance to apoptosis (Arlt *et al.*, 2003; Brach *et al.*, 1991; Hwang and Ding, 1995). The fact that cancer cells have high NF- κ B activity

together with the enhanced activation of NF- κ B could be an important strategy of cancer therapy (Lee *et al.*, 2007). NF- κ B inhibition enhances apoptotic response to chemotherapy (Jones *et al.*, 2000; Wang *et al.*, 1999) and radiotherapy (Shao *et al.*, 1997; Yamagishi *et al.*, 1997).

4.4.4.6. NF- κ B inhibition.

NF- κ B is a key-factor in cancer and many inflammatory diseases and this signaling pathway provides attractive targets for treatment of these diseases (Calzado *et al.*, 2007). Rational inhibition of unfavorable NF- κ B activity can be obtained by many pathways (Fig. 4.9) (Calzado *et al.*, 2007). One of these regulatory levels to interfere with NF- κ B activation is to target membrane receptor signaling (antiTNF α) (Pikarsky and Ben-Neriah, 2006). Anti TNF α treatments are also in clinical use (Etanercept[®], Enbrel[®] and Amgen[®]) or by infliximab (Remicade[®]) which is an injectable antibody that binds and neutralize TNF α (Calzado *et al.*, 2007). Antioxidants were also suggested as possible NF- κ B inhibitors (Staal *et al.*, 1990; Mihm *et al.*, 1991). PDTC as an antioxidant inhibits NF- κ B through I κ B ligase inhibition (Hayakawa *et al.*, 2003). Moreover, at least 18 IKK inhibitors have been developed, 3 of them are tested in phase II (Calzado *et al.*, 2007). The compound SPC-839 inhibits IKK β with an IC₅₀ of 62 nM (Karin *et al.*, 2004). Other IKK β selective inhibitors include PS-1145, BMS-345541 and SC-514 (Calzado *et al.*, 2007).

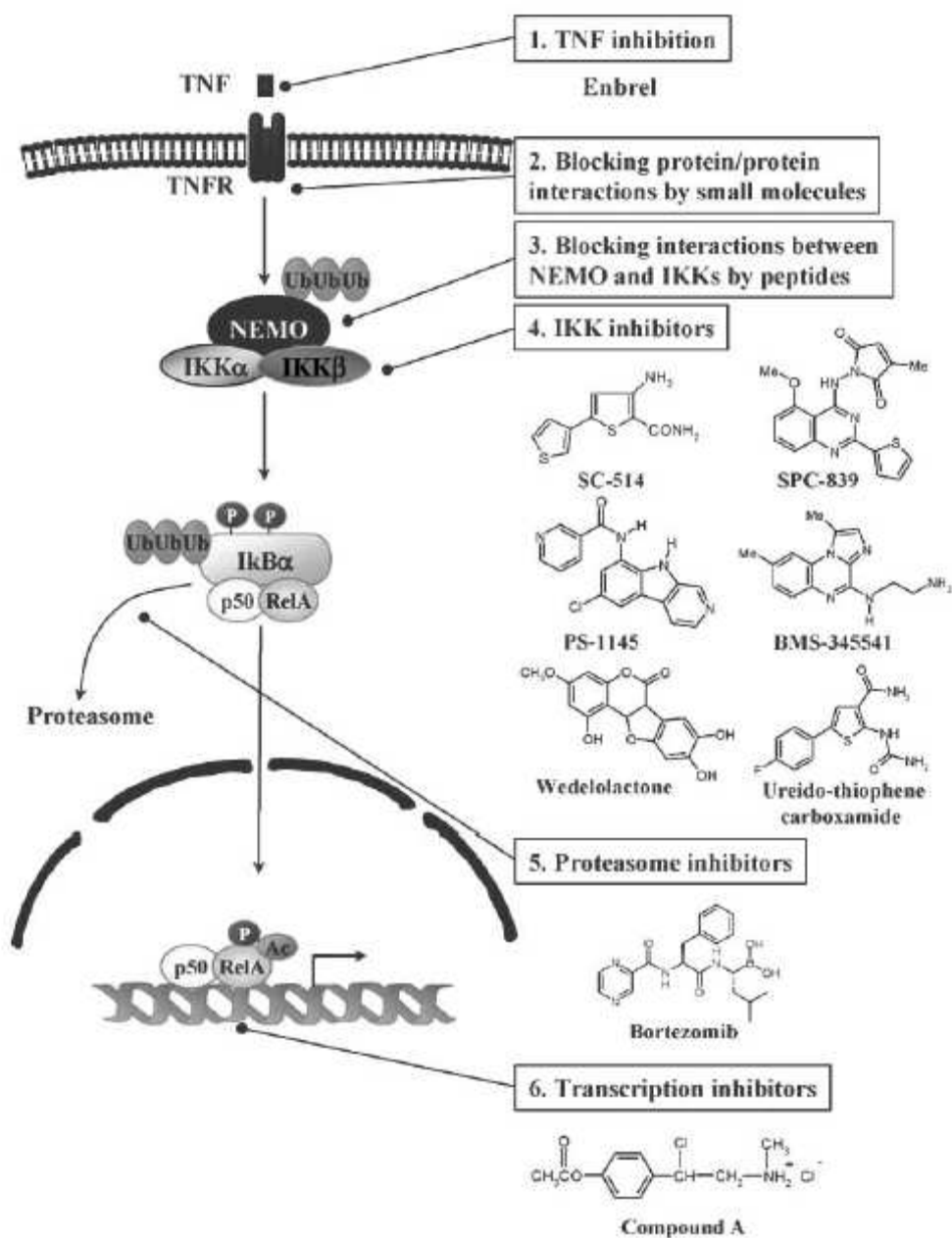


Fig. 4.9: NF-κB inhibitors (Calzado *et al.*, 2007).

Plant endophytic fungi produce natural products with a large diversity of chemical structures which might prove to be suitable for specific medicinal or agrochemical applications. Most of these secondary metabolites show biological activities in pharmaceutically relevant bioassay systems and thus represent potential lead structures which could be optimized to yield effective therapeutic and bioactive agents.

The aim of this work was the isolation of secondary metabolites from endophytic fungi, followed by structure elucidation and examination of their pharmacological potential. Four endophytic fungal strains (*Corynespora cassiicola*, *Stemphylium botryosum*, *Stemphylium solani* and *Embellisia eureka*) were selected as biological sources. The fungi were grown in liquid Wickerham medium as well as in solid rice medium for a period of three to four weeks. The extracts obtained were then subjected to different chromatographic separation techniques in order to isolate the secondary metabolites.

Structure elucidation of secondary metabolites was performed using state-of-the-art analytical techniques, including mass spectrometry (MS) and nuclear magnetic resonance (NMR) experiments. In addition, in the case of selected optically active natural products, chiral derivatisation methods were applied in order to determine their absolute configuration. Finally, the isolated compounds were subjected to various bioassays to examine their cytotoxic activities.

1. *Corynespora cassiicola*

Corynespora cassiicola was isolated from the Mangrove plant *Laguncularia racemosa* (Combretaceae). Eighteen compounds were isolated from different cultures of *Corynespora cassiicola*. These compounds belong to naphthaquinones, octalactones, decalactones and depsidones. Fourteen compounds are new natural products.

2. *Stemphylium botryosum*

Eight compounds were isolated from solid rice cultures of *Stemphylium botryosum*. These compounds represent mainly pyrones. Two compounds are new natural products.

3. *Stemphylium solani*

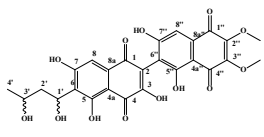
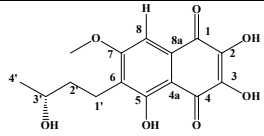
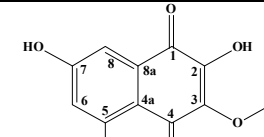
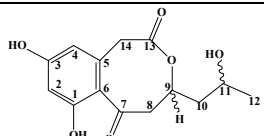
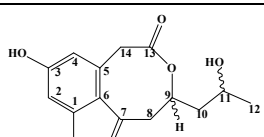
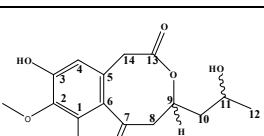
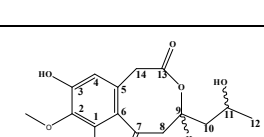
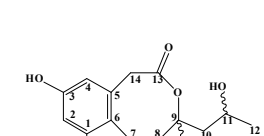
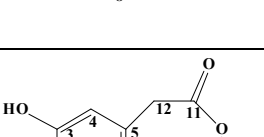
Two compounds were isolated from solid rice cultures of *Stemphylium solani*. One compound of these isolated compounds is a new natural product.

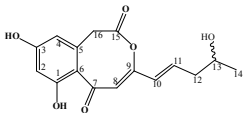
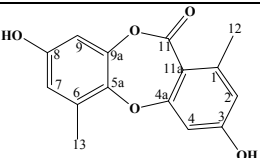
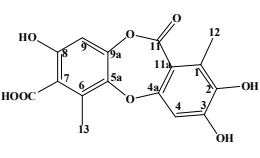
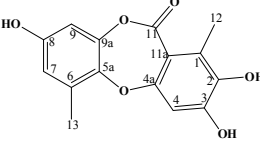
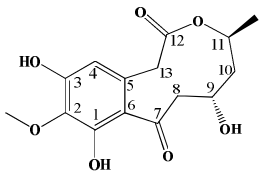
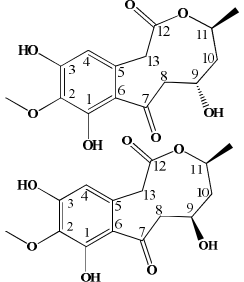
4. *Embellisia eureka*

Thirteen compounds were isolated from solid rice cultures of *Embellisia eureka*. These compounds include phthalides, isocoumarines and pyrrocidines. Ten compounds are new natural products. The two pyrrocidines derivatives show potent cytotoxic activity against L5178Y, A2780sens., A2780CisR. and many other cell lines.

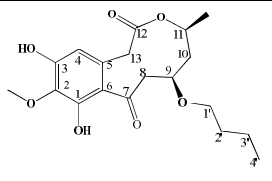
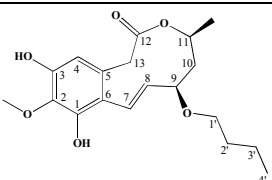
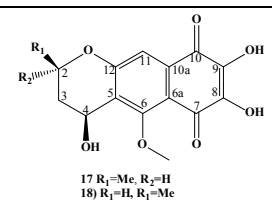
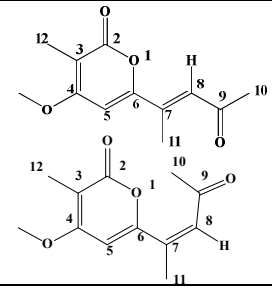
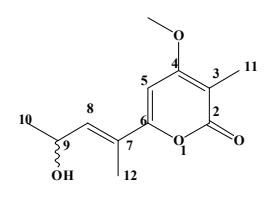
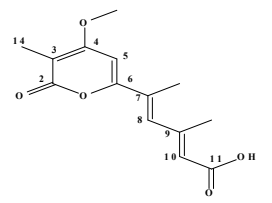
A total of forty-one compounds were isolated in this study, twenty seven of which were identified as new natural products. Both known and new compounds were tested for their biological activities using different bioassay systems.

Table 5.1: Summary of the isolated compounds

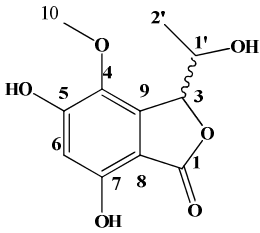
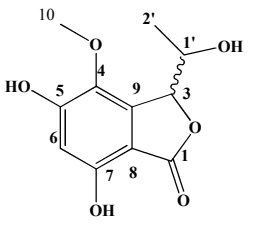
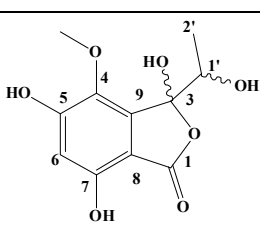
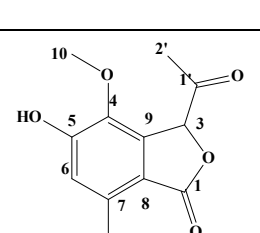
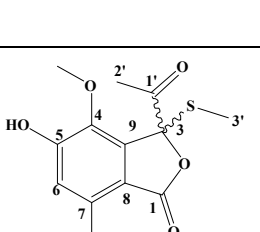
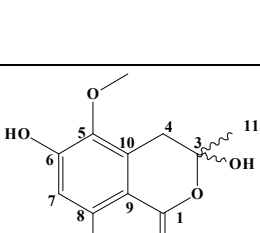
Compound name	Structure	Source	Comment
Corynecassiidiol		<i>Corynespora cassicola</i>	New
6-(3'-hydroxy- <i>n</i> -butyl)-7- <i>O</i> -methyl spinochrome B		<i>Corynespora cassicola</i>	Known
7- <i>O</i> -methyl spinochrome B		<i>Corynespora cassicola</i>	Known
Coryneoctalactone A		<i>Corynespora cassicola</i>	New
Coryneoctalactone B		<i>Corynespora cassicola</i>	New
Coryneoctalactone C		<i>Corynespora cassicola</i>	New
Coryneoctalactone D/A	 	<i>Corynespora cassicola</i>	New
Coryneoctalactone E		<i>Corynespora cassicola</i>	New

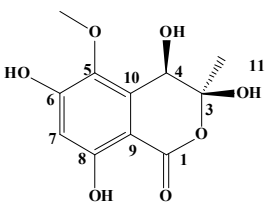
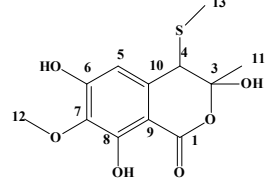
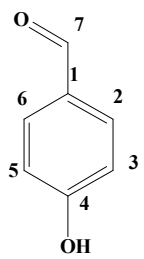
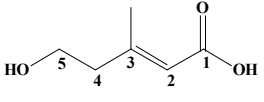
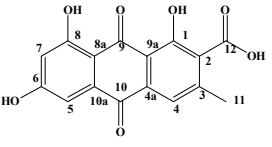
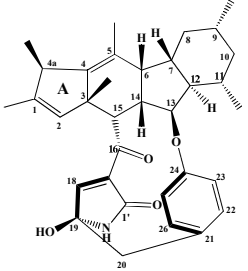
Coryneoctalactone F		<i>Corynespora cassicola</i>	New
Corynesidone A		<i>Corynespora cassicola</i>	Known
Corynesidone B		<i>Corynespora cassicola</i>	Known
Corynesidone D		<i>Corynespora cassicola</i>	New
Xestodecalactone D		<i>Corynespora cassicola</i>	New
Xestodecalactone D/E		<i>Corynespora cassicola</i>	New

Conclusion

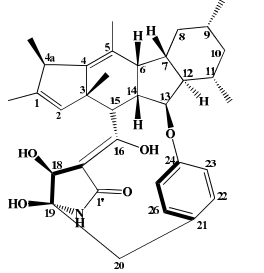
Xestodecalactone F		<i>Corynespora cassicola</i>	New
Xestodecalactone G		<i>Corynespora cassicola</i>	New
Corynecassiicol A/B	 <p>17 R₁=Me, R₂=H 18) R₁=H, R₂=Me</p>	<i>Corynespora cassicola</i>	New
Phomapyrone D/H		<i>Stemphylium botryosum</i>	Phomapyrone H (New) Phomapyrone (Known)
stemphpyrone		<i>Stemphylium botryosum</i>	Known
Infectopyrone		<i>Stemphylium botryosum</i>	Known

Stemphbotrydione		<i>Stemphylium botryosum</i>	New
Stemphperyleneol		<i>Stemphylium botryosum</i>	Known
Macrosporin		<i>Stemphylium botryosum</i> <i>Stemphylium solani</i>	Known
Indole-3-carbaldehyde		<i>Stemphylium botryosum</i>	Known
Altersolanol A		<i>Stemphylium solani</i>	Known
Stemphsolantrione		<i>Stemphylium solani</i>	New

Embepthalide A		<i>Embellisia eureka</i>	New
Embepthalide B		<i>Embellisia eureka</i>	New
Embepthalide C		<i>Embellisia eureka</i>	New
Embepthalide D		<i>Embellisia eureka</i>	New
Embepthalide D		<i>Embellisia eureka</i>	New
Embeurekol A		<i>Embellisia eureka</i>	New

Embeurekol B		<i>Embellisia eureka</i>	New
Embeurekol C		<i>Embellisia eureka</i>	New
p-hydroxybenzaldehyde		<i>Embellisia eureka</i>	Known
2-Anydromevalonic acid		<i>Embellisia eureka</i>	Known
Endocrocin		<i>Embellisia eureka</i>	Known
Pyrrocidine D		<i>Embellisia eureka</i>	New

| *Conclusion*

Pyrrocidine E		<i>Embellisia eureka</i>	New
---------------	---	--------------------------	-----

6. References

- Aggarwal, B. B., Schwarz, L., Hogan, M. E., and Rando, R. F. (1996). Triple helix-forming oligodeoxyribonucleotides targeted to the human tumor necrosis factor (TNF) gene inhibit TNF production and block the TNF-dependent growth of human glioblastoma tumor cells. *Cancer Res.*, **56(22)**, 5156-5164.
- Aggarwal, B. B., Shishodia, S., Sandur, S. K., Pandey, M. K., and Sethi, G. (2006). Inflammation and cancer: how hot is the link? *Biochem. Pharmacol.*, **72(11)**, 1605-1621.
- Ahn, K. S. and Aggarwal, B. B. (2005). Transcription factor NF-kappa B: a sensor for smoke and stress signals. *Ann. N. Y. Acad. Sci.*, **1056**, 218-233.
- Aly, A. H., Debbab, A., and Proksch, P. (2011a). Fifty years of drug discovery from fungi. *Fungal Divers.*, **50(1)**, 3-19.
- Aly, A. H., Debbab, A., and Proksch, P. (2011b). Fungal endophytes: unique plant inhabitants with great promises. *App. Microb. Biot.*, **90(6)**, 1829-1845.
- Arlt, A., Gehrz, A., Muerkoster, S., Vorndamm, J., Kruse, M. L., Folsch, U. R., and Schafer, H. (2003). Role of NF-kappaB and Akt/PI3K in the resistance of pancreatic carcinoma cell lines against gemcitabine-induced cell death. *Oncogene*, **22(21)**, 3243-3251.
- Arnone, A., Nasini, G., Merlini L., and Assante G. (1986). Secondary mould metabolites. Part 16. Stemphytoxins, new reduced perylenequinone metabolites from *Stemphylium botryosum* var. *lactucum*. *J. Chem. Soc. Perkin Trans. I*, 525-530.

- Assante, G., Locci, R., Camarda, L., Merlint, and L., Nasini, G. (1977). Screening of the genus *Cercospora* for secondary metabolites, *Phytochemistry*, **16**, 243-247.
- Azevedo, J. L., Maccheroni W. Jr., Pereira, J. O., and Araujo, W. L. (2000). Endophytic microorganisms: a review on insect control and recent advances on tropical plants. *Electron. J. Biotechnol.*, **3**, 40-65.
- Bacon, C. W., and White, J. F. (2000). Microbial endophytes, New York, NY, USA, Marcel Dekker, 341-388.
- Badisa, R. B., Tzakou, O., Couladis, M., and Pilarinou E. (2003). Cytotoxic activities of some Greek Labiatae herbs. *Phytother. Res.*, **17**(5), 472-76.
- Bauer, A. W., Kirby, W. M. M., Sherriss, J. C., and Turck, M. (1966). Antibiotic susceptibility testing by a standardized single disc method. *Amer. J. Clin. Pathol.*, **45**(4), 493-496.
- Becker, A. M., Rickards, R. W., Schmalzl, K. J., and Yick, H. C. (1978). Metabolites of *Dactylaria lutea*. *J. Antibiot.*, **31**(4), 324-329.
- Beistel, D. W., and Edwards, W. D. J. (1976). The internal chemical shift - a key to bonding in aromatic molecules. 2. Substituent effects on the carbon-13 magnetic resonance spectra of the 1,4-disubstituted benzenes. *J. Phys. Chem.*, **80**, 2023- 2027.
- Bergmann, S., Schumann, J., Scherlach, K., Lange, C., Brakhage, A. A. and C. Hertweck. (2007). Genomics-driven discovery of PKS-NRPS hybrid metabolites from *Aspergillus nidulans*. *Nat. Chem. Biol.*, **3**, 213.
- Bernays, E. A. (1993). Plant sterols and host-plant affiliations of herbivores. In: Bernays, E. A. (ed), Insect-plant interactions, vol IV. CRC, Boca Raton, Fla, USA, pp 45-57.

- Bharti, A. C., Donato, N., Singh, S., and Aggarwal, B. B. (2003). Curcumin (diferuloylmethane) down-regulates the constitutive activation of nuclear factor-kappa B and I kappa B alpha kinase in human multiple myeloma cells, leading to suppression of proliferation and induction of apoptosis. *Blood*, **101**(3), 1053-1062.
- Bills, G. F. (1995). Analysis of microfungal diversity from a user's perspective. *Can. J. Bot.*, **73** (1), 33-41.
- Birch, A. J., Musgrave, O. C., Rickards, R. W., and Smith, H. (1959). Studies in relation to biosynthesis. Part XX. The structure and biosynthesis of curvularin. *J. Chem. Soc.*, **4**, 3146-3152.
- Bond, M., Fabunmi, R. P., Baker, A. H., and Newby, A. C. (1998). Synergistic upregulation of metalloproteinase-9 by growth factors and inflammatory cytokines: an absolute requirement for transcription factor NF-kappa B. *Febs Lett.*, **435**(1), 29-34.
- Bouchra, C., Achouri, M., Idrissi Hassani, L. M., and Hmamouchi, M. (2003). Chemical composition and antifungal activity of essential oils of seven Moroccan Lamiaceae against *Botrytis cinerea* Pers.,. *Fr. J. Ethnopharmacol.*, **89**, 165-169.
- Brach, M. A., Hass, R., Sherman, M. L., Gunji, H., Weichselbaum, R., and Kufe, D. (1991). Ionizing radiation induces expression and binding activity of the nuclear factor kappa B. *J. Clin. Invest.*, **88**(2), 691-695.
- Braun, T., Carvalho, G., Fabre, C., Grosjean, J., Fenaux, P., and Kroemer, G. (2006). Targeting NF-kappa B in hematologic malignancies. *Cell Death Differ.*, **13**(5), 748-758.

- Buss, A. D., Cox, B., and Waigh, R. D. (2003). In Burger's Medicinal Chemistry and Drug Discovery, 6th ed.; Volume 1: Drug Discovery; Abraham, D. J., Ed.; Wiley: Hoboken, N. J., Chapter 20, 847-900.
- Butler, M. S. (2004). The role of natural product chemistry in drug discovery. *J. Nat. Prod.*, **67**(12), 2141-2153.
- Calzado, M. A., Bacher, S., and Schmitz, M. L. (2007). NF-kappa B inhibitors for the treatment of inflammatory diseases and cancer. *Curr. Med. Chem.*, **14**(3), 367-376.
- Camara, M. P. S., O'Neill, N. R., and Van Berkum, P. (2002). Phylogeny of *Stemphylium* spp. based on ITS and glyceraldehyde-3-phosphate dehydrogenase gene sequences. *Mycologia*, **94**(4), 660-672.
- Cannall, R. J. P. (1998). Methods in Biotechnology, Vol. 4: Natural products isolation, *Humana Press Inc.*, Totowa, N. J., pp.1.
- Carmichael, J., DeGraff, W. G., Gazdar, A. F., Minna, J. D., and Mitchell, J. B. (1987). Evaluation of a tetrazolium-based semiautomated colorimetric assay: Assessment of radiosensitivity. *Cancer Res.*, **47**(4), 943-946.
- Cetin, H., Cinbilgel, I., Yanikoglu, A., and Gokceoglu, M. (2006). Larvicidal activity of some Labiate (Lamiaceae) plant extracts from Turkey. *Phytother. Res.*, **12**(20): 1088-90.
- Chimura, H., Sawa, T., Kumada, Y., Nakamura, F., and Matsuzaki, M. (1973). 7-O-Methylspinochrome B and its 6-(3-hydroxybutyl) derivative, catechol O-methyltransferase inhibitors, produced by Fungi imperfecti, *J. antibiot.*, **26**(10), 618-20.
- Chomcheon, P., Wiyakrutta, S., Sriubolmas, N., Ngamrojanavanich, N.; Kengtong, S., Mahidol, C., Ruchirawat, S. and Kittakoop, P. (2009). Aromatase inhibitory, radical scavenging and antioxidant activities of

- depsidones and diaryl ethers from the endophytic fungus *Corynespora cassiicola* L36, *Phytochemistry*, **70**, 407-413.
- Clay, K. (1988). Fungal endophytes of grasses: A defensive mutualism between plants and fungi. *Ecology*, **69**(1), 10-16.
- Clay, K. (1990). Fungal endophytes of grasses. *Annu. Rev. Ecol. Syst.*, **21**, 255-297
- Coombe, R. G., Jacobs, J. J., and Watson, T. R. (1968). Constituents of some *Curvularia* species., *Aust. J. Chem.*, **21**(3), 783-788.
- Cragg, G. M., Newman, D. J. and Snader, K. M. (1997). Natural products in drug discovery and development. *J. Nat. Prod.*, 60, 52-60.
- Cribb, A. B. and Cribb, J. W. (1955). Marine fungi from Queensland I. University of Queensland Papers., Department of Botany, **3**, 77-81.
- Debbab, A., Aly, A. H., and Proksch, P. (2011). Bioactive secondary metabolites from endophytes and associated marine derived fungi. *Fungal Divers.*, **49**(1), 1-12.
- Debbab, A., Aly, A. H., Edrada-Ebel, R., Wray, V., Mueller, W. E., Totzke, F., Zirrgiebel, U., Schaechtele, C., Kubbutat, M. H., Lin, WH., Mosaddak, M., Hakiki, A., Proksch P., and Ebel, R. (2009). Bioactive metabolites from the endophytic fungus *Stemphylium globuliferum* isolated from *Mentha pulegium*. *J. Nat. Prod.*, **72**, 626-631.
- DeBusk, L. M., Chen, Y., Nishishita, T., Chen, J., Thomas, J. W., and Lin, P.C. (2003). Tie2 receptor tyrosine kinase, a major mediator of tumor necrosis factor alpha-induced angiogenesis in rheumatoid arthritis. *Arthritis Rheum.*, **48**(9), 2461-2471.

- Dehm, S., Senger M. A., and Bonham, K. (2001). SRC transcriptional activation in a subset of human colon cancer cell lines, *FEBS Lett.*, **487** (3), 367-371.
- Demain, A. L. (2000). Microbial natural products: A past with a future. In: Biodiversity: New leads for pharmaceutical and agrochemical industries. Wrigley, S. K., Hayes, M. A., Thomas, R., Chrystal, E. J. T., and Nicholson, N. (ed.), The Royal Society of Chemistry, Cambridge, UK, p. 3-16.
- Dewick P. M. (2002), Medicinal natural products: a biosynthetic approach, p35. John Wiley & Sons, Chichester.
- Dewick, P. M. (2006). Medicinal natural products. A biosynthetic approach. John Wiley & Sons Ltd, Baffins Lane, Chichester, England.
- Dhanasekaran, S. M., Barrette, T. R., Ghosh, D., Shah, R., Varambally, S., Kurachi, K., Pienta, K. J., Rubin, M. A., Chinnaiyan, A. M. (2001). Delineation of prognostic biomarkers in prostate cancer. *Nature*, **412**, 822-826.
- Diekmann, H. (1968). Stoffwechselprodukte von Mikroorganismen. 68. Mitteilung. Die Isolierung und Darstellung von trans-5-Hydroxy-3-methylpenten-(2)-säure. *Arch. Mikrobiol.*, **62**, 322- 327.
- Edrada, R., Heubes, M., Brauers, G., Wray, V., Berg, A., Graefe, U., Wohlfarth, M., Muehlbacher, J., Schaumann, K., Sudarsono, Bringmann, G., and Proksch, P. (2002), Online analysis of xestodecalactones A-C, novel bioactive metabolites from the fungus *Penicillium cf. montanense* and their subsequent isolation from the sponge *Xestospongia exigua*, *J. Nat. Prod.*, **65**(11), 1598-1604.

- Endo, A. (1979). Monacolin K, a new hypercholesterolemic agent produced by *Monascus* species. *J. Antibiot.*, **32**, 852-854.
- Estrov, Z., Thall, P. F., Talpaz, M., Estey, E. H., Kantarjian, H. M., Andreeff, M., Harris, D., Van, Q., Walterscheid, M., and Kornblau, S. M. (1998). Caspase 2 and caspase 3 protein levels as predictors of survival in acute myelogenous leukemia. *Blood*, **92(9)**, 3090-3097.
- Eyberger, A. L., Dondapati, R., and Porter, J. R. (2006). Two endophyte fungal isolates from *Podophyllum peltatum* produce podophyllotoxin.” *J. of Nat. Prod.*, **69** (8), 1121-1124.
- Faeth, S. H. (2002). Are endophytic fungi generally plant mutualists?, *Oikos*, **98**, 25-36
- Faeth, S. H. and Fagan, W. F. (2002). Fungal endophytes: Common host plant symbionts but uncommon mutualists., *Integr. Comp. Biol.*, **42** (2), 360-368.
- Fehler, M. and Schmidt, J. M. (2003). Property distributions: differences between drugs, natural products and molecules from combinatorial chemistry. *J. Chem. Inf. Comput. Sci.*, **43**, 218-227.
- Garces, C. A., Kurenova, E. V., Golubovska, V. M., and Cance, W. G. (2006). Vascular endothelial growth factor receptor-3 and focal adhesion kinase bind and suppress apoptosis in breast cancer cells. *Cancer Res.*, **66**, 1446-1454.
- Garg, A. and Aggarwal, B. B. (2002). Nuclear transcription factor-kappa B as a target for cancer drug development. *Leukemia*, **16(6)**, 1053-1068.
- Ge, F., Wang, L. S., and Kim J. (2005). The cobweb of life revealed by genome-scale estimates of horizontal gene transfer. *PLoS. Biol.*, **3**, 316.

- Gerondakis, S., Grumont, R., Gugasyan, R., Wong, L., Isomura, I., Ho, W., and Banerjee, A. (2006). Unravelling the complexities of the NF-kappa B signalling pathway using mouse knockout and transgenic models. *Oncogene*, **25(51)**, 6781-6799.
- Gilmore, T. D. (1999). Multiple mutations contribute to the oncogenicity of the retroviral oncoprotein v-Rel. *Oncogene*, **18(49)**, 6925-6937.
- Gilmore, T. D. (2006). Introduction to NF-kappa B: players, pathways, perspectives. *Oncogene*, **25(51)**, 6680-6684.
- Gilmore, T. D., and Herscovitch, M. (2006). Inhibitors of NF-kappa B signaling: 785 and counting. *Oncogene*, **25(51)**, 6887-6899.
- Giri, D. K. and Aggarwal, B. B. 1998. Constitutive activation of NF-kappa B causes resistance to apoptosis in human cutaneous T cell lymphoma HuT-78 cells - Autocrine role of tumor necrosis factor and reactive oxygen intermediates. *J. Biol. Chem.*, **273(22)**, 14008-14014.
- Grove, J. F., MacMillan, J., Mulholland, T. P. C., and Rogers, M. A. T. (1952). Griseofulvin. Part IV. Structure. *J. Chem. Soc.*, 3977-3987.
- Hartley, S. E. and Gange, A. C. (2009) Impacts of plant symbiotic fungi on insect herbivores: mutualism in a multitrophic context. *Annu. Rev. Entomol.*, **54**, 323-342.
- Hayakawa, M., Miyashita, H., Sakamoto, I., Kitagawa, M., Tanaka, H., Yasuda, H., Karin, M., and Kikugawa, K. (2003). Evidence that reactive oxygen species do not mediate NF-kappaB activation. *Embo J.*, **22(13)**, 3356-3366.
- He, H., Yang, H. Y., Bigelis, R., Solum, E. H., Greenstein, M., and Carter, G. T. (2002). Pyrrocidines A and B, new antibiotics produced by a filamentous fungus., *Tetrahedron Lett.*, **43**, 1633-1636.

- Hofer, M. D., Fecko, A., Shen, R., Setlur, S. R., Pienta, K. G., Tomlins, S. A., Chinnaiya, A. M. and Rubin, M. A. (2004). Expression of the platelet-derived growth factor receptor in prostate cancer and treatment implications with tyrosine kinase inhibitors. *Neoplasia*, **6** (5), 503-512.
- Hosoe, T., Nozawa, K., Udagawa, S.-I., Nakajima, S., and Kawai, K.-I. (1990). An anthraquinone derivative from *Dichotomophthora lutea*. *Phytochemistry*, **29** (3), 997-999.
- Hradil, C. M., Hallock, Y. F., Clardy, J., Kenfield, D. S., and Strobel, G. (1989). Phytotoxins from *Alternaria cassiae*. *Phytochemistry*, **28** (1), 73-75.
- Hwang, S. and Ding, A. (1995). Activation of NF-kappa B in murine macrophages by taxol. *Cancer Bioch. Biophys.*, **14**(4), 265-272.
- Hyde, K. D. and Lee, S. Y. (1995). Ecology of mangrove fungi and their role in nutrient cycling. What gaps occur in our knowledge? *Hydrobiologia*, **295**, 107-118.
- Ibrahim, S. R. M. (2005). Isolation and Structure Elucidation of Bioactive Secondary Metabolites from Marine Sponges. Dissertation, Heinrich-Heine-Universität Düsseldorf.
- Isaka, M., Rugserree, N., Maithip, P., Kongsaree, P., Prabpai, S., and Thebtaranonth, Y. (2005). Hirsutellones A-E, antimycobacterial alkaloids from the insect pathogenic fungus *Hirsutella nivea* BCC 2594. *Tetrahedron*, **61**(23), 5577-5583.
- Iseki, H., Ko, T. C., Xue, X. Y., Seapan, A., and Townsend, C. M. Jr. (1998). A novel strategy for inhibiting growth of human pancreatic cancer cells by blocking cyclin dependent kinase activity. *J. Gastrointest. Surg.*, **2**(1), 36-43.

- Ivanova, L., Petersen, D., and Uhlig, S. (2010). Phomenins and fatty acids from *Alternaria infectoria*., *Toxicon*, **55** (6): 1107-14
- Izeradjene, K., Douglas, L., Delaney, A., and Houghton, J. A. (2004). Influence of casein kinase II in tumor necrosis factor-related apoptosis-inducing ligand-induced apoptosis in human rhabdomyosarcoma cells. *Clin. Cancer Res.*, **10**, 6650-6660.
- Jones, D. R., Broad, R. M., Madrid, L. V., Baldwin, A. S., Jr., and Mayo, M. W. (2000). Inhibition of NF-kappaB sensitizes non-small cell lung cancer cells to chemotherapy-induced apoptosis. *Ann. Thorac. Surg.*, **70**(3), 930-936; discussion 936-937.
- Jones, E. R. G. and Mitchell, L. L. (1996). Biodiversity of marine fungi. In: Biodiversity: International Biodiversity Seminar (eds A. Cirnerman and N. Gunde-Cirnerman). National Institute of Chemistry and Slovenia National Commission for UNESCO, Ljubljana, Slovenia: 31-42.
- Jung, H. J., Lee, H. B., Kim, C. J., Rho, J. R., Shin, J., and Kwon, H. J. (2003). Anti-Angiogenic activity of terpestacin, a bicyclo sesterterpene from *Embellisia chlamydospora*, *J. Antibiot.*, **56**, 492.
- Kalli, K. R., Falowo, O. I., Bale, L. K., Zschunke, M. A., Roche, P. C., and Conover, C. A. (2002). Functional insulin receptors on human epithelial ovarian carcinoma cells: Implications for IGF-II mitogenic signalling. *Endocrinology*, **143** (9), 3259-3267.
- Karin, M., Cao, Y. X., Greten, F. R., and Li, Z. W. (2002). NF-kappa B in cancer: From innocent bystander to major culprit. *Nature Rev. Cancer*, **2**(4), 301-310.

- Karin, M., Yamamoto, Y., and Wang, Q. M. (2004). The IKK NF-kappa B system: a treasure trove for drug development. *Nat. Rev. Drug Discov.*, **3**(1), 17-26.
- Kato, T., Duffey, D. C., Ondrey, F. G., Dong, G., Chen, Z., Cook, J. A., Mitchell, J. B., and Van Waes, C. (2000). Cisplatin and radiation sensitivity in human head and neck squamous carcinomas are independently modulated by glutathione and transcription factor NF-kappa B. *Head Neck-J. Sci. Spec.*, **22**(8), 748-759.
- Keen, N., and Taylor, S. (2004). Aurora-kinase inhibitors as anticancer agents. *Nat. Rev. Cancers*, **4**, 927-936.
- Keil, G. (1989). Das Lorsch'sche Arzneibuch. Wiss. Verl.-Ges., Stuttgart.
- Kim, H. J., Hawke, N., and Baldwin, A. S. (2006). NF-kappa B and IKK as therapeutic targets in cancer. *Cell Death and Differ.*, **13**(5), 738-747.
- Kingston, D. G. I. (1996). Natural Products as Pharmaceuticals and Sources for Lead Structures. In *The Practice of Medicinal Chemistry*; Wermuth, C. G., Ed.; Academic Press: London, 101-116.
- Knight, V., Sanglier, J. J., DiTullio, D., Braccili, S., Bonner, P., Waters, J., Hughes, D., and Zhang, L. (2003). Diversifying microbial natural products for drug discovery. *Appl. Microbiol. Biotechnol.*, **62** (5-6), 446-458.
- Knoch, T. R., Faeth, S. H., and Arnott, D. L. (1993). Endophytic fungi alter foraging and dispersal by desert seed-harvesting ants. *Oecologia*, **95** (4), 470-475.
- Kobayashi, J. and Kubota T. (2007). Bioactive macrolides and polyketides from marine dinoflagellates of the genus *Amphidinium*, *J. Nat. Prod.*, **70**, 451-460.

- Korff, T., and Augustin, H. G. (1998). Integration of endothelial cells in multicellular spheroids prevents apoptosis and induces differentiation. *J.Cell. Biol.*, **143**, 1341-1352.
- Korff, T., and Augustin, H. G. (1999). Tensional forces in fibrillar extracellular matrices control directional capillary sprouting. *J.Cell. Biol.*, **112**, 3249-3258.
- Kurobane, I. and Vinng, L. C. (1979). Biosynthesis relationships among the secalonic acid, isolation of emodin, endocrocin and secalonic acids from *Pyrenochaeta terrestris* and *Aspergillus aculeatus*, *J. Antibiot.*, **32**, 1256-1266.
- Kusakai, G., Suzuki, A., Ogura, T., Miyamoto, S., Ochiai, A., Kaminishi, M., and Esumi, H. (2004). ARK5 expression in colorectal cancer and its implications for tumor progression. *Am. J. Pathol.*, **164**, 987-995.
- Kwon, H. J., Jung, H., Shin, J. H., Kim, C. J., Rho, J., and Lee, H. (2005). Heptatrienoic acid-substituted bicyclic ketone derivative, pharmaceutical compositions, isolation, and use in inhibiting angiogenesis, *Int. Appl.*, WO 2005003076 A1 20050113.
- Lai, S., Shizuri, Y., Yamamura, S., Kawai, K., and Furukawa, H. (1991). Three new phenolic metabolites from *Penicillium* species. *Heterocycles*, **32** (2), 297-305.
- Lai, S., Shizuri, Y., Yamamura, S., Kawai, K., Terada, Y., and Furukawa, H. (1989). Novel curvularin-type metabolites of a hybrid strain ME0005 derived from *Penicillium citreovirdie* B. IF0 6200 and 4692, *Tetrahedron lett.*, **30** (17), 2241-2244.

- Larsen, T. O., Smedsgaard, J., Nielsen, K. F., Hansen, M. E., and Frisvad, J. C. (2005). Phenotypic taxonomy and metabolite profiling in microbial drug discovery. *Nat. Prod. Rep.*, **22** (6), 672-695.
- Lazarovits, G., Steele, R. W., and Stoessl, A. (1988). Dimers of altersolanol A from *Alternaria solani*., *Z. Naturforsch. Sect. C*, **43c** (11-12), 813-817.
- Lee, C. H., Jeon, Y. T., Kim, S. H., and Song, Y. S. (2007). NF-kappa B as a potential molecular target for cancer therapy. *Biofactors*, **29**(1), 19-35.
- Lee, J. W., Soung, Y. H., Kim, S. Y., Park, W. S., Nam, S. W., Kim, S. H., Lee, J. Y., Yoo, N. J., and Lee, S. H. (2005). ERBB2 kinase domain mutation in a gastric cancer metastasis. *APMIS*, **113**, 683-687.
- Levine, L., Lucci, J. A., 3rd, Pazdrak, B., Cheng, J. Z., Guo, Y. S., Townsend, C. M., Jr., and Hellmich, M. R. (2003). Bombesin stimulates nuclear factor kappa B activation and expression of proangiogenic factors in prostate cancer cells. *Cancer Res.*, **63**(13), 3495-3502.
- Li, D., Zhu, J., Firozi, P., Abbruzzesse, J. L., Evans, D. B., Cleary, K., Fries, H., and Sen, S. (2003). Overexpression of oncogenic STK15/BTAK/Aurora A kinase in human pancreatic cancer. *Clin.Cancer Res.* **9**, 991-997.
- Li, J. Y., Strobel, G. A., Sidhu, R., Hess, W. M. and Ford, E. (1996). Endophytic taxol producing fungi from bald cypress *Taxodium distichum*. *Microbiology*, **142**, 2223-2226.
- Li, M. Z., Yu, L., Liu, Q., Chu, J. Y., Zhao, S. Y. (1999). Assignment of NEK6, a NIMA-related gene, to human chromosome 9q33.3-q34.11 by radiation hybrid mapping. *Cytogenet. Cell Genet.*, **87**, 271-272.
- Liu, E., Hjelle, B., Bishop, J. M. (1988). Transforming genes in chronic myelogenous leukemia. *Proc. Nat. Acad. Sci.*, **85**, 1952-1956.

- Liu, Y., Li, Z., and Vederas, J. C. (1998). Biosynthetic incorporation of advanced precursors into dehydrocurvularin, a polyketide phytotoxin from *Alternaria cinerariae*. *Tetrahedron*, **54** (52), 15937-15958.
- Loch, T., Michalski, B., Mazurek, U., and Graniczka, M. (2001). [Vascular endothelial growth factor (VEGF) and its role in neoplastic processes]. *Postepy Hig. Med. Dosw.*, **55**(2), 257-274.
- Lugo, A. E. and Snedaker, S. C. (1974). The ecology of mangroves. *Annu. Rev. Ecol. Sys.*, **5**, 39-64.
- Lutzoni, F., Kauff, F., Cox, C. J., McLaughlin, D., Celio, G., Dentinger, B., Padamsee, M., Hibbett, D., James, T. J., Baloch, E., Grube, M., Reeb, V., Hofstetter, V., Schoch, C., Arnold, A. E., Miadlikowska, J., Spatafora, J., Johnson, D., Hambleton, S., Crockett, M., Shoemaker, R., Sung, G.-H., Lücking, R., Lumbsch, T., O'Donnell, K., Binder, M., Diederich, P., Ertz, D., Gueidan, C., Hansen, K., Harris, R. C., Hosaka, K., Lim, Y.-W., Matheny, B., Nishida, H., Pfister, D., Rogers, J., Rossman, A., Schmitt, I., Sipman, H., Stone, J., Sugiyama, J., Yahr, R., and Vilgalys, R. (2004). Assembling the fungal tree of life: Progress, classification, and evolution of subcellular traits. *American Journal of Botany*, **91** (10), 1446-1480.
- Macmillan, J. C., Hudson J. W., Bull, S., Dennis, J. W., and Swallow, C. J. (2001). Comparative expression of the mitotic regulators SAK and PLK in colorectal cancer. *Ann. Surg. Oncol.*, **8**, 729-740.
- Mann, J. (1999). *The Elusive Magic Bullet: The Search for the Perfect Drug*; Oxford University Press: Oxford, UK, 39-78
- Manser, E., Leung, T., Salihuddin, H., Zhao, Z., Lim, L. (1994). A brain serine/threonine protein kinase activated by Cdc42 and Rac1. *Nature*, **367**, 40-46.

- Menezes, D. E. L., Peng, J., Garrett, E. N., Louie, S. G., Lee, S. H., Wiesmann, M., Tang, Y., Shephard, L., Goldbeck, C., Oei, Y., Ye, H., Aukerman, S. L., and Heise, C. (2005). CHIR-258: A potent inhibitor of FLT3 kinase in experimental tumor xenograft models of human acute myelogenous leukemia. *Clin. Cancer Res.*, **11**, 5281-5291.
- Metz, A., Haddad, A., Worapong, J., Long, D., Ford, E., Hess, W. M., and Strobel, G. A. (2000). Induction of the sexual stage of *Pestalotiopsis microspora*, a taxol producing fungus. *Microbiology*, **146** (8), 2079-2089.
- Mihm, S., Ennen, J., Pessara, U., Kurth, R., and Droge, W. (1991). Inhibition of HIV-1 replication and NF-kappa B activity by cysteine and cysteine derivatives. *AIDS*, **5**(5), 497-503.
- Morris, S. W., Kirstein, M. N., Valentine, M. B., Dittmer, K. G., Shapiro, D. N., Saltman, D. L., Look, A. T. (1994). Fusion of a kinase gene, ALK, to a nucleolar protein gene, NPM, in non-Hodgkin's lymphoma. *Science*, **263**, 1281-1284.
- Mukhopadhyay, A., Banerjee, S., Stafford, L. J., Xia, C. Z., Liu, M. Y., and Aggarwal, B. B. (2002). Curcumin-induced suppression of cell proliferation correlates with down-regulation of cyclin D1 expression and CDK4-mediated retinoblastoma protein phosphorylation. *Oncogene*, **21**(57), 8852-8861.
- Müller, H., Kassack, M. U. and Wiese, M. (2004). Comparison of the usefulness of the MTT, ATP, and calcein assays to predict the potency of cytotoxic agents in various human cancer cell lines. *J. Biomol. Screen*, **9**, 506-515
- National Cancer Institute. (22 November 2005). Mutations in glioblastoma in multiforme predict responded to target therapies. NCI Cancer Bulletin (online), **2** (45).

- Newman, D. J., Cragg, G. M., and Snader, K. M. (2000). The influence of natural products upon drug discovery. *Nat. Prod. Rep.*, **17**, 215-234.
- Nielsen, K. F., Larsen T. O., and Frisvad, J. C. (2004). Lightweight expanded clay aggregates (LECA), a new up-scaleable matrix for production of microfungal metabolites. *J. Antibiot.*, **57** (1), 29-36.
- Novak, U., Cocks, B. G., and Hamilton, J. A. (1991). A labile repressor acts through the NF κ B-like binding sites of the human urokinase gene. *Nucleic Acids Res.*, **19**(12), 3389-3393.
- Odum, N. E. and Heald, E. J. (1972). Trophic analyses of an estuarine mangrove community. *B. Mar. Sci.*, **22**, 671-738.
- Ohnishi, K., Suemitsu, R., Kubota, M., Matano, H., and Yamada, Y. (1991). Biosynthesis of alterporriol D and E by *Alternaria porri*. *Phytochemistry*, **30** (8), 2593-2595.
- Ohtani, I., Kusumi, T., Kashman, Y., and Kakisawa, H. (1991). High-field FT NMR application of Mosher's method. The absolute configurations of marine terpenoids. *J. Am. Chem. Soc.*, **113** (11), 4092-4096.
- Oikawa, H. (2003). Biosynthesis of structurally unique fungal metabolite GKK1032A₂: Indication of novel carbocyclic formation mechanism in polyketide biosynthesis, *J. Org. Chem.*, **68**, 3553-3557.
- Okamura, N., Haraguchi, H., Hashimoto, K., and Yagi, A. (1993). Altersolanol-related antimicrobial compounds from a strain of *Alternaria solani*. *Phytochemistry*, **34** (4), 1005-1009.
- Okamura, N., Mimura, K., Haraguchi, H., Shingu, K., Miyahara, K., and Yagi, A. (1996). Altersolanol-related compounds from the culture liquid of *Alternaria solani*. *Phytochemistry*, **42** (1), 77-80.

- Okuno, T., Natsume, I., Sawai, K., Sawamura, K., Furusaki, A., and Matsumoto, T. (1983). Structure of antifungal and phytotoxic pigments produced by *Alternaria* sps. *Tetrahedron Lett.*, **24** (50), 5653-5656.
- Ong, J. E. (1995). The ecology of mangrove conservation and management. *Hydrobiologia*, **295**, 343-351.
- Ouyang, B., Knauf, J. A., Smith, E. P., Zhang, L., Ramsey, T., Yusuff, N., Batt, D., and Fagin, J. A. (2006). Inhibitors of Raf kinase activity block growth of thyroid cancer cells with RET/PTC or BRAF mutations in vitro and in vivo. *Clin. Cancer Res.*, **12**, 1785-1793.
- Pahl, H. L. 1999. Activators and target genes of Rel/NF-kappa B transcription factors. *Oncogene*, **18(49)**, 6853-6866.
- Paranagama, P. A., Wijeratne, E. M. K., Burns, A. M., Marron, M. T., Gunatilaka, M. K., Arnold, A. E., and Gunatilaka, A. A. L. (2007), Heptaketides from *Corynespora* sp. inhabiting the cavern beard lichen, *Usnea cavernosa*: first report of metabolites of an endolichemic fungus, *J. Nat. Prod.*, **70**, 1700-1705.
- Pastre, R., Marinho, A. M. R., Rodrigues, E., Souza, A. Q. L., and Pereira, J. O. (2007). Diversity of polyketides produced by *Penicillium* species isolated from *Melia azedarach* and *Murraya paniculata*. *Quim. Nova*, **30(8)**, 1867-1871.
- Patwardhan, B., Vaidya, A. D. B., and Chorgade, M. (2004). Ayurveda and natural products drug discovery. *Curr. Sci.*, **86** (6), 789-799.
- Pedras, M. S. C. and Chumala, P. B. (2005). Phomapyrones from blackleg causing phytopathogenic fungi: isolation, structure determination, biosynthesis and biological activity, *Phytochemistry*, **66**, 81-87.

- Pikarsky, E. and Ben-Neriah, Y. (2006). NF-kappa B inhibition: A double-edged sword in cancer? *Eur. J.Cancer*, **42(6)**, 779-784.
- Qiao, H., Hung, W., Tremblay, E., Wojcik, J., Gui, J., Ho, J., Klassen, J., Campling, B., and Elliot, B. (2002). Constitutive activation of met kinase in non-small-cell lung carcinomas correlates with anchorage-independent cell survival. *J. Cell. Biochem.*, **86** (4), 665-677.
- Rajagopal, K., Suryanarayanan, T. S. (2000). Isolation of endophytic fungi from leaves of neem (*Azadirachta indica* A. Juss). *Curr. Sci.*, **78**, 1375-1377.
- Rawlings, B. J. (1999). Biosynthesis of polyketides (other than *actinomycete* macrolides), *Nat. Prod. Rep.*, **16**, 425-484.
- Rayet, B. and Gelinas, C. (1999). Aberrant rel/nfkb genes and activity in human cancer. *Oncogene*, **18(49)**, 6938-6947.
- Redman, R. S., Sheehan, K. B., Stout, T.G., Rodriguez, R. J., Henson, J. M. (2002). Thermotolerance generated by plant/fungal symbiosis. *Science*, **298**, 1581.
- Rim, I. S. and Jee, C. H. (2006). Acaricidal effects of herb essential oils against *Dermatophagoides farinae* and *D. pteronyssinus* (Acari: Pyroglyphidae) and qualitative analysis of a herb *Mentha pulegium* (pennyroyal). *Kororean J. Parasitol.*, **44**, 133-138.
- Robeson, D. J. and Strobel, G. A. (1981). $\alpha\beta$ -Dehydrocurvularin and curvularin from *Alternaria cinerariae*., *Z. Naturforsch.*, **36c**, 1081-1083.
- Rodriguez, R. J., Henson, J., Van Volkenburgh, E., Hoy, M., Wright, L., Beckwith, F., Kim, Y., and Redman, R. S. (2008). Stress tolerance in plants via habitat-adapted symbiosis. *ISME Nat*, **2**, 404-416.

- Rudgers, J. A., Koslow, J. M., and Clay, K. (2004). Endophytic fungi alter relationships between diversity and ecosystem properties. *Ecology Lett.*, **7**(1), 42-51.
- Ryan, K. M., Ernst, M. K., Rice, N. R., Vousden, K. H. (2000). Role of NF-kappa-B in p53-mediated programmed cell death. *Nature*, **404**, 892-897.
- Saikkonen, K., Faeth, S. H., Helander, M., and Sullivan, T. J. (1998). Fungal endophytes: A continuum of interactions with host plants. *Annu. Rev. Ecol. Syst.*, **29**, 319-343.
- Scheidereit, C. (2006). I kappa B kinase complexes: gateways to NF-kappa B activation and transcription. *Oncogene*, **25**(51), 6685-6705.
- Schmitz, K. J., Grabellus, F., Callies, R., Otterbach, F., Wohlschlaeger, J., Levkau, B., Kimmig, R., Schmid, K. W., and Baba, H. A. (2005). High expression of focal adhesion kinase (p125FAK) in node-negative breast cancer is related to overexpression of HER2/neu and activated Akt kinase but does not predict outcome. *Breast Cancer Res.*, **7**(2), R194-R203.
- Schultz, S. J., Fry, A. M., Sutterlin, C., Ried, T., Nigg, E. A. (1994). Cell cycle-dependent expression of Nek2, a novel human protein kinase related to the NIMA mitotic regulator of *Aspergillus nidulans*. *Cell Growth Diff.*, **5**, 625-635.
- Schulz, B., and Boyle, C. (2005). The endophytic continuum. *Mycol. Res.*, **109** (6), 661-686.
- Sethi, G., Sung, B., and Aggarwal, B. B. (2008). Nuclear factor-kappaB activation: from bench to bedside. *Exp. Biol. Med.*, **233**(1), 21-31.
- Shao, R., Karunakaran, D., Zhou, B. P., Li, K., Lo, S. S., Deng, J., Chiao, P., and Hung, M. C. (1997). Inhibition of nuclear factor-kappaB activity is

- involved in E1A-mediated sensitization of radiation-induced apoptosis. *J. Biol. Chem.*, **272(52)**, 32739-32742.
- Shi, D., Li, L., Zheng, M., Li, G., Zhang, H., and Wang, Q. (2009). Preliminary study on the isolation and purification of active secondary metabolites in the fermentation broth of *Embellisia oxytropis*, *Anhui Nongye Kexue*, **37(33)**, 16213-16215.
- Shiono, Y., Kosukegawa, A., Koseki, T., Murayama, T., Kwon, E., Uesugi, S., & Kimura, K. (2012). A dimeric pyrrocidine from *Neonectria ramulariae* is an inhibitor of prolyl oligopeptidase. *Phytochemistry Lett.*, **5(1)**, 91-95.
- Smedsgaard, J., and Frisvad, J. C. (1996). Using direct electrospray mass spectrometry in taxonomy and secondary metabolite profiling of crude fungal extracts. *J. Microbiol. Meth.*, **25** (1), 5-17.
- Sourvinos, G., Tsatsanis, C., and Spandidos, D. A. (1999). Overexpression of the Tpl-2/Cot oncogene in human breast cancer. *Oncogene*, **18**, 4968-4973.
- Staal, F. J., Roederer, M., and Herzenberg, L. A. (1990). Intracellular thiols regulate activation of nuclear factor kappa B and transcription of human immunodeficiency virus. *Proc. Natl. Acad. Sci. U S A*, **87(24)**, 9943-9947.
- Staal, S. P. (1987). Molecular cloning of the akt oncogene and its human homologues AKT1 and AKT2: Amplification of AKT1 in a primary human gastric adenocarcinoma, *Proc. Natl. Acad. Sci. USA*, **84** (14), 5034-5037.
- Stahl-Biskup, E. and Schulz, *Mentha pulegium* L. Pulegii herba. In Hagers Handbuch der Drogen und Arzneistoffe. (2006). Blaschek, W., Ebel,

- S., Hackenthal, E., Holzgrabe, U., Keller, K., and Reichling, J., Eds. ; Hager ROM; Springer Electronic Media.
- Stierle, A., Strobel, G. A., and Stierle, D. (1993). Taxol and taxane production by *Taxomyces andreanae*, an endophytic fungus of Pacific yew. *Science*, **260** (5105), 214-216.
- Stoessl, A. (1969). Relative stereochemistry of altersolanol A. *Can. J. Chem.*, **47** (5), 777-784.
- Stoessl, A., Unwin, C. H., and Stothers, J. B. (1983). On the biosynthesis of some polyketide metabolites in *Alternaria solani*: ^{13}C and ^1H NMR studies. *Can. J. Chem.*, **61** (2), 372-377.
- Strobel, G. A. (2002). Microbial gifts from rain forests. *Can. J. Plant Pathol.*, **24** (1), 14-20.
- Strobel, G. and Daisy, B. (2003). Bioprospecting for microbial endophytes and their natural products. *Microbiol. Mol. Biol. Rev.*, **67**(4), 491-502.
- Strobel, G., Yang, X. S., Sears, J., Kramer, R., Sidhu, R. S., and Hess, W. M. 1996. Taxol from *Pestalotiopsis microspora*, an endophytic fungus of *Taxus wallachiana*. *Microbiology-Uk*, **142**, 435-440.
- Su, B.-N., Park, E. J., Mbwambo, Z. H., Santarsiero, B. D., Mesecar, A. D., Fong, H. H. S., Pezzuto, J. M., and Kinghorn, A. D. (2002). New chemical constituents of *Euphorbia quinquecostata* and absolute configuration assignment by a convenient Mosher ester procedure carried out in NMR tubes. *J. Nat. Prod.*, **65** (9), 1278-1282.
- Suemitsu, R., Ohnishi, K., Yanagawase, S., Yamamoto, K., and Yamada, Y. (1989). Biosynthesis of macrosporin by *Alternaria porri*. *Phytochemistry*, **28** (6), 1621-1622.

- Suemitsu, R., Sano, T., Yamamoto, M., Arimoto, Y., Morimatsu, F., and Nabeshima, T. (1984). Structural elucidation of alterporriol B, a novel metabolic pigment produced by *Alternaria porri* (Ellis). *Ciferri. Agric. Biol. Chem.*, **48** (10), 2611-2613.
- Tan, R. X., and Zou (2001). Endophytes: a rich source of functional metabolites., *Nat. Prod. Rep.* **18**, 448-459.
- Traber, R., Hofmann, H., Kuhn, M., and von Wartburg, A. (1982). Isolierung und Strukturermittlung der neuen Cyclosporine E, F, G, H und I. *Helv. Chim. Acta*, **65**, 1655-1677.
- Traber, R., Hofmann, H., Loosli, H.R., Ponelle, M., and von Wartburg, A. (1987). Neue cyclosporine aus *Tolypocladium inflatum*. Die Cyclosporine K – Z. *Helv. Chim. Acta*, **70**, 13-36.
- Unterseher, M., and Schnittler, M. (2009). Dilution-to-extinction cultivation of leaf-inhabiting endophytic fungi in beech (*Fagus sylvatica* L.)-different cultivation techniques influence fungal biodiversity. *Assessment. Mycol. Res.*, **113**, 645-654.
- van de Stolpe, A., Caldenhoven, E., Stade, B. G., Koenderman, L., Raaijmakers, J. A., Johnson, J. P., and van der Saag, P. T. 1994. 12-O-tetradecanoylphorbol-13-acetate- and tumor necrosis factor alpha-mediated induction of intercellular adhesion molecule-1 is inhibited by dexamethasone. Functional analysis of the human intercellular adhesion molecular-1 promoter. *J. Biol. Chem.*, **269**(8), 6185-6192.
- Verdine, G. L. (1996). The Combinatorial Chemistry of Nature. *Nature*, **384**, 11-13.
- Wainwright, M. (1990). Miracle Cure: The Story of Penicillin and the Golden Age of Antibiotics; Blackwell: Oxford, UK.

- Wang, C. Y., Cusack, J. C., Jr., Liu, R., and Baldwin, A. S., Jr. (1999). Control of inducible chemoresistance: enhanced anti-tumor therapy through increased apoptosis by inhibition of NF-kappaB. *Nat. Med.*, **5**(4), 412-417.
- Watanabe, A., Fujii, I., Sankawa, U., Mayoorga, M. E., Timberlake, W. E., and Ebizuka, Y. (1999). Re-identification of *Aspergillus nidulans* wA gene to code for a polyketide synthase of naphthopyrone. *Tetrahedron Lett.*, **40** (1), 91-94.
- Weichert, W., Schmidt, M., Gekeler, V., Denkert, C., Stephan, C., Jung, K., Loening, S., Dietel, M., and Kristiansen, G. (2004). Polo-like kinase 1 is overexpressed in prostate cancer and linked to higher tumor grades. *Prostate*, **60** (3), 240-245.
- Wheeler, M. M., and Wheeler, D. M. S. (1975). Anthraquinone pigments from the phytopathogen *Phomopsis juniperovora* Hahn. *Phytochemistry*, **14** (1), 288-289.
- White, J. F., Morgan-Jones, G., and Morrow, A. C. (1993). Taxonomy, life cycle, reproduction and detection of *Acremonium endophytes*. *Agric. Ecosyst. Environ.*, **44** (1-4), 13-37.
- Wilson, D. (1995). Endophyte—the evolution of a term, and clarification of its use and definition. *Oikos*, **73**, 274-276
- Woese, C. R., Balch, W. E., Magrum, L. J., Fox, G. E., and Wolfe, R. S. (1977). An ancient divergence among the bacteria. *J. Mol. Evol.*, **9**, 305-311.
- Wolfender, J. L., Queiroz, E. F., and Hostettmann, K. (2005). Phytochemistry in the microgram domain—a LC-NMR perspective. *Magn. Reson. Chem.*, **43** (9), 697-709.

- Wolock-Madej, C. and Clay, K. (1991). Avian seed preference and weight loss experiment: The role of fungal-infected fescue seeds. *Oecologia*, **88**(2), 296-302.
- Xia, G., Kumar, S. R., Masood, R., Zu, S., Reddy, R., Krasnapetrov, V., Quinn, D. I., Henshal, S. M., Sutherland, R. L., Pinski, J. K., Daneshmand, S., Buscarini, M., Stein, J. P., Zong, C., Broek, D., Roy-Burman, P., and Gill, P. S. (2005). EphB4 expression and biological significance in prostate. *Cancer Res.*, **65** (11), 4623-4632.
- Yagi, A., Okamura, N., Haraguchi, H., Abo, T., and Hashimoto, K. (1993). Antimicrobial tetrahydroanthraquinones from a strain of *Alternaria solani*. *Phytochemistry*, **33** (1), 87- 91.
- Yamagishi, N., Miyakoshi, J., and Takebe, H. (1997). Enhanced radiosensitivity by inhibition of nuclear factor kappa B activation in human malignant glioma cells. *Int. J. Radiat. Biol.*, **72**(2), 157-162.
- Yamaoka, S., Inoue, H., Sakurai, M., Sugiyama, T., Hazama, M., Yamada, T., and Hatanaka, M. (1996). Constitutive activation of NF-kappa B is essential for transformation of rat fibroblasts by the human T-cell leukemia virus type I Tax protein. *Embo J.*, **15**(4), 873-887.
- Yu, Q., Sicinska, E., Geng, Y., Ahnstrom, M., Zagozdou, A., Kong, Y., Gardner, H., Kiyokawa, H., Harris, L. N., Stal, O., and Sicinski, P. (2006). Requirement for CDK4 kinase function in breast cancer. *Cancer cell*, **9** (1), 23-32.
- Zhang, X. and Yee, D. (2000). Tyrosine kinase signalling in breast cancer: Insulin-like growth factors and their receptors in breast cancer. *Breast Cancer Res.*, **2** (3), 170-175.

7. List of abbreviation

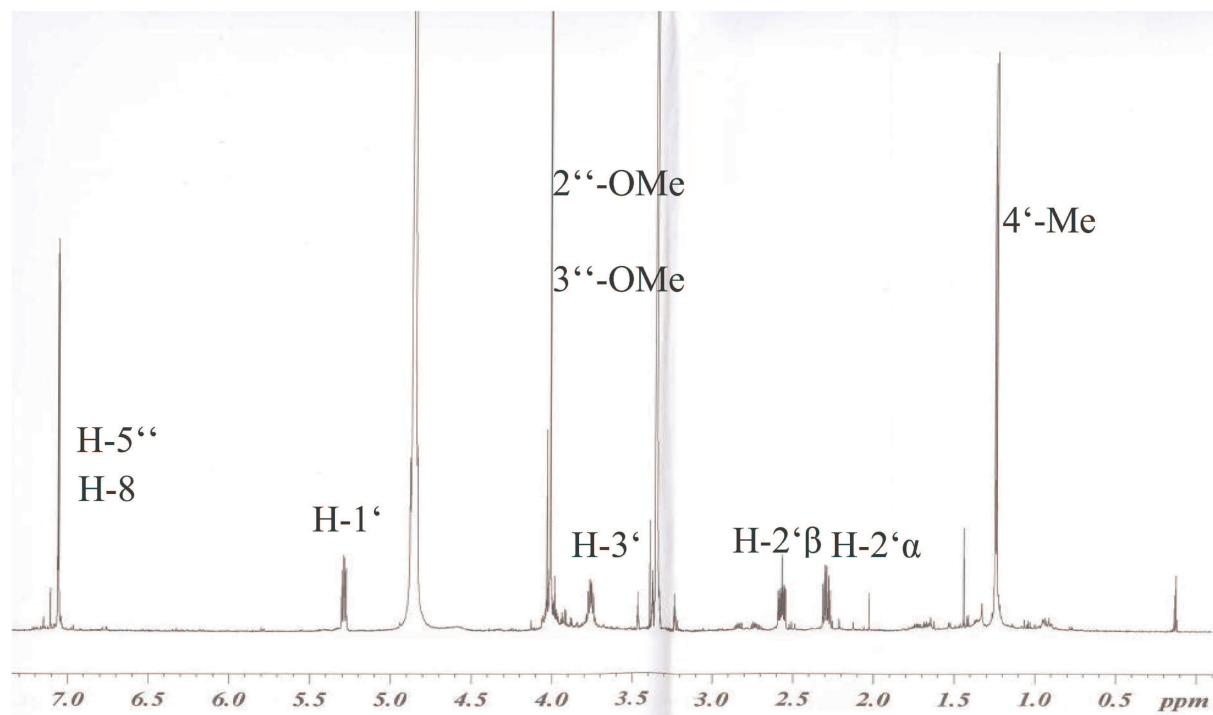
$[\alpha]^D$	specific rotation at the sodium D-line
br	broad signal
$CDCl_3$	deuterated chloroform
$CHCl_3$	chloroform
CI	chemical ionization
COSY	correlation spectroscopy
d	doublet
DCM	dichloromethane
dd	doublet of doublet
DEPT	distortionless enhancement by polarization transfer
DMSO	dimethyl sulfoxide
DNA	Deoxyribonucleic acid
ED	effective dose
EI	electron impact ionization
ESI	electrospray ionization
<i>et al.</i>	<i>et altera</i> (and others)
EtOAc	ethyl acetate
eV	electronvolt
FAB	fast atom bombardment
g	gram
HMBC	heteronuclear multiple bond connectivity
HMQC	heteronuclear multiple quantum
H ₂ O	coherence water
HPLC	high performance liquid chromatography
H ₃ PO ₄	phosphoric acid
hr	hour
HR-MS	high resolution mass spectrometry

Hz	Herz
IZ	inhibition zone
L	liter
LC	liquid chromatography
LC/MS	liquid chromatography-mass spectrometry
m	multiplet
M	molar
MeOD	deuterated methanol
MeOH	methanol
mg	milligram
MHz	mega Herz
min	minute
mL	milliliter
mm	millimeter
MS	mass spectrometry
MTT	microculture tetrazolium assay
m/z	mass per charge
μg	microgram
μL	microliter
μM	micromol
ng	nanogram
NMR	nuclear magnetic resonance
NOE	nuclear Overhauser effect
NOESY	nuclear Overhauser and exchange spectroscopy
PCR	polymerase chain reaction
ppm	parts per million
q	quartet
ROESY	rotating frame Overhauser enhancement spectroscopy

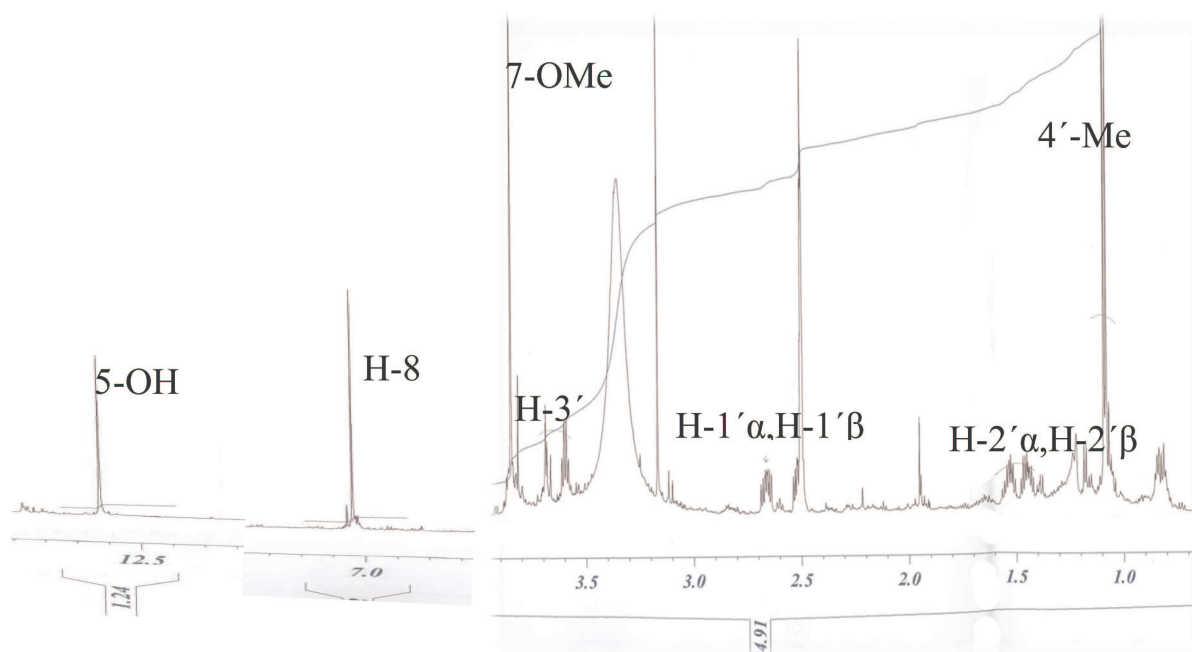
| *Abbreviations*

RP 18	reversed phase C-18
s	singlet
t	triplet
TFA	trifluoroacetic acid
THF	tetrahydrofuran
TLC	thin layer chromatography
UV	ultra-violet
VLC	vacuum liquid chromatography

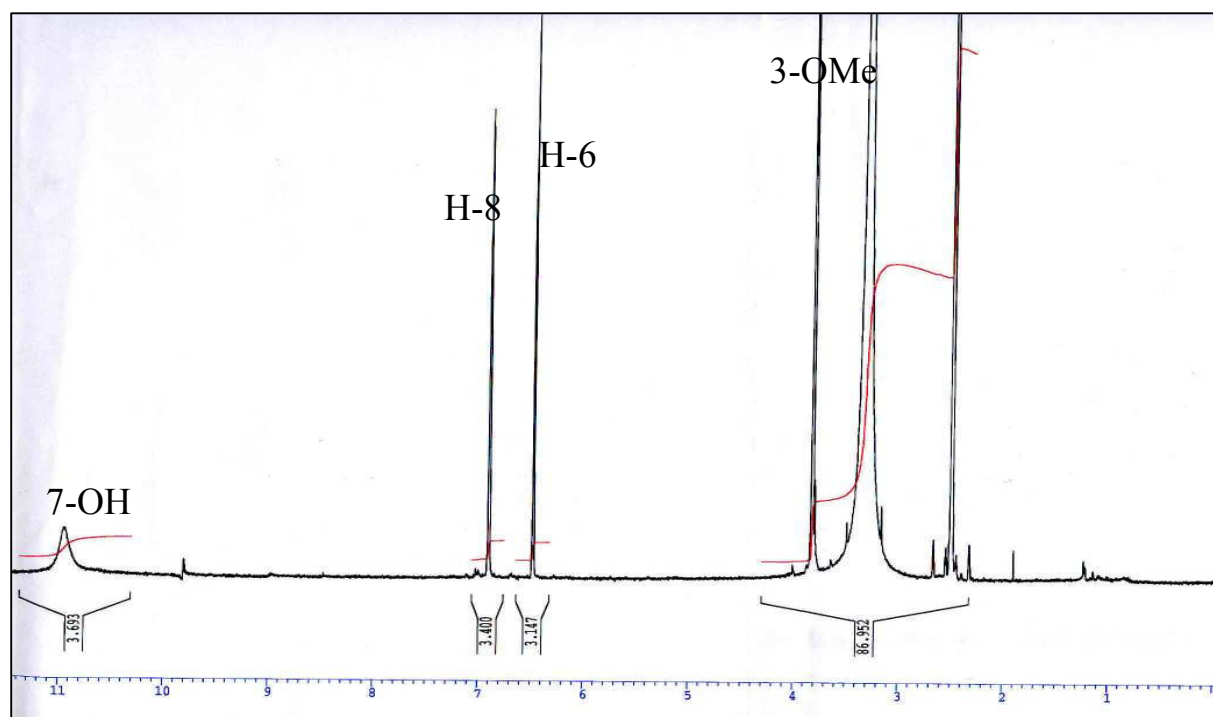
Attachment 1: The ^1H NMR spectrum of corynecassiidiol (1).



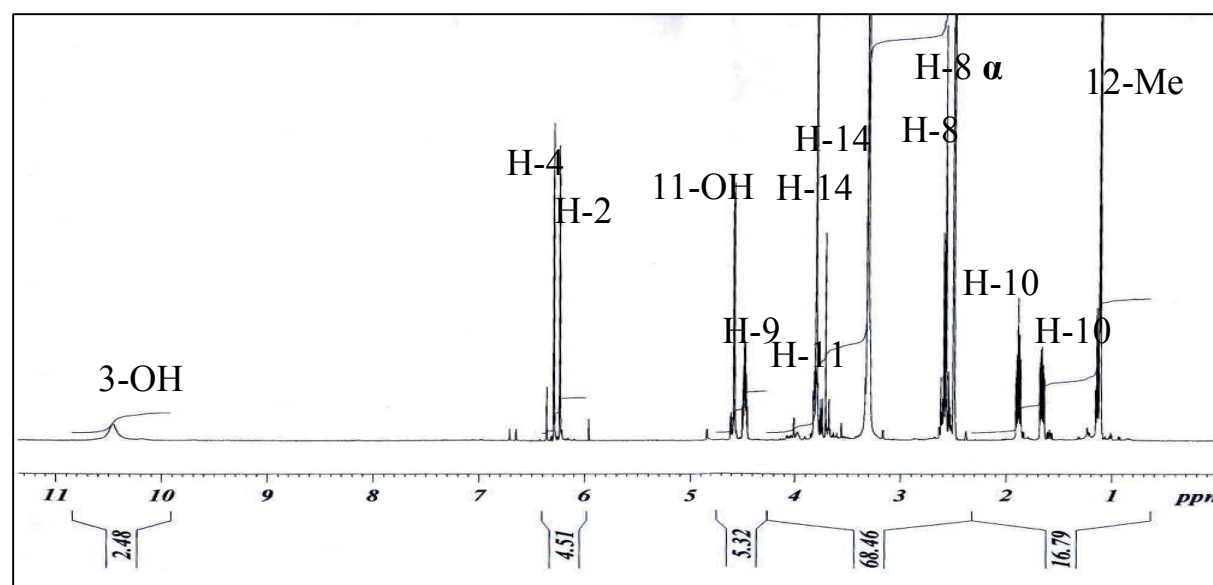
Attachment 2: The ^1H NMR spectrum of 6-(3'-hydroxy-*n*-butyl)-7-*O*-methyl spinochrome B (2).



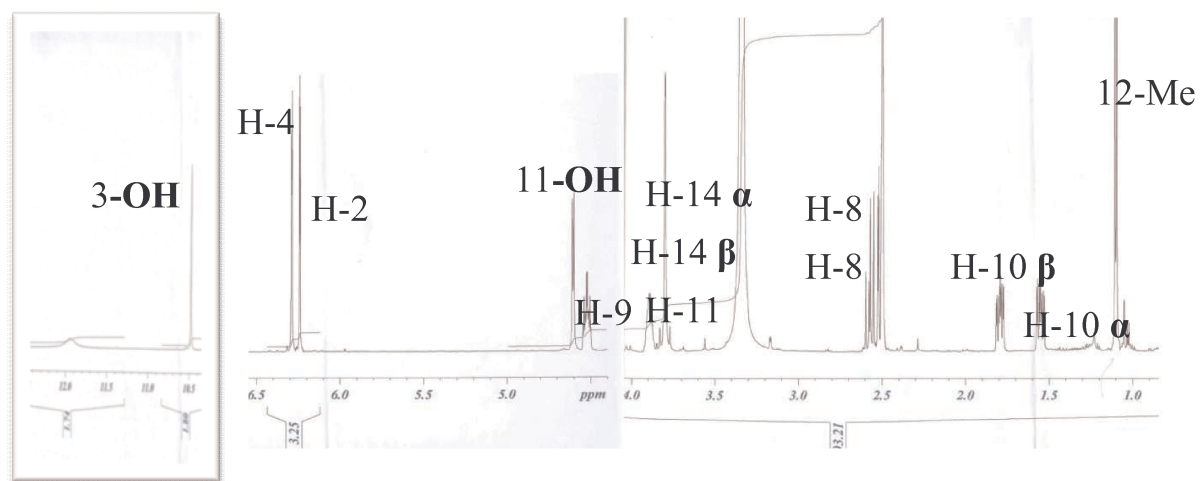
Attachment 3: The ^1H NMR spectrum of 7-O-methyl spinochrome B (3).



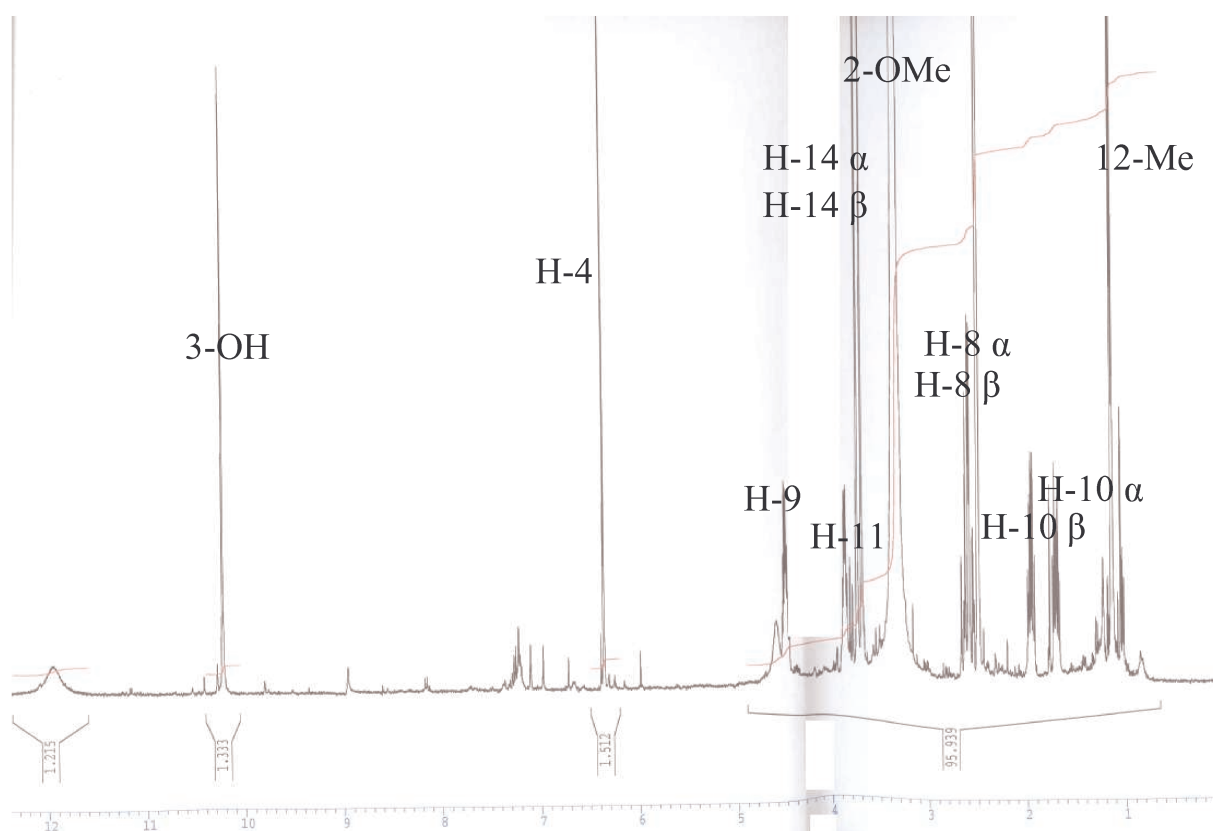
Attachment 4: The ^1H NMR spectrum of coryneoctalactone A (4).



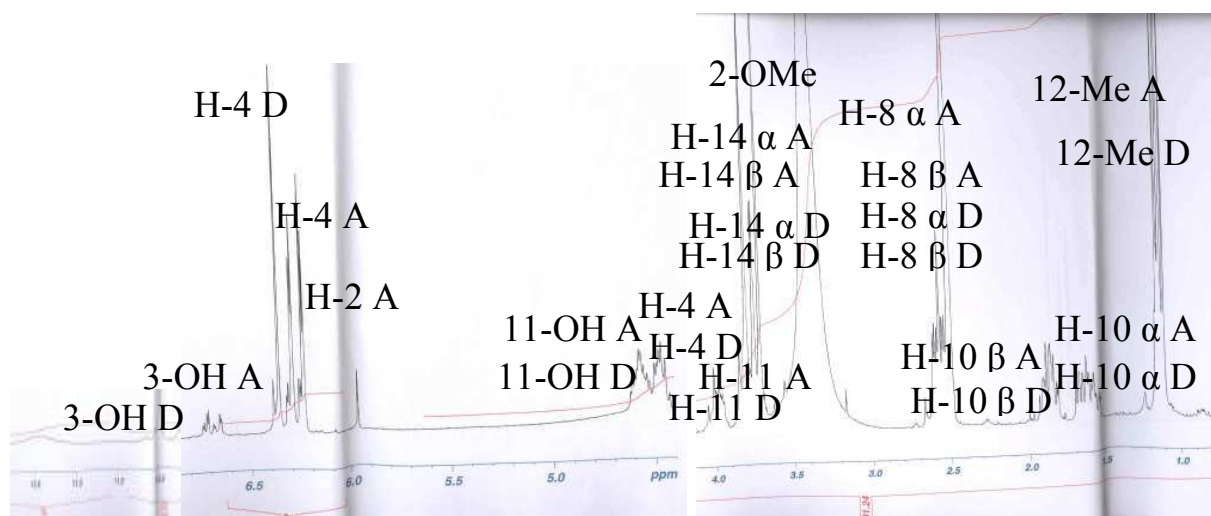
Attachment 5: The ^1H NMR spectrum of coryneoctalactone B (**5**).



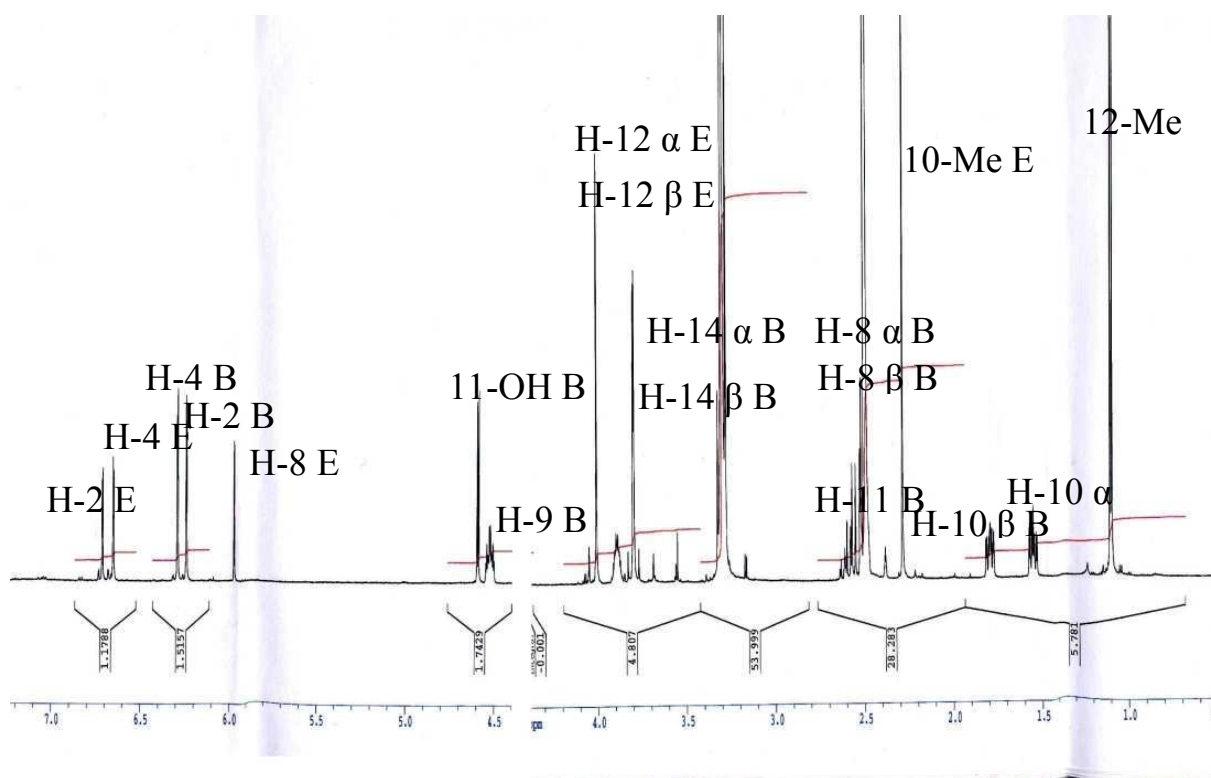
Attachment 6: The ^1H NMR spectrum of coryneoctalactone C (**6**).



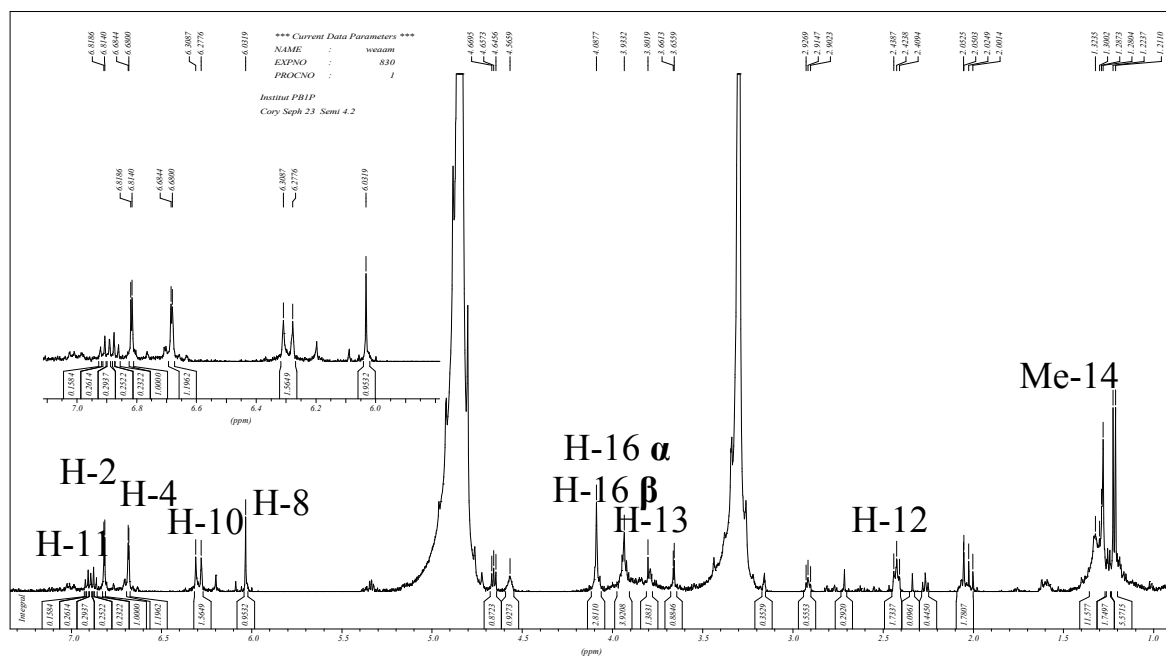
Attachment 7: The ^1H NMR spectrum of coryneoctalactone D/A (7/1).



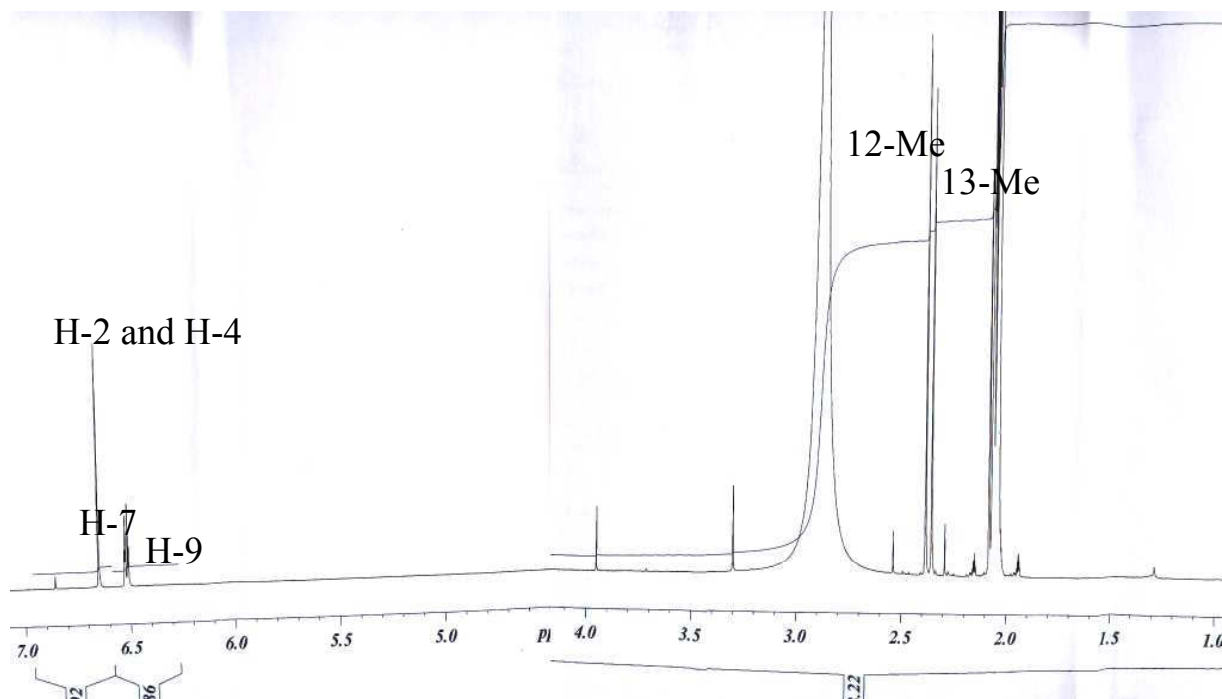
Attachment 8: The ^1H NMR spectrum of coryneoctalactone E/B (8/2).



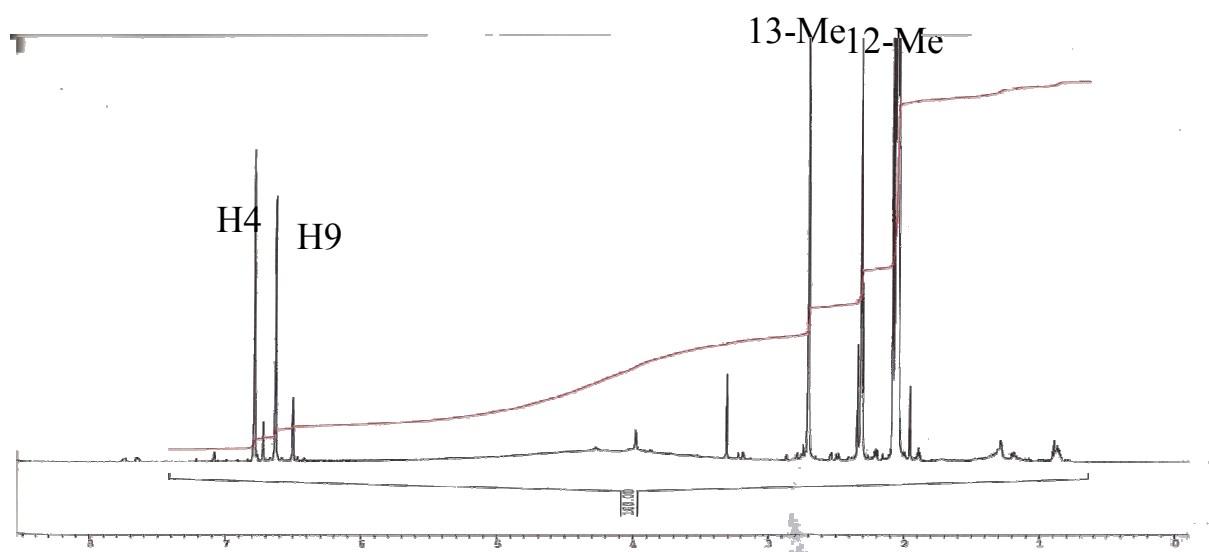
Attachment 9: The ^1H NMR spectrum of coryneoctalactone F (9).



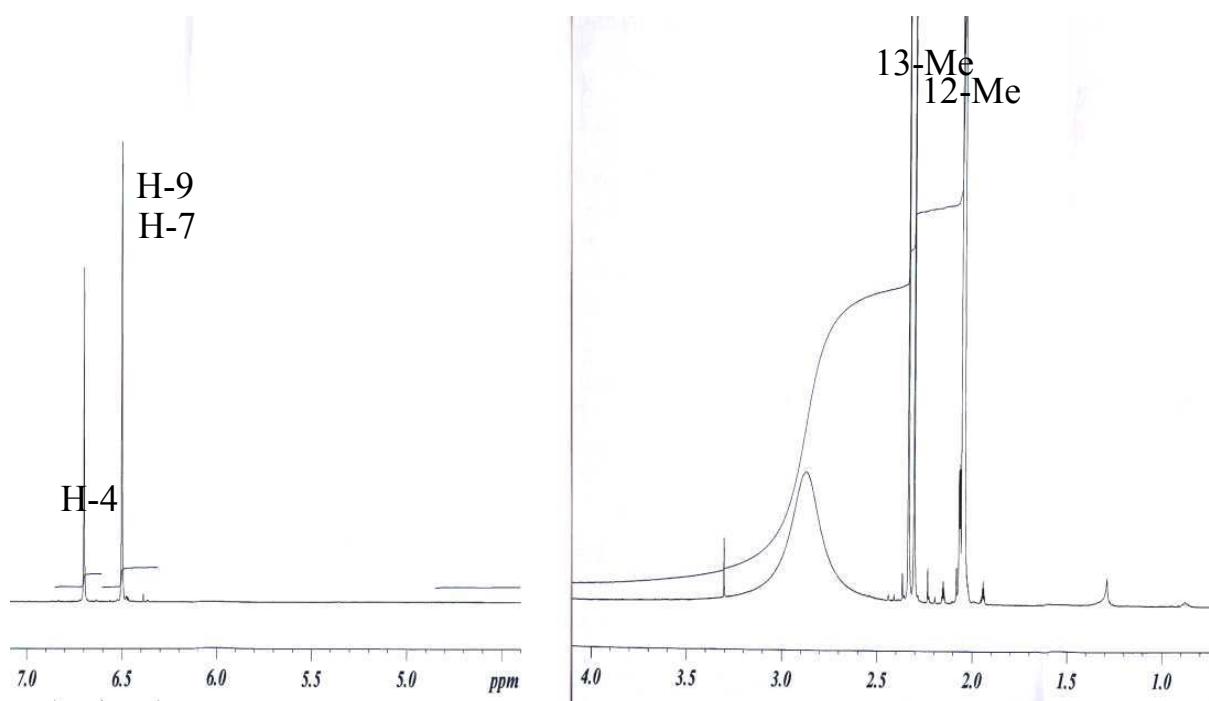
Attachment 10: The ^1H NMR spectrum of corynesidone A (10).



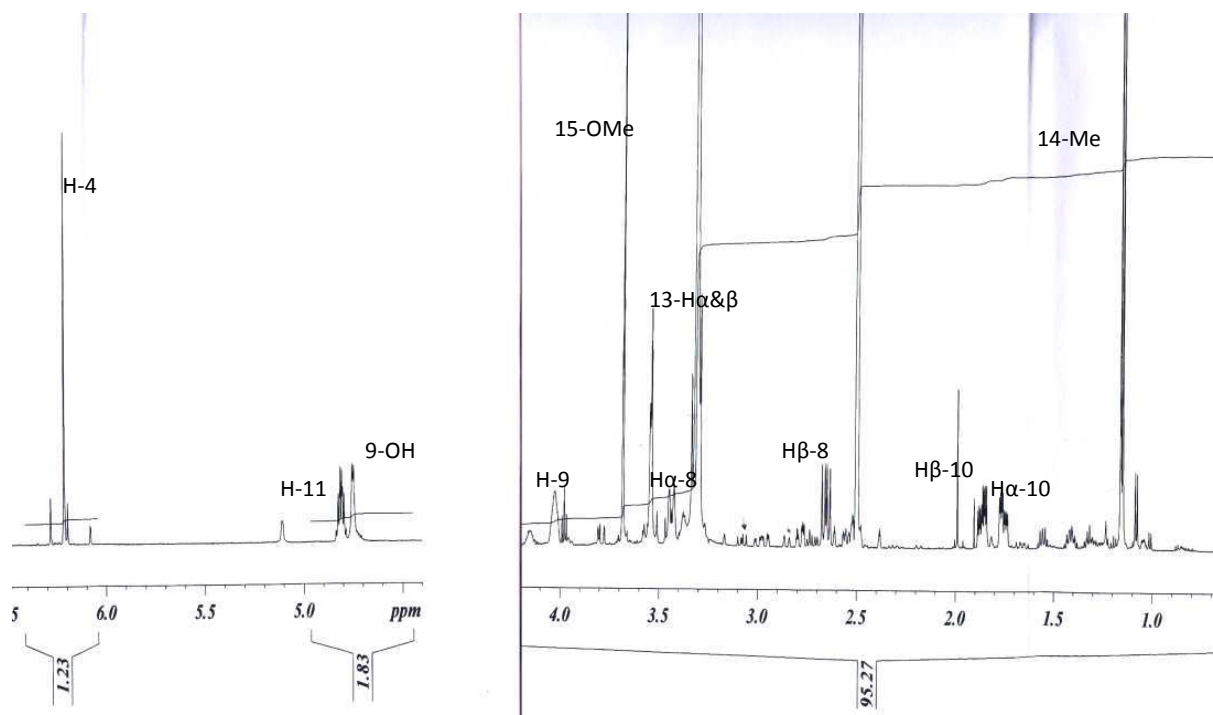
Attachment 11: The ^1H NMR spectrum of corynesidone B (**11**).



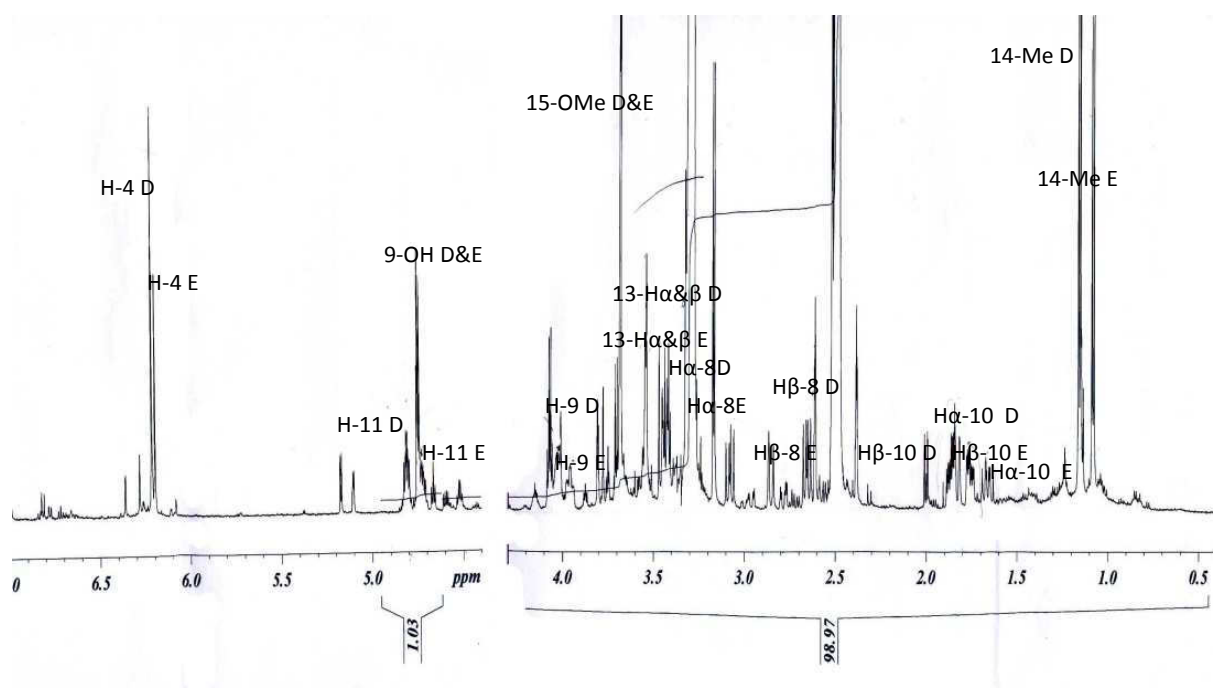
Attachment 12: The ^1H NMR spectrum of corynesidone D (**12**).



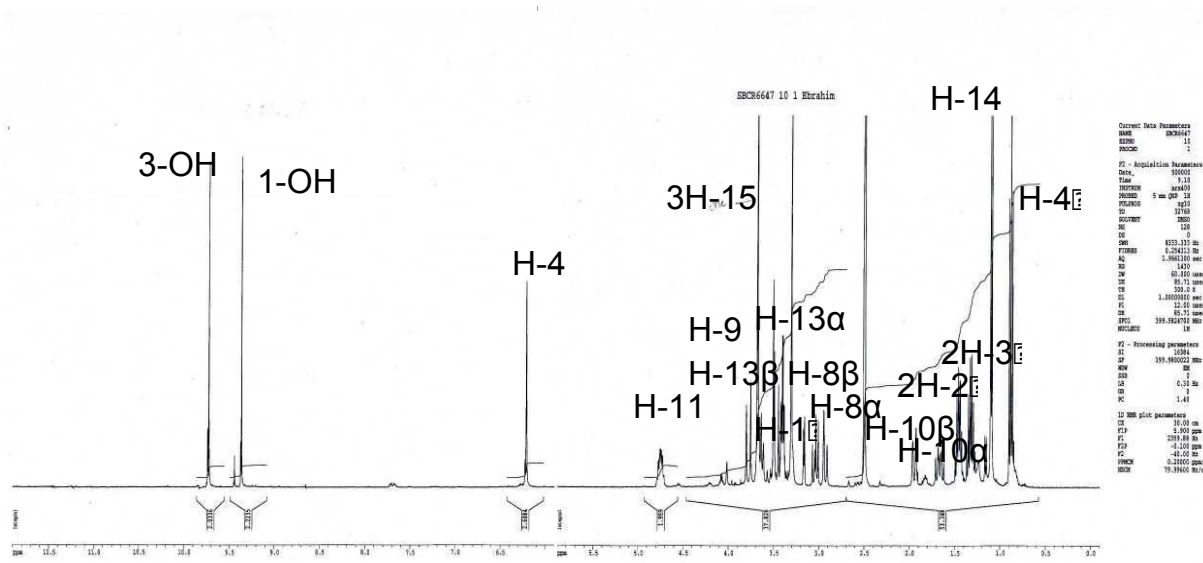
Attachment 13: The ^1H NMR spectrum of xestodecalactone D (**13**).



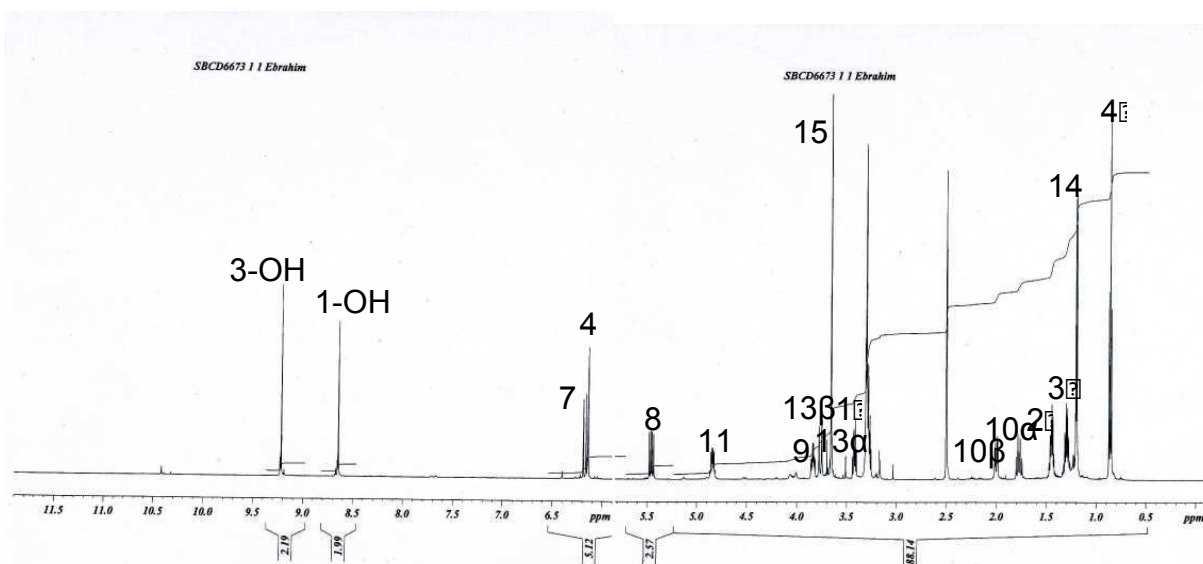
Attachment 14: The ^1H NMR spectrum of xestodecalactone D/E (**13/14**).



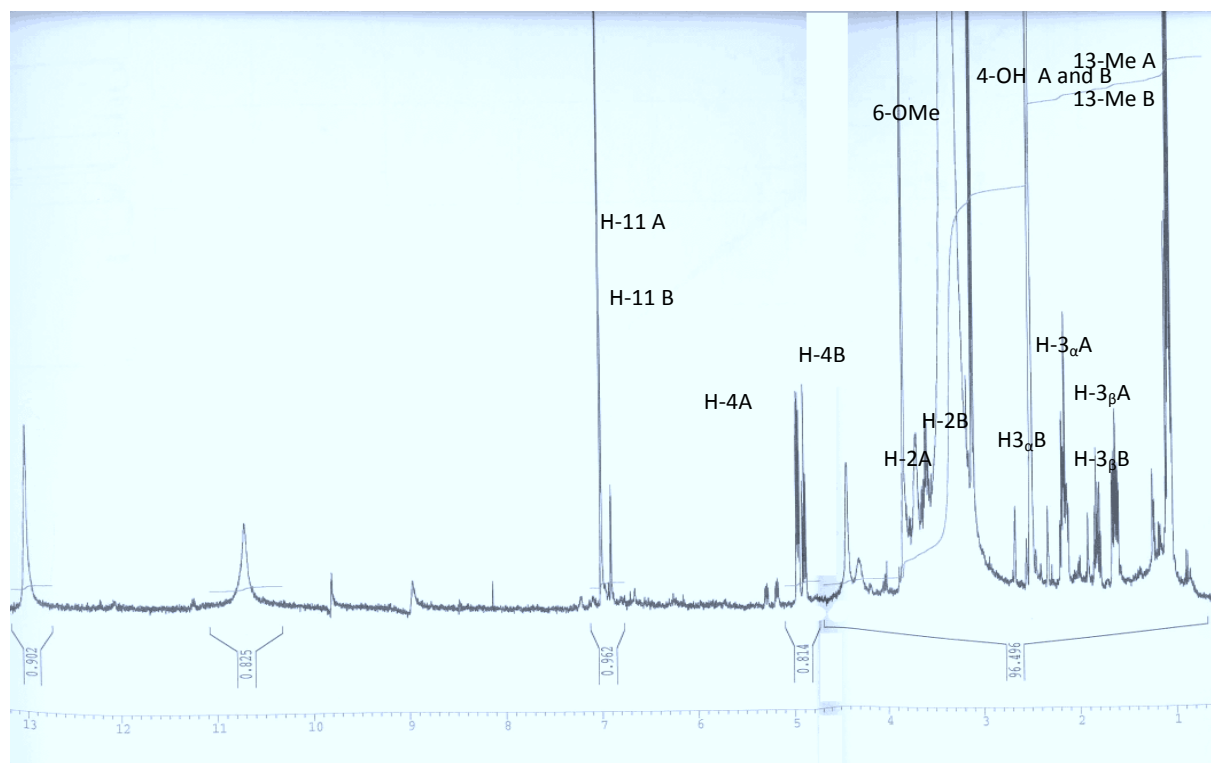
Attachment 15: The ^1H NMR spectrum of xestodecalactone F (**15**).



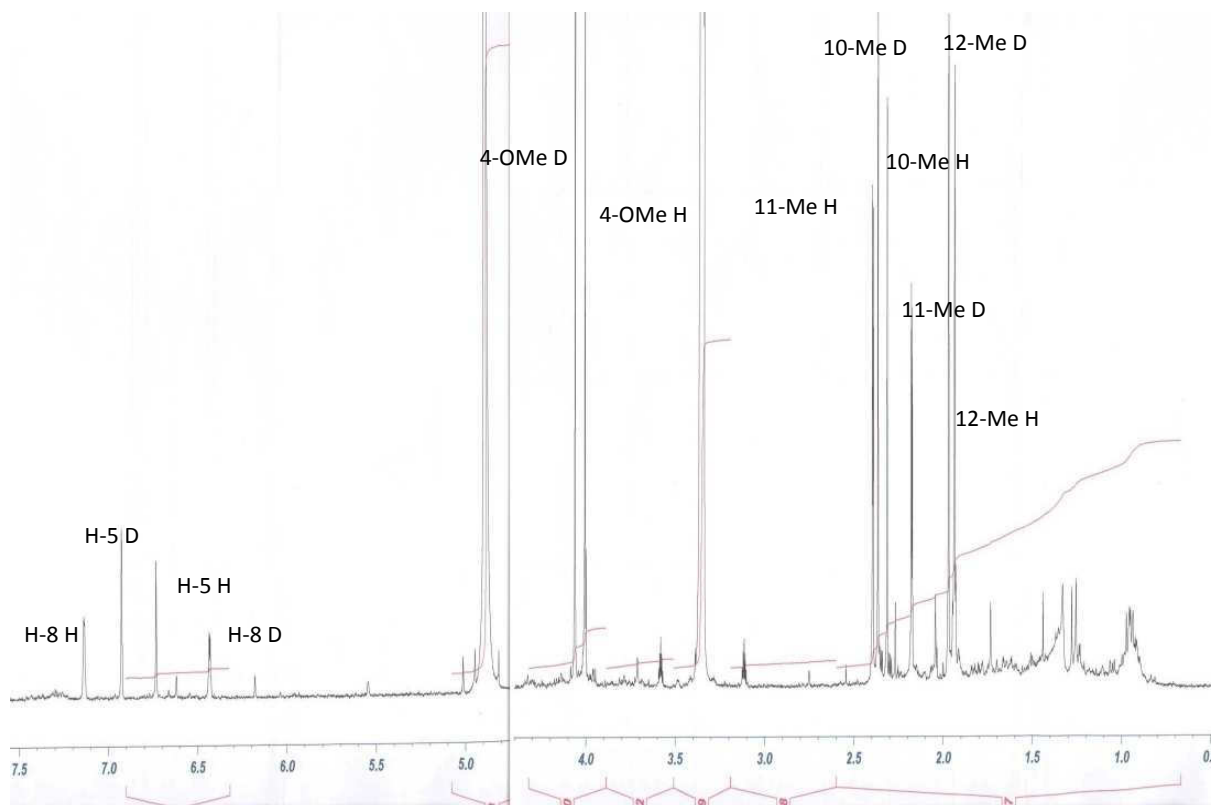
Attachment 16: The ^1H NMR spectrum of xestodecalactone G (**16**).



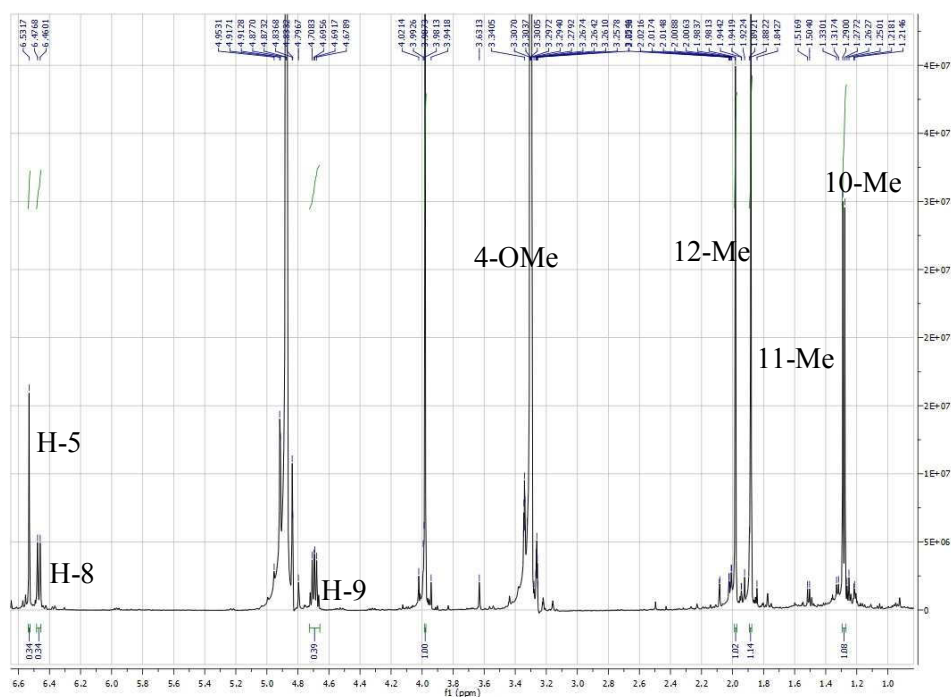
Attachment 17: The ^1H NMR spectrum of corynecassiicol A/B (**17/18**).



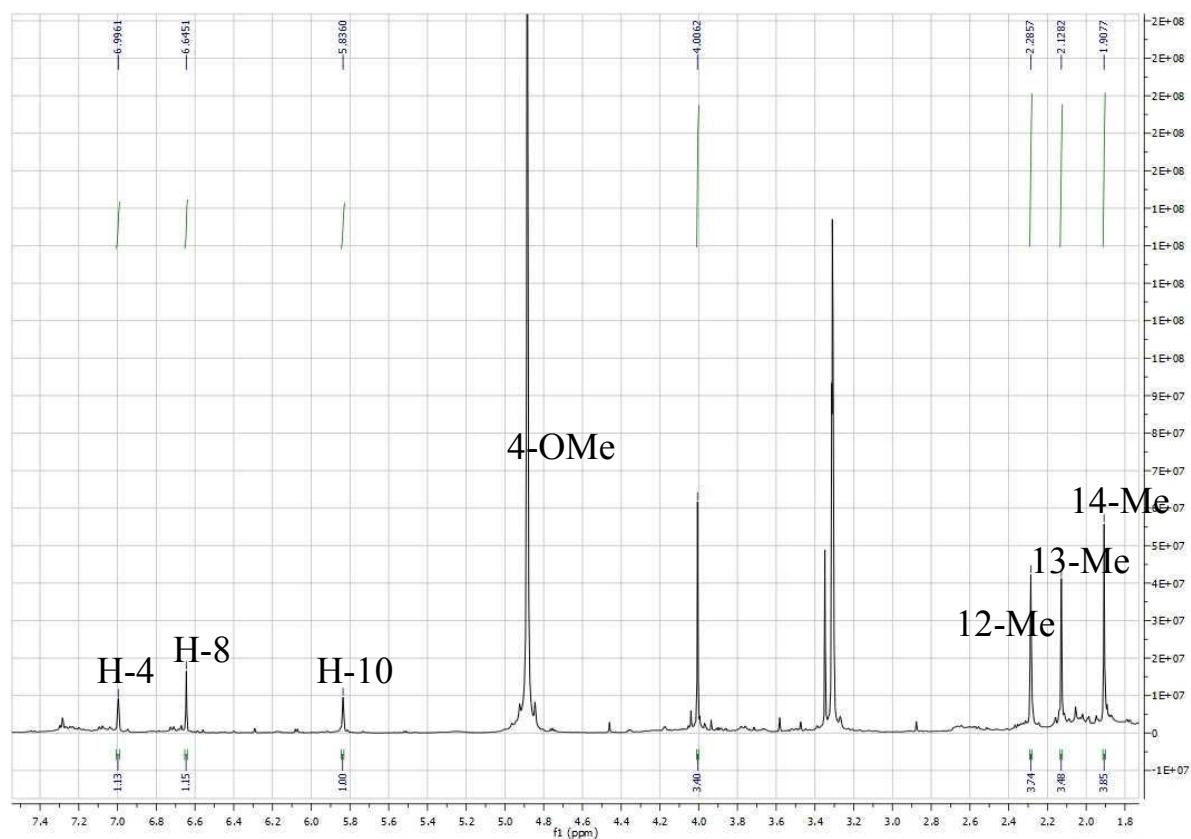
Attachment 18: The ^1H NMR spectrum of phomapyrone D/H (**19/20**).



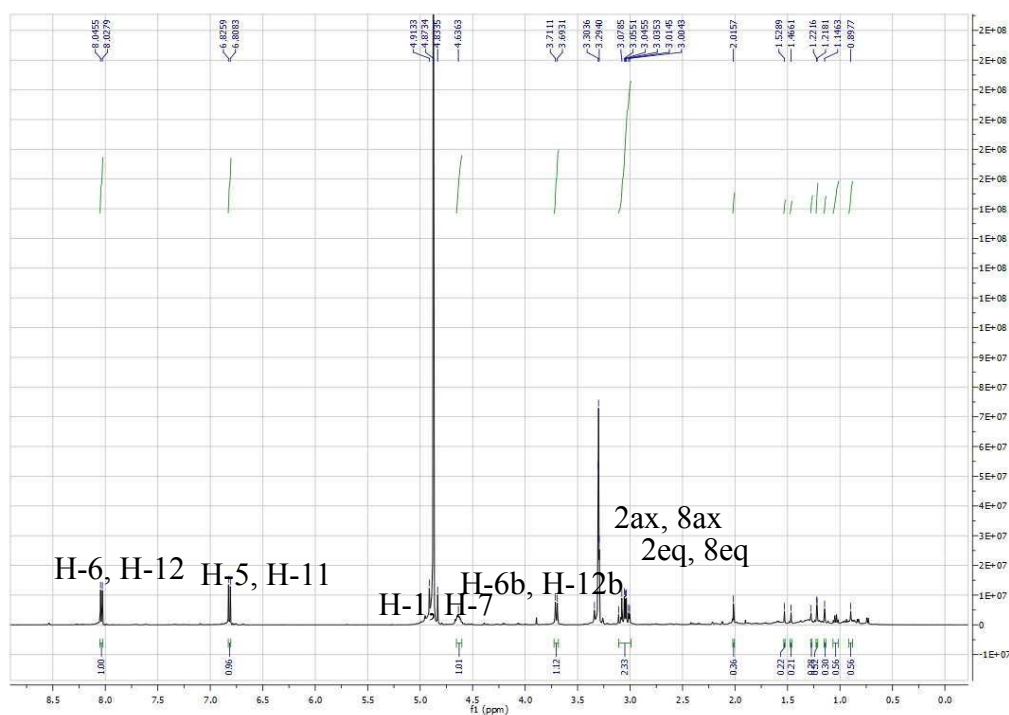
Attachment 19: The ^1H NMR spectrum of stemphyrone (21).



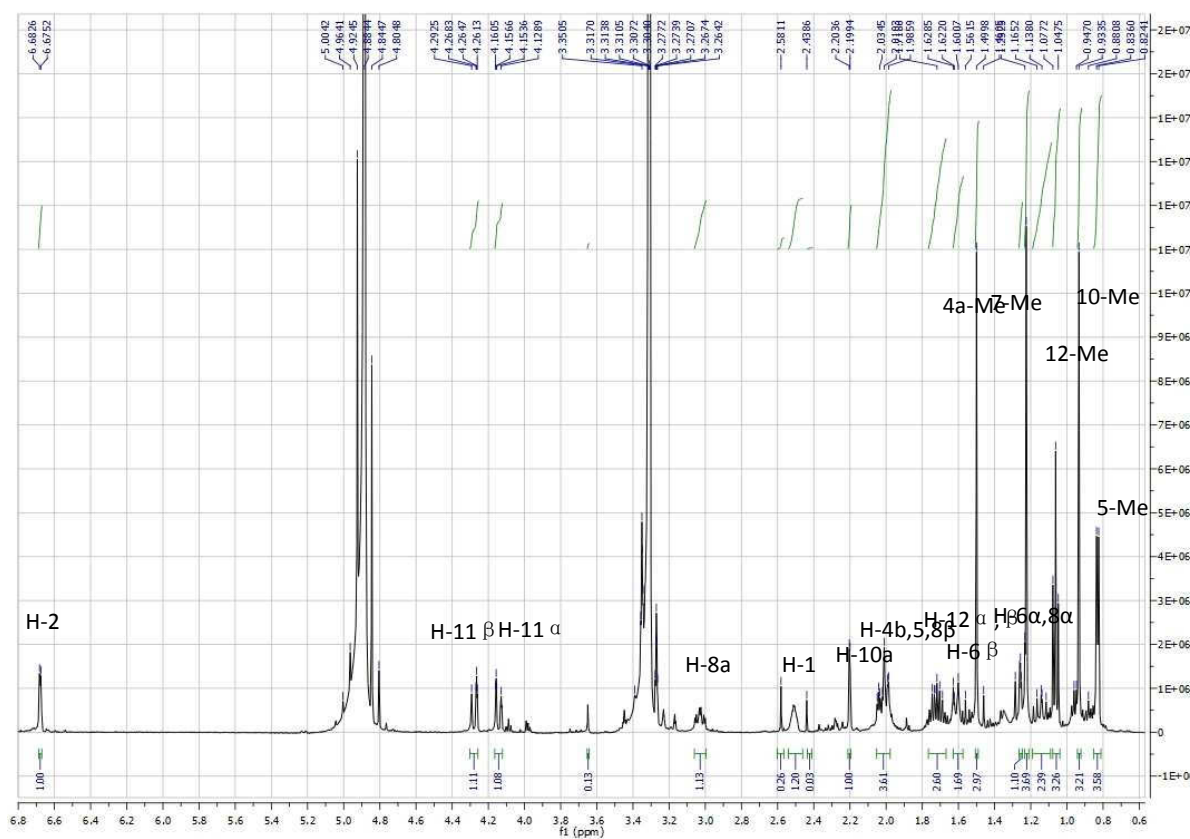
Attachment 20: The ^1H NMR spectrum of infectopyrone (22).



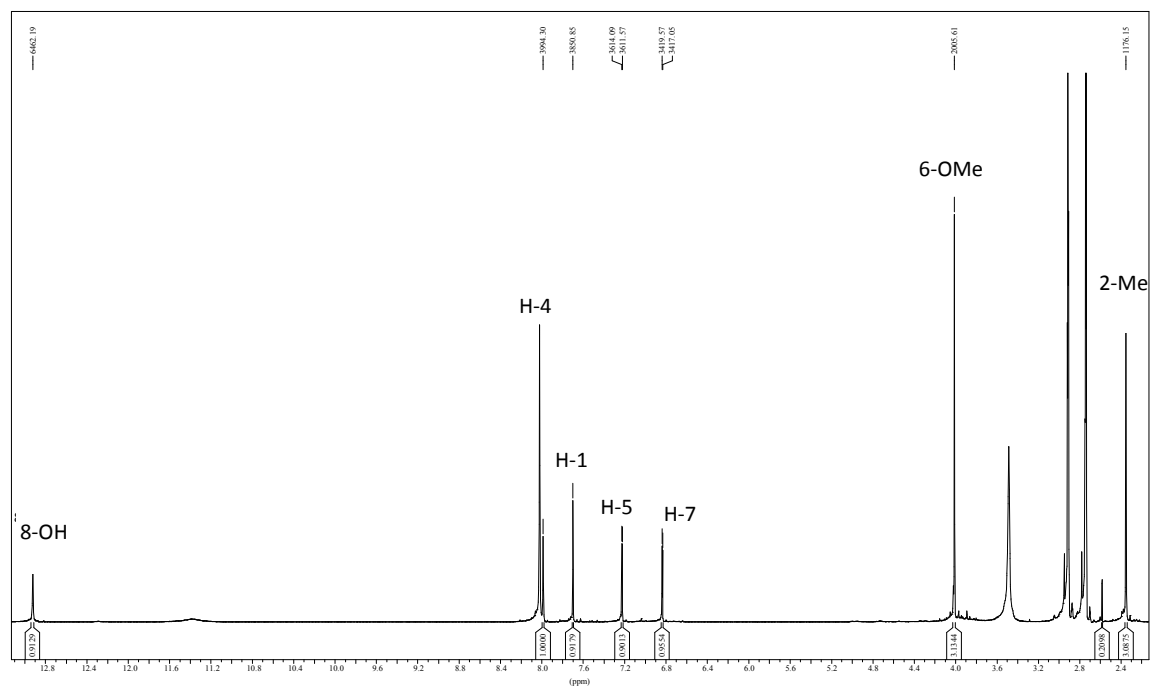
Attachment 21: The ^1H NMR spectrum of stemphyperlenol (**23**).



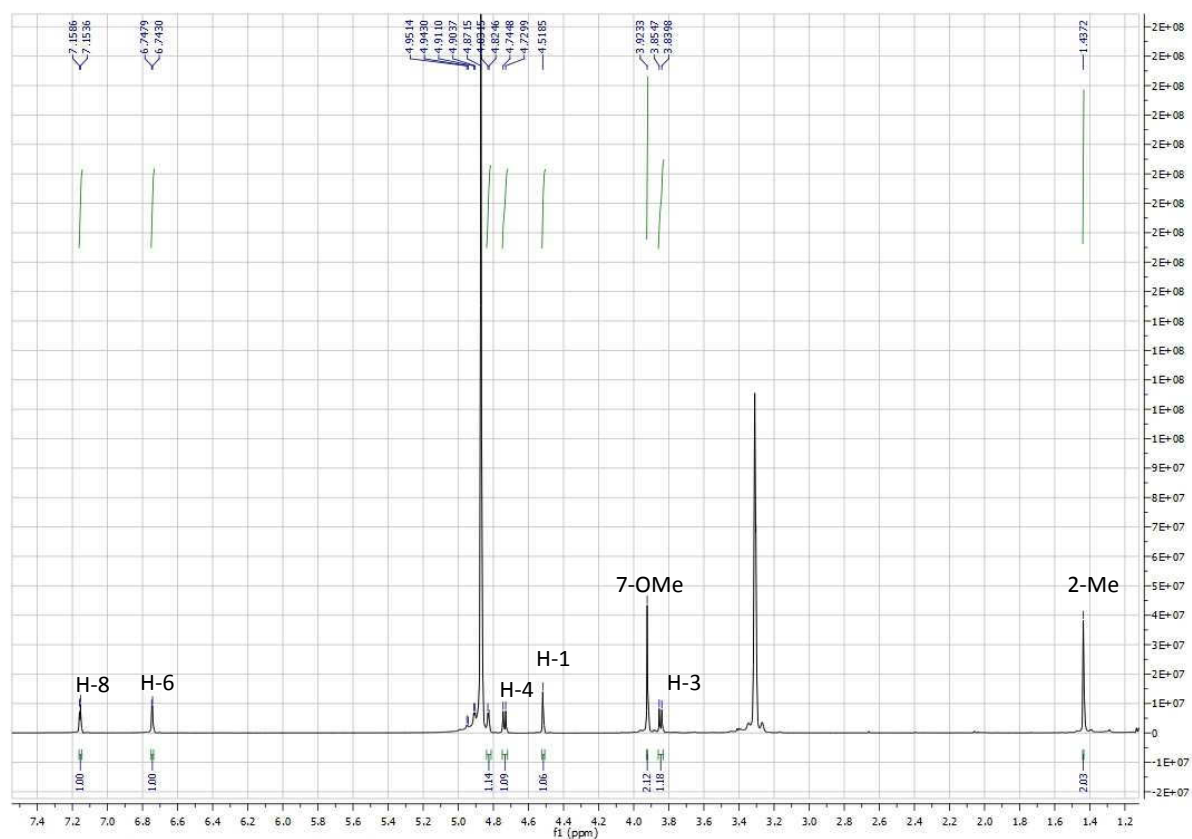
Attachment 22: The ^1H NMR spectrum of stemphbotrydione (**24**).



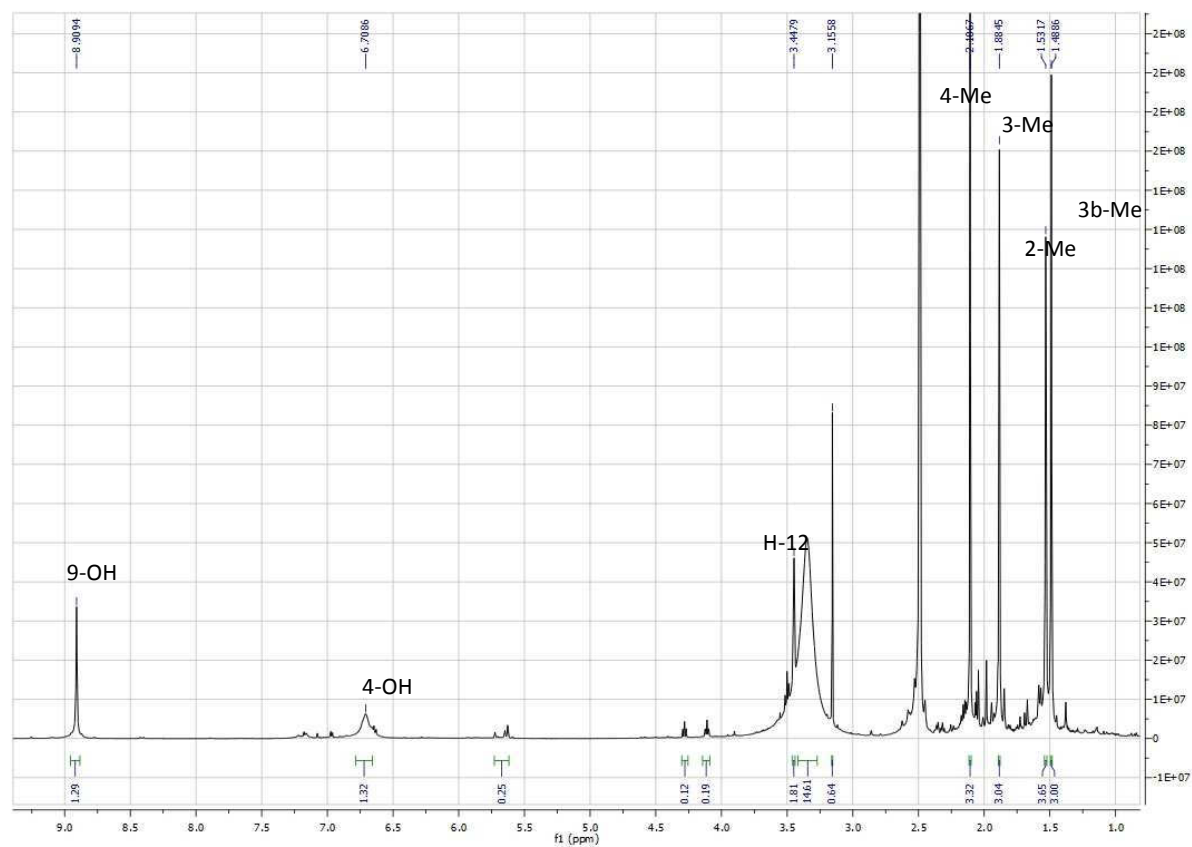
Attachment 23: The ^1H NMR spectrum of macrosporin (25).



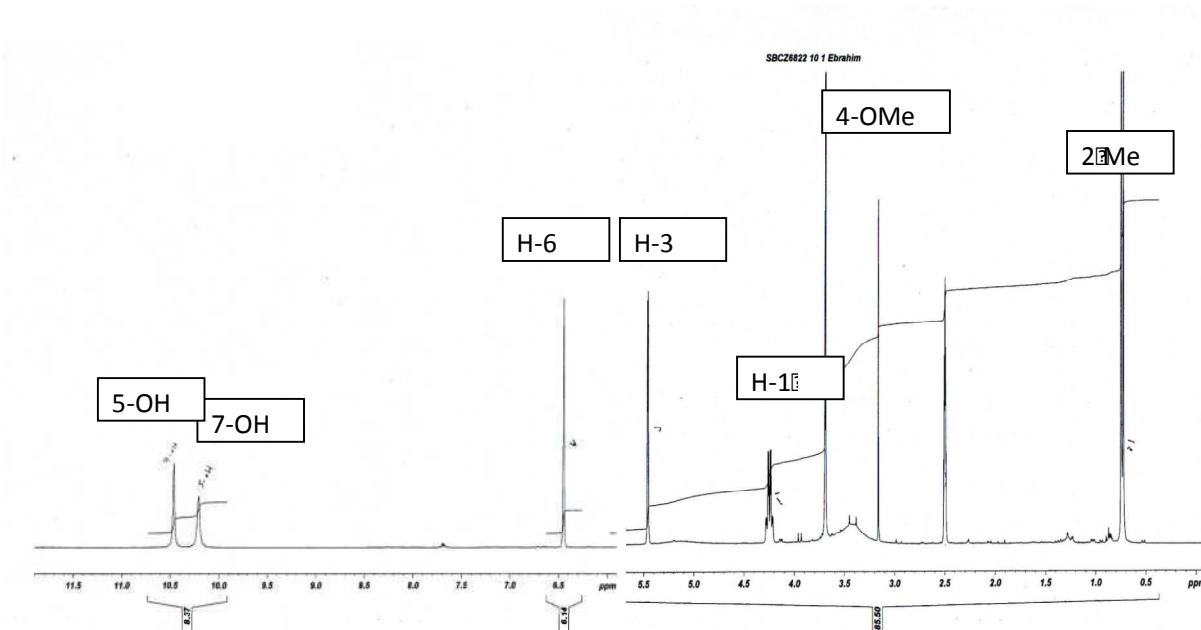
Attachment 24: The ^1H NMR spectrum of altersolanol A (27).



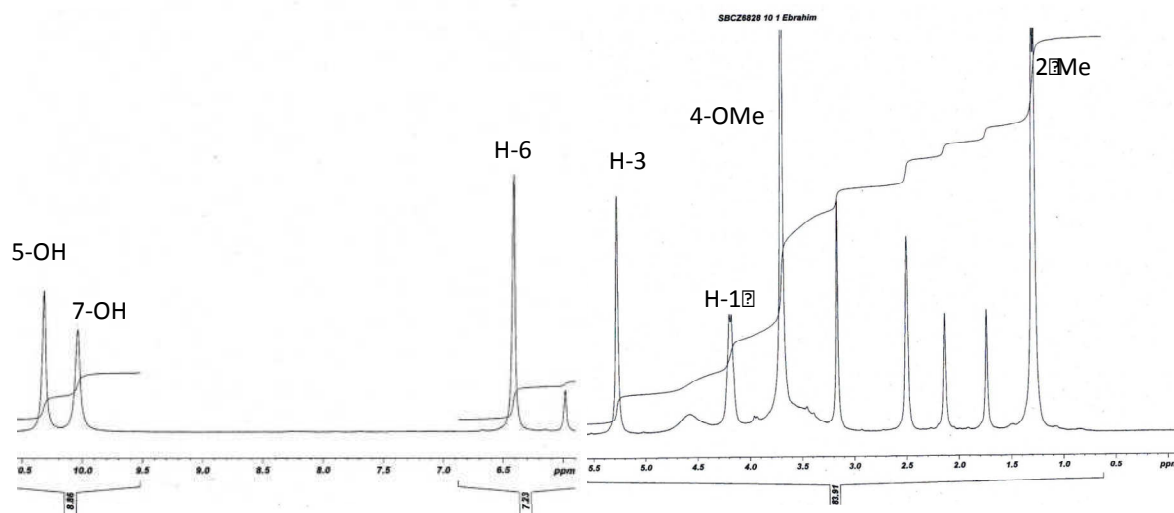
Attachment 25: The ^1H NMR spectrum of stempholantrione (**28**).



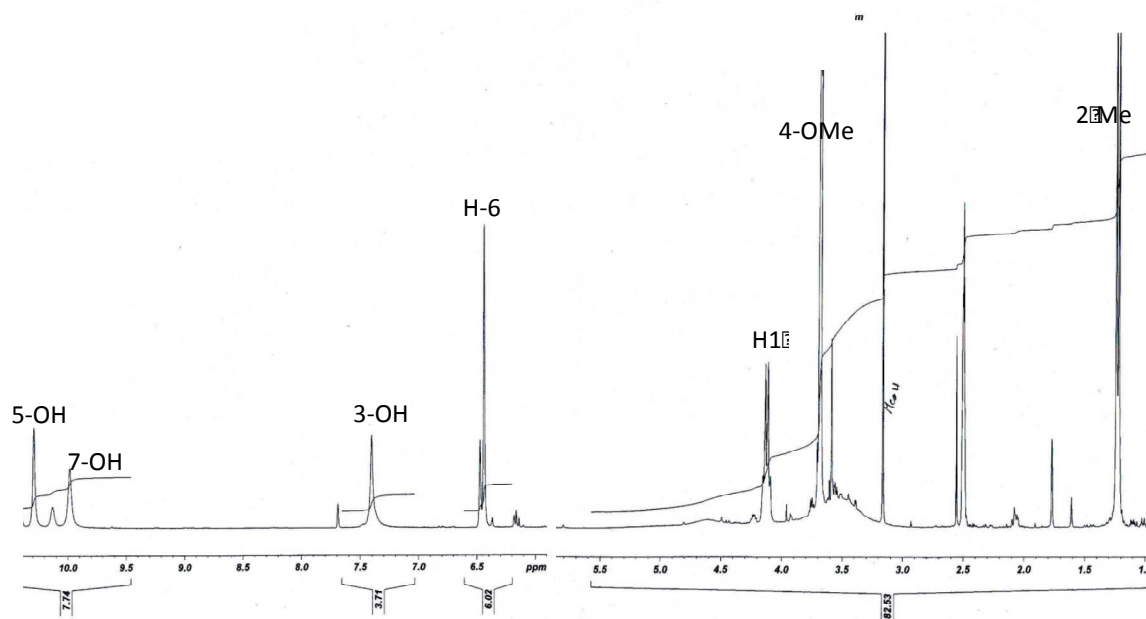
Attachment 26: The ^1H NMR spectrum of embepthalide A (**29**).



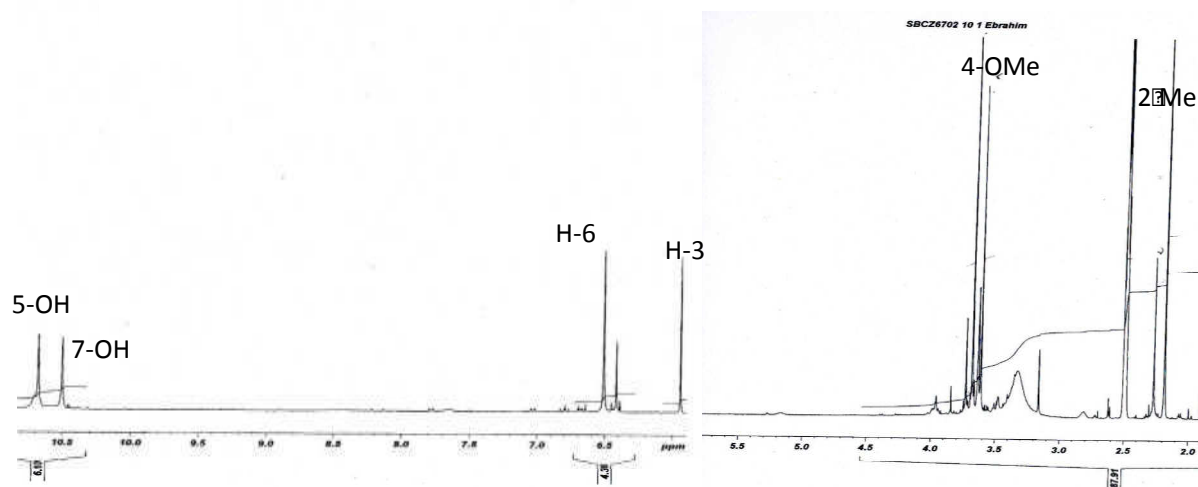
Attachment 27: The ^1H NMR spectrum of embepthalide B (**30**).



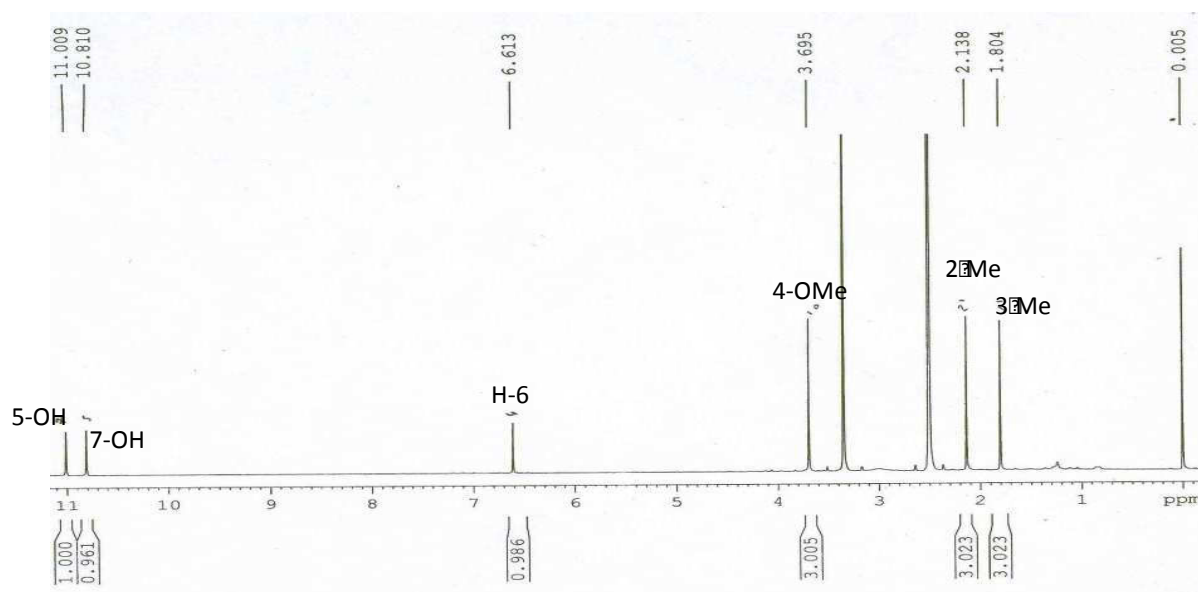
Attachment 28: The ^1H NMR spectrum of embepthalide C (**31**).



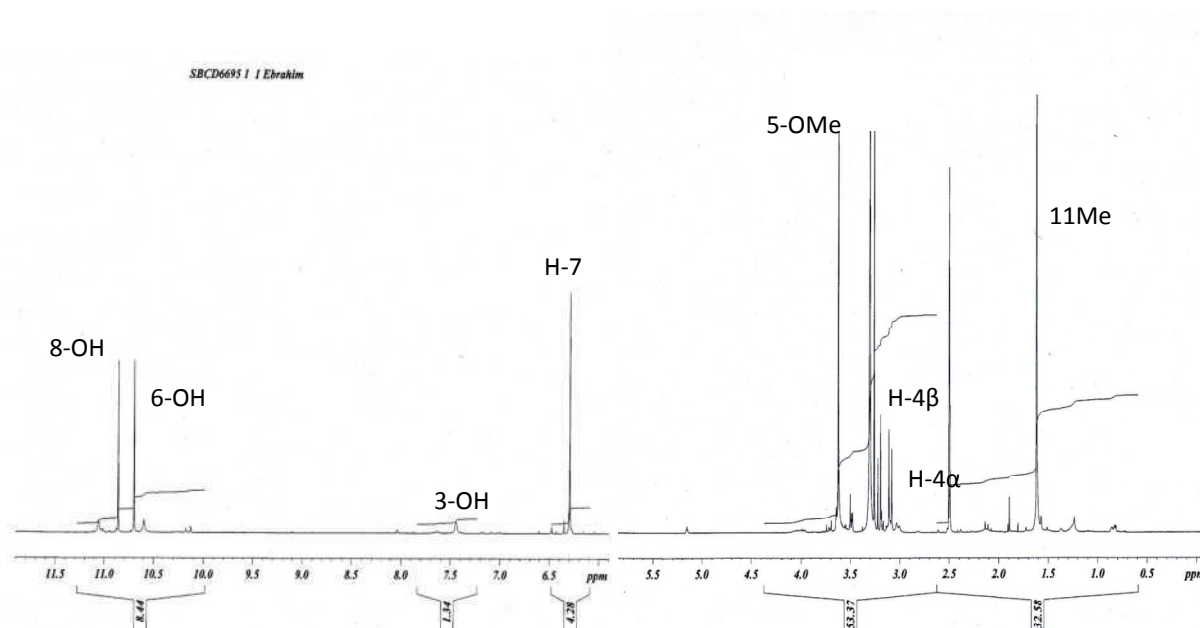
Attachment 29: The ^1H NMR spectrum of embepthalide D (32).



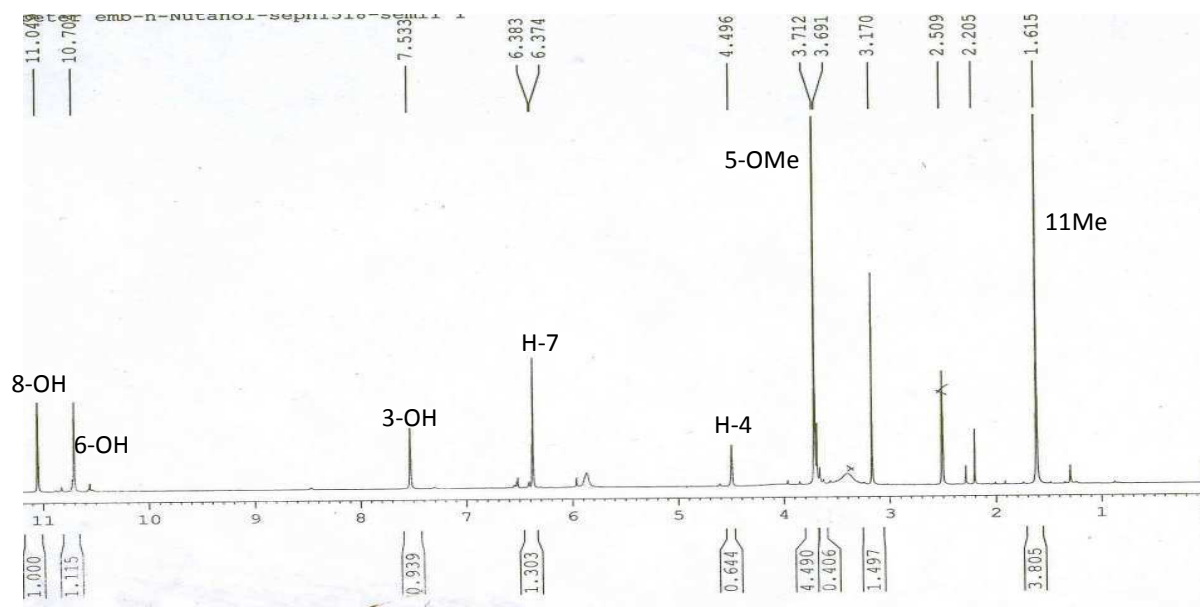
Attachment 30: The ^1H NMR spectrum of embepthalide E (33).



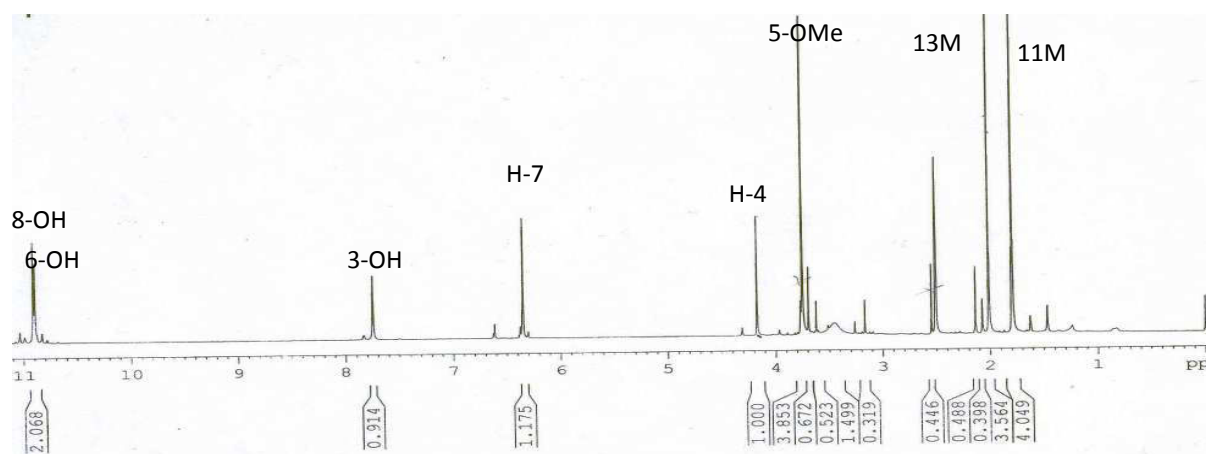
Attachment 31: The ^1H NMR spectrum of embeurekol A (**34**).



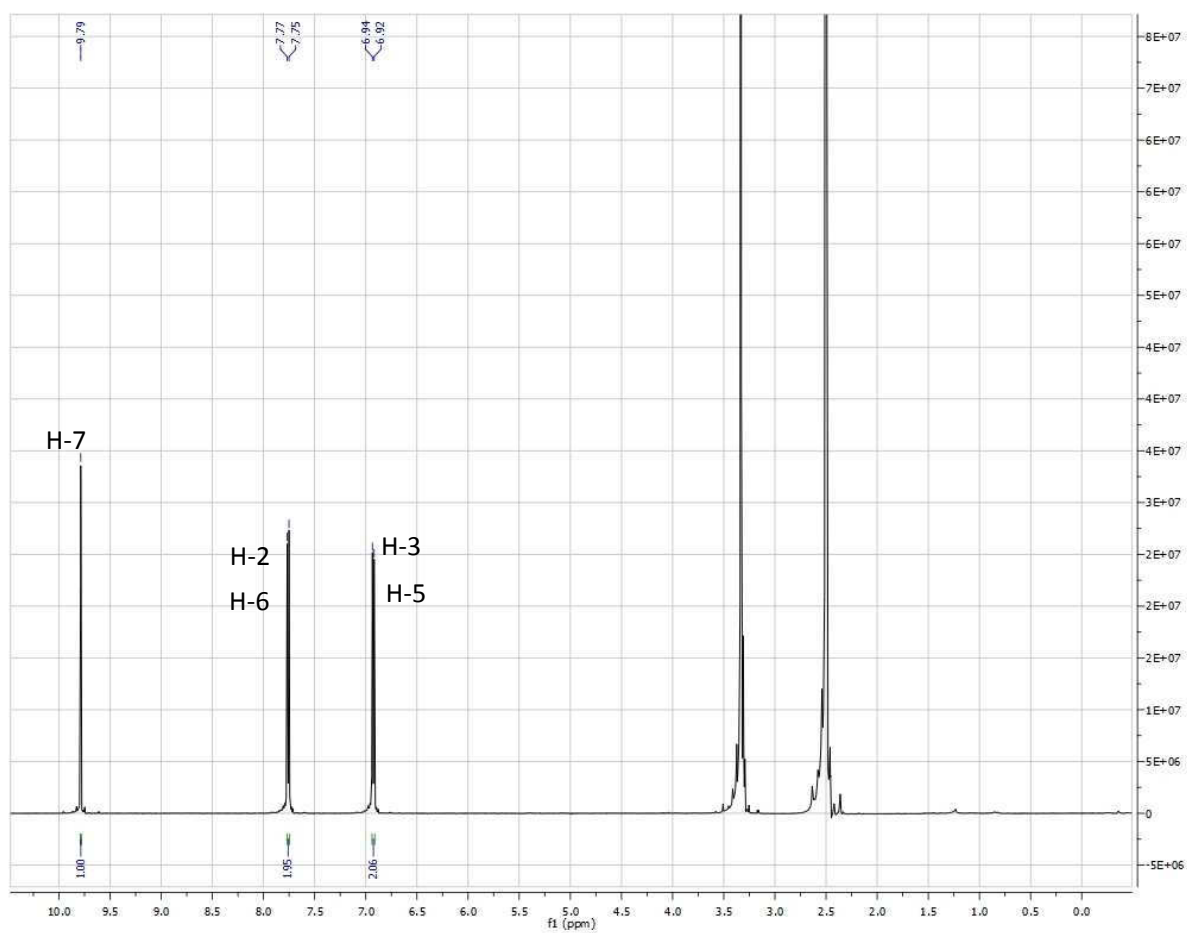
Attachment 32: The ^1H NMR spectrum of embeurekol B (**35**).



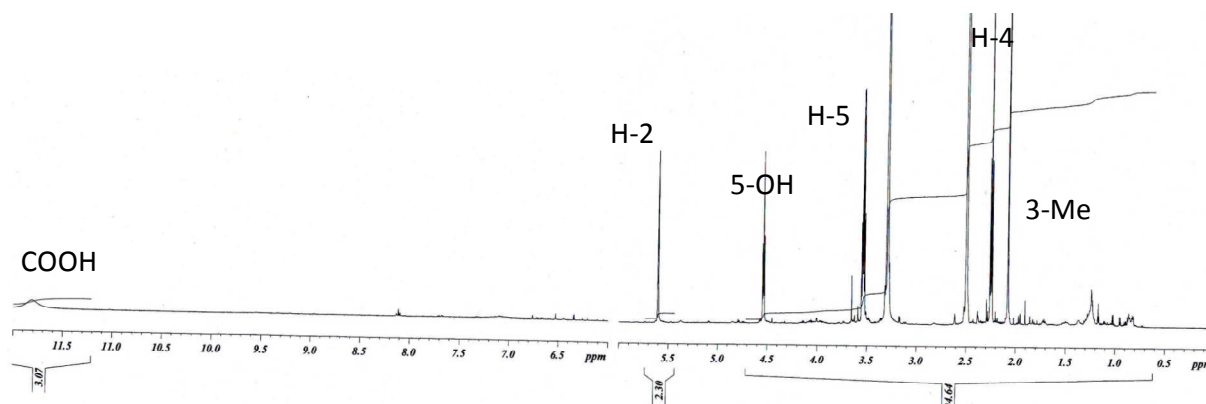
Attachment 33: The ^1H NMR spectrum of embeurekol D (36).



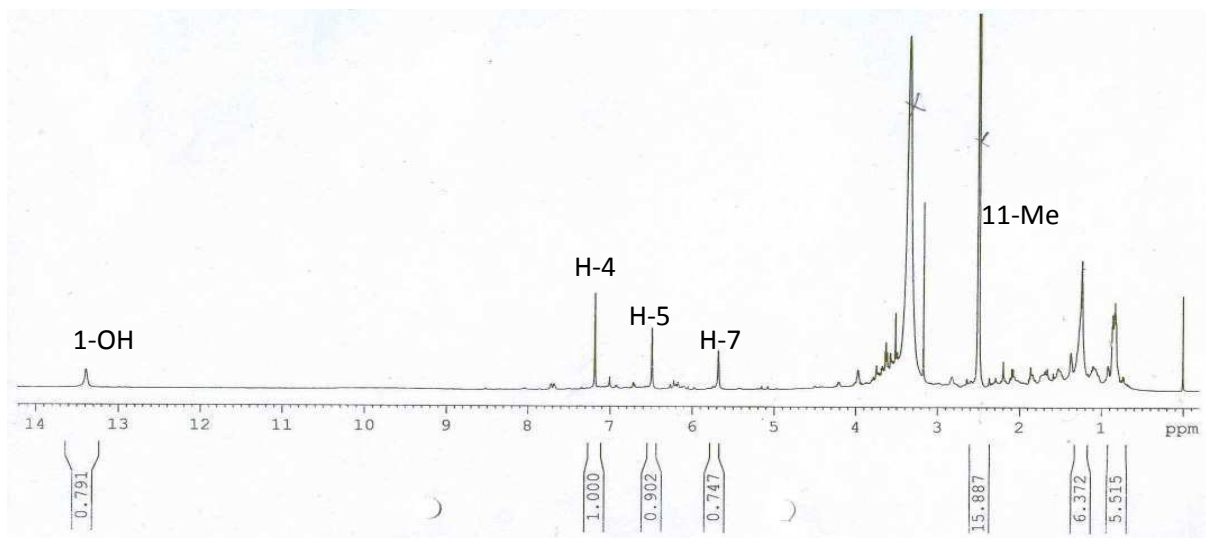
Attachment 34: The ^1H NMR spectrum of *P*-hydroxybezoic acid (37).



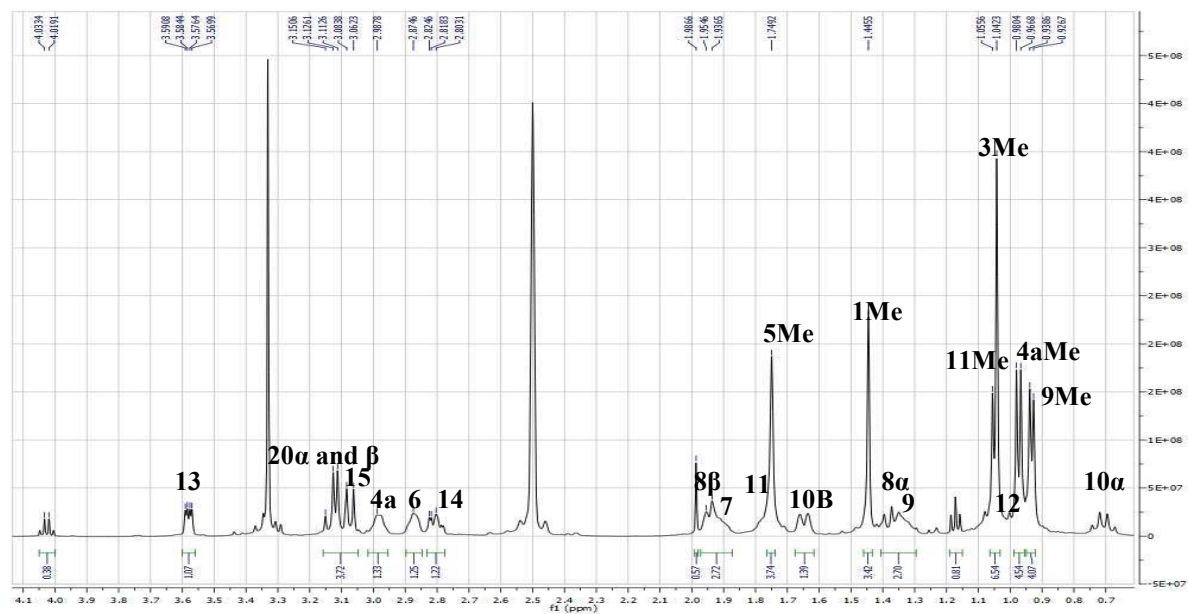
Attachment 35: The ^1H NMR spectrum of 2-anhydromevalonic acid (**38**).



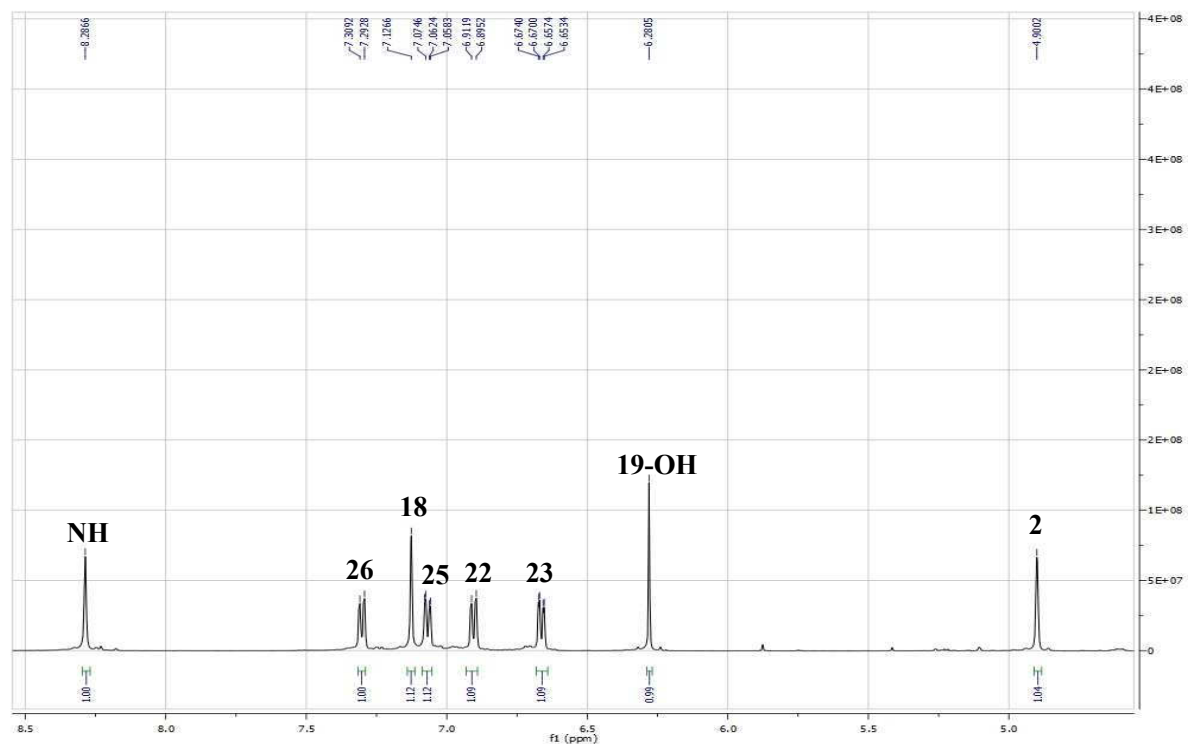
Attachment 36: The ^1H NMR spectrum of endocrocin (**39**).



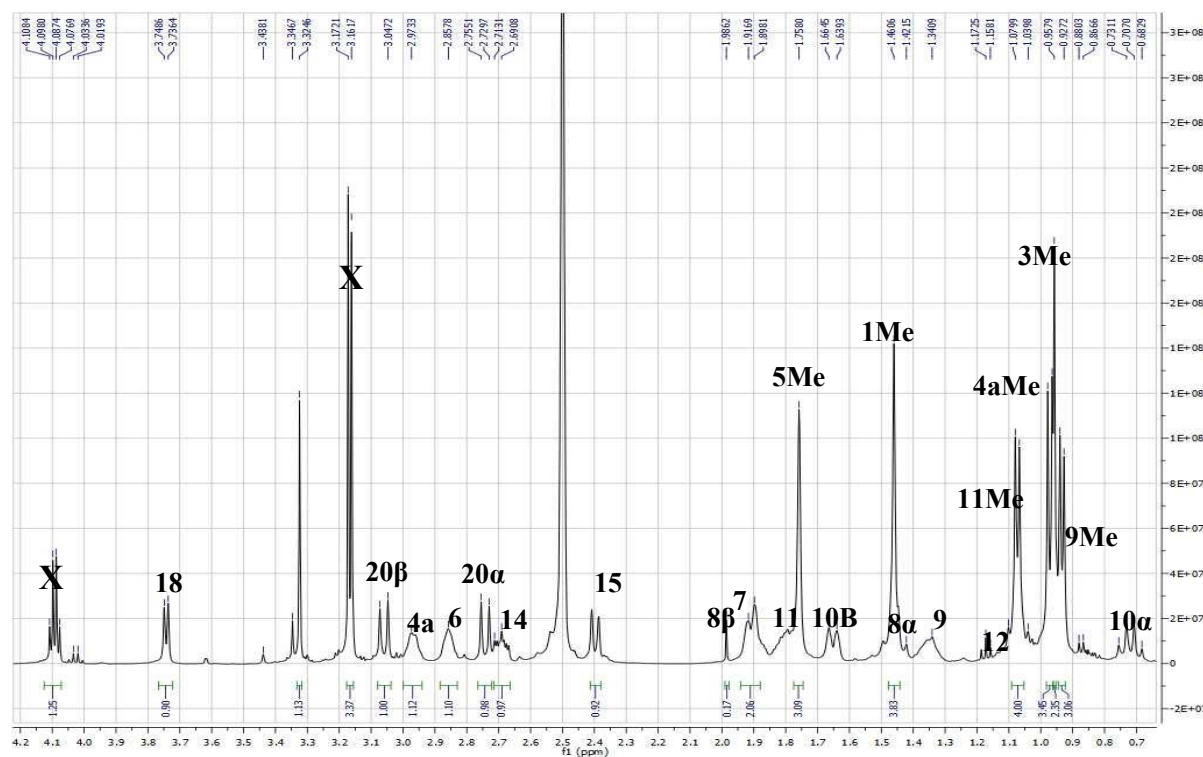
Attachment 37: The ^1H NMR spectrum of pyrrocidine D (40).



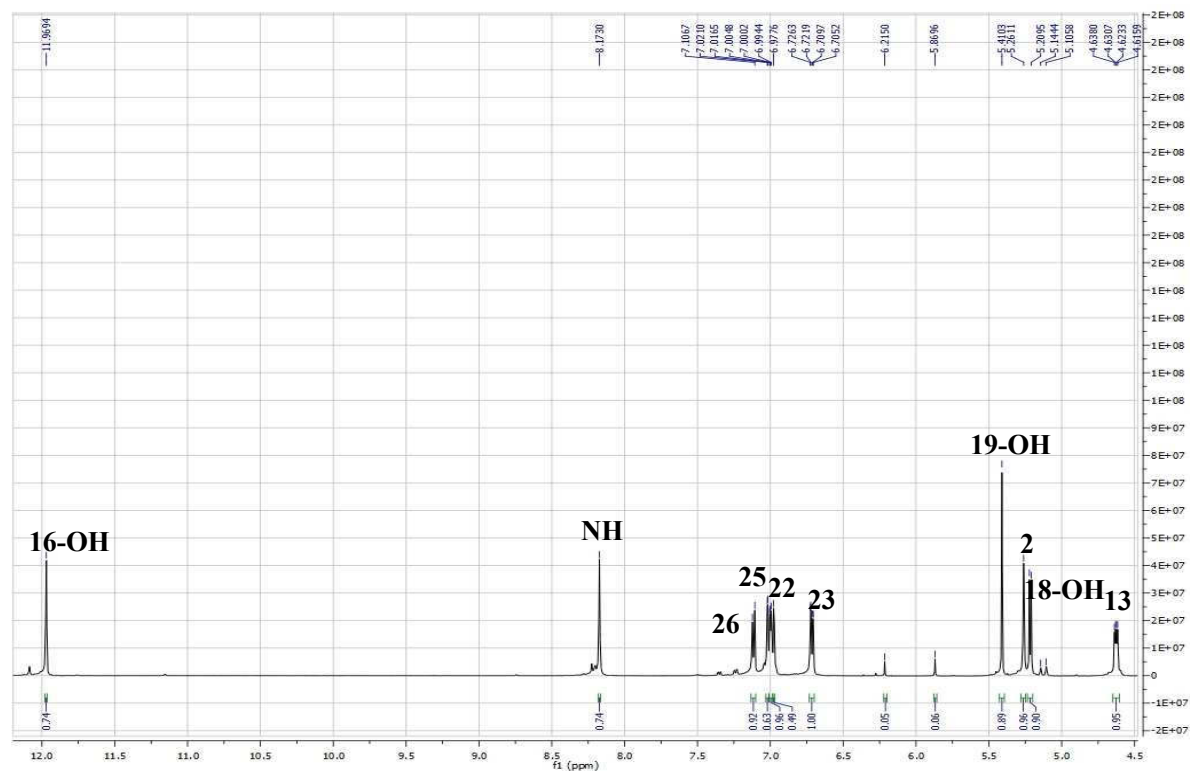
Attachment 37a: The ^1H NMR spectrum of pyrrocidine D (40).



Attachment 38: The ^1H NMR spectrum of pyrrocidine E (41).



Attachment 38a: The ^1H NMR spectrum of pyrrocidine E (41).



Curriculum Vitae

Weaam Nabil El-Sayed Ebrahim



CURRENT ADDRESS

Home address	Himmelgeister Str. 85 40225, Düsseldorf. Phone: 0176-62912538 E-mail: weel-001@uni-duesseldorf.de
Work address	Institute für pharmazeutische Biologie und Biotechnologie Heinrich-Heine-Universität Universitätsstr. 1 40225, Düsseldorf.
Permenant address	Department of Pharmacognosy, Faculty of Pharmacy, Mansoura University, Mansoura 35516, Egypt.

PERSONAL

Sex	Male
Marital Status	Married-No children
Nationality	Egyptian
Date of Birth	05.05.1977

EDUCATION

11.2008- Present	Graduate PhD Student, Institute für pharmazeutische Biologie und Biotechnologie, HHU, Düsseldorf.
09.2006	Master degree in pharmaceutical sciences (Pharmacognosy and Natural Products Chemistry), Mansoura University, Mansoura, Egypt.
09.2002	Premaster studies at Department of Pharmacognosy, Faculty of Pharmacy, Mansoura University, Mansoura, Egypt. General and special preparatory courses of the M. Sc. in Pharmaceutical Sciences (Pharmacognosy) at Faculty of Pharmacy, Mansoura University, Mansoura, Egypt.
09.2001	
09.1995-05.2000	Bachelor of Pharmacy, Degree very good with honor, Faculty of Pharmacy, Mansoura University, Mansoura, Egypt.
09.1995	Graduate study in Pharmaceutical Sciences at Faculty of Pharmacy, Mansoura University, Mansoura, Egypt.
05.1995	Graduating in Elmansoura Army Secondary School, Cairo, Egypt.

SCIENTIFIC EXPERIENCE

- 11.2008-Present** Graduate PhD Student, Institute für pharmazeutische Biologie und Biotechnologie, HHU, Düsseldorf.
- 16.09.2006** Assistant lecturer at Department of Pharmacognosy, Faculty of Pharmacy, Mansoura University, Mansoura, Egypt.
- 24.10.2000-03.02.2007** Supervising and teaching the graduate practical courses of pharmacognosy and Phytochemistry for 1st, 2nd, 3rd, 4th, 5th, 6th, 7th and 8th semester students at Department of Pharmacognosy, Faculty of Pharmacy, Mansoura University, Mansoura, Egypt.
- 24.10-2000-16.9.2006** Demonstrator in Pharmacognosy Department, Faculty of Pharmacy, Mansoura University, Mansoura, EGYPT.
The same teaching duties as an assistant lecturer.

COMPUTER SKILLS

UNESCO certified **International Computer Driving Licence certificate** (ICDL) which involve the following: 1-Basic Concepts of Information Technology 2-Using the Computer and Managing Files 3-Word Processing 4-Spread Sheets (Excel) 5-Database (Access) 6-Presentation (PowerPoint) 7-Information and Communication (Internet).

RESEARCH SKILLS

1. Chromatographical separation Techniques using column and preparative TLC.
2. Phytochemical screening of different plant extracts.
3. Microscopical examination of plant tissues.
4. Structure elucidation of different natural organic compounds using spectral data such as UV, IR, NMR and mass spectroscopy.
5. Handling experimental animals (mice, rats), blood withdrawal through retro-orbital plexus vein, and anaesthesia.
6. DNA binding using TLC, antibacterial using inhibitory zone and hepatotoxicity in mice and rats.

LANGUAGE PROFICIENCY

Arabic	Mother tongue
English	Excellent (Reading, Writing, Speaking, Listening) International TOEFL iBT .
Germany	Very good (ZD) level B1 (Goethe Institute, Cairo)
French	Basic knowledge

RESEARCH INTERESTS

1. Isolation and structure elucidation of bioactive compounds from higher plants using bioassay-guided techniques.
2. Conducting studies to utilize micro-organisms and semi-synthetic reactions to effect specific changes in structures of biologically active substances.
3. Analysis of compounds in extracts and biological fluids using TLC, HPLC and GC.

CONFERENCES, WORKSHOPS AND SYMPOSIUMS

1. Assiut University Third Pharmaceutical Sciences, Faculty of Pharmacy, Assiut, Egypt, 5-6 March (2002) (Poster Presentation).

2. 22. Irseer Naturstofftage (Poster Presentation)-February 2010.
3. 58th International Congress and Annual Meeting of the Society for Medicinal Plant and Natural Products Research and the 7th Tannin Conference, Berlin, 29th August-2nd September 2010 (Poster Presentation).
4. ScieTalk NRW (Poster Presentation)- Münster-23th November 2011.
5. 24. Irseer Naturstofftage (Poster Presentation)-February 2012.
6. Young Researcher Meeting (Oral Presentation)-Münster-2nd and 3rd March 2012.

PUBLICATION IN PEER-REVIEWED JOURNALS

- 1-**"Phytochemical and biological Study of Monsonia Nivea Growing in Egypt"** M.S. Afifi, M. A. Hassan, Z.A.M. Naeim and W.N.El-Sayed.*Mans.J.Pharm.Sci.* Vol.23, Part 1(2007).
- 2-**"A Pharmacognostical Study of Monsonia Nivea Growing in Egypt"**. M. S. Afifi, M.A Hassan, Z. A. M. Naeim and W. N. El-Sayed. *Bull. Pharm. Sci.*, Assiut University. Vol.30, Part 1, (2007).
- 3-**"Chemical Characterization and Insecticidal Evaluation of the Essential Oil of *Mentha suaveolens* L. and *Mentha pulegium* L. Growing in Morocco"**. N. Benayad, W. Ebrahim, A. Hakiki and M. Mosadak *SCSCC6*, Vol. 13 (1), (2012).
- 4-**"Decalactone Derivatives from *Corynespora cassiicola*, an Endophytic Fungus of the Mangrove Plant *Laguncularia racemosa*"**. W. Ebrahim, A. H. Aly, V. Wray, H. Dai, F. Totzke, M. H. G. Kubbutat, P. Proksch and A. Debbab. *Eur. Jour. Org. Chem.* (DOI: 10.1002/ejoc.201200245).
- 5-**"Pullularins E and F, Two New Peptides from the Endophytic Fungus *Bionectria ochroleuca* Isolated from the Mangrove Plant *Sonneratia caseolaris*"**. Weaam Ebrahim, Julia Kjer, Mustapha El Amrani, Victor Wray, Wenhan Lin, Rainer Ebel, Daowan Lai, and Peter Proksch. *Mar. Drugs* (Accepted).
- 6-**"New Octalactone Derivatives from the Endophyte *Corynespora cassiicola* Isolated from *Laguncularia racemosa*"**. W. Ebrahim, A. H. Aly, V. Wray, H. Dai, P. Proksch and A. Debbab. *Nat. Prod. Comm.* (Submitted).
- 7-**"NF-kappa B Inhibitors from the endophytic fungus *Embellisia eureka*"**. W. Ebrahim, A. H. Aly, V. Wray, A. Hamacher, M. U. Kassack, F. Totzke, M. H. G. Kubbutat, P. Proksch and A. Debbab. (Submitted to *Journal of Medicinal Chemistry*).
- 8-**"New naphthoquinone derivative from *Corynespora cassiicola*, an endophytic fungus of the mangrove plant *Laguncularia racemosa*"**. W. Ebrahim, A. H. Aly, V. Wray, H. Dai, P. Proksch and A. Debbab. (Submitted to *Mycosphere*).